Application of an atmospheric mesoscale modelling system to analysis of air pollution dispersion in the Christchurch area

A thesis
submitted in fulfilment
of the requirements for the degree
of
Master of Science in Environmental Science
in the
University of Canterbury

by

Mikhail Titov

University of Canterbury
2004

Table of Contents

List of Figures

Figures **Page**

List of Tables

Acknowledgements

First and foremost my sincerest thanks to Professor Andy Sturman (principal supervisor) and Dr Peyman Zawar-Reza (associate supervisor), who supervised my work and provided all possible and impossible assistance (including the language problems) to guide me, not only during my 16-month Masters research, but also in my everyday working life in the Department of Geography at the University of Canterbury. I am very grateful to them for their support, which provided me with the opportunity to make full use of the Department's computer and other resources, as well as for commenting on the final drafts of the thesis. Their enthusiasm and advice are greatly appreciated.

I also especially want to express my gratitude to Professor Andy Sturman for his strong support of my successful application for a Masters Scholarship, as well as to thank Dr Simon Krichak (Tel-Aviv University, Tel Aviv, Israel) for his reference.

I am grateful to the Department of Geography and Environment Canterbury (Ecan) for providing meteorological and air pollution data (for CAPS2000 and winter 2003), both from fixed observation sites and vertical atmospheric balloon soundings that had been used in this research as the ultimate 'tuning fork' in the process of utilization, assimilation and fine tuning of the MM5–CAMx4 numerical system. I also want to thank the Meteorological Service of New Zealand (Wellington), and particularly Dr Norm Henry, who found time to send me the MM5 input data with the MetService MM5 configuration giving me an opportunity to compare their version of MM5 tuning with the one I used for the Christchurch region.

Many thanks are due to the technical staff of the Geography Department for their support of my everyday work, especially to John Thyne (for his vital help in the creation of landuse files), to computing administrator Steven Sykes, and to software analyst Graham Furniss. Separately, I want to acknowledge the work of my colleague researcher James Sturman for the very big and complex job of creating CAMx4 input gridded aerosol and gaseous concentration files, as well as for his advice with regard to the chemistry involved during application of the chemical model.

In reviewing drafts of this thesis, the guidance of Professor Andy Sturman, Dr Peyman Zawar-Reza, and Mr Henry Wrassky was greatly appreciated. Other people around me also continued to provide their friendship and support. In particular, I would like to thank my family, especially my mother Olga, my wife Elena for their inspiration, and my office-mates James Sturman and Mike Green.

Abstract

The study is concerned with the significant and historically well-known problem of winter air pollution in Christchurch and its vicinity (especially associated with particulate matter–PM_{10}) during nights dominated by stagnant synoptic weather situations. This pollution results from active use of domestic log-burners and open-fires, on nights of strong near-surface temperature inversion.

In this study, a numerical modelling research approach is used with the application of a regional atmospheric model (Mesoscale Model, 5th generation-MM5) and an air quality-air pollution model (Comprehensive Air quality Model with extensions, version 4-CAMx4), coupled together for more sophisticated investigation of space-time PM_{10} dispersion over the Christchurch region during heavy smog nights.

In the thesis, the theoretical and practical background of limited area models is described, with reference to basic limited area meteorological models such as MM5, RAMS and WRF. The potential of limited area meteorological modelling (MM5), air pollution chemical modelling (CAMx4), and the use of coupled numerical systems (MM5-CAMx4) for numerical investigations are also discussed. The basic types of coupled meteorological-chemical models, the application of the main limited area models, and the level of precision of the various modelling systems are briefly discussed.

The factors controlling atmospheric circulation over Canterbury and the Christchurch region are described, and their influence on heavy night-time air pollution in Christchurch and its vicinity, with particular reference to the winter situation and the possibility of prediction and control of the aerosol air pollution. The study analyses input data for numerical modelling, including global analysis data, the CAPS2000 and winter 2003 field experimental sites, and particulate monitoring observations.

Several methods of MM5 modelling are applied to replicate the local air circulation over Christchurch and its environs: single run modelling, series of runs with different levels of nesting with use of the CAPS2000 observed data for MM5 fine tuning. Particulars of 2003 winter MM5 modelling using global analysis input data, and Meteorological Service input data are covered separately.

The numerical modelling system (meteorological-chemical) was created with application of CAMx4 as a basic air quality model. The procedures for assimilation of MM5 data as basic input meteorology for the chemistry model, and use of particulate matter monitoring data were investigated. Different versions of MM5-CAMx4 optimal combination have been compared, and quasi-operation possibilities of the MM5-CAMx4 modelling system have also been considered

on the basis of winter 2000 and winter 2003 PM_{10} experimental modelling.

Chapter 1
Introduction

1.1 Research rationale

Atmospheric pollution is a major problem for big and small cities all over the world. The bigger the city the more complex the problem of air pollution from domestic, industrial and transport exhausts or natural pollutants. In such major centres as Mexico City, Tokyo, Beijing, Moscow and New York people are affected by polluted air, especially during the summer time. A lot of respiratory diseases of varying severity strike inhabitants of these cities, from an increase in the number of cold suffer to heavy attacks of asthma and anaphylactic shocks (Arya, 1999).

Acute respiratory disease is not only associated with big cities (with millions of people). In smaller (less than 1 million population) cities the situation can sometimes be much worse under the specific local atmospheric conditions resulting from such things as orographic effects and land-water distribution (Cogliani, 2001), as well as historical traditions and/or fast growing industry (in a city and/or it's suburbs). The situation of air deterioration in the near-surface layer can be worsened by particular combinations of human and environmental factors (Owens, Tapper, 1977; Kossmann, Sturman, 2002). Research into the influence of human activity on the air quality is one of the major tasks of mesoscale numerical modelling (Pielke, 1984; Otte, 2001).

International demand for regional (mesoscale) models appeared many years ago and is associated with an increase in the number of meteorological and environmental problems to be solved at this scale. This situation has been important for Canterbury, the South Island and the whole of New Zealand for many years, as illustrated in many published papers (Sturman, 1985; 2000).

The increasing needs of New Zealand organizations such as Ecan (Environment Canterbury) and the Ministry for the Environment to establish strategies for environment protection (for example, the 'Clean Heat Project 2003') demand innovation in the application of modelling techniques (Moody, 1983). New high-resolution modelling systems like the meteorological prognostic model MM5 (Mesoscale Model, 5th generation) described by Grell, Dudhia, and Stauffer (1994), and chemistry numerical model CAMx4 (Comprehensive Air quality Model with extensions Version 4) described in the Technical report of Hurley (2002) can be used for fine-scale simulation and research of air pollution over complex terrain in areas like Christchurch and the surrounding small towns. The problem of air pollution over the Christchurch region during cold winter nights under clear skies and associated air stagnation

requires serious numerical research and comparison with available observations (Sturman, Zawar-Reza, 2000; 2002). Comparison with observations is necessary for creating more realistic and accurately tuned numerical modelling of 'air circulation – air quality' systems (McKendry and Sturman, 1983).

The demands for higher resolution modelling in space and time of air pollution over Christchurch are the main reasons for this thesis (Mass *et al.*, 1997). The ultimate aim is to provide quasi-operational predictions of approximate levels of air pollution in different parts of the city, which requires installation, utilization and adjustment of the limited area model MM5 and Chemical Modelling System (CMS) CAMx for more sophisticated investigation of air pollution situations.

From history, it can be traced that the problem of air pollution has it's roots several centuries ago, in an era of increased house building and industrial development using a range of different kinds of fuel (e.g. wood, peat and coal) for heating and industrial processes. For example, in the late 17th century a special English law prohibited the burning of coal during misty days and nights to prevent heavy air pollution. The punishment for noncompliance was execution! New Zealanders, mostly descendants of Great Britain, have inherited the tradition of using log-burners and open-fires. This tradition of house heating allowed the builders to build cheaper houses, but it reduced air quality especially during the cold time of the year. Christchurch represents an excellent example of traditional domestic heating during wintertime when clear skies enhance outgoing long wave radiation and cold nights (Spronken-Smith *et al.*, 2001). Absence of double glazing, big windows and glass doors (including so-called 'sun rooms' or 'conservatories'), poorly insulated walls, high ceilings and a lot of gaps in the structure are distinctive characteristics of the houses built during the 19th century and much of the 20th century. Until recently, the builders have preferred not to put double-glazing in new houses (except for special projects), trying to spend less money and gain more return. Hence the habit of heating using open fires and log-burners continues to encourage traditional styles of building (e.g. many new houses have open fires as a tribute to tradition). This process is made worse by the increase in cost of real estate and electricity prices, which makes it impossible to decrease the total number of domestic fires over Christchurch and its suburbs.

The effect of increasing development of small and medium sized industry must be added to the domestic factor to provide an overall assessment of solid fuel use, which is affected by a reluctance to move from this kind of fuel because of the high price of more efficient and clean kinds of fuel, like electricity and natural gas.

The complex and unique orographic landscape of the Canterbury region and the ocean increase the problem of air pollution during cold winter nights because of the very frequent

situation of stagnant air in the atmospheric boundary layer (ABL) under strong, low level temperature inversions (Ryan, 1975; 1987). Accumulation of products of combustion in the lowest level of the ABL during winter nighttime is considered to be the most important environmental problem of Christchurch and its suburbs.

1.2 The research in context

1.2.1 Numerical research approaches

Twenty years ago only the meteorological organizations in a few countries (e.g. the United States, the Soviet Union, Japan, Great Britain, Australia and Canada) had the ability to create their own Global Atmospheric Models (GAM). However, various problems limited the extent of development of global numerical atmospheric models for researching different kinds of meteorological–environmental phenomena. These problems were mostly technical and associated with restricted access to super computers, restricted computer speed, and with the absence of reliable gridded input data (Smagorinsky, 1983).

Also, it was nearly impossible to investigate meso- and local scale atmospheric circulations using global numerical models. Theoretical formulation and numerical realization of limited area models using nested grids has provided a great tool for researchers all over the world, who can now take a regional modelling approach, evaluated using local observations, for modelling a range of local climate situations (Sturman, 2000).

Hence the theory and practice of using nested grids in mesoscale models to investigate more accurately different scales of phenomena in meteorology, climatology and environment pollution started to develop very rapidly in the middle of the 1980s (Dudhia, 1993). The possibility to research small-scale features using limited area models in the different geographical areas all over the world has been an outstanding step in the development of regional numerical modelling. Local models with regional initial data have been used for a lot of special meteorological purposes (Dudhia and Bresh, 2000; Klausmann *et al.,* 2001; Dailey and Keller, 2002; Low-Nam and Davis, 2002; Miranda and Borrego, 1996; Smallcomb, 2002; Someshwar *et al.,* 2002; Spronken-Smith *et al.,* 2004). Global and regional modelling are now two essential parts of one main aim, to investigate atmosphere circulation across the whole range of scales (Fast *et al.,* 1995).

1.2.2 Global atmospheric models

Global Atmospheric Models (GAM) started to develop in the late 1960s based on the system of primitive hydrodynamic equations transformed in finite-difference form using time schemes with different levels of precision (Pedlosky, 1979; Manabe, Hahn, 1981). Nowadays, global models are run on super computers with speeds of about several teraflops (n x 10^{14}), because of the enormous number of nodes (due to increased spatial and temporal resolution), which allow global models to be applied over a wide range of scales.

We can split global numerical models into two types based on whether they are finite-difference or spectral models. Finite-difference models were developed earlier, basically at the Geophysics Fluid Dynamic Laboratory (Smagorinsky, 1963) and at the Goddard's Laboratory of the National Centre for Atmospheric Research (NCAR) from the late sixties to early seventies of the 20th century. The United Kingdom Meteorological Office (UKMO) and Environment Protection Agency (EPA) global models are examples of global finite-difference, meteorological, prognostic–diagnostic–data assimilation systems (Arakawa, Mintz, 1974).

Spectral models appeared approximately the same time (in the middle to late 1960s) and were actively developed by GFDL (Gordon, Stern, 1974) and at the European Centre for Medium-range Weather Forecast (ECMWF) (Bourke, 1974) that had been established in Reading (England). Spectral models are considered to be more stable and more precise from the point of view of integration in time, and they provide the possibility of choosing the exact space–time scale oscillations suitable for modelling particular phenomena (Kurihara, 1965). However, they have their limitations: choosing the exact range of the spectrum removes other scale processes and the ability to model different scale energy exchange processes.

1.2.3 Regional atmospheric models

Many problems have limited the extent to which research groups could develop global atmospheric models for modelling meteorological-environmental problems:

1. Complex numerical global models with a spatial resolution better than 110 km (about 1° of longitude at 45° latitude) require huge computer resources, although the situation is improving because of technological developments
2. The development of global models requires a global network of meteorological data that has to cover the whole Earth using a grid that is regular in space and time. This situation has been improved by using meteorological satellite data, but has not been properly resolved
3. The resolution of global models did not allow them to represent accurately regional and local scale meteorological and pollution situations that included the effects of complex terrain (Krishnamurti *et al.*, 1984).

All these problems led to the appearance of Limited Area Models (LAM): firstly, as part of a global model (as a nested grid) and then as completely independent numerical models with an unlimited number of nested grids (Pielke, 1984; Pielke *et al.,* 1992). Also, it is impossible to use nested grids in spectral global models because of the inability to stipulate boundary conditions inside such models.

The practice of using nested grids in mesoscale models to investigate more accurately the different scales of phenomena in meteorology, climatology and environment pollution started to develop very rapidly in the middle of the 1980s (Dadhia, 1993). The global meteorological community now has the possibility to install and adjust regional numerical models they can download free from the big national and international meteorological research centres. These centres have started to accumulate the results of research undertaken by local scientific groups, to use these results for additional improvement and development of regional models and for the improvement of global numerical atmospheric models for better weather prediction. Numerical regional modelling is now possible in every atmospheric research department that has basic computational resources. For example, in New Zealand five scientific centres use various versions of Mesoscale Model (MM5) (McKendry, 1989; McGill, 1987), and more than 10 institutes use some other kind of regional Weather Prediction Model (WPM), such as TAPM (The Air Pollution Model) or RAMS (Regional Atmospheric Modeling System) (Spronken-Smith *et al.,* 2004). MM5 (WRF) and RAMS are considered to be the most widespread limited area models among the international modelling community.

In the early 1990s, there were several attempts to create a Limited Area Spectral Model (LASM, Chen, *et al.*, 1996) in ECMWF, but these attempts were not supported by the world meteorological community, because of the complexity of LASM compared with finite-difference ones, and also because of heavy acoustic noise generated on the spectral model boundaries and the absence of the ability to transform spectral functions on a flat surface without serious loss of meteorological information.

1.2.4 Air quality – air pollution models

Photochemical numerical models started to develop approximately at the same time as the meteorological limited area models (Arya, 1999) as they use meteorological information from these models (especially in the Planetary Boundary Layer-PBL (Arya, 1988; Oke, 1978)) as an input for analysis of different kinds of case study. Examples include the influence of pollen on asthma increase (Pietrowicz, 2002), as well as such global problems as ozone layer migration and of its depletion in the middle stratosphere (Goldfrey, Clackson, 1998), regional tropospheric ozone concentration research (Stein *et al.*, 2000), scenarios of nuclear winter resulting from

nuclear war, and the effects of reactor accidents such as the Chernobyl catastrophe (Ackermann *et al.,* 1998). Limited area and Eulerian dispersion models play a dominant part in chemical-air pollution models (Russel, 1997). Some pollution models can be applied to the entire hemisphere (e.g. Modal Aerosol Dynamic model for Europe – MADE and the variable grid Urban Airshed Model system – UAM-V) and include a well-developed plotting, visualization and decision support system (CAMx can be used with Environment Decision Supporting System – EDSS that includes Plotting, Analysis and Visualization of the Environmental data program – PAVE).

There is also a large variety of air pollution models tuned to specific conditions to investigate a limited range of problems. The Denver Air Quality Model Version 2 (DAQM-V2) and Advanced Texas Air Quality Model (ATAQM) are good examples of such pollution models. However, most air pollution–air quality models are developed for application to study different problems anywhere in the world: CAMx, SMOKE (Sparse Matrix Operator Kernel Emission System), MAQSIP (Multiscale Air Quality Simulation Platform), CMAQ (Community Multiscale Air Quality system), EURAD (European Air Pollution Dispersion model system) (Byun, Ching, 1999; Coats, Tryanov *et al.,* 1999; Ebel, *et al.,* 1997). All of the above-mentioned models include calculations of PM_{10} and $PM_{2.5}$ as an essential part of their Chemistry Mechanism Compiler (CMC).

Usually, air pollution models receive meteorological information from limited area models (MM5 or RAMS) or from global models (EPA, ECMWF, NOGAPS – Navy Operational Global Analysis and Prediction System) (Davis *et al.*, 1998). Some chemical models have their own meteorological module and well-developed Graphic User Interface, for example TAPM vX (The Air Pollution Model Version X) described in the technical report of Hurley (2002). Also it is worth mentioning that some systems have a combination of meteorological limited (global) area models with an additional chemistry module: MM5- chemistry block, WRF-chemistry block.

1.2.5 Coupled models

Coupling of two or more numerical models has become a normal feature of the air 'circulation–pollution' modelling systems. Classical examples are nested grids in limited area models. In these cases, so-called **direct coupling** between two numerical models describing different levels of the circulation can be run in parallel, exchanging results and creating multi-scale two-way interaction during a numerical experiment.

Indirect coupling means use of output results from one numerical model for use by a second numerical model (as basic input data, additional input data, correction data and correction coefficients). In such situations, we deal with so-called one-way interaction with **postponed backward response**. **Postponed backward response** means representing the indirect influence of the results of the second numerical model on a process in the first model, with the aim of

achieving more finely tuned experimental results. There is no direct interaction between the two models, except through experimental repetition using corrected model parameters. The link created in most coupled meteorological and air pollution models is an illustration of indirect coupling.

There are many examples of coupled models in environmental research, such as MM5 – UAM, MM5–CMAQ, MM5–CAMx, RAMS–CAMx, MM5–DAQM (Byun and Ching, 1999; Kotroni, *et al.,* 1999; Michelson *et al.*, 2002) and so on (Peters-Lidard *et al.*, 2002). Depending on the aims of a particular study, the coupling methods can differ. The most consistent component of the air circulation–air pollution modelling system is the use of particular limited area meteorological models. In most cases, research groups prefer to work with MM5 or RAMS.

1.3 Research main aims

The coupled modelling system MM5–CAMx4 is used in this research for fine-scale examination of the relationship between air circulation and air pollution (basically PM_{10} and $PM_{2.5}$ from domestic, industry and transport sources) over Christchurch and its suburbs. It is used to investigate the effects of complex terrain and the ocean shoreline on temporal and spatial variations in air pollution under stagnation situations associated with clear sky nights and intensive outgoing long wave radiation.

The main aims of the thesis are:

1. To utilize and adjust the regional meteorological model MM5 v3.5.3 and MM5 v3.6.1-2;
2. To utilize CAMx (version 4.02–4.03) for more sophisticated investigation of air pollution situations than has previously been possible, especially during wintertime under conditions of strong temperature inversions
3. To debug and fine tune the coupled system MM5–CAMx4, so that it can be used to undertake a full range of experiments aimed at reproducing the development of smog nights in Christchurch
4. To run a series of test experiments using data collected during the Christchurch Air Pollution Study (CAPS2000) and during winter 2003, including comparison of CAMx4 results with observations of PM_{10}, and the effects of additional tuning of the MM5–CAMx4 system for the Christchurch situation.

1.4 Thesis structure

The thesis consists of six chapters with the first one being the introduction. The second chapter provides a theoretical background of limited area atmospheric and chemical models, and describes their possibilities and limitations. A discussion covers basic test problems of regional meteorological and chemical modelling, and the principles and effectiveness of coupling atmospheric circulation and air pollution models (e.g. MM5–CAMx4).

Chapter 3 goes on to outline different kinds of atmospheric circulation and air pollution regimes over the Christchurch region and its vicinity for the winter season.

Chapter 4, being the biggest of the thesis, firstly describes the structure (dynamical, physical, chemical and program) of the Mesoscale Model 5 (MM5) and the Comprehensive Air quality Model version 4 (CAMx4). Visualisation facilities of each model are also discussed in this chapter. Chapter 4 outlines the methodology and settings of MM5 and CAMx, which are used for fine adjustment to reproduce the air circulation over the complex terrain of the Christchurch area. In the second part, Chapter 4 includes description of the input data available for meteorological and chemical models, and description of the observed data (Christchurch Air Pollution Study 2000–CAPS2000, and winter 2003 measurements) available for comparison with model output. It also discusses the methods of optimal MM5–CAMx4 coupling for more realistic modelling, and the possibilities of a quasi-operational regime for the MM5–CAMx4 system. The third part of Chapter 4 introduces the results of MM5 modelling over the Christchurch area during winters 2000 and 2003, with discussion of the problems of regional modelling using global analysis data for MM5 input at different levels of resolution (nesting). Possibilities and constraints of MM5 modelling of the Christchurch region wintertime air circulation are discussed as well. The fourth part of the Chapter 4 includes analysis of the creation of high quality input information for CAMx4, and the problems of chemistry modelling over the Christchurch region and surrounding small towns.

The fifth chapter shows the results of the particulate matter (PM_{10}) dispersion studies during winter cold nights, using the MM5–CAMx4 coupled numerical system and compares the model output with the observations. Observations made by Environment Canterbury (Ecan) at Coles Place (St. Albans, Christchurch) and two additional sites, during the CAPS2000 (winter 2000) and winter 2003 periods were used as the main sources of near-surface air pollution data to compare with the output of the MM5–CAMx4 modelling system. The results of the comparison for winter 2000 and winter 2003 are described in two parts of Chapter 5.

Chapter 6 re-examines the research objectives, and summarises the main findings, implications of the thesis research, and suggestions for future research.

1.5 Summary

This chapter has introduced the thesis by outlining the rationale and the main research aims, as well as the temporal and spatial scale of the research. It has discussed the essential importance of the work for Christchurch and its surroundings due to the health problems associated with cold winter nights when very high concentrations of PM can accumulate. This work aims to show how a complex numerical modelling system can be used to predict approximate levels of PM concentration over the Christchurch region during extremely polluted winter nights.

Chapter 2

Theoretical background

2.1 Introduction

The main aim of this chapter is to elucidate the theoretical and practical background of numerical modelling in meteorology and air pollution chemistry. It also describes different ways of coupling meteorological and chemical models, including advantages and limitations of such procedures. The first part of the chapter introduces the main aspects of limited area meteorological and air pollution models, and their application as research tools. The second part describes the basic features of MM5 and CAMx, and of the application this numerical modelling system for sophisticated research into the problem of air pollution dispersion under conditions conducive to poor air quality.

2.2 Meteorological modelling

2.2.1 Theoretical and practical background of limited area models

The theoretical background of limited area meteorological models is considered here in terms of the general equations of geophysical fluid dynamics applied to atmosphere and ocean (Gill, 1982). There are the basic analytical equations starting with the equation of mass continuity

$$\rho^{-1} D\rho/Dt + \nabla \cdot u = 0 \qquad (2.1)$$

where ρ is air density, u is a wind vector, D/Dt is a total derivative, ∇ is the Laplacian, This also includes the general equation of motion (Lighthill, 1966):

$$Du/Dt + 2\Omega x\, u = -\rho^{-1} \nabla p - g + \upsilon \nabla^2 u \qquad (2.2)$$

where Ω is the rotational speed of the Earth, $2\Omega x$ is the Coriolis force, p is air pressure, g is acceleration due to gravity, $\upsilon = \mu/\rho$, or the coefficient of kinematic viscosity, and μ is dynamic viscosity.

The thermodynamics or energy equation is

$$\rho T c_p(p_r, \theta)\, \theta^{-1} D\theta/Dt = \nabla \cdot (k \nabla T - F^{rad.}) + Q_H \qquad (2.3),$$

where T is air temperature, θ is potential temperature of air, c_p is specific heat at constant pressure, k is thermal conductivity, and heating function Q_H is derived from the equation of radiation comprising F^{rad} and T as a function of ρ, s (humidity) and θ (Morse, 1964). With s as a humidity variable, we add to the system of equations (2.1 – 2.3) the equation of humidity:

$$\rho \, Ds / Dt = \nabla \bullet (\rho \, \chi_D \, \nabla s) \qquad (2.4)$$

where χ_D is a water vapor diffusion coefficient, and the condition equation is

$$\rho = \rho (p, s, \theta) \qquad (2.5)$$

The last equation can be combined with the equation of mass continuity (2.1), depending on variables used to describe system conditions. If using variables p, s and θ, as in equation 2.5, then the derivative of the density in equation (2.1) can be expressed as:

$$1/\rho \, D\rho/Dt = 1/\rho \, \partial\rho/\partial p \, Dp/Dt + 1/\rho \, \partial\rho/\partial s \, Ds/Dt + 1/\rho \, \partial\rho/\partial \theta \, D\theta/Dt \qquad (2.6)$$

where during calculation of every primary derivative, two other variables are considered to be constant.

The most interesting primary case is when the movement is isentropic, with absence of effects of viscosity and diffusion. In such cases, the equations (2.3) and (2.4) transform to

$$D\theta / Dt = 0 \qquad (2.7)$$

$$Ds / Dt = 0 \qquad (2.8)$$

The equation of mass continuity (2.4) does not change, but if it is applied to equations (2.6 – 2.8) it can be rewritten in the following form

$$(\rho \, c_s^2)^{-1} \, Dp/Dt + \nabla \bullet u = 0 \qquad (2.9)$$

where c_s is the speed of sound, and the general equation of motion (equation 2.2) is rewritten in the form (Pedlosky, 1979):

$$Du/Dt + 2\Omega \, x \, u = -\rho^{-1} \, \nabla p - g \qquad (2.10)$$

To the above system of primitive theoretical equations describing the atmosphere should be added top and bottom boundary conditions for an ideal fluid without diffusion, or for a viscous fluid with or without diffusion (free atmosphere / boundary layers).

Practical application of limited area meteorological models requires consideration of:

1. Global Data Analysis System (GDAS) development
2. Global data assimilation (with application of global atmospheric models) and global data redistribution among research centres all over the world
3. Additional regional to local meteorological data collection and use through Four Dimensional Data Assimilation (FDDA) procedures
4. Possibilities of creating local databases resulting from regional experiments (like the Christchurch Air Pollution Experiment, conducted during winter 2000 – CAPS2000) so, that the information in these databases can be compared with the output meteorology of limited area models for fine tuning of regional models to local air circulation.

To the above list could be added the availability and level of computer and human resources that can support regional numerical modelling tasks. The intellectual expertise required

to undertake research in this area has to be built up over relatively long periods of time, often involving establishment of specialist research groups.

2.2.2 *Basic limited area models: MM5, RAMS, WRF*

MM5 and Regional Atmospheric Modelling System (RAMS) are the most widespread limited area models that are used in more than 80 countries and in hundreds of different research divisions and departments.

Mesoscale Model–MM was developed by Pennsylvania State University (PSU) and the National Centre for Atmospheric Research (NCAR) Mesoscale and Microscale Meteorology division (MMM) from 1978 and by the University Corporation for Atmospheric Research (UCAR) since 1986 (Grell *et al.*, 1994). It is developed on a multi-platform principle (it can be run on such platforms as Compaq, IBM, SGI, Sun, and PC Linux) and has the option of multi-nesting (stationary, moving and overlapping) as an essential feature of the model. The first complete release of this model appeared in the USA in 1988 (MM2) and contained not only a dynamical part, but also physical and surface-orographic sections. The ability to assimilate 2-dimensional and 3-dimensional data from global databases and local observations was installed in MM version 3 (Grell *et al.,* 1994). The model is the most popular and is run in more than 60 countries and in more than 250 officially registered research institutes and divisions. MM5 is also available as a multi-parallel version, mainly for PC Linux.

The most recent versions of MM (MM5 V.3.5.4-5 and MM5 V.3.6.1-2) were released in October–December 2002 and May–August 2003. The latest versions include all the improvements that have been created during the more than 20-year history of model use. MM5 is considered to be a prognostic model with sufficient spatial resolution to undertake research into the development of miscroscale eddy fluxes up to studies of hemispherical energy redistribution from the tropics toward the poles. It is mostly used for multi-purpose prognostic or basic research simulations from mesoscale up to hemispherical applications. A special Antarctic Mesoscale Prediction System (AMPS) was based on MM5 and four dimensional data assimilation to undertake research on the influence of the Antarctic continent on the weather and climate of the Southern Hemisphere, as well as the reverse influence of the Southern Hemisphere air circulation in the upper troposphere and stratosphere on the seasonal and annual migration processes affecting the Antarctic ozone layer. A more detailed description of the latest versions of MM5 will be given later in this chapter (Dudhia, 2002).

Regional Atmospheric Modelling System (RAMS), developed by Colorado State University and Meteorological Research Centre (MRC), is a multipurpose, multi-nested numerical prediction model (Pielke *et al.*, 1992) that simulates atmospheric circulations ranging

in scale from an entire hemisphere down to Large Eddy Simulations (LES) within the planetary boundary layer. It is most frequently used to simulate mesoscale atmospheric phenomena in applications from operational weather forecasting to air pollution dispersion. RAMS is used nowadays in more than 150 officially registered research divisions in more than 40 different countries. Initially, RAMS was run exclusively on the NCAR CRAY–1 machine and later the program code was rewritten to make RAMS a multi-platform model. The first version of the 'new' RAMS was released in 1988 as version 0a, and the first widely distributed version, version 2c, was released in 1991. The current version of RAMS that is released to the general RAMS community is version 4.4, which includes modification for distributed-memory parallel computer platforms.

The Weather Research and Forecasting (WRF) model was developed in 1992 to become the replacement for the MM5 model. It is now released as a beta version for 'friendly' users, offering an opportunity for wide involvement in its development. The WRF model is not yet considered a 'research quality' model, but as a prototype until future improvements allow it to be considered a fully-fledged model. WRF includes two dynamic cores, height and mass ones, and can be run with either idealized initialization or real-data initialization (Klemp *et al.,* 2000). The time-dependent (modelled) fields consist of 3-dimensional wind, potential temperature, water vapor and a number of 2-dimensional fields. The standard output is in netCDF format, the model is written in standard free formatted Fortran 90 with shared memory parallelism (open MP) and with MPI-C compilers for multi-platform purposes. In WRF, the following features are used: fully compressible non-hydrostatic primitive equations, Coriolis and curvature terms for a single domain or multiple domains (nested grids), and a height-based terrain following (zeta) coordinate system for height version or a mass-based terrain following (eta) coordinate system for the mass (Klemp *et al.,* 2000) version of WRF. The future development of WRF (including nesting and data assimilation) will mainly be based on the mass model, as the future 'official' WRF model (Klemp *et al.,* 2000).

2.2.3 Potential of limited area modelling

The potential of the limited area models includes ideal and real simulation of atmospheric circulations ranging in scale from an entire hemisphere down to eddy flux simulations of the planetary boundary layer. Most frequently, limited area modelling is used to simulate atmospheric phenomena at the mesoscale level (horizontal scales from 2000 km to 2 km – Otte and Loscer, 2001) for applications from operational weather forecasting to air quality dispersion, and in fundamental research. Limited area models are also successfully used at much higher resolutions to simulate boundary layer near-surface fine scale processes (boundary layer eddies

with 10–100 m grid spacing), individual building simulation (1 m grid spacing) or direct wind tunnel simulations (1 cm grid spacing).

Such limited area models as RAMS and MM5 were developed to undertake research in modelling physiographically-driven weather systems and simulation of convective clouds, mesoscale systems, cirrus clouds, precipitation weather systems in general and extreme precipitation events (Someshwar *et al.,* 2002). Limited area modelling is also a basic numerical tool in teleconnection research (Krichak *et al.*, 2002), in back- and forward trajectory numerical methods (Sturman and Zawar-Reza, 2001), and in investigation of many other atmospheric phenomena.

Mostly, the resolution of limited area modelling depends on the scale at which data observations are available (for realistic simulations), the availability of computer resources, and the skills of the research group involved.

2.3 Numerical modelling of air pollution

2.3.1 Air pollution chemical models

Chemical models of various types play an increasingly important role in air quality management in most developed, and in some developing, countries (like Brazil, Mexico and Russia). Air pollution composition in the urban environment is very complex, both spatially and temporally. Initially, air pollution models that have provided the most useful empirical tools for prediction of air pollution concentrations in a variety of situations were the products of the standard statistical approaches involving linear and non-linear regression, correlation methods with a number of input parameters, and various time-series techniques. Baldasano *et al.* (1998) applied principal components analysis and the multiple linear regression method to a receptor modelling study in Spain with the aim identifying potential sources of volatile organic components (VOC). A number of new artificial intelligence techniques have also been applied in air pollution meteorology and climatology (Gardner and Dorling, 1998; 1999), including the application of neural networks to model non-linear relationships.

For many years, so-called Gaussian-based grid or box models were used in pollution research studies to predict the impact of particulate emission sources on a change of air pollution concentrations over time. But these models had significant limitations that have been discussed in many studies. 'Haggkvist (1997) evaluated the possibility of Gaussian grid-based (box) models to create reliable pollutants distribution in time and found that the accuracy of the pollution forecast varied greatly with the mean difference from observations up to 50–60 % depending on input data assimilation and a complexity of a case study' (Sturman, 2000, p. 132). Including turbulence structure in these models, de Haan and Rotach (1998) attempted to improve

the representation and reliability of near-surface 3-dimensional structure in more advanced multi-source Gaussian dispersion models. A complex Gaussian dispersion model has been used to predict long-term annual and monthly average concentrations of a number of pollutants using a limited area centred on London (Seika *et al.,* 1998). However, the more meteorologically realistic three-dimensional mesoscale airflow models have tended to dominate in the field of air pollution dispersion.

Three-dimensional prognostic pollution chemistry models have been developed with the growth of three-dimensional prognostic, mesoscale meteorological models. Limited area meteorological models are now commonly used to provide meteorological fields with the purpose of estimating the urban air pollution, especially over complex terrain dominated by local air circulations (Souto *et al.,* 1998). A whole generation of chemical models was developed at the same time as the growth of mesoscale models in atmosphere numerical prediction centres of the USA and Europe. Three-dimensional Lagrangian particle models and Eulerian pollution models were developed and used in parallel (Kotroni *et al.,* 1999). However, although some recent dispersion models use a Lagrangian particle model to reproduce air pollutant emission, transport and redistribution in time, it was suggested (de Haan and Rotach, 1998) that the integration of a Gaussian emission-based (gridded or source emission) 3-dimensional prognostic meteorologically based model with a stochastic Lagrangian particle module provides a good compromise in reproducing more closely the observed air pollution patterns. A large amount of research was conducted in Europe to improve urban-scale air pollution dispersion models, that first of all concerned such models as Urban Air-shed Model with Variable grid–UAM-V, EURopean Air pollution Dispersion model system–EURAD, and Modal Aerosol Dynamic model for Europe–MADE (Arya, 1999; ENVIRON, 2002).

It should be stressed that modern 3-dimensional air pollution models with different kinds of Chemistry Mechanisms (CM) and Chemistry Mechanism Compilers (CMC) are becoming increasingly complex, often consisting of several modular components simulating emission sources, atmospheric boundary layer processes, upper troposphere–lower stratosphere processes, and a complex representation of different kinds of primary and secondary chemical reactions. For example, a 3-dimensional Eulerian Comprehensive Air quality Model with extensions – CAMx (ENVIRON, 2002), designed for the urban environment and ozone studies by ENVIRON (an environment protection agency in the USA) includes 56 chemical species and 175 primary reactions for Carbon Bond Mechanism 5 (CBM5–SAPRC 99); while the model described by Jaeckervoirol et al (1998) includes 83 chemical species and 191 reactions. Therefore, complex models are able to compute the chemical reactions of various species in space and time as they are transported by the wind, diffused by turbulence and affected by precipitation (dry and wet

deposition). Community Multi-scale Air Quality model (CMAQ) and Multi-scale Air Quality Simulation Platform (MAQSIP) serve as examples of such complex models.

In Europe, there have also been attempts made to incorporate effects of aerosols and their processes of dispersion (i.e. coagulation and condensation) and movement (transport and deposition) in 3-dimensional long-range dispersion models (Ackermann *et al.,* 1998). 'A rather unusual application of operational air quality models to extreme conditions was made by Godfrey and Clarkson (1998), who applied the diagnostic model CALMET (CALifornia METeorology) and puff-dispersion model CALPUFF (CALifornia PUFF dispersion) to simulate extreme-case situations for emission of air pollution from two source emission points at Scott Base, Ross Island, and Antarctica' (Sturman, 2000, p. 134).

It is evident that several different modelling approaches are being explored today. They include different model types that consist of empirical, statistical, neural network, Gaussian, Lagrangian, physical/numerical/chemical and Geographic Information System (GIS) model components and models. Improvements in research and development in computer technology have moved air pollution modelling towards more complex hybrid models, often based around mesoscale airflow models, including atmospheric dispersion modules and a range of chemical processes.

2.3.2 Applications of basic chemistry models

All the models described in Section 2.3.1 are being applied to the range of scales from local to inter-regional and almost hemispherical, from individual street canyons and tunnel portals to pollution redistribution calculations of long-range transport between different continents. The role of air pollution models in the life of any society has been discussed up to now, but the recognition of the significance of chemical modelling for environmental and human life is increasing in developed countries. For instance, 'Cirillo *et al.* in 1997 have reviewed the debate over the function of regulatory models in new European directives on air quality' (Sturman, 2000). They suggested that acceptance of chemical models requires elimination of prejudices against models and emphasized the complementary role of models with monitoring networks as essential tools for air quality management. The main applications of air quality models appear to be in satisfying regulation requirements and for general assessments of air pollution problems.

Observational meteorological and pollution studies provide an indispensable background for air chemical modelling, by contributing to improvements in the understanding of air pollution dispersion and the role of atmosphere circulation in this complex artificially induced air deterioration. For instance, St. John and Chameides (1997) have undertaken analysis of high

ozone incidences and their dependence on meteorological conditions in Atlanta. 'Multi-day severe pollution episodes were found to be the result of plume recirculation by local wind systems during stagnant anticyclonic situations' (Sturman, 2000, p. 130). They classified 11 mesoscale airflow patterns over the area with seven pollution categories based on a range of different gaseous pollutants, including volatile non-organic components (VNOC). They identified clear relationships between wind speed and direction and pollution, with the highest concentrations of ozone, nitrogen dioxide and sulphur dioxide during warm weather with sea breeze development occurrence.

Applications of different kinds of statistical techniques used to forecast daily maximum ozone concentration for Athens were compared by Chaloulakau *et al.* (1999). In their work, 'three multiple regression models and one time-series regression model were described that provided prediction of the maximum daily one-hour mean ozone concentration based on several years of observation data' (Sturman, 2000, p 131). The most reliable was considered to be a regression model with six independent input variables (predictants), including mean wind speed and direction and near-surface temperature profiles. 'Clai *et al.* in 1998 provided an example of the application of statistical models to the prediction of CO, SO_2 and NO_2 concentrations in the Bologna region, and found quite a clear weekly cycle in the pollutants and reasonable predictability for a few days ahead' (Sturman, 2000, p 130).

In application of multiple linear regression to a study of VOC in Spain, Baldasano *et al.* (1998) were able to identify vehicle traffic as the main source of air pollution. In the study, the authors were able to identify (relying on principal components analysis) that wind direction affected the dispersion and redistribution of VOC in different ways, and helped to identify more closely the role of individual sources of emission. 'Davis with collaborators applied a cluster analysis technique to a study of the influence of meteorological near-surface conditions on ozone in Houston' (Sturman, 2000, p 131) and managed to categorize seven distinct meteorological regimes associated with different patterns of daily one-hour mean maximum concentration of ozone (using 12 years of data observations).

The application of neural networks and expert systems involves, as an essential part of research, the training of models using previous observation data or formerly produced results with application of models to more recent input data as a next step of research – the training process. Gardner and Dorling (1998; 1999) emphasized the ability of neural networks to model non-linear relationships between boundary layer meteorology and air pollutants. That seems to be a natural conclusion, as the theory of neural networks had been created to research highly organized stochastic conduction/perception processes of the central nervous system and had been based initially on the theory of random processes (e.g. the Monte-Carlo method). 'The models of

Gardner and Dorling were able to predict the normal range of nitrogen oxide concentrations, but failed to predict extreme values during severe smog nights in London' (Sturman, 2000, p 131), which could be easily explained by the basic theory of neural processes that had been created to research stochastic processes without a distinctive time trend. However, the comparison of neural networks, applied to short and medium-term prediction of air pollutant concentrations, with regression-based techniques has shown a significant improvement in prediction (Nunnari *et al.,* 1998).

Grid or box and Gaussian-based modelling have been applied in air pollution studies for many years. For instance, there was an attempt to use a Gaussian model (Seika *et al.,* 1998) that included modules of point and area sources and components representing a range of atmospheric and chemical processes. As a result, monthly averaged levels of NO_x concentrations were predicted with a high level of accuracy, while the results of modelling for shorter time periods were unsuccessful.

Three-dimensional, prognostic, limited area meteorological models have a lot of advantages over the earlier models described, especially from the point of view of representing important pollution prediction factors such as very complex terrain and the complex distribution and redistribution of gridded and point emission sources in space and time. Numerical mesoscale models, firstly predict the wind fields and then the predicted wind, temperature and humidity fields are used to drive an air pollution or particle dispersion model to estimate the dispersion of air pollutants from different kinds of source (Finardi *et al.,* 1997; Hernandez, *et al.,* 1997). These numerical chemistry models are usually based on a Gaussian puff module (like Comprehensive Air quality Model–CAMx4), but can also include an additional Lagrangian particle module. The integration of airflow and particle transport models has been applied to environmental situations dominated by both topographic and thermally induced local air circulations (Lamprecht and Berlowitz, 1998). 'An analysis of the effects of thermally induced wind systems on air pollution transport near Sao Paulo showed the combined effect of topography and the land-sea interface (strong onshore and upslope–downslope flows) on local air pollution dispersion (Bischoff-Gauss *et al.,* 1998)' (Sturman, 2000, p 132). Cox *et al.* (1998) developed a modelling scheme for use in providing short-term (1–4 hour) predictions for accidental release of hazardous materials. This approach requires good real-time weather data at a high resolution (resolution depends on the local scale of the hazardous process and surroundings) to produce useful results.

Some new studies have applied 3-dimensional pollution models to much longer-range pollutant transport than city-scale pollution dispersion (Jaeckervoirol *et al.,* 1998). 'Kallos *et al.* (1998) applied a combined wind-field and Lagrangian particle dispersion model to study of the transport of pollutants from Europe to North Africa' (Sturman, 2000, p 133). As emitted

pollutants undergo a range of chemical reactions resulting in the production of secondary volatile organic components (SVOC), a significant amount of research work has been devoted to trying to incorporate important chemical processes into air pollution dispersion models (Russell, 1997). Bergin *et al.* (1998) have illustrated the importance of getting correct parameterisations of chemical reactions into applied dispersion models and stressed the significant variation in the sensitivity of the predictions from chemical models to different chemical processes. Chemical composition and particle size distribution have become important factors during consideration of interactions between aerosol and gas phases. Ackermann *et al.* (1998) successfully coupled an aerosol model with an atmospheric dispersion model and applied it to Western Europe. Although the general patterns were realistic, insufficient input field data seriously reduced the quality of the final research results.

The intercomparison of models from 24 different institutions and sensitivity analyses (Brandt *et al.,* 1998) suggests that predictions depend significantly on high-resolution good-quality meteorological data. Significant discrepancies in the results suggest that there is still a lot of work to be done (especially in parameterisation of convection and turbulence schemes) before atmospheric dispersion models will be satisfactorily reliable for real-time forecasting (especially of Chernobyl-type accidents).

Specialized applications of air pollution dispersion models include (after Sturman, 2000):

1. Development of a technique for identifying individual street canyons that are worse affected by vehicular pollution (Buckland and Middleton, 1999)
2. Prediction of potential forest fires and their spread in conditions of complex orography and local air circulation (Miranda and Borrego, 1996)
3. Transport of material from instantaneous explosions or continuous source emissions (Makviadze, 1995).

Geographic Information System (GIS)–based pollution dispersion models allow the interactions between spatial fields of such variables as land use, population distribution and economic activity, meteorological parameters, vegetation and surface roughness to be evaluated with regard to their influence on ambient air pollution concentrations. Beyea and Hatch (1999) showed how this approach could be used to define areas of potentially high exposure to air pollution.

2.3.3 Numerical model evaluation

It is obvious that the study of the air pollution problem is an active topic in applied numerical meteorology. Several special collections of contributions on the air pollution problem have been published and the majority of the works are dedicated to air pollution modelling in

one form or another (Sturman, 2000), or descriptive analysis of air quality deterioration problems in a range of different environments. This research illustrates the complex interactions between the atmosphere, topography and resulting quality of air for defined regions.

Understanding mesoscale and miscroscale controls on local airflow and atmospheric boundary layer structure is a principal step in studying a particular air pollution problem. For instance, the problems created by recirculation of local wind systems and near-surface air pollution redistribution because of the stagnation and local circulation over complex orographic areas is now well known, and dominates in a number of numerical chemical studies using 3-dimensional dispersion models. Air quality prediction models can mostly reproduce accurately these processes and provide hope for realistic forecasts of air pollution concentrations in the nearest future (Arya, 1988; 1999).

In any way, 'it is evident that several different modelling approaches will be explored in future, including empirical–descriptive methods such as statistical regression modelling, and neural network approaches, Gaussian–Lagrangian physical and 3-dimensional numerical modelling and GIS modelling' (Sturman, 2000, p.134).

Improvements in knowledge and rapid developments of computer technology make a move in air pollution research towards more complex hybrid numerical models. Complex chemical hybrid models, often based around mesoscale limited area meteorological models, include very complex atmospheric dispersion modules and incorporate a large number of input chemical species and a large range of primary and secondary chemical reactions of gases and pollutants.

2.4 Coupling of limited area models for predicting air quality

2.4.1 Types of coupled meteorology-chemistry models

The most popular type of coupled meteorology–chemistry model includes global or regional (limited area) numerical atmospheric models as an independent first step and some kind of prototype chemical/numerical (mostly Eulerian) model, which is dependent on the meteorological model output fields. Examples of such coupled systems include MM5–Comprehensive Air quality Model version x (CAMx), MM5–Modal Aerosol Dynamical model for Europe (MADE), MM5–Community Multi-scale Air Quality model (CMAQ), MM5–Variable grid Urban Airshed Model with extensions (V-UAM), MM5–Advanced Texas Air Quality Model (ATAQM), MM5–TOPOMODEL-based Land Atmosphere Transfer Scheme (TOPLAST) (Peters-Lidard *et al.,* 2001), MM5–Sparse Matrix Operation Kernel Emission system (SMOKE), MM5–EURopean Air pollution Dispersion model (EURAD), MM5–Multiscale Air Quality Simulation Platform (MAQSIP), Regional Atmospheric modelling

System (RAMS)–Multi-component Aerosol Dynamics Modelling–Model Approach System version X (MADMAS X), RAMS – Regional Atmospheric Chemistry Mechanism model (RACM) and RAMS – Alpine Hydrochemical Model (AHM). To this group can be added such meteorological model amalgamations as MM5 – chemistry block (MM5–meteo) and Weather Research and Forecasting system (WRF) – chemistry block (WRF–meteo).

There are also so-called joint meteorological–air quality modelling systems, which include such models as The Air Pollution Model (TAPM) of the Commonwealth Scientific and Industrial Research Organisation (CSIRO, Australia) described by Hurley (2002), and CALPUFF (created initially by CALifornia Air Resources Board–CARB) described by Allwine *et al.* (1998). The first one includes in one numerical–graphical user interface (GUI) the ability to simulate air pollution episodes with meteorology calculated in another part of the same model. CALPUFF is an advanced non-steady-state meteorological and air quality modelling system that consists of three main components with a GUI and a set of meteorological conditions: CALMET (a diagnostic 3-dimensional meteorological model), CALPUFF (an air quality dispersion model) and CALPOST (a postprocessing statistical–plotting package). As mentioned in Chapter 1, this diagnostic model had been used for global scale tracing of long term dispersion of a particular chemical species.

2.4.2 Main limited area model applications

Regional and local meteorological-air quality models have become important tools for environmental research, application to environmental assessment and assessing possible impacts of different kinds of air pollution. For any air pollution study it is important to use highly developed limited area meteorological models as a basic tool in a coupled meteorology–air pollution system. On one hand, it is important to use air quality models as a research tool to understand the simulations carried out with them, and on the other, properly evaluated highly improved models should be used to forecast atmospheric pollutants in an operational or quasi-operational state. Recently, these two tasks have been explored together for more efficient realization of modelling system potential. A few examples of optimised use of coupled limited area models are now described.

In Texas, evaluation of real-time forecasts from weather–chemistry forecasting system and meteorological observations taken during Texas Air Quality Study 2000 (TAQS2000) were used in the forecast of a real-time coupled numerical model by comparing the model output results with data sets from NCAR's Electra aircraft, wind profiles and rawinsondes (Michelson *et al.*, 2002). The coupled weather–chemistry forecasting model combined a modified version of MM5 and the chemical mechanism of the Regional Acid Deposition Model (RADM) version 2 (Grell

et al., 2002). The transport of chemical species was treated simultaneously with meteorology and photolysis, with biogenic emissions and deposition also calculated 'online'. The model system was run on multiple 1-way nested grids of 60, 15, 5 and 1.67 km spatial resolutions. The 60-km grid was initialised using the Forecast System Laboratory/Rapid Update Cycle (FSL/RUC) analyses and the boundary conditions were provided by NCEP's ETA model forecasts. The chemical fields were initialised with the previous forecast to take into account the effect of pollutant accumulation. The emission inventory was compiled with databases from EPA and TNRCC (Texas Natural Resource Conservation Commission) (Bao *et al.,* 2002).

Since summer 2001, a real-time forecast system based on the EURAD chemistry model was tested and established in Germany to predict the main atmospheric pollutants on different scales in Europe. The EURAD forecasting system consists mainly of the mesoscale meteorological model MM5, the emission processor EEM (EURAD Emission Model) and the EURAD Chemistry Transport Model (EURAD–CTM). The initial and boundary data for MM5 were obtained from the global AVN forecast (NCEP) at the start of every day forecast cycle (0000 UTC). The emissions data were interpolated from the EMEP (Cooperative Program for Monitoring and Evaluation of the Long-range Transmission of Air Pollutants in Europe) database in time and space for 3 different regions (MM5 domains): for a Europe grid with grid size 125 km, for Central Europe with grid size 25 km, and for one of the German states with 5 km grid size. In this case, MM5 is used separately without nested grids for each grid, but the coarse grid is used as a first-guess field for finer grids. The system starts automatically with the download of the AVN global meteorological forecast and initialisation of boundary conditions of MM5 for the coarse domain to predict the meteorology 48 hours ahead. After this, together with the emissions data for the selected time and region of the Europe domain, the EURAD–CTM predicts the concentrations of the atmospheric constituents. Then, the forecast of the coarse grid is used as initial data for finer grids. In addition, a special aerosol option of the EURAD–CTM is applied for the chemistry transport calculations (Otte, 2001).

In research conducted by the Texas Natural Resources Conservation Commission (TNRCC) the Advanced Texas Air Quality Model (ATAQM Phase II) has been implemented to support simulations of the August 1998 ozone episode in the Houston-Galveston area. ATAQM consists of MM5 version 3 (MM5v3); the TOPMODEL-based Land Atmosphere Transfer Scheme (TOPLATS, Peters-Lidard *et al.,* 2002); land-surface hydrology model and a Sea-Surface Atmosphere Transfer Scheme (SSATS). The TOPLATS model is driven with both in situ and remotely sensed estimates of key meteorological variables, including solar radiation and precipitation, and the SSATS is driven with observed sea surface temperature (SST) data.

2.4.3 *Level of precision of the model systems*

The level of precision of coupled limited area atmospheric–air pollution models is very difficult to assess and, first of all is much more difficult to obtain, as the quality level of research/forecast results is created not only inside one model, but also between different models of one modelling system.

With all kinds of improvements in modelling systems it is now possible not only to develop a very complex numerical system, but to predict concentrations of atmospheric pollutants every day within a sufficient time range and with quite high forecast reliability (in the range of 70–85 % consistency) depending on the input data, spatial resolution of the grid, and complexity of the region. It is very important to have good quality input data for gaseous and particulate matter compounds of the main air pollutants to be able to maintain a relatively good agreement between observed and predicted data (up to 90%). Level of reliability also depends on the type of species predicted. The level of reliability is higher for aerosol forecasts than for gases, and for inert gases it is higher than for active and unstable gases (like O_3). The mean level of predictability of research models is higher than for forecast applications of numerical air pollution systems, but there is a tendency toward equalizing the levels of reliability of the two modelling time regimes (Peters-Lidard *et al.*, 2002; Stein *et al.*, 2000).

2.5 *Mesoscale Model, 5th generation*

2.5.1 *Dynamical scheme*

In terms of terrain following coordinates (x, y, σ) the basic primitive equations for the non-hydrostatic MM5 basic variables (excluding moisture) are the pressure and momentum prognostic equations, and the diagnostic equation of thermodynamics (Holton, 1992; Dudhia *et al.,* 2000). It is important to mention that prognostic equations also exist for water vapour and microphysical variables, such as cloud and precipitation (if used). These equations include the advection and various source/sink terms.

The modelling system usually gets and analyses its data on pressure surfaces, but they have to be interpolated to the model's vertical coordinates before being input into MM5. The vertical terrain following coordinate system means that the lower grid levels follow the terrain while the upper level is flat. Intermediate levels are progressively flattened as the pressure decreases toward the fixed (chosen) top pressure level. A dimensionless quantity σ is used to define MM5 levels, where:

$$\sigma = (p - p_t) / (p_s - p_t), \qquad (2.5.1)$$

and p is the pressure, p_t is a specified constant top pressure and p_s is the surface pressure.

The model vertical resolution is therefore defined by a list of values between zero and one that do not necessarily have to be evenly spaced. In cases of complex terrain and research into near-surface local processes the resolution in the boundary layer is much finer than above; the number of levels may vary unlimitedly, but in most case studies lies in the range of 20–45 full σ levels (Figure2.1).

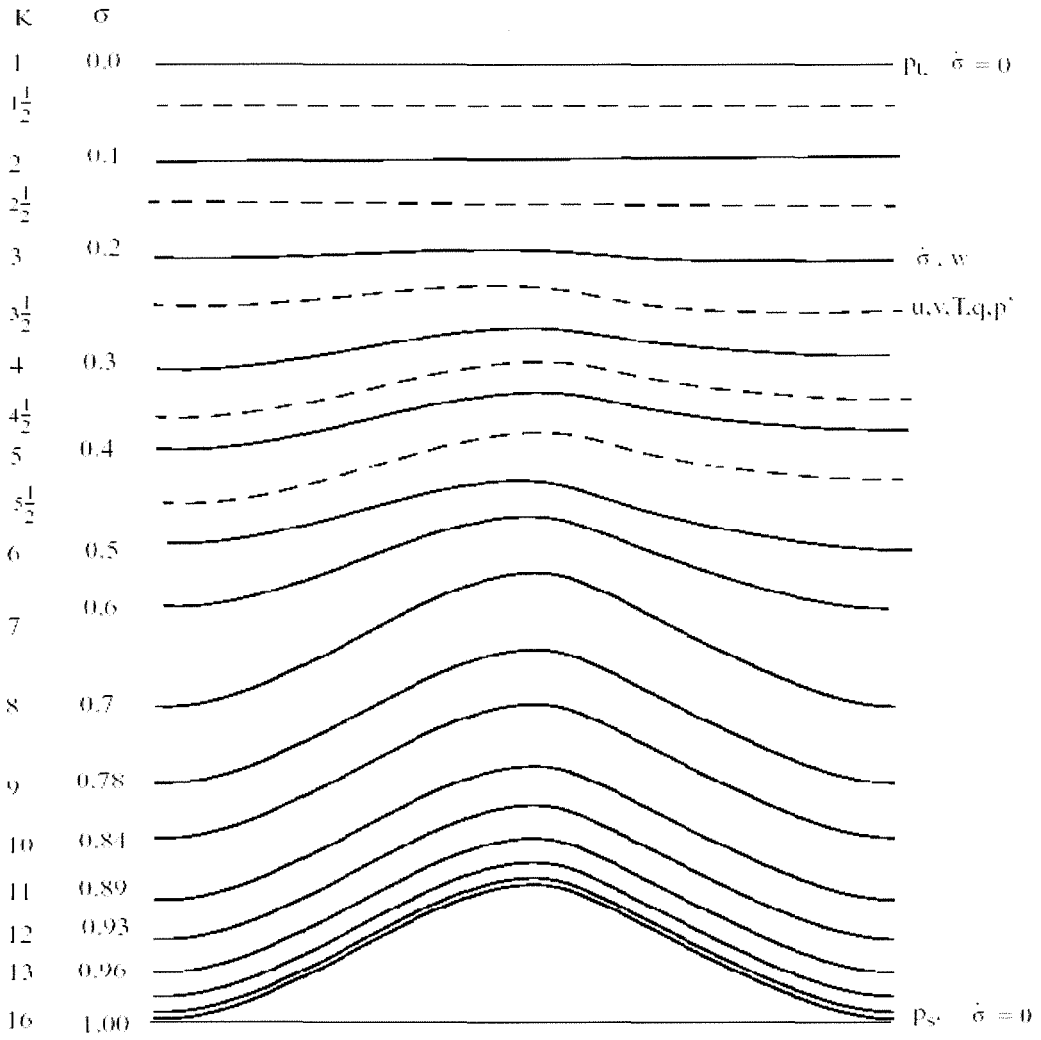

Figure 2.1 Schematic representation of the vertical structure of MM5. The example is for 15 vertical layers. Dashed lines denote half-sigma levels and solid lines denote full-sigma levels (after MM5 Modelling System Version 3–user's guide).

The horizontal grid has an Arakawa-Lamb (Arakawa and Lamb, 1977) B-staggering of the velocity variables with respect to the scalar: the scalars (T, q, etc.) are defined at the centre of the grid square, while the velocity components are collocated at the corners (Figure 2.2). From the picture it is seen that horizontal velocity is defined at dot points and scalar variables are defined at cross points.

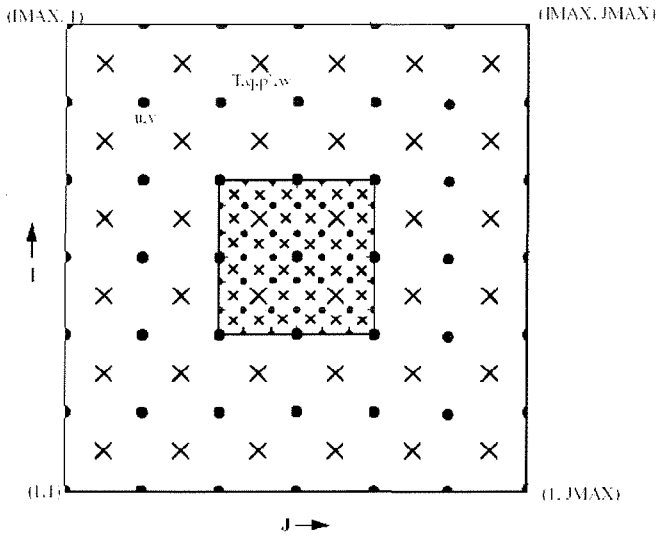

Figure 2.2 Schematic representation of the horizontal Arakawa-Lamb B-grid staggering of the dot and cross grid points. The nested domain is a representative grid staggering for a 3:1 coarse grid distance to fine-grid distance ratio (after MM5 Modelling System Version 3–user's guide).

All scalars and vector wind are defined in the middle of each model vertical level referred to as half-sigma levels and represented by the dashed lines in Figure 2.1. Vertical velocity is calculated at the full sigma levels (solid line in Figure 2.1). As the full sigma levels range from 1 to 0, the total number of MM5 layers is always one less than the number of full-sigma levels.

Second-order centred finite differences scheme represents the spatial gradients of prognostic equations except for the precipitation term, which uses a first-order upstream scheme for positive definiteness (Grell *et al.,* 1994). A second-order leapfrog time-step scheme is used for the equations described above, but some terms are handled using a time-splitting scheme of Martchuk (Pedlosky, 1979). Shorter time steps are applied for so-called fast terms that are responsible for sound waves, using the same second order precision. When a time step is split, certain variables and tendencies are updated more frequently, such as sound waves when u, v, w and p' all need to be updated each short step using the tendency terms. For diffusion and microphysics, a forward step is used. Some radiation and cumulus options of MM5 use a constant time step (determined in the input parameters of MM5) over periods of many model time steps and are only recalculated at specific time steps (30 minutes or so) as determined in the input file.

MM5 contains the capability of multiple nesting with up to 9 domains at the same time, which are completely interacting (Figure 2.3). The nesting ratio is always 3:1 for two-way interaction, which means that the input of information to the grid nests from the coarse grid comes via its boundaries, while the feedback to the coarser grid occurs over the daughter nest

interior 3-dimensional space. However, the ratio 1:3 is not required for one-way interacting mother–daughter grids (Dudhia *et al.,* 2003). Nested domains are allowed on one given level. They are also allowed to overlap, can be turned on and off at any time in the simulation, noting that whenever a mother domain is terminated all its descendent nests are also turned off. Moving a domain is possible during a simulation, excluding the mother or coarsest grid.

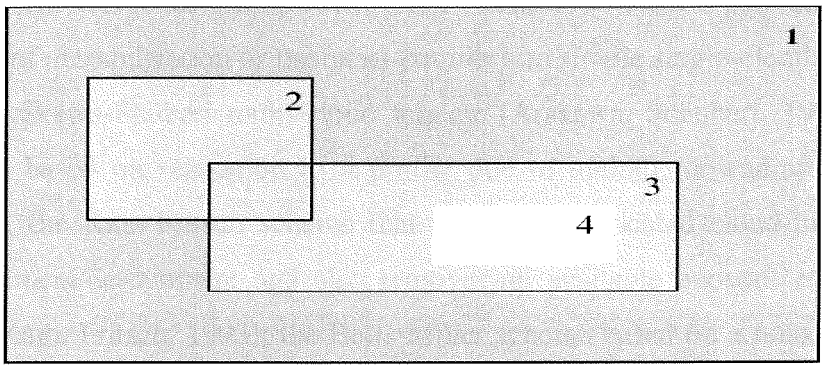

Figure 2.3 Example of different levels of nesting configuration for the mother (coarse) grid (grid1) (after MM5 Modelling System Version 3–user's guide).

Calculation of lateral boundary conditions in MM5 means that horizontal winds, temperature, pressure and moisture fields are specified for all four boundaries, while microphysical fields can also be specified if necessary. For research, and especially for real-time forecasts (as MM5 has been created as a prognostic model from the beginning,) the lateral boundaries ultimately depend on global model analysis/forecast fields (from the Global Data Assimilation System–GDAS). Where upper-air analysis are used (radiosondes, meteorological balloons, etc.) the boundary values may be available only 12-hourly, although it may be a higher frequency (from 6 to 1 hourly) for model-generated boundary conditions obtained from global analysis data assimilation. The basic stipulation for boundary conditions of the coarse grid is a situation of relaxation of MM5 fields toward the global analysis – the model is nudged towards the analysis with a smoothing term. Two-way nest boundary conditions are similar to the mother domain, but are updated every coarse-mesh time-step and have no relaxation process (Dudhia *et al.,* 2003).

2.5.2 Physical options of MM5

Physical options in MM5 include choice of appropriate cumulus parameterisation scheme, explicit moisture scheme, and type of Land-Surface Model (LSM) parameterisation. However, the LSM parameterisation will be considered later in Section 2.5.4 (Dudhia *et al.,* 2003). The chosen schemes of physical processes used in MM5 are directly and strongly related to the

dynamical properties of realistic MM5 tuning, and especially with the number of vertical levels and depth of the modelled atmosphere, spatial resolution, time step and number of one (or two) way interacting nested grids. But first of all, the parameterisation scheme chosen depends on application of MM5 to the particular local meteorological and topographic situation.

MM5 cumulus parameterisation includes 8 schemes, including the scheme of Anthes-Kuo based on moisture convergence (Kuo, 1974; Grell *et al.,* 1994); Grell parameterisation that is based on the rate of destabilization or the quasi-equilibrium simple single-cloud scheme (Grell *et al.,* 1994); the Arakawa-Shubert multi-cloud scheme (Arakawa, Schubert, 1974); the Fritsch-Chappell scheme based on relaxation to a profile due to updraft, downdraft and subsidence region properties; the Kain-Fritsch scheme that uses a sophisticated cloud-mixing scheme to determine entrainment/detrainment and also removes all available buoyant energy during the relaxation time (Kain, Fritsch, 1993); the Betts-Miller scheme based on a relaxation adjustment to a reference post-convective thermodynamic profile; and the Kain–Fritsch 2/new cumulus scheme that includes also shallow convection with a spatial scale between 15–10 km (Dudhia, 2002).

MM5 has seven options of explicit moisture parameterisation that include:

1. a stable precipitation scheme that is nonconvective
2. a warm rain scheme including cloud and rain water grids
3. Dudhia's simple ice scheme with ice phase processes in addition to the warm rain scheme (Grell *et al.*, 1994)
4. a mixed-phase (Reisner *et al.,* 1998) scheme, which adds a supercooled water phase to the above 2 schemes
5. the Goddard microphysics scheme, including an additional equation for prediction of graupel (Tao and Simpson, 1993)
6. the Reisner graupel scheme (Reisner 2), suitable for cloud-resolving
7. Schultz microphysics scheme, which is a highly efficient and simplified scheme and is designed for fast running, containing ice and graupel/hail processes.

2.5.3 Radiative scheme

Radiation parameterisation (as the main source of energy for atmospheric processes) is essentially important for realistic modelling of energy distribution and redistribution (especially in the atmospheric boundary layer), as short term fluctuations in dry bulb and potential temperature fields determine most of the variations in local circulation. Figure 2.4 illustrates a system of free atmosphere radiation processes. MM5 includes 5 possibilities of radiation processes parameterisation (Dudhia *et al.,* 2003).

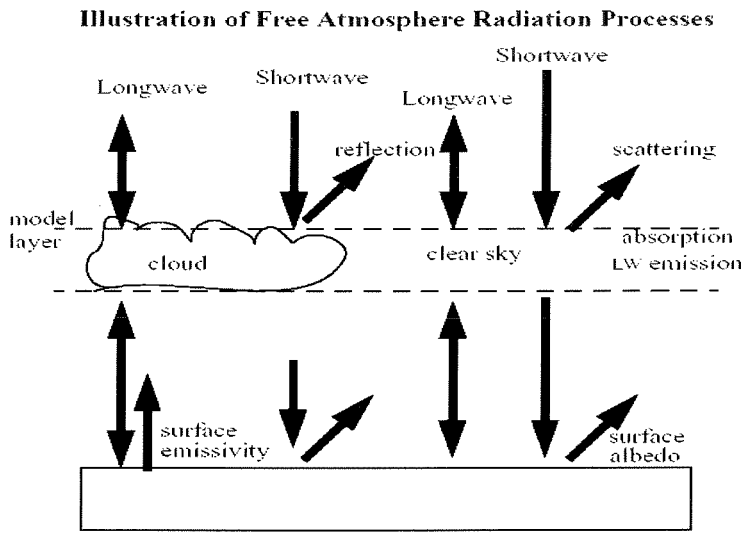

Figure 2.4 Schematic illustration of radiation processes for the surface and free atmosphere (after MM5 Modelling System Version 3–user's guide).

2.5.4 *Planetary boundary layer parameterisation*

MM5 has 7 options of different kinds of PBL schemes to run, including:

1. a bulk PBL scheme, suitable for coarse vertical resolution in the boundary layer
2. a high-resolution Blackadar scheme, suitable for high resolution PBL (Blackadar, 1979)
3. a bulk-Thompson PBL scheme, based on Mellor–Yamada formula
4. an ETA global model PBL, based on the Mellor–Yamada scheme but used for scheme stability using long time steps
5. the MRF or Hong–Pan PBL, suitable for high-resolution PBL
6. the Gayano-Seaman PBL scheme, which is close to the MRF scheme, but using split time steps instead of surface temperature from the LSM (Land Surface Model)
7. the Pleim–Chang PBL scheme, which was developed to use with LSM parameterisation type 3 (Chang *et. al.*, 1987).

It is also important to mention the MM5 options of vertical diffusion in cloudy air, resulting in mixing toward a moist adiabat by basing atmospheric mixing on moist stability instead of dry stability, and the calculation of different thermal roughness lengths for heat/moisture that affects the partitioning of sensible and latent heat fluxes (Zaengl, 2002). The Land Surface Model (LSM) is a basic block of most PBL schemes and there are 4 types of LSM in MM5 (described by Dudhia *et al.,* 2000).

2.5.5 *Non-hydrostatic requirements*

The scope of application of MM5 has increased and for some investigated processes the ratio between horizontal and vertical scales has approached unity, while in some research (such

as cloud development and lee waves) the horizontal scale has become shorter than the vertical one, and it is impossible to neglect non-hydrostatic dynamics. The additional term in non-hydrostatic dynamics is the vertical acceleration that contributes to the vertical pressure gradient, so that hydrostatic balance is no longer exact.

The reference state in the non-hydrostatic MM5 is an idealized temperature profile in hydrostatic equilibrium. It is specified by the equation

$$T_0 = T_{s0} + A\log_e(p_0/(p_{00})) \qquad (2.5.2)$$

T_0 (p_0) is specified by 3 constants: p_{00} is sea-level pressure (taken to be 1013 hPa), T_{s0} is the reference temperature at p_{00}, and A is a measure of the lapse rate. Since MM5 Version 3.1, the reference state can include an isothermal layer at the top to better approximate the stratosphere. This is defined by a single additional temperature (T_{iso}), which acts as a lower limit for the base-state temperature. Using this, effectively raises the model top height (Dudhia *et al.*, 2003).

2.5.6 *Grid nudging*

MM5 grid nudging can be of two types, and each type has 2 options to choose between. The first type of nudging (one-way interaction) is founded in nested grid possibility for any LAM using nested grids (number of nested grids for each mother domain and a level of nesting don't play any role in the grid nudging process). During MM5 runs there can be two options for interaction between mother (coarse) and daughter (fine) grids: one-way interaction nudging means a numerical process of downward movement of calculated information from large-scale processes (mother grid) to the higher resolution processes of the nested/daughter grid(s). Two-way interaction nudging allows two-way interaction between grids of any level of nesting with downward–upward transition, redistribution and assimilation of time-dependent meteorological information during a numerical experiment (Grell *et al.*, 1994).

The second type of grid nudging consists of the ability to switch on the grid nudging procedure for separate meteorological fields (e.g. wind, temperature, mixing ratio and rotational component of the wind fields) during an MM5 run.

2.5.7 *Four-dimensional data assimilation/analysis and observation nudging*

In situations where data are to be input to the model over an extended time period, Four-Dimensional Data Assimilation (FDDA) is an option that allows this to be done (Wang, 2002). Essentially, FDDA allows the model to be run with forcing terms that 'nudge' it towards the observations or an analysis field. Newtonian relaxation terms are added to the prognostic equations for wind, temperature and water vapor to relax the model values towards a given 4-

dimensional analysis field (Stauffer and Seaman, 1994). The benefit of this is that after a period of nudging, the model has been adjusted to some extent to all data available for that time interval while also remaining close to a dynamical balance. This has advantages over just initializing with analysis data at a single synoptic time, because adding data over a period effectively increases the data resolution. Observations at a station are carried downstream by the model and may help fill data voids at later times.

2.5.8 *Output plotting options*

A number of files are written out during MM5 runs, including output files of several meteorological and derived fields for every grid domain and at specified time intervals (these files are called MM5 history files), as well as restart files for every grid in case of a run interruption, so that calculations can be resumed from the last time output fields were dumped. For each time period, the history output includes a general header of MM5 configuration, a subheader describing the field following the subheader, 14 3-dimensional (V3) forecast fields for each domain, 30 2-dimensional (V2) variable-in-time forecast fields for each domain (like snow cover depth) and 11 constant in time 2-dimensional (V2) fields (like orography or land use distribution). MM5 has a few 1, 2 and 3 dimensional graphical programs to process the output of any grid domain in MM5 format (IEEE), binary format, ASCII format and into any kind of plot (Dudhia *et al.,* 2003).

2.5.9 *MM5 as a prognostic model*

MM initially was created and developed as a prognostic model. Through more than 25 years of MM (now MM5) development it has undergone many changes designed to broaden and improve its use in real-time mode (Bao *et. al.*, 2002; Smallcomb, 2002). These changes include multiple-nest capability, non-hydrostatic dynamics and four-dimensional data assimilation capability. The assimilation of local observations is a very important feature of the model and MM5 is used as a prognostic model (with FDDA) in many regional meteorological centres all over the world (the Meteorological Service of New Zealand in Wellington is an example of MM5 use as a prognostic model).

Fast and accurate assimilation of global and local observation data is an important feature of MM5 as a prognostic model, not only for everyday weather forecasting, but for predicting severe events such as tropical cyclones (MM5 includes a special option of moving nested grids) (Low-Nam, Davis, 2002), heavy monsoon rain based on prediction of ITCZ (InterTropical Convergence Zone) movement (Someshwar *et al.*, 2002), gusting winds as a result of drainage of cold air masses (Dailey, Keller, 2002), severe cold frontogenesis as a result of local conditions

(Brown, Locatelli, *et al.*, 1999), and simulation of ozone episodes (Boucouvala *et al.*, 2003). It is useful to mention that MM5 was successfully applied during the 2002 winter Olympic games (Steenburg *et al.*, 2001) and was also used as a basic prognostic model during the summer Olympic games 2004 in Athens (Kotroni *et al.*, 1999; Kotroni, Lagouvardos, 2002).

2.5.10 MM5 as a regional, polar or global model

MM5 has a choice of several map projections:

1. Lambert Conformal projection is best suitable for mid-latitudes and represents a method of interpolation from latitude/longitude grid to Lambert projection centered on 45 latitude degree;
2. Mercator projection is best for the equator and low latitudes;
3. Polar Stereographic projection was specially developed for application of MM5 to Antarctic and Arctic meteorological research. The Arctic/Antarctic Mesoscale Prediction System (AMPS) was created to use MM5 as a prognostic model for Arctic/Antarctic weather forecasting (see Figure 2.5).

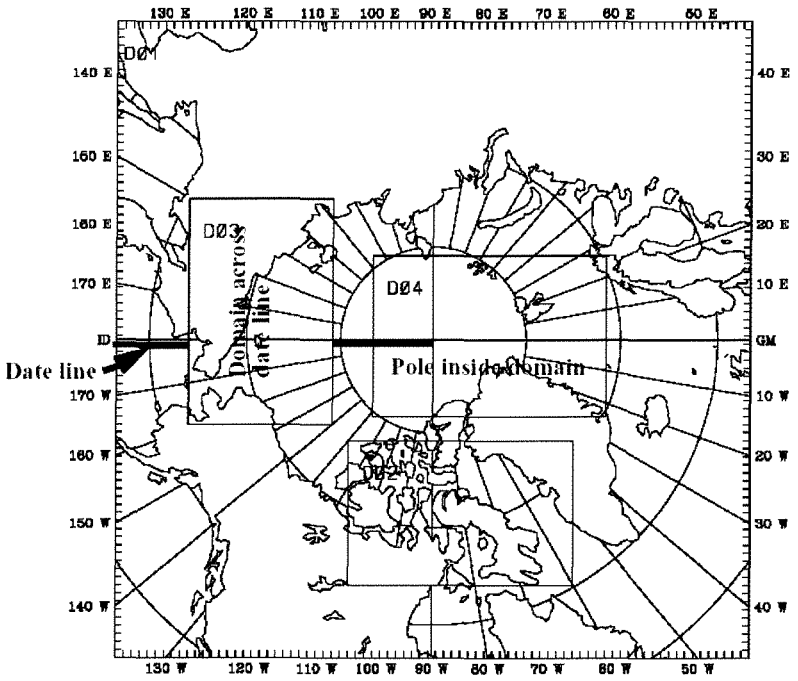

Figure 2.5 Polar Stereographic projection over Arctic (after MM5 Modelling System Version 3 – user's guide).

MM5 can be used as a global (hemispherical) model for creation of first-guess fields with use of nesting for research involving spatial scales of more than 1000 km and time scales more than 48–72 hours (e.g. teleconnection studies, long range air pollution studies) (Dudhia and Bresh, 2000).

2.6 *Comprehensive Air Quality Model (CAMx), version IV*

2.6.1 *Basic description, dynamical scheme and links to MM5*

The Comprehensive Air quality Model with □meteorology (CAMx) is a Eulerian photochemical dispersion model that allows for an integrated 'one-atmosphere' assessment of gaseous and particulate air pollution over many scales ranging from urban to 'super-regional'. It is designed to unify all of the technical features required of 'state-of-the-science' air quality models into a single efficient system, which is publicly available. The input/output formats are based on the Urban Airshed Model (UAM-IV) and are compatible with many existing formats.

CAMx simulates the emission, chemical reactions during dispersion, and removal of pollutants in the lower troposphere by solving the pollutant continuity equation for each chemical species (l) on a system of nested three-dimensional grids. The Eulerian continuity equation describes the time dependency of the averaged species concentration ($c_l(t)$) within each grid cell volume as a sum of all of the physical and chemical processes operating in that volume:

$$\partial c_l/\partial t = -\nabla_H \bullet \boldsymbol{V}_H c_l + [\,\partial(c_l\eta)/(\partial z) - c_l\,\partial/\partial z(\partial h/\partial t)\,] + \nabla \bullet \rho K\nabla(c_l/\rho) + \partial c_l/\partial t\,|_{Chemistry} + \partial c_l/\partial t\,|_{Emission} + \partial c_l/\partial t\,|_{Removal} \qquad (2.6.1)$$

where $\boldsymbol{V}_H$ is the horizontal wind vector, η is the net vertical 'entrainment rate', h is the layer interface height, ρ is atmospheric density, K is the turbulence exchange (diffusion) coefficient (CAMx receives all these characteristics from the meteorological numerical model – MM5).

The physical representations and the numerical methods used in CAMx for each of the terms of the pollutant continuity equation (2.6.1) include 6 modules (ENVIRON Int. Corp., 2003): horizontal advection/diffusion, vertical transport/diffusion, chemistry module with Carbon Bond IV (CB IV) mechanism, dry deposition module, wet deposition, and plume in grid (PiG) with inorganic chemistry (ENVIRON Int. Corp., User's Guide, 2003).

CAMx carries concentrations at the centre of each grid cell, representing the average concentration over the entire cell. CAMx internally carries meteorological fields in an arrangement of the 'Arakawa C' grid configuration: temperature, pressure, water vapour and cloud water are located at the cell centre together with concentrations; wind components and diffusion coefficients are carried at cell interfaces to describe the transfer of mass in and out of each cell. In the vertical, most variables are carried at each layer midpoint except those variables that describe the rate of mass transport across the layer interface, which include the vertical diffusion coefficient K_v and the vertical entrainment rate η. These variables are carried in the centre of each cell horizontally, but are located at the top of the layer (i.e. interface) vertically.

CAMx can perform simulations on the three types of Cartesian map projections: Universal Transverse Mercator, Rotated Polar Stereographic and Lambert Conic Conformal. CAMx also offers the option of operating on a curvi-linear geodetic latitude/longitude grid system. The

vertical grid structure is defined externally, so that layer interface heights may be specified as any arbitrary function of space and time.

CAMx incorporates two-way grid nesting, which means that pollutant concentration information propagates into and out of all grid nests. Any number of grid nests can be specified in a single run, while grid spacing and vertical layer structures can vary from one grid nest to another. Nesting in the vertical is allowed, but only by sub-dividing parent grid layers into a series of finer layers. To maximize flexibility in the vertical structure, each parent grid layer may be individually split into a unique set of fine layers, or not split at all. The flexi-nest option in CAMx allows users to redefine the nested grid configuration at any point in a simulation. Nested grids can be introduced or removed only at the time of a model restart, when users can redefine nested grids structure in the CAMx input general configuration information file (CAMx.in file). Flexi-nesting provides suppleness to both meteorological and emissions input files for a nested grid and allow CAMx to interpolate data that are not provided from the parent grid.

The approach of pollutant transport solving in CAMx provides both mass conservation and mass consistency. To be mass conservative, CAMx carries concentrations of each species internally as a density and solves the advection equations in flux form. Mass consistency refers to CAMx's ability to transport pollutant mass exactly equivalent to the input atmospheric momentum field. Sources of mass inconsistency in CAMx can be from: supplying meteorology that is inherently inconsistent from an interpolated objective analysis with meteorological fields independently developed; spatial interpolating or averaging MM5 three-dimensional wind vector fields to a different size grid of CAMx; and employing different numerical and physical methods and techniques in CAMx and MM5. It is therefore best if translation of meteorological data to CAMx is achieved with as few additional manipulations as possible. Horizontal advection is performed using the area preserving flux-form advection solver from Bott (Bott, 1989) or the Piecewise Parabolic Method (PPM) of Colella and Woodward (Colella and Woodward, 1984), as implemented by Odman (Odman *et al.,* 1996).

2.6.2 Chemistry

The chemical mechanisms supported in CAMx4 are based on version 4 of the Carbon Bond mechanism (CB4, Gery *et al.,* 1989) and the SAPRC99 mechanism (Carter, 2000). CAMx includes five chemistry mechanisms: two versions of the 'standard' CB4 mechanism, chlorine chemistry mechanism, the mechanism of aerosol modelling and the fixed parameter version of the SAPRC99 mechanism. The basic features of each chemistry mechanism are explained below:

1. CB4 (mechanism 3) with reactive chlorine chemistry: 110 primary reactions and 48 species (34 state gases and 14 radicals)

2. CB4 with revised radical-radical termination reactions that are necessary for regional modelling: 91 primary reactions and 36 species (24 state gases and 12 radicals)
3. Mechanism 2 with updated isoprene chemistry based on Carter (2000) as implemented for the Ozone Transport Assessment Group (OTAG): 96 reactions and 37 species (25 state gases and 12 radicals)
4. Mechanism 3 with extension for aerosol modelling: 100 primary reactions and 62 species (35 state gases, 12 radicals and 15 aerosols)
5. The fixed parameter version of the SAPRC99 mechanism: 211 primary reactions and 74 species (56 state gases and 18 radicals).

2.6.3 *Chemistry solver and pollutant removal*

Numerically solving the time evolution of the gas and particle phase chemistry is typically the most 'expensive' part of a photochemical grid model simulation, especially for the aerosol phase. Two chemistry solver options are available in CAMx, the Implicit-Explicit Hybrid (IEH) solver (Sun *et al.,* 1994) and the Chemistry Mechanism Compiler (CMC) fast solver. CMC solver is nearly three times faster than IEH, and solutions of both solvers are very similar for daytime conditions, but differ at night. The accuracy of the CMC fast solver is an improvement over many commonly used solvers and the availability of the IEH solver option provides a way to evaluate the CMC solver performance and provides an alternative for users who choose to accept longer run-times (more than 24 hours).

Trace gases and small particles are removed from the atmosphere via deposition: dry deposition refers to the direct sedimentation and/or diffusion of material to various terrestrial surfaces and uptake into biota, wet deposition refers to the uptake of material via chemical absorption (gases) or nucleation/impaction (particles) into cloud water, and the subsequent transfer to the Earth surface by precipitation.

Wet deposition is an important removal process for particles, as they act as cloud condensation nuclei. The cloud droplets grow and collect into sufficiently large sizes to fall as precipitation. A fraction of particles that are subsequently entrained into the cloud are scavenged by liquid precipitation via impaction. The rates of nucleation and impaction depend upon cloud type, rainfall rate and particle size distribution. Wet deposition occurs through the following series of steps: mixing of trace gas and condensed water in common air space, absorption of gas molecules by water droplets, possible reactions of the pollutant within water droplets, precipitation of droplets and diffusion of ambient gases into falling precipitation.

2.6.4 *Gridded and source emissions*

Initial gridded concentrations of gases and particulate matter are used by the mother grid of CAMx when gridded emissions of pollutants are to be modelled. Gridded emissions of gases and aerosols are supplied at specific time intervals during CAMx runs (the time interval can range from 1.5 minutes to a few hours depending on the process to be investigated and computer resources), but only for the lowest (boundary) layer of the model.

The CAMx PiG is used to treat the near-surface impacts of large NO_x point sources, when just inorganic chemistry is important. The method is called the Greatly Reduced Execution and Simplified Dynamics (GREASD) PiG, which is much faster and structurally simpler than other PiG approaches. The streamlining employed in the recent version of CAMx was based upon former experience in developing, utilizing and studying the responses of the more detailed Urban Airshed Model with a grid variable (UAM-V) PiG algorithm.

2.6.5 *Gases and ozone chemistry problems in CAMx4*

Ozone Source Appointment Technology (OSAT–Yarwood *et al.,* 1996) and its derivatives allow CAMx to track source region and/or source category contributions to predicted grid cell ozone concentrations. Thus, for any selected receptor point and time, the model gives a clear picture of the likely distribution of ozone and ozone precursors by source category and/or source region, as well as an indication as to whether the ozone at the selected time and location would more likely respond to upwind NO_x or Volatile Organic Components (VOC) components. This method was originally implemented in the Urban Airshed Model and was then built into CAMx. OSAT provides a method for estimating the contributions of multiple source areas, categories, and pollutant types to ozone formation in a single model run. OSAT also includes a methodology for diagnosing the temporal relationships between ozone and emissions from groups of sources.

2.6.6 *Input-output software and its improvement*

Before a run, CAMx needs several fields to be prepared and attached to the model as input fields and files including meteorological fields (from MM5 output), chemical, photochemical, landuse, gridded emission, source emission, top concentration, boundary and initial condition files that are listed below:

1. The rates for primary photolysis reactions are supplied via the photolysis rates file, and the file must be supplied if chemistry is invoked. It is essentially in a large look-up table that provides the photolysis rates in five dimensions, including variations with solar zenith angle, height above the ground, ultraviolet albedo of the ground, atmospheric turbidity, and total ozone column density and is configured by the user.

2. Albedo/ozone/haze file contains the spatial and temporal distribution of surface UV albedo, ozone column density, and turbidity for a specific CAMx domain or episode and must be supplied if chemistry is invoked. The values in this file depend on the latitude/longitude position and specific time of year. The UV albedo is supplied for each cell of the master grid and optionally for nested grids, while the ozone and turbidity fields are supplied for the coarse grid and are assigned to nested grids.
3. The top concentration file contains the time- and space-invariant species concentrations that are assumed to exist above the top boundary of the entire modelling grid. Top concentrations may and should be specified for a sub-set of the total number of modelled species that are of most interest for a specific task.
4. The landuse input file contains time-invariant two-dimensional gridded fields of landuse distribution. The file must be provided for the master grid and should be created for all nested grids for as accurate as possible reproduction of gridded land cover categories associated with exact surface roughness (in metres) for precise dry deposition scavenging calculations. Surface roughness can be edited for every land cover category by the user.
5. Meteorological input files are three dimensional fields that are variant not only in space, but also in time, with a specific time interval (nudging time interval for CAMx4), and are provided to the model through all runs for the master grid and optionally can be provided for all nested grids from MM5 output fields. Meteorological fields include height/pressure, wind, temperature, water vapour, cloud/rain and vertical diffusivity as four-dimensional fields.
6. The boundary condition file contains two-dimensional gridded concentration fields on the lateral edges of the master grid boundary. The initial conditions file contains 3-D gridded concentration fields for the master grid and must be specified for a sub-set of the total number of modelled species listed in the CAMx.in information/reference file.
7. The gridded emissions fields contain two-dimensional gridded fields of near-surface emission rates for all the emitted species to be modelled. The format of the file follows the format of the UAM model and pre-existing emission pre-processor software may be used to develop this file. If gridded emissions are to be modelled, a gridded emissions file must be created in advance by a user for the master grid and optionally for any nested fine grid.
8. Elevated point source emissions file contains stack parameters and emission rates for all elevated point sources, and for all emitted species to be modelled.

The output master and fine grid instantaneous files contain full three-dimensional fields of all species modelled, but the master and fine grid and deposition files contain only those species that are specified in the run control file CAMx.in. For flexibility, CAMx offers the option to write full three-dimensional average concentration fields or just surface layer two-dimensional

fields. Additional statistical software (like the CAMxPOST program package) is developed by ENVIRON for the primary statistical analysis of the CAMx output and comparison with observations. Windows and Golden software are widely applied to the model output to analysis and visualise the calculated results.

2.7 Summary

In the first part of Chapter 2, basic primitive equations of the atmosphere numerical modelling are described. The main modern trends in development and application of limited area meteorological and chemical modelling were then described. The second part provides a basic understanding of the MM5 and CAMx4 configurations, and the research and forecast potential of the models.

Chapter 3
Regional context

3.1 Introduction

This chapter describes firstly the main features of synoptic and local scale air circulation over Christchurch and its vicinity, and secondly the problem of particulate matter air pollution resulting from active use of domestic open fires. Examination of historical aspects of PM_{10} night-time peaks, as well as the possibility of winter air pollution prediction and control are considered in the third part of the chapter.

3.2 Atmospheric circulation over Canterbury and the Christchurch region during winter

The city of Christchurch is situated on the coastal edge of the Canterbury Plains (Figure 3.1). The plains slope gently from the Southern Alps to the eastern coast and average 40 km in width and 150 km in length from the hills of north Canterbury to the Hunter Hills in the south. Banks Peninsula lies on the southern border of Christchurch and reaches a height of 906 m (Herbert Peak).

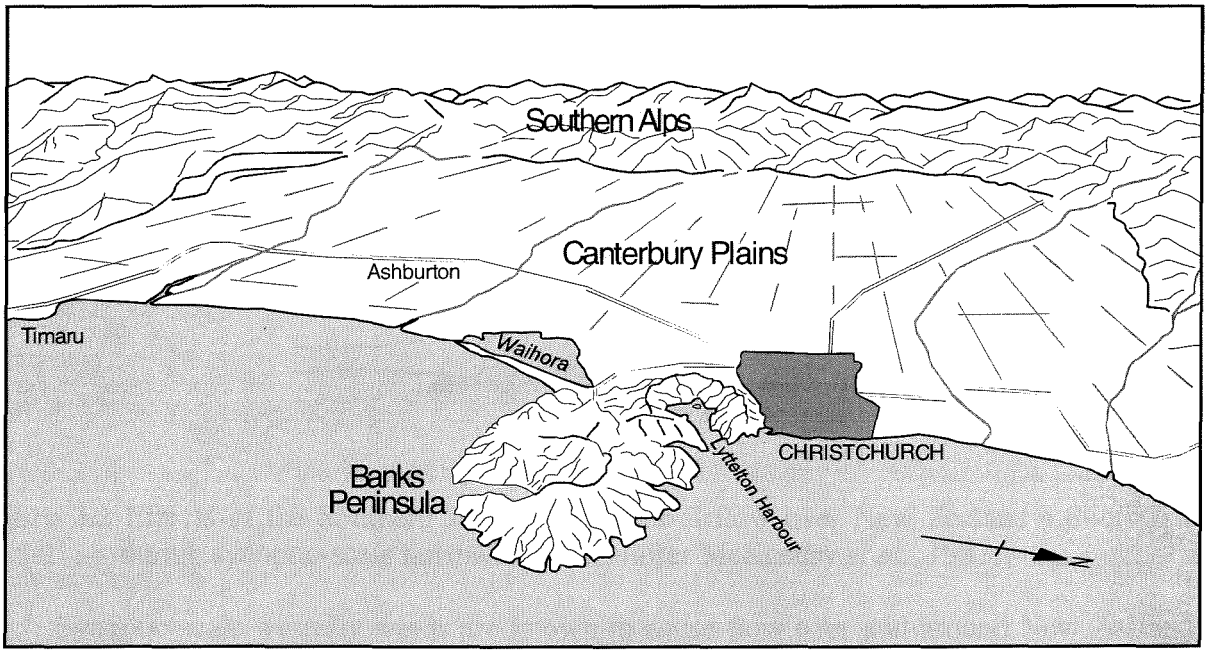

Figure 3.1 The Canterbury Plains, Christchurch and the Port Hills (Kossmann and Sturman, 2002).

The Christchurch urban area covers more than 20,000 hectares of land with an immediate rural fringe of 30,000 hectares. Ninety-seven percent of the population of Christchurch live in the urban area and the total population of Christchurch city is estimated at more than 405,000 (from the National Census 2002, Statistics New Zealand, 2003). Topographically induced local

wind fields over Canterbury and the Christchurch region play an important role in the microclimate of Christchurch.

New Zealand is located in the mid-latitudes of the Southern Hemisphere and its wind climate is largely controlled by eastward travelling high- and low-pressure systems (Sturman and Tapper, 2002). In the Canterbury region, located on the eastern side of the South Island of New Zealand (Figure 3.2), the synoptic-scale wind is strongly modified by dynamic and thermotopographic effects caused by the land-sea discontinuity, the Southern Alps and Banks Peninsula (McKendry, 1983).

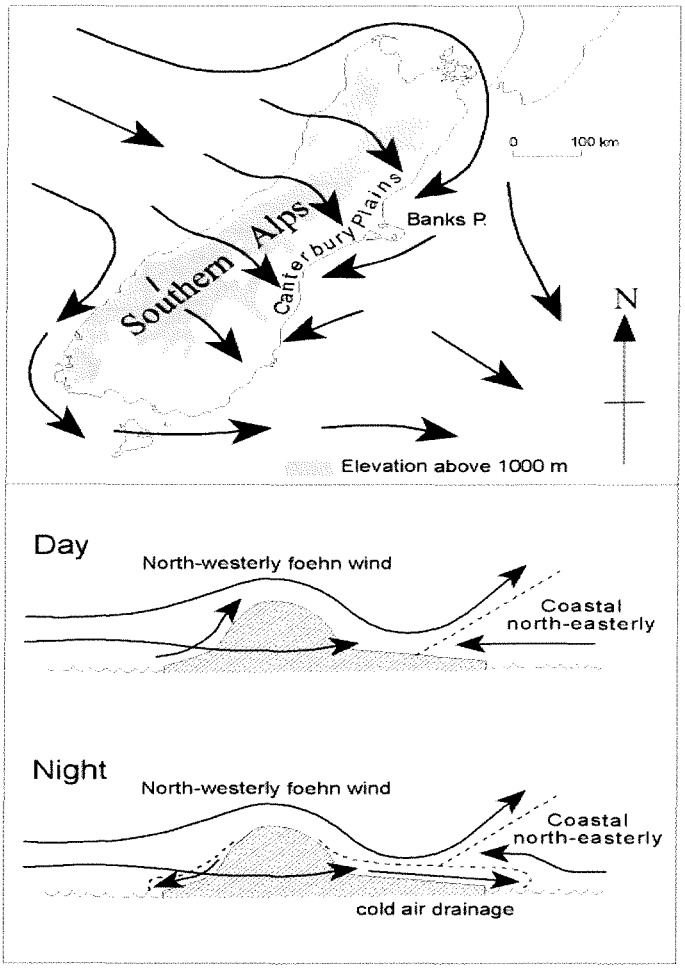

Figure 3.2 Effects of the Southern Alps on regional airflow over New Zealand's South Island during synoptic-scale northwest winds (after McKendry *et al.,* 1987)

'Synoptic-scale westerly winds are known to cause flow over and around New Zealand's South Island, resulting in frequent foehn winds and onshore northeasterly winds over the Canterbury Plains' (Kossmann and Sturman, 2002, page 452), as shown in Figure 3.2 (Sturman *et al.,* 1985; McKendry *et al.,* 1987). The onshore northeasterlies appear to be due to localized pressure gradients resulting from the development of lee troughs over the Canterbury region, as described by McKendry *et al.* (1986). In the initial stages of a westerly wind event (caused by a trough approaching New Zealand from the west), the convergence zone between the northwesterly foehn winds and the northeasterly onshore flow occurs at some distance inland,

whereas during the prefrontal final stage the convergence zone often moves out to sea. 'After the passage of a cold front, Canterbury usually experiences a period of cold southwesterly airflow (parallel to the main divide of the Southern Alps) and the development of a short-lived high-pressure system. The arrival of the next trough signals the repetition of the sequence of wind changes.' (Kossmann and Sturman, 2002, page 452).

'Superimposed on these synoptic-scale wind changes are diurnal variations caused by the frequent development of easterly sea breezes during daytime (Sturman and Tyson, 1981) and night-time decoupling of the lowest air layers, in which offshore drainage winds and land breezes are observed (Sturman and McKendry, 1984; Ryan, 1987)' (Kossmann and Sturman, 2002, page 452). These occur particularly when synoptic pressure gradients are weak (Figure 3.3).

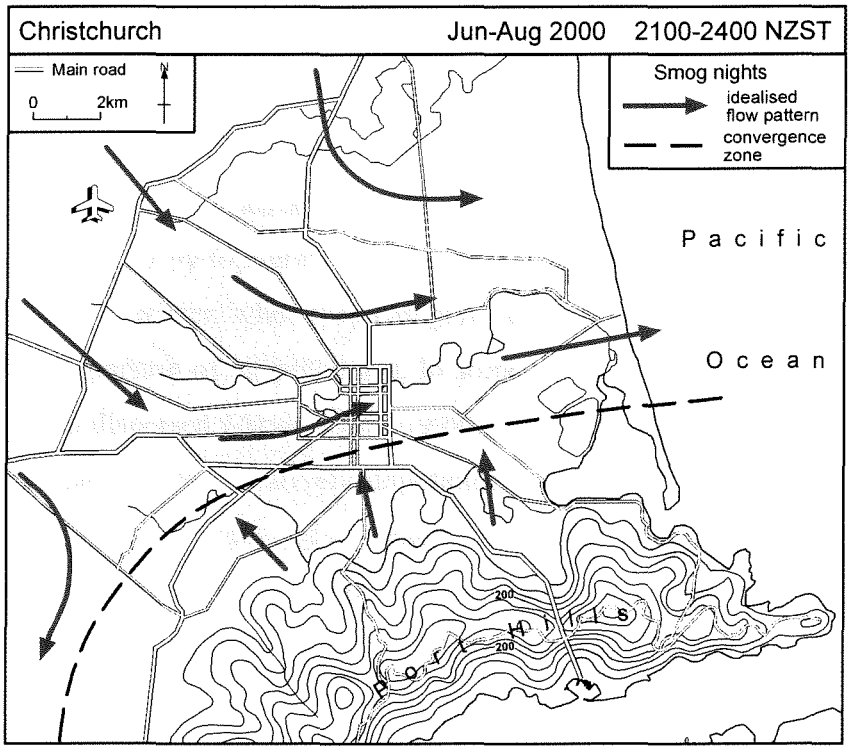

Figure 3.3 Night-time decoupling of observed downslope and offshore drainage winds and land breezes and the migrating convergence zone in the near-surface air layer (after Kossmann and Sturman, 2004).

As can be seen, radiative cooling of hill slopes on clear, calm nights and subsequent cooling of the air in contact with them by conduction and convection, results in cold air drainage, which follows the terrain to its lowest sections, where it may become slow moving or stagnant. Knowledge of these atmospheric boundary layer flows is important for predicting dispersion of air pollution from near-surface sources in complex terrain (Arya, 1999). The term 'airshed' is defined as 'The conceptual boundary of an atmospheric 'catchment' used in crude modelling of air pollution around known sources of pollution under expected conditions of air movement and rates of chemical change' (Goudie *et al.,* 1994). The airshed for many cities is difficult to define

because of the complex geography of the surrounding area (Sortberg *et al.,* 2001) and this is the case for Christchurch, where the airshed can be delimited clearly to the south of the city by the ridgeline of the Port Hills, but to the west and north, it is much more difficult to delimit because of the configuration of the plains and foothills of the Southern Alps (Sturman and Zawar-Reza, 2001). This makes the catchment for cold air drainage potentially extremely large. 'However, much of the air over this extensive area has little significance for air pollution in Christchurch because of the time frame involved, particularly the time when it moves across the city relative to the period of maximum night time pollution emission' (Sturman and Zawar-Reza, 2002, page 3339).

3.3 Air pollution in Christchurch and its vicinity

3.3.1 The winter situation

Topographically induced local wind fields play an important part in the dispersion of air pollution (Arya, 1988). Recent international research (Alexandrova *et al.,* 2003) illustrates the importance of such local wind systems in creating variability in the spatial distribution of air pollution. Local winds induced by topography are particularly significant during relatively calm synoptic conditions, often in winter, when they can generate quite complex airflow patterns that are able to control the dispersion of air pollutants. In some cases, they are the main mechanism by which air pollution is dispersed (Arya, 1988; 1999). However, they may be responsible for advection of either polluted or comparatively unpolluted air across an area, depending on the relative location of air pollution sources and scavenging points. On occasion, they can be closed-cell circulations that can produce recirculation of pollution over a diurnal time frame (Oke, 1978). The effects of topographically induced flow splitting and flow separation, and of non-stationary drainage wind convergence, on air pollution dispersion are so far only partly understood (McCauley and Sturman, 1999). However, they appear to be of great importance in the case of wintertime air pollution events in the Christchurch area, which is the focus of this thesis. Improved understanding of the relationship between the temporal development of mesoscale local winds and ambient air pollution concentrations of particulate matter (PM) can contribute to the development of appropriate air quality management tools.

Christchurch has a significant wintertime air pollution problem that is dominated by smoke generated by domestic fires burning coal and wood (Spronken-Smith *et al.,* 2001). The emissions consist mostly of particulate matter originating within the near-surface atmospheric layer, generally within 10 m of the ground. Under anticyclonic weather conditions, a strong surface-based radiative temperature inversion traps the air close to the ground, resulting in high air pollution concentrations exhibiting a characteristic daily variation with high levels at night when

people use their log-burners and open-fires (Figure 3.4). The winter season over the Christchurch region can be characterized by the frequent occurrence of severe nocturnal smog events in Christchurch, surrounding suburbs and nearby smaller towns and cities (e.g. Ashburton and Timaru), where health guidelines are regularly exceeded (McGowan and Sturman, 1993; Chilton, 1999, pers.comm.; Sturman *et al.,* 2002; Wilton *et al.,* 2002). These smogs are experienced usually during cold and calm nights when atmospheric stability and emissions of PM, mostly from home heating (but also partly from traffic), are high. A synoptic climatology of such events has shown that situations with post-frontal southwesterly winds, or with northwesterly winds aloft (but undeveloped at the surface), or with weak easterly synoptic-scale flows are favourable for the development of severe smog events in Christchurch (Owens and Tapper, 1977). The near-surface airflow during smog nights is often dominated by westerly cold air drainage from the Southern Alps, which can enhance the strength of near-surface temperature inversions (Johnstone, 2000, pers.comm.; Sturman, 2000, pers.comm.) and generate zones of stagnant air resulting from convergence with drainage winds down the slopes of Banks Peninsula.

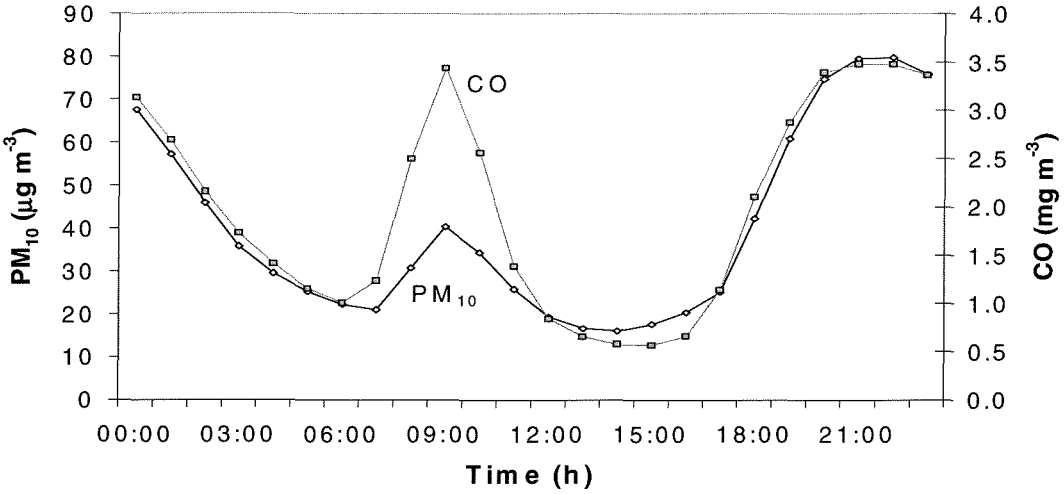

Figure 3.4 Diurnal cycle of hourly average concentrations of particulate material < 10 µm in diameter (PM_{10}) and carbon monoxide (CO) during winter (June–August), averaged for the years 1988–1999 (data supplied by Environment Canterbury).

It is important to stress that although regions such as Christchurch may initially appear to represent relatively simple environments, the complexity of the local wind systems can create significant problems for agencies responsible for air quality management (van den Assem *et al.,* 1996). For purposes of detailed study of Christchurch aerosol pollution, a special unique high density network of surface wind, temperature (and additional PM_{10}) measurements was established (the Christchurch Air Pollution Study 2000–CAPS2000) to analyse spatial and

temporal variability of surface wind fields in coastal Canterbury in winter, with special emphasis on flow conditions found during smog nights (Sturman *et al.*, 2001).

In considering more precisely the origin and 24-hour trends of PM_{10} and CO (carbon monoxide) it should be noted that emissions of PM_{10} (mostly from home heating) are highest between sunset and midnight (Figure 3.4). Emissions of CO are also highest and largely from home heating during the first half of the night, whereas during daytime they originate mostly from traffic (Figure 3.5). Owing to these emission characteristics and the diurnal variation in ventilation, including mixing depth and wind speed, wintertime smog events in coastal Canterbury and over the Christchurch region are found to be mainly a nocturnal phenomenon (Wilton *et al.*, 2002).

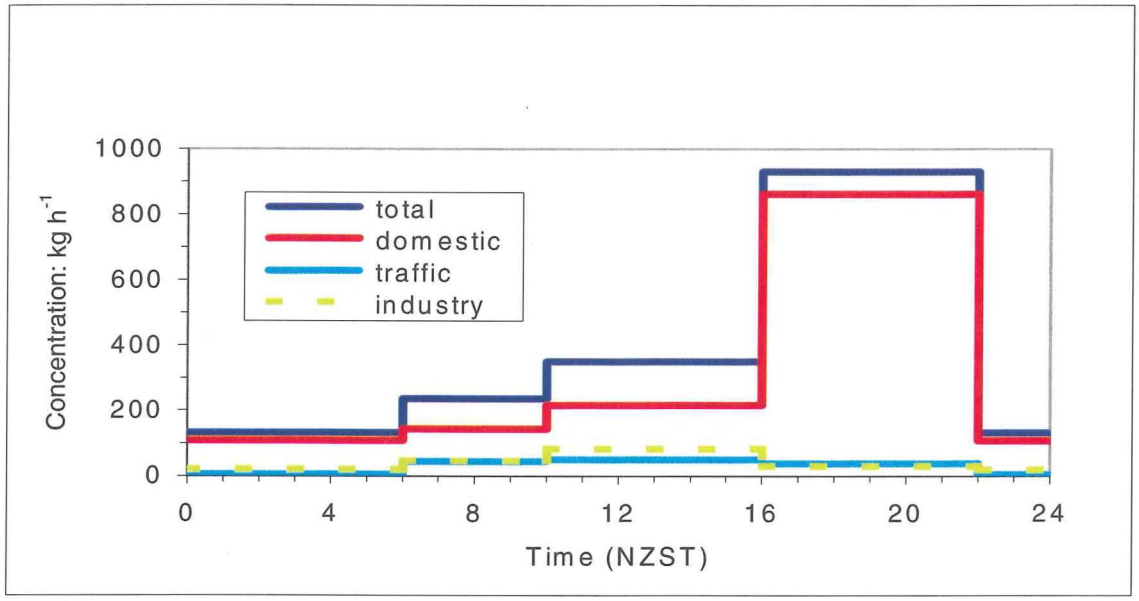

Figure 3.5 Contribution of domestic heating, traffic and industry to emissions of PM_{10} during winter 1999, Christchurch 25 suburbs area – 177.6 km^2 (after Spronken-Smith *et al.*, 2001).

The average 24-hour values of PM_{10} and CO measured during smog nights at the monitoring sites at Timaru Main School and at Coles Place, Christchurch are shown in Figure 3.6. The data in this figure illustrate the significant variations in air pollution and wind characteristics that can occur over relatively small distances across the city.

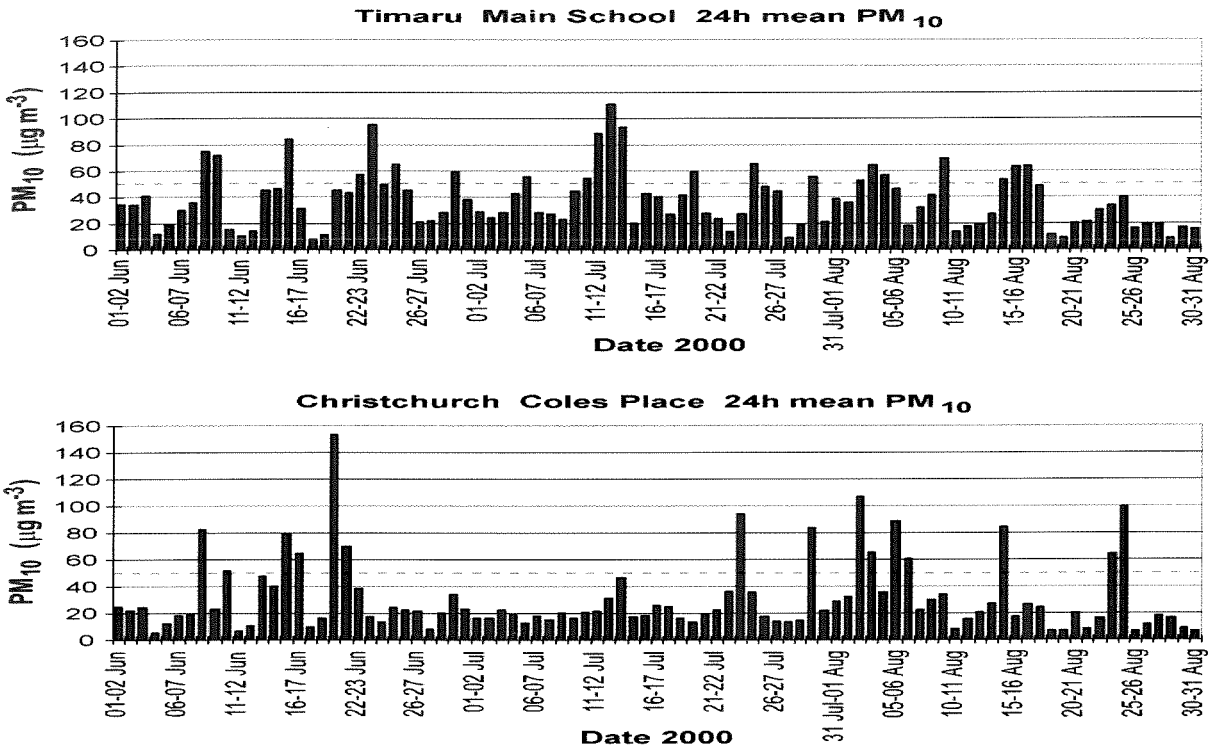

Figure 3.6 The 24-hour average PM_{10} concentrations for the period 1 June – 31 August 2000 measured at: a) Main School in Timaru, and b) Coles Place in Christchurch. The 50 $\mu g\ m^{-3}$ health guideline is indicated by a dashed line (after Ecan winter 2000 report).

Wind-rose maps show the characteristic airflow features that contribute to heavy smog winter nights in Christchurch, including the frequent development of weak westerly to northwesterly cold air drainage down the Canterbury Plains during night time and the Canterbury Plains northeasterly winds, which are stronger during daytime, but less frequent and much weaker towards the southern parts of coastal Canterbury (Kossmann and Sturman, 2002).

3.3.2 Possibilities of prediction and control of winter air pollution

Despite evidence of an air pollution problem since the 1880s, there has been little progress in ameliorating the problem, and effective air quality management strategies have yet to become operative. Early research on air pollution in Christchurch focused on smoke and sulphur dioxide as the main contaminants. Gray (1910) measured dissolved matter contained in rainwater at Lincoln, 20 km southwest of Christchurch city centre, while in the 1930s the Christchurch Sunlight League initiated measurements of the precipitation of solid matter, such as smoke.

In June 1954, systematic monitoring of sulphur dioxide began in central Christchurch, and this was extended in 1956 to include deposited particulate matter and smoke in a further three suburbs. Wilkinson (1959) was the first to show that the air pollution problem in Christchurch was clearly seasonal with a winter maximum, when pollutant concentrations

reached levels warranting serious consideration of their significance. Wilkinson's report initiated further research by the Christchurch Regional Planning Authority (1966), leading to a comprehensive city study of air pollution and associated fuel use from 1960–1964. Wilkinson's study found that pollution was more severe in residential areas, and that domestic fires produced double the amount of smoke compared to all other sources combined (industry, commercial and transport).

Despite having established the facts of air pollution in the mid-1960s, it was several years before the Clean Air Act (1972) was passed, and during this time significant improvements in air quality occurred. Moody (1983) discussed the findings of a three-year survey and noticed that a decline in solid fuel use for domestic heating had been matched by a decrease in the aerosol part of smoke concentrations. In 1988, a continuous air quality monitoring site was established in the residential suburb of St. Albans, just north of the central business district, to measure basic boundary layer meteorology and gas and aerosol (PM_{10}) pollutants. While monitoring in the St. Albans area continues to provide the main measurements of air pollution for Christchurch, three more sites in Beckenham, Hornby and Opawa were established in 1995 to identify spatial variability across the city. Since recordings began in St. Albans in 1988, the 24-hour average PM_{10} concentrations have exceeded the local guideline (50 $\mu g\ m^{-3}$) about 30 times each year on average.

The Christchurch City Council recently adopted a new motto for the city – 'Fresh Each Day', which is rather ironic given the continuing air pollution problem in winter. Although the maximum 24-hour concentrations of PM_{10} have decreased dramatically (from as high as 800–1300 $\mu g\ m^{-3}$ total suspended particulates in the late 1950s to 280–320 $\mu g\ m^{-3}$ PM_{10} in 2002–2003) they are still too high compared to World Health Organization standards, especially for the size of the city. Furthermore, the statistical 24-hour averages obscure extremely high hourly and 10-minute values that occur overnight (see Figures 3.4 and 3.5) that can be more than 400–500 $\mu g\ m^{-3}$ and influence dramatically health conditions of vulnerable sections of the Christchurch community. The methods of home heating were also assessed to determine which method contributed the most to particulate matter levels. Figure 3.7 indicates that the main emitters of PM are open fires and older woodburners. Given that urban Christchurch has an estimated 52,000 households using solid fuel burners the potential for significant air pollution from particulate matter is high.

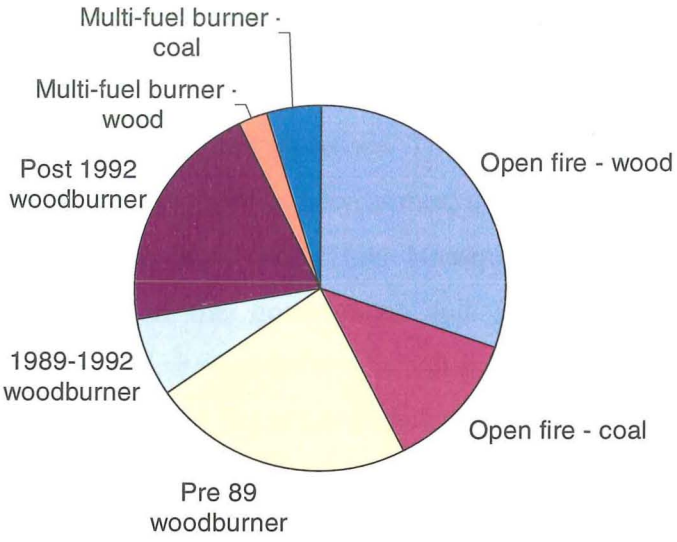

Figure 3.7 Contribution of different methods of home heating to total domestic emissions of PM_{10} (after Ecan annual report, 2000).

Concerns about the state of Christchurch's air quality have been raised since the 1930s and in 1959, Wilkinson concluded that although air pollution in Christchurch was not as serious as London, Los Angeles or Auckland (McKendry, 1989), there was sufficient pollution to warrant consideration of abatement measures. The Health Act (1956) and the Chemical Works Orders (1960s) resulted in the introduction of smoke restriction regulations by the Christchurch City Council. These regulations controlled fuel burning in industrial and commercial premises. The Clean Air Act 1972 was implemented by the City Council and the former Department of Health. Clean Air Zone Orders (1974 and 1984) established under this Act focused on domestic heating, as this was considered a significant source of air pollution. These orders prohibited the installation of open fires and restricted the installation of wood burners to models meeting the specifications set by the Council. There was an attempt by the City Council to establish a ban on the use of existing open fires that failed when the issue was taken to a public hearing, as the opponents of the bill described the ban as 'draconian' because of its social and economical consequences.

The introduction of the Resource Management Act (RMA) in 1991 gave Environment Canterbury (Ecan) the responsibility for air quality management in Christchurch. One of the methods specified in Ecan's Regional Policy Statement (RPS) was addressing air quality issues through an air chapter in a Natural Resources Regional Plan. The first draft of the Air Plan was released in 1998, including an air-quality target for PM_{10} of 50 $\mu g\ m^{-3}$ (24-hour average) and rules prohibiting the use of open fires, and requiring that solid fuel burners were replaced 15 years after installation. Also, in an attempt to reduce PM_{10} concentrations in Christchurch in a

shorter time frame, Environment Canterbury in 1997 publicly notified its intention to prohibit the use of coal for domestic heating. However, in mid-2000 Ecan decided against a coal ban because of the likely social and economic impacts on the community and the need for a financial assistance package to accompany any such processes. The latest proposed Air Plan involves a ban on the installation of solid fuel burners in new homes, a ban on the use of open fires from 2005, and a ban on the use of enclosed solid fuel burners if they are 15 years old, with appropriate financial support from the government and local government organizations. Whatever plan becomes operational, it appears that it will have an extremely long time frame, meaning that the air quality problem will remain in Christchurch for at least another 20–30 years.

The ultimate aim of air pollution research is to provide knowledge required to ameliorate air quality problems, including source apportionment using chemical analysis of aerosols and particulate matter, identifying the causes of reduced visibility, and evaluation of pollution sinks in the urban landscape (Baty, 1999).

There is also a major programme under way to investigate the role of boundary layer meteorology in Christchurch's air pollution problem in more detail. A key aspect of this initiative is the creation and fine-tuning of a numerical regional coupled (meteorological–chemical) model system (e.g. MM5–CAMx4), which will provide the city with the unique possibility of simulating the dispersion of air pollution (especially PM_{10}) across the urban landscape. A major outcome of this research will be the ability to provide short-time air pollution forecasts using a numerically coupled meteorological–chemical model system (de Haan *et al.*, 1998). Also, such a numerical system would allow prediction of the potential impact of proposed new industrial or residential development, as well as the effectiveness of proposed amelioration strategies through inclusion of differing pollution emission levels and origins of sources in the initial gridded concentrations for the chemical part of the MM5–CAMx4 numerical system. This project is being developed in parallel with an interdisciplinary Health Research Council funded project investigating in greater detail the links between air pollution and health in New Zealand (Dockerty and Pope, 1994; Foster, 1996). Part of this work involves the application of dispersion modelling techniques to mapping exposure of humans to air pollution across Christchurch and other New Zealand cities, as well as the relationship between indoor and outdoor air pollution in houses using a range of home heating methods. The main aim of such research programmes is to improve the scientific understanding that forms the basis of management strategies developed by national and regional authorities (Arya, 1999).

3.4 Summary

In the first part of this study, the mean synoptic situation over the South Island of New Zealand during wintertime is discussed, as well as the complexity of air circulation that is formed under the influence of complex orography and the surrounding ocean. The Christchurch area PBL air circulation is shown to depend not only on synoptic scale airflow, but furthermore from local air circulation in situations affected by ocean–land discontinuities, especially under wintertime stagnant synoptic situations.

The second part of the chapter provides a history of the air pollution problem in Christchurch and its vicinity, particularly during wintertime calm nights under temperature inversions. During winter months, the mean diurnal cycle of hourly averaged concentrations of particulate matter (< 10 μm in diameter–PM_{10}), the contribution of domestic heating, traffic and industry emissions to PM_{10}, and the different methods of heating to domestic emission of PM_{10} are discussed.

Chapter 4

Settings and methodology

4.1 Introduction

This chapter has a multi-purpose objective, although the main aims of it are to illustrate the ability of the limited area meteorological model MM5 to reproduce local air circulation over Christchurch using databases from the winters of 2000 and 2003, and to show what input fields are necessary for CAMx4 to simulate air pollution (especially the aerosol component of it) over the Christchurch region during winter. The settings and methodology of both models, as they are applied to the Christchurch region, will be shown in the context of global data assimilation by MM5, and in the context of regional databases of land use and air pollution that allow precise calibration and adjustment of both MM5 and CAMx4. The ability of MM5 to simulate the complex local air circulation observed in this region during cold calm winter nights is evaluated (Hauge and Hole, 2002).

The first part of the chapter is devoted to description of the main sources of input data for MM5 and CAMx4, and available regional observation information used for comparison with model output. The second part of the chapter describes the methods used in numerical experiments over the Christchurch area, including application of multi-nested grids for different physical and numerical parameterisation schemes of MM5. The last part of the chapter discusses the main possibilities of particulate matter (PM_{10}) modelling and some aspects of gaseous air pollution during wintertime in Christchurch. All the results of numerical modelling are compared with observations taken from data collection sites.

4.2 Controlling factors

4.2.1 Global data analysis

Input data in regular horizontal and vertical grids provide essential information for the evaluation of MM5, and the finer the resolution of input data (in the form of global model analysis) the greater the possibilities to utilize and adjust MM5 for fine scale reproduction of the air circulation over the Christchurch area. In this case, the vertical resolution of input data plays as important a role as horizontal resolution because baroclinic factors are expected to play a very significant role in the complex topographic influence on mesoscale air circulation over Christchurch (Sorteberg *et al.*, 2001).

Before choosing an appropriate Global Database (GD), the mesoscale modelling section of the Meteorological Service of New Zealand (Wellington) was consulted. As a result, global

analysis data of the NCEP Global Tropospheric Analysis (NCEP GTA) were used. The full description of the data is as follows: ds083.2 (dataset 083.2), collected 6-hourly, with 1 x 1 degree global coverage resolution, derived from the FNL (final) run of the global data assimilation model. This included use of additional observations that had been collected through at least six hours after the synoptic time, making the data more accurate and therefore more suitable for this research. The advantages of the ds083.2 data set for this application include:

1. Global coverage with quite fine 3-dimensional and time resolution
2. Database is written in GRIB format, that is one of the commonly used input meteorological data formats easily assimilated by MM5
3. Cheap price of the ds083.2 analysis data (only US$120 for 12 days of global meteorological information), compared to other global meteorological data centres, such as ECMWF
4. The possibility of fast download of the data via ftp (file translate protocol) from the NCEP site
5. The possibility to download free current analysis data for model testing, and the possibility to accumulate these data for future experiments (starting from 2004, ds083.2 data are available for any time period since the beginning of 2002 without any charge).

The basic parameters of the NCEP global tropospheric analysis dataset are:

1. 1 x 1-degree grid coverage (360 x 181 points) of the entire globe every six hours from 15 September 1999 to the present
2. Up to twenty-two 2- and 3-dimensional input meteorological variables, including the fundamental ones, such as wind, temperature and relative humidity fields
3. 26 vertical levels from the surface layer up to the mid-stratosphere top level of 10 hPa
4. Use of GRIB format as one of the basic MM5 regular input grid formats.

Two 12-day time periods of analysis data were purchased for winter 2000 (July and August), while nearly all the winter 2003 global meteorological data were freely downloaded and archived on disk.

4.2.2 *The CAPS2000 and winter 2003 field experiments*

The Christchurch Air Pollution Study 2000 (CAPS2000) was a major field campaign that was undertaken during winter 2000 to provide measurements of both meteorology and air pollution, with the main aim of improving the fundamental theoretical and practical knowledge of air pollution dispersion over Christchurch and surrounding small towns, and to evaluate modelling tools for use in air quality numerical modelling and management (Spronken-Smith *et al.,* 2002).

As shown in Chapter 3 (see Figure 3.2), synoptic scale westerly airflow frequently results in foehn winds and onshore northeasterly winds over the Canterbury Plains. In the initial stages of westerly wind events, the convergence zone between the north-westerly foehn and the north-easterly onshore flow is often found at some distance inland, whereas during the prefrontal final stage the convergence zone often moves out to sea (Sturman, 1986; Sturman *et al.*, 1984). Local circulations are superimposed on weak synoptic scale winds, producing diurnal variations associated with easterly sea breezes, and night-time decoupling of the offshore drainage winds and land see breezes is a characteristic mesoscale air circulation (Sturman and Tyson, 1981). Such features are typical of the mesoscale air circulation frequently associated with severe nocturnal smog events during cold and calm nights in Christchurch and other towns during the winter season, when the health guidelines are regularly exceeded. Before the CAPS2000 study, the wintertime wind field studies in Canterbury were mainly based on data composited from different years and did not focus on near-surface meteorological conditions during night smog events (McKendry, 1983; McKendry *et al.,* 1987), or they were limited to only parts of coastal Canterbury (Ryan, 1973; McGowan and Sturman, 1993; Chilton, 1999, pers.comm.).

Several large environmental research organisations took part in the CAPS2000 winter experiment, including the National Institute of Water and Atmospheric research (NIWA), the Geography Department of the University of Canterbury (Geography), Environment Canterbury (Ecan), Landcare Research, the University of Auckland, the Institute for Meteorology and Climate Research at the University of Karlsruhe (Germany), the Fire Weather Service (FWS), Meteorological Service of New Zealand (MetService), Christchurch City Council (CCC), and the Selwyn Plantation Board (SPB).

'A major field campaign was mounted in the Christchurch area in the winter of 2000, when meteorological data were collected using a network of 7 existing and 8 additional automatic weather stations' (Kossmann, Sturman, 2002, page 453) within the city (with standard wind, temperature and relative humidity sensors – see Figure 4.1), as well as two instrumented towers with two levels each measuring net radiation, temperature, relative humidity, and wind speed and wind direction. In addition, surface energy exchanges were measured over a suburban neighbourhood at one of the towers, and continuous vertical profiles of wind and atmospheric stability were obtained from a SODAR at another site. The observation programme ran from June to August with an intensive period during the month of July, when several special observation periods were undertaken. These involved measurements of vertical profiles of the atmosphere using radiosondes and tethered balloons.

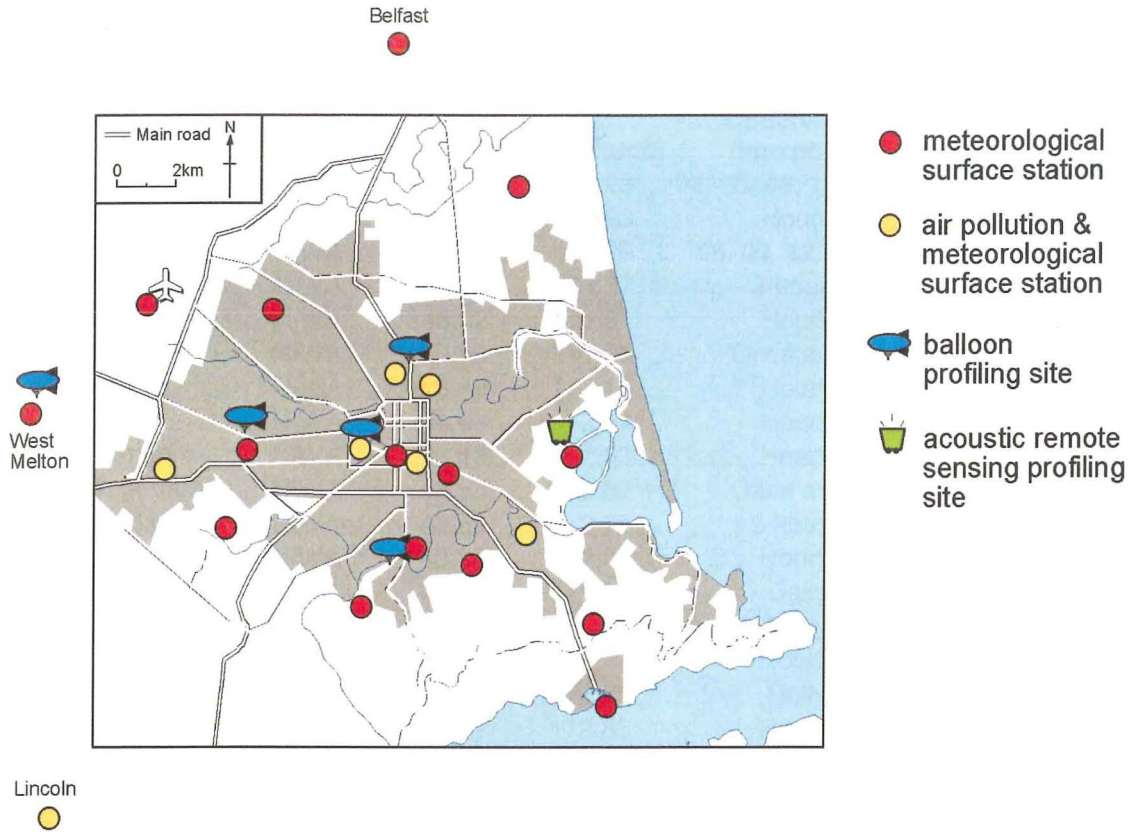

Figure 4.1 Network of observation sites in Christchurch during the winter period of CAPS2000 (after Sturman *et al.*, 2001).

A full list of place names and coordinates, with a list of meteorological measurements and time intervals, is provided in Table 4.1. The near-surface meteorological observations were made at various sites on the Canterbury Plains (not just in Christchurch and its suburbs) and at differing time frames (from daily to 10 minutes intervals). The sites located outside of Christchurch were at varying heights above sea level, especially those closer to the foothills of the Southern Alps (e.g. some NIWA and FWS sites).

July 2000 was the warmest on record with a mean temperature of 8.4^{0}C – two degrees higher than the long-term average (Sturman *et al.*, 2001). Warmer than usual nights resulted in a reduced incidence of frost, with only two air frosts recorded. Rainfall for the month was only 25% of normal and sunshine was 92% of normal.

Table 4.1 List of observation sites during CAPS200, where: T–Temperature, RH–Relative Humidity, U–zonal wind component, V–meridional wind component, DIR–wind direction, P–pressure, AP–air pollutant (after Titov, 2003, pers. comm.).

Place Name	Organi-sation	Latitude	Longitude	Observation time points	Measured meteorology
Timaru aero	NIWA	-44.32	171.23	02, 05, 06, 19, 20, 21	T, RH, U, V, DIR
Timaru aero	NIWA	-44.33	171.23	Hourly	T, RH, U, V, DIR
Timaru harbour	NIWA	-44.44	171.25	06, 09, 12, 15, 18	T, RH, U, V, DIR
Ashburton	NIWA	-43.91	171.77	3-hourly	T, RH, U, V, DIR
Winchmore	NIWA	-43.82	171.81	Hourly	T, RH, U, V, DIR
Hororata, Illiana	NIWA	-43.53	171.95	Once a day	T, RH, U, V, DIR
Darfield	NIWA	-43.49	172.15	Hourly	T, RH, U, V, DIR
Lincoln	NIWA	-43.63	172.47	Hourly	T, RH, U, V, DIR
Christchurch aero	NIWA	-43.48	172.53	Hourly	T, RH, U, V, DIR
Christchurch gardens	NIWA	-43.53	172.62	Once a day	T, RH, U, V, DIR
Lyttelton harbour	NIWA	-43.62	172.72	3-hourly	T, RH, U, V, DIR
Rangiora	NIWA	-43.33	172.61	Hourly	T, RH, U, V, DIR
Akaroa, rue Lavaud	NIWA	-43.83	172.97	Daily	T, RH, U, V, DIR
Waipara west	NIWA	-43.07	172.65	Daily	T, RH, U, V, DIR
Le bons bay	NIWA	-43.73	173.12	Hourly	T, RH, U, V, DIR
Culverden	NIWA	-42.77	172.85	Daily	T, RH, U, V, DIR
Hanmer forest	NIWA	-42.55	172.85	Hourly	T, RH, U, V, DIR
Kaikura	NIWA	-42.42	173.68	Hourly	T, RH, U, V, DIR
Hanmer springs	FWS	-42.33	172.47	Hourly	T, RH, U, V, DIR
Balmoral	FWS	-42.49	172.44	Hourly	T, RH, U, V, DIR
Lees valley	FWS	-43.83	172.11	Hourly	T, RH, U, V, DIR
Ashley	FWS	-43.17	172.36	Hourly	T, RH, U, V, DIR
Mount Somers	FWS	-43.42	171.23	Hourly	T, RH, U, V, DIR
Ashburton plains	FWS	-43.54	171.45	Hourly	T, RH, U, V, DIR
Snowdon	SPB	-43.27	171.39	Hourly	T, RH, U, V, DIR
Darfield	SPB	-43.29	172.68	Hourly	T, RH, U, V, DIR
Bottle lake	SPB	-43.62	172.41	Hourly	T, RH, U, V, DIR
Hororata forestry	FWS	-43.33	172.33	Daily	T, U, V, DIR
Agricultural park	Geography	-43.330	172.331	Hourly	U, V, DIR
Belfast	Geography	-43.268	172.375	Hourly	U, V, DIR
CCC, Tuam Street	CCC	-43.322	172.382	15 minutes	T, U, V, DIR, P
Colombo Street	Geography	-43.336	172.382	10 minutes	RH, T, U, V, DIR
Cracroft	Geography	-43.347	172.368	10 minutes	RH, T, U, V, DIR
Mount Vernon park	Geography	-43.342	172.396	Hourly	U, V, DIR
Canterbury University	Geography	-43.318	172.345	10 minutes	RH, T, U, V, DIR
West Melton	Geography	-43.286	172.237	10 minutes	RH, T, U, V, DIR
Woolston Jubilee park	NIWA	-43.333	172.408	Hourly	U, V, DIR
Bromley	Geography	-43.322	172.425	Daily	RH, T, U, V, DIR
Coles Place	Ecan	-43.305	172.382	Hourly	RH, T, U, V, DIR, **AP**
Polytechnic	Ecan	-43.323	172.388	Hourly	RH, T, U, V, DIR, **AP**
Hornby	Ecan	-43.326	172.311	Hourly	RH, T, U, V, DIR, **AP**
Packe Street	Ecan	-43.311	172.385	I0 minutes	RH, T, U, V, DIR, **AP**
Hagley park	Ecan	-43.317	172.369	Hourly, JUNE, JULY	RH, T, U, V, DIR, **AP**
Airport, Christchurch	Metservice	-43.331	172.332	850 hPa surface	U, V, DIR
New Brighton	Geography	-43.304	172.437	Hourly, JULY	RH, T, U, V, DIR, **AP**
Rangiora, Airdrome	Ecan	-43.176	172.311	10 minutes	RH, T, U, V, DIR, **AP**
Timaru, Airdrome	Ecan	-44.181	171.135	10 minutes	RH, T, U, V, DIR, **AP**
Ashburton	Ecan	-43.543	171.477	10 minutes	RH, T, U, V, DIR, **AP**
Jade Stadium	Geography	-43.326	172.393	10 minutes	RH, T, U, V, DIR
Greers Road	Geography	-43.326	172.393	10 minutes	RH, T, U, V, DIR

Unfortunately, some of the surface meteorological data collected did not cover the special observation periods of August 2000 when one of the two most significant smog events occurred (see Figure 3.6). There were also some errors in the CAPS2000 database, including such things as the non-precise location of a site, and errors in data entry to the spreadsheets. In spite of these minor problems, these data were sufficient to allow tuning of the meteorological regional model for winter circulation conditions over the Canterbury Plains and Christchurch area.

During winter 2003, a more focused examination of vertical profiles of both meteorological variables and PM_{10} was undertaken with the aim of investigating the layering of air pollution and its causes. Figure 4.1 shows the location of sites at which measurements of vertical profiles of the atmosphere were made using tethered balloons (English Park) and a Doppler SODAR wind profiler (Sound Direction And Ranging, at Bromley). Data were also available from the main meteorological and air pollution monitoring site at Coles Place (St. Albans) and 2 additional sites in Hoon Hay and Aranui, operated by Environment Canterbury.

4.2.3 Particulate monitoring sites and observations

As mentioned before, 'winter 2000 was somewhat unusual, with easterly airflow unusually dominant in northern Canterbury as a result of long persistent periods of synoptic scale easterly winds generated by frequent lows over the North Island and highs located near the southern end of the South Island (Johnstone, 2000)' (Kossmann and Sturman, 2002, page 454). Christchurch experienced an unusually low number of smog nights, and during winter 2000 there were only 21 days in Christchurch and 31 days in Timaru when the 24-hour mean concentration guideline of 50 $\mu g\ m^{-3}$ for PM_{10} was exceeded. This is in contrast to the average numbers of 30 and 19 exceedence days for Christchurch and Timaru, respectively. For the CAPS2000 measurement period of 1 June to 31 August 2000, only 15 and 22 exceedence days were monitored in Christchurch and Timaru, respectively (see Figure 3.6).

During the active winter period of CAPS2000, particulate and gaseous pollutants were measured at six locations throughout the city (Coles Place, the Polytechnic, Hornby, Packe Street, Hagley Park and New Brighton – see Table 4.1) operated by Ecan, with a time frequency of either 10 minute or 1-hour averages. Three of these sites (Coles Place, the Polytechnic and Packe Street) were operated permanently during the observation period from the 1st of June till the 31st of August 2000. The three other sites hold fragmentary information about near-surface PM_{10}, CO and NO_2 air pollution concentrations, which can be used only occasionally for very specific short-term studies.

The winter was warm and pollutant concentrations were much lower than the long term average, although the daily cycle of PM_{10} concentrations still showed the typical pattern of low

values during late afternoon and a rapid increase after sunset (from about 16:45 NZST) due to both an increase in emissions from traffic (around rush hour) and as domestic fires were lit in the evening. The reduced capacity for dispersion in the atmospheric boundary layer was also evident, with radiative cooling creating a dramatic reduction of mixing depth as nocturnal surface inversions developed in association with minimal vertical energy fluxes (due to strong stability and negative buoyancy), resulting in accumulation of aerosol and gaseous air pollution during night time (Figure 4.2).

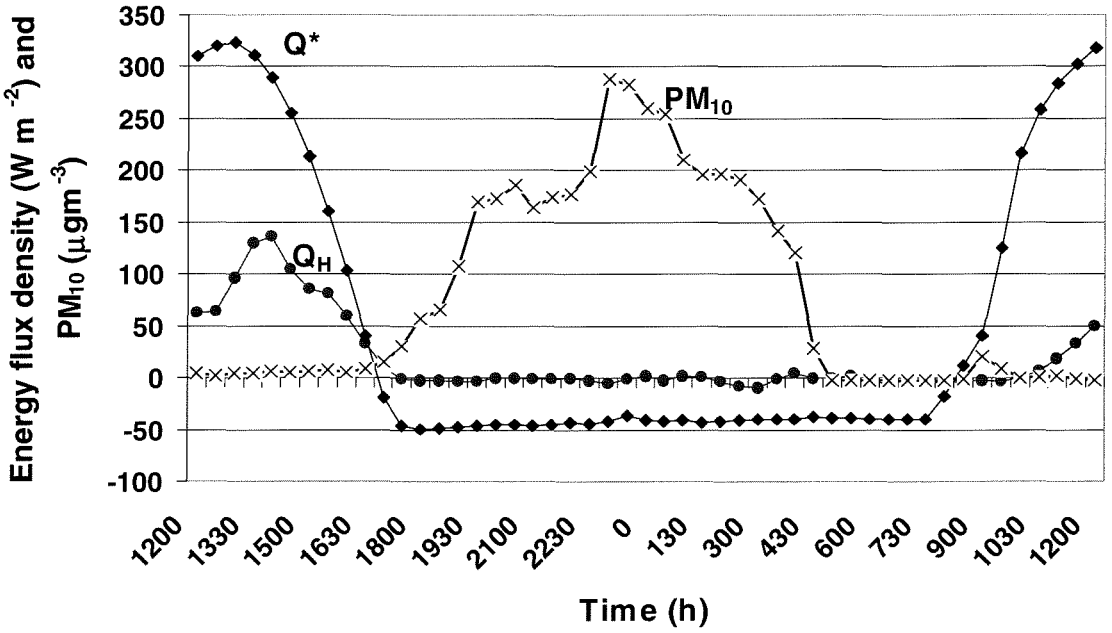

Figure 4.2 Vertical energy fluxes and PM_{10} for July 29-30, 2000, Coles Place (after Kossmann and Sturman, 2002).

From observations, the concentrations of PM_{10} increased through the night and typically peaked in the one to two hours before midnight, after which they started to decline as emission from domestic fires decreased (Figure 4.2). This example of an observed PM_{10} time trend from CAPS2000 stresses the complexity of the relationship between different meteorological and human factors in controlling the accumulation and redistribution of near-surface pollutants.

During winter 2003, three air pollution monitoring sites measured not only PM_{10} (and $PM_{2.5}$) concentrations, but also several gaseous pollutants including CO, NO, NO_2, SO and SO_2. A GRIMM particle sampler was also carried on a tethered balloon (Figure 4.3) that was operated at English Park in late July, providing vertical profiles of particulate material and meteorological variables in the PBL (Sturman *et al.*, 2003). These were also used to compare with results from the MM5–CAMx4 numerical modelling system.

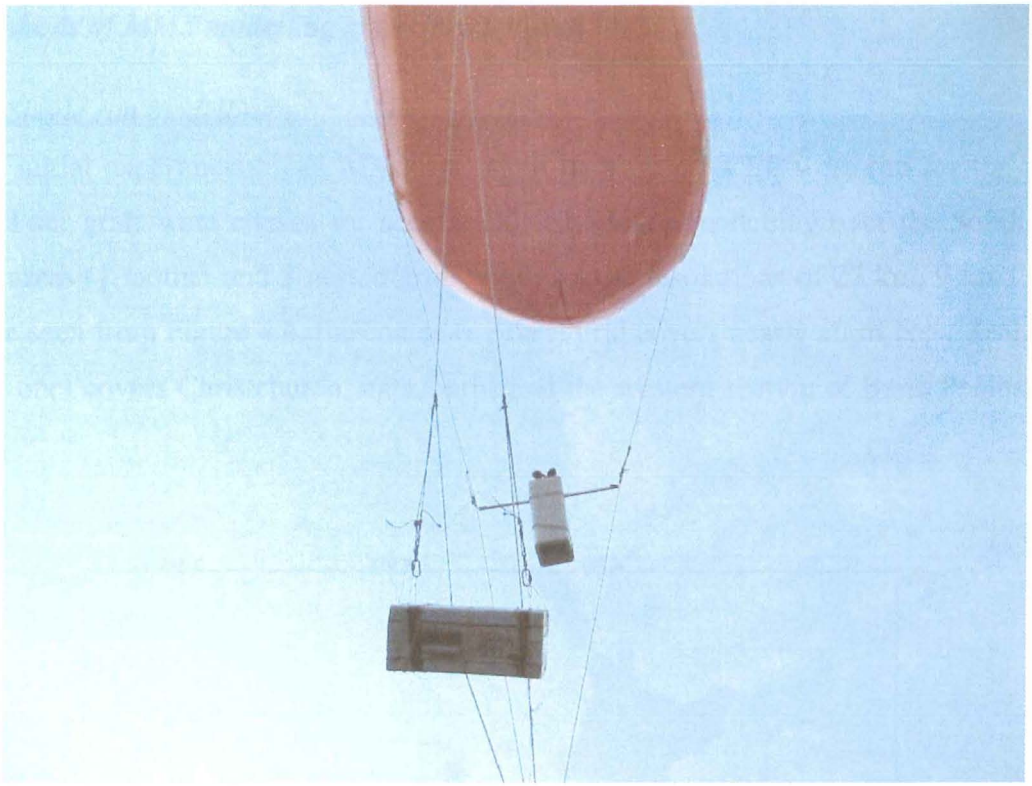

Figure 4.3 A GRIMM particle sampler and tethersonde carried on a tethered balloon at English Park, 21 July 2003 (after Sturman *et al.,* 2003, pers.comm.).

4.2.4 The Air Pollution Model (TAPM) output

As an additional opportunity to evaluate the MM5-CAMx4 modelling system output for particulate matter (PM_{10} and $PM_{2.5}$) against other sources of modelled data, an inter-comparison of MM5-CAMx4 output with output of The Air Pollution Model (TAPM) (from the Commonwealth Industrial and Research Organization CSIRO, Australia) was also undertaken. TAPM is a limited area numerical modelling system and it predicts three-dimensional meteorology and air pollution concentrations. Technical details of the model equations, parameterisation and numerical methods are described in a technical paper by Hurley (2002). A summary of some verification studies using TAPM is also provided. TAPM has a PC-based Graphic User Interface (GUI) that allows the user to set up and run the model under the Windows 98/ME/NT4/2000/XP operating systems. It is connected to databases of terrain, vegetation and soil type, sea-surface temperature, and synoptic-scale meteorological analyses for various regions around the world. Model output can be analysed using a graphic user interface and can be used for comparison with MM5 (MM5–CAMx4) outputs by calculating an Index Of Agreement (IOA) as well as systematic and unsystematic root mean square errors for both modelling systems in comparison with observation data.

4.3 Methods of MM5 modelling over Christchurch

4.3.1 Single run modelling with all nested grids

Several initial experiments with MM5 and input data from NCEP were run for the mother and nested grids. Four grids were chosen for accurate air circulation modelling over the South Island and Christchurch areas (1 mother and 3 nested grids) with spatial resolutions of 27 km, 9 km, 3 km and 1 km. As can be seen from Figure 4.4, the coarse (mother) grid covers nearly all of New Zealand and the 4th (the finest one) covers Christchurch, its suburbs and the western section of Bank Peninsula (Jacobs *et al.,* 1995).

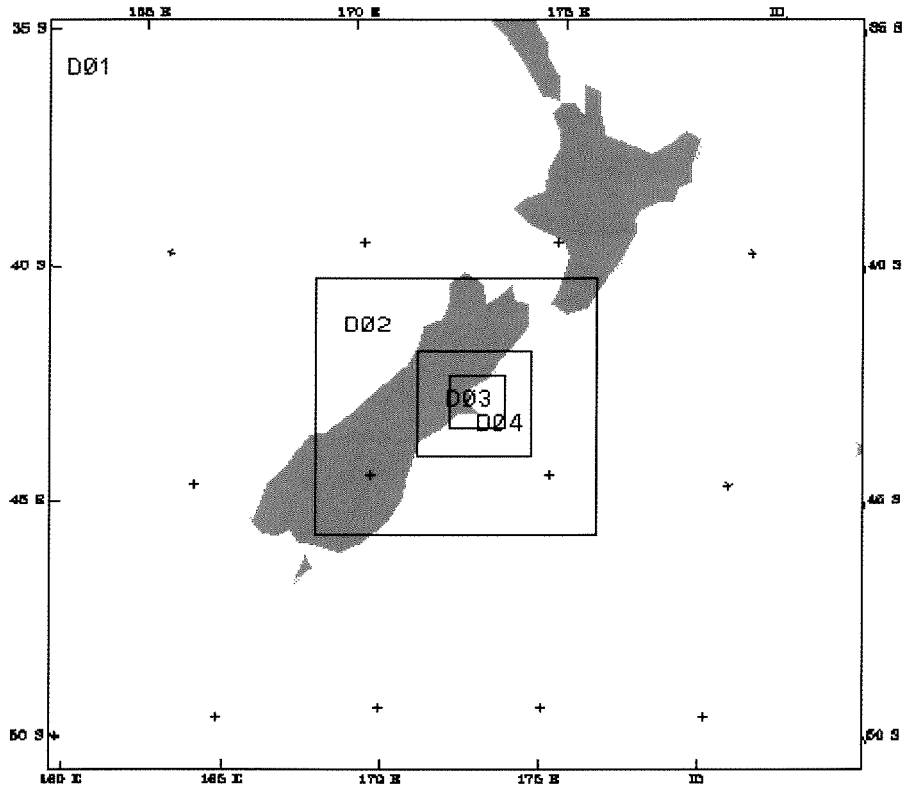

Figure 4.4 Coarse (outer or mother) grid and 3 nested (daughter) MM5 grids (RIP, MM5).

The centre of all 4 grids was pinpointed on the University of Canterbury in Christchurch, with latitude φ = - 43°.3183 and longitude λ = 172°.345. The total number of spatial nodes for every grid remains constant throughout the research. The respective values are as follows: grid 1 (27 km resolution) – 65 x 65 nodes, grid 2 (9 km resolution) – 67 x 67 nodes, grid 3 (3 km resolution) – 82 x 82 nodes, and grid 4 (1 km resolution) – 121 x 121 nodes. Spatial resolution of every grid is a constant and agrees with grid number (for example, grid 3 has 3 km resolution) to compare with domain number. Domain number depends of an actual MM5 run and can vary from four (for grid 4) if all 4 grids start together (4 domains–4 grids) in one experiment to one

(for grid 4) if only one domain (domain with 4th grid) takes part in the experiment. So a number of domain depends of an actual MM5 experiment and can varies in different MM5 runs.

For all four grids, information regarding orography and landuse distribution was taken from the United States Geological Survey (USGS) global database and interpolated regularly over all four grids. Different resolution input databases were used to represent orography for the different resolution grids: from 30-minute resolution for grid 1 up to 2-minute resolution for grid 4 (an example of interpolated orography for grid 4 is shown in Figure 4.5). The difference between real orography and the interpolated one is not more than a 25% reduction of mean height in modelled topography, resulting from application of the mean square procedure and the process of interpolation. In the USA, it is possible to use the 30-second global database of USGS, but this information is not extended to other countries. In future, it will be possible to improve the representation of initial orography by deriving height information using GIS techniques.

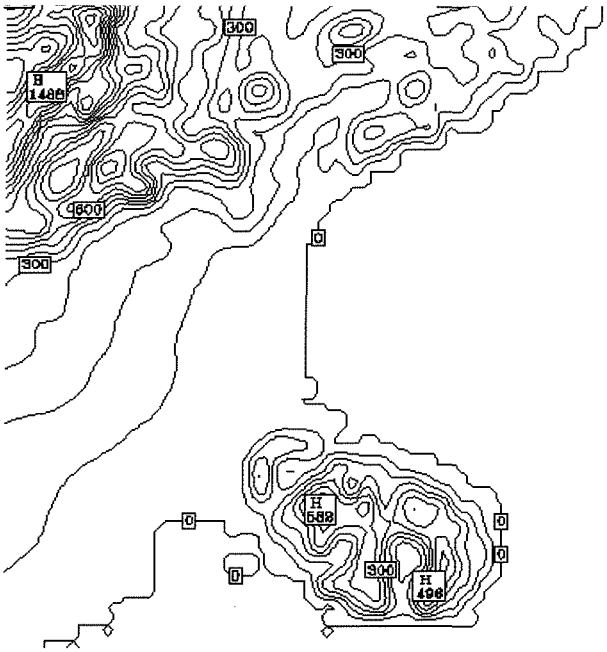

Figure 4.5 Interpolated 2-minute global database topography for grid 4 (RIP, MM5).

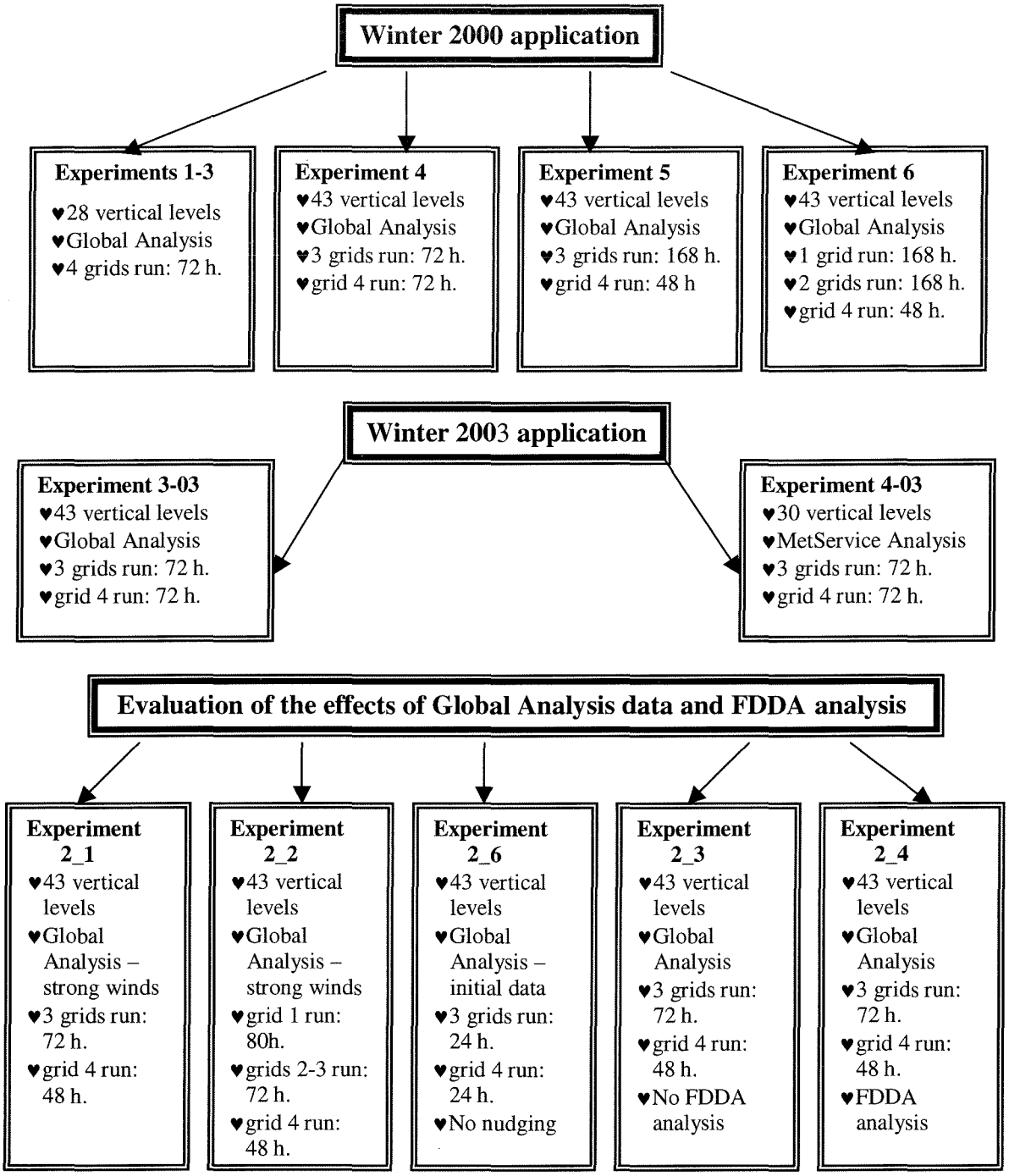

Figure 4.6 Overview of the logical standing of the modelling programme used in the thesis.

In Figure 4.6 is presented a scheme of the modelling programme and the overview of the logical standing of the experimental sequence used in the thesis with specification of particulars of every experiment. In Table 4.2, all experiments described in Chapter 4 are listed with additional information about input–output meteorological data for every experiment.

Table 4.2 List of MM5 experiments described in Chapter 4 with additional information about: domain number to be run (2 means domain 2 of MM5); origin of meteorological observations (FWS–Fire Weather Stations, Geography–the Department of Geography, the University of Canterbury, NIWA–National Institute of Water and Atmosphere research, CCC–Christchurch City Council, Ecan–Environment Canterbury, Towers–Stadium observation mast points, Geography); nudging time interval during MM5 runs; origin of input meteorological data (DS 083.2–NCEP Global Analysis, MS – Meteorological service, Wellington, Domain 3 – from mother grid); and output dump frequency during MM5 domain run.

Experiment Name	Domain Number	Observations Origin	Nudging Frequency	Origin of Nudging Data	Output Frequency
Experiments 1-3	2 & 3	NIWA, Ecan, Geography, FWS, SPB	6-hourly	DS 083.2	6-hourly
Experiment 4a	4	Geography, Ecan	3-hourly	DS 083.2	Hourly
Experiment 4b	4	Geography, CCC	3-hourly	DS 083.2	Hourly
Experiment 4c	2 & 3	NIWA, SPB	3-hourly	DS 083.2	Hourly
Experiment 4d	4	Towers – Geography	3-hourly	DS 083.2	Hourly
Experiment 4x1a	4	Geography, Ecan	3-hourly	Domain 3	Hourly
Experiment 4x1b	4	Geography, CCC	3-hourly	Domain 3	Hourly
Experiment 4x1c	2 & 3	NIWA, SPB	6-hourly	DS 083.2	Hourly
Experiment 4x1d	4	Towers – Geography	3-hourly	Domain 3	Hourly
Experiment 5a	4	Geography, Ecan	Hourly	Domain 3	Hourly
Experiment 5b	4	Geography, CCC	Hourly	Domain 3	Hourly
Experiment 6a	4	Ecan Geography, CCC	6-hourly	Domain 2	Hourly
Experiment 6b	4	Ecan Geography, CCC	3-hourly	Domain 3	Hourly
Experiment 3-03a	4	Coles Place	3-hourly	Domain 3	Hourly
Experiment 3-03b	4	Hoon Hay	3-hourly	Domain 3	Hourly
Experiment 3-03c	4	Aranui	3-hourly	Domain 3	Hourly
Experiment 4-03a	4	Coles Place	3-hourly	Domain 3 – MS	Hourly
Experiment 4-03b	4	Hoon Hay	3-hourly	Domain 3 – MS	Hourly
Experiment 4-03c	4	Aranui	3-hourly	Domain 3 – MS	Hourly
Experiment 2_1a	3	NIWA, Geography, Ecan, SPB	6-hourly	DS 083.2	Hourly
Experiment 2_1b	4	Geography, Ecan, CCC	Hourly	Domain 3	Hourly
Experiment 2_2	4	Geography, Ecan, CCC	Hourly	Domain 3	Hourly
Experiment 2_6	4	Geography, Ecan, CCC	24-hourly	Domain 3	Hourly
Experiment 2_3	4	Geography, Ecan, CCC	3-hourly	Domain 3	Hourly
Experiment 2_4	4	Geography, Ecan, CCC	3-hourly	Domain 3	Hourly

In the first three experiments (experiments 1, 2 & 3), the main purpose was to model the local circulations that develop over the Christchurch region during relatively stagnant synoptic situations. The daily cycle of wind direction changes resulting from the collective effects of local topographical factors on the atmospheric boundary layer have to be simulated. For the first three experiments, 28 vertical levels were used in MM5 for all 4 grids with the top σ-level equal to 100 hPa (about 12.5 km above mean sea level) and output meteorological information was damped 6-hourly for all 4 grids to compare with observed results. However, MM5 was not able to clearly reproduce the 24-hour wind direction cycle from easterlies to north-westerlies, and vice versa. To resolve this problem, additional levels were included in experiment 4, with a total number of 43 vertical levels. The levels are (in hPa): 1000, **998**, **995**, **990**, **985**, **980**, 975, **970**, **965**, **960**, **955**, 950, **940**, **925**, **910**, 900, 875, 850, 835, 800, 785, 750, 725, 700, 650, 625, 600, 550, 500, 450, 400, 350, 300, 250, 200, 150, 125, 100, **70**, **50**, **30**, **20**, **10** (additional levels are

marked **bold**). The number of vertical levels in the PBL was increased to 12, and an additional five upper tropospheric-lower stratospheric levels were used with the top σ-level equal to 0.010 (approximately 36 km above mean sea level) to create a 'deep' atmosphere. The increased number of vertical levels in the PBL was planned not only to increase model resolution in the BL, but also to help resolve daily observations of positive and negative peaks of near-surface modelled temperature that were very important for the realistic simulation of near-surface wind field magnitude (via a localised thermal wind effect).

Evaluation of the four grids in the experiment was undertaken in the following way:

1. Calculation of the first three grids with resolutions 27, 9 and 3 km after 72 hours of simulation time, with all three grids starting at the same time ('cold' start) at 1200 UTC on 31 July 2000 (0000 NZST on 1 August 2000) and finishing all together at 1200 UTC on 3 August 2000 (0000 NZST on 4 August 2000)
2. Fourth grid started at 1200 UTC on 1 August 2000 (0000 NZST 2 August 2000) with a 24 hours spin up period
3. Two-way interaction between mother and daughter grids for all levels of nesting during the whole run, with the output information dumped hourly for grids 3 and 4 (the finest ones)
4. Grids 1–3 are nudged by global data analysis every six hours and the 4th domain is nudged 3-hourly.

The experiment was run with the following MM5 parameterisation of physical processes:

1. Explicit moisture scheme is Dudhia's simple ice scheme for all 4 domains
2. Cumulus parameterisation is the Kain-Fritsch scheme one for domains one and two, and cumulus parameterisation is switched of in grids 3 and 4
3. Boundary layer parameterisation is the MRF PBL scheme (see Chapter 2) for domains 1 and the Blackadar scheme for the other three domains (for all nested grids)
4. Radiation scheme – cloud-radiation scheme for all 4 grids
5. Five-layer soil model with bucket soil moisture scheme in all 4 domains
6. Roughness model is Zilitinkevich's scheme.

The first three domains started at 1200 UTC on 31 July 2000 and the fourth domain started 24 hours later at 1200 UTC on 1 August 2000, and all domains finished at 1200 UTC on 3 August 2000. Accumulated central processor time to run the experiment was more than 300 hours on the Sun workstation 'Tornado'.

Results: The wind fields presented in Figure 4.7 result from the MM5 run for domain 4 (nested grid 3) for σ-level=0.999 (that is approximately 7.0–8.5 metres above surface topography) for two time points of the experiment: at 1700 NZST on 3 August 2000, showing daytime easterly–northeasterly winds over the Christchurch area (the daytime breeze circulation

– Figure 4.7a) and at 0000 NZST on 4 August 2000 with obvious westerly–southwesterly near-surface winds (the nocturnal breeze and drainage circulation – Figure 4.7b).

a) **b)**

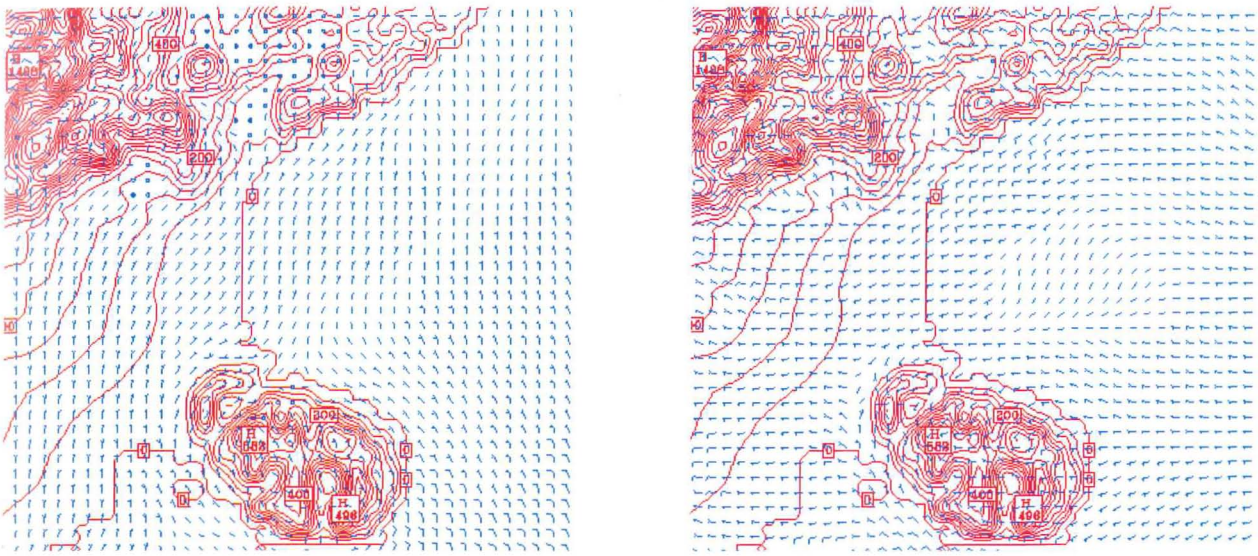

Figure 4.7 Spatial distribution of MM5 modelled near-surface wind for experiment 4, grid 4, σ = 0.999 (7.0-8.5 metres): a) at 1700 NZST on 3 August 2000 (41 hour forecast); and b) at 0000 NZST on 4 August 2000 (48 hour forecast).

The ability of MM5 to model rapid day-night changes of near-surface wind direction was evaluated using a 'deep' atmosphere during the fourth model run, with additional vertical levels in the PBL and upper troposphere–lower stratosphere. This step allowed more realistic replication of the mesoscale baroclinity of the real atmosphere corresponding to orographic–thermal effects over very complex terrain in the Christchurch area. Figure 4.8 shows vertical profiles of dry-bulb (red line) and dew-point (green line) temperatures, and wind as a function of height derived from MM5 modelled output for a point at Christchurch Airport (domain 4) at 1700 NZST on 3 August 2000 (daytime dry-bulb temperature profile – red one in Figure 4.8a) and at 0000 NZST on 4 August 2000 (night time dry-bulb temperature profile with negative height buoyancy – Figure 4.8b). Diurnal and nocturnal modelled temperature profiles (Figures 4.8a & 4.8b respectively) confirm the ability of MM5 to reproduce daytime temperature lapses with height and nighttime temperature inversions in Christchurch for fine grids (domains 3 and 4).

a) b)

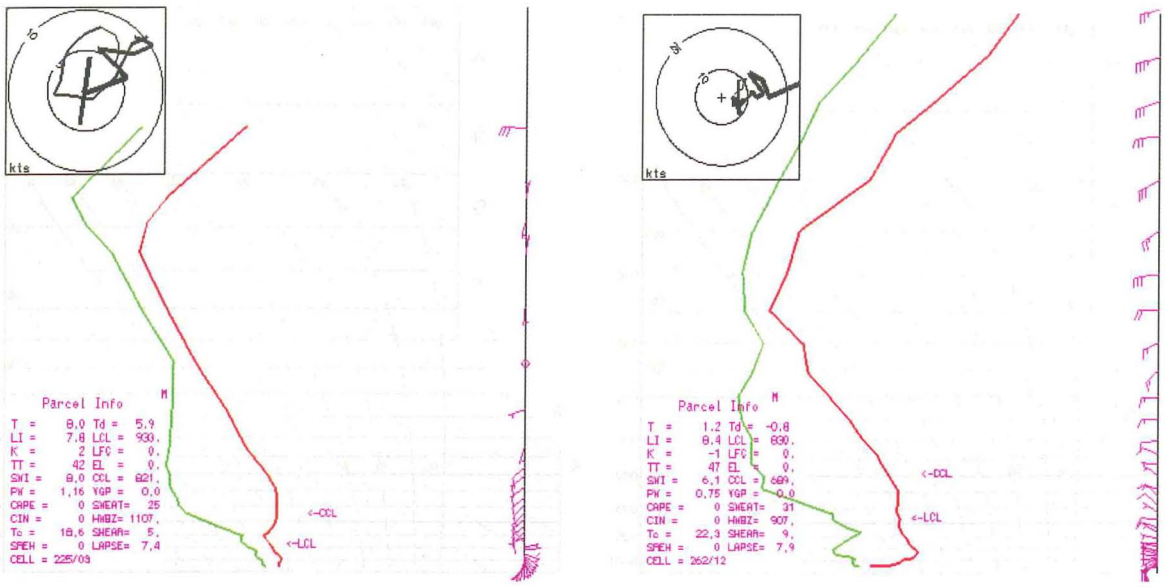

Figure 4.8 Vertical profiles of wind direction, and modelled dry-bulb (red) and dew-point (green) temperatures for experiment 4, grid 4: at a) 1700 NZST on 3 August 2000 (41 hour forecast); b) 2400 NZST on 3 August 2000 (48 hour forecast).

The Index of Agreement (IOA) between modelled and observed data was calculated and additional statistics used to compare more accurately the modelled near-surface fields of wind, temperature and relative humidity (for grid 4 with 1 km spatial resolution) with the observation sites established over the Christchurch area for CAPS2000. The special program package *MM5toGrADS* was applied to obtain time variations of the basic near-surface meteorological variables at fixed points coinciding with the location of observation sites during the intensive winter period of the CAPS2000. Additional statistics include total number of observation (in space and time) points compared with modelled results for the same space coordinates and the same time (TOTAL NUMBER of OBSERVATIONS), mean observed and modelled values (OBSERVED MEAN, MODELLED MEAN), the standard deviation from the mean of the observed and modelled data (OBSERVED DEVIATION, MODELLED DEVIATION), Pearson correlation coefficient between observed and modelled meteorological spatial information for the same site (PCC), and systematic and unsystematic (stochastic) root mean square errors (RMSE) between modelled and observed data (S-RMSE, U-RMSE). The Index Of Agreement (IOF) provides the most important assessment of reliability of the modelled data (Willmot *et al.*, 1985) and was applied to compare observed modelled spatial variations of wind speed, zonal (U) and meridional (V) components of near-surface wind, temperature and relative humidity (Rostkier-Edelstein *et al.*, 2002). All this information is shown in Table 4.3 for 12 surface observation sites

(see Table 4.2) that were operated during CAPS2000 by Environment Canterbury, the Geography Department of the University of Canterbury and the Christchurch City Council.

Table 4.3 Index Of Agreement (IOA), Pearson Correlation Coefficient (PCC), Systematic & Unsystematic Root Mean Square Errors (S-RMSE & U-RMSE), and additional statistics for observed-modelled data for the time period from 0000 NZST on 2 August 2000 to 0000 NZST on 4 August 2000: near-surface wind (m/s), temperature (^{0}C) and relative humidity (%).

EXPERMENT	NUMBER OF OBSERATIONS	OBSERVED MEAN	MODELLED MEAN	OBSERVED DEVIATION	MODELLED DEVIATION	PCC	S-MSE	U-RMSE	IOA
WIND SPEED (m/s)									
Experiment 4a	643	1.5	1.2	0.9	1.1	0.78	0.50	0.55	0.77
Experiment 4b	305	1.6	1.3	1.2	1.5	0.89	0.61	0.66	0.73
AVERAGE	**474**	**1.4**	**1.3**	**1.0**	**1.3**	**0.83**	**0.76**	**0.83**	**0.75**
U-COMPONENT (m/s)									
Experiment 4a	643	0.3	0.7	2.4	2.4	0.80	1.15	1.25	0.74
Experiment 4b	305	0.2	0.3	1.4	1.5	0.78	0.78	0.80	0.67
AVERAGE	**474**	**0.3**	**0.5**	**1.9**	**2.0**	**0.79**	**1.14**	**1.27**	**0.71**
V-COMPONENT (m/s)									
Experiment 4a	643	0.0	0.0	1.5	1.8	0.68	0.86	0.92	0.71
Experiment 4b	305	0.0	0.2	0.8	0.7	0.71	0.33	0.35	0.65
AVERAGE	**474**	**0.0**	**0.1**	**1.1**	**1.3**	**0.70**	**0.86**	**0.96**	**0.68**
TEMPERATURE (^{0}C)									
Experiment 4a	460	3.3	0.7	4.1	3.6	0.85	2.02	2.13	0.69
Experiment 4b	306	3.8	1.4	4.2	3.8	0.77	1.98	2.56	0.68
AVERAGE	**383**	**3.5**	**1.1**	**4.2**	**3.7**	**0.81**	**2.00**	**2.35**	**0.69**
RELATIVE HUMIDITY (%)									
Experiment 4a	460	76.6	76.5	15.7	14.4	0.86	5.81	6.02	0.68
Experiment 4b	306	78.5	75.9	15.6	15.8	0.83	5.78	6.24	0.71
AVERAGE	**383**	**77.6**	**76.2**	**15.7**	**15.1**	**0.85**	**5.80**	**6.13**	**0.70**

IOA is quite good (0.75) for wind speed and wind components (0.71–0.68). IOA and Pearson correlation coefficients are quite good for near-surface temperature (0.69 and 0.80) and relative humidity (0.70 and 0.85), but modelled temperature time trends corresponding to observation points showed underprediction of daytime (night-time) near-surface temperature maxima (minima), underestimation of modelled wind speed and overestimation of relative humidity. In Figure 4.9, modelled near-surface wind speed, wind direction and temperature

values (black empty circles) taken from MM5 output are compared with the observation data values (red crosses) obtained from the Coles Place measuring site of Environment Canterbury in Christchurch for 60 hours modelling for early August 2000. Modelled data are obtained from experiment 4 with hourly damping of output MM5 results.

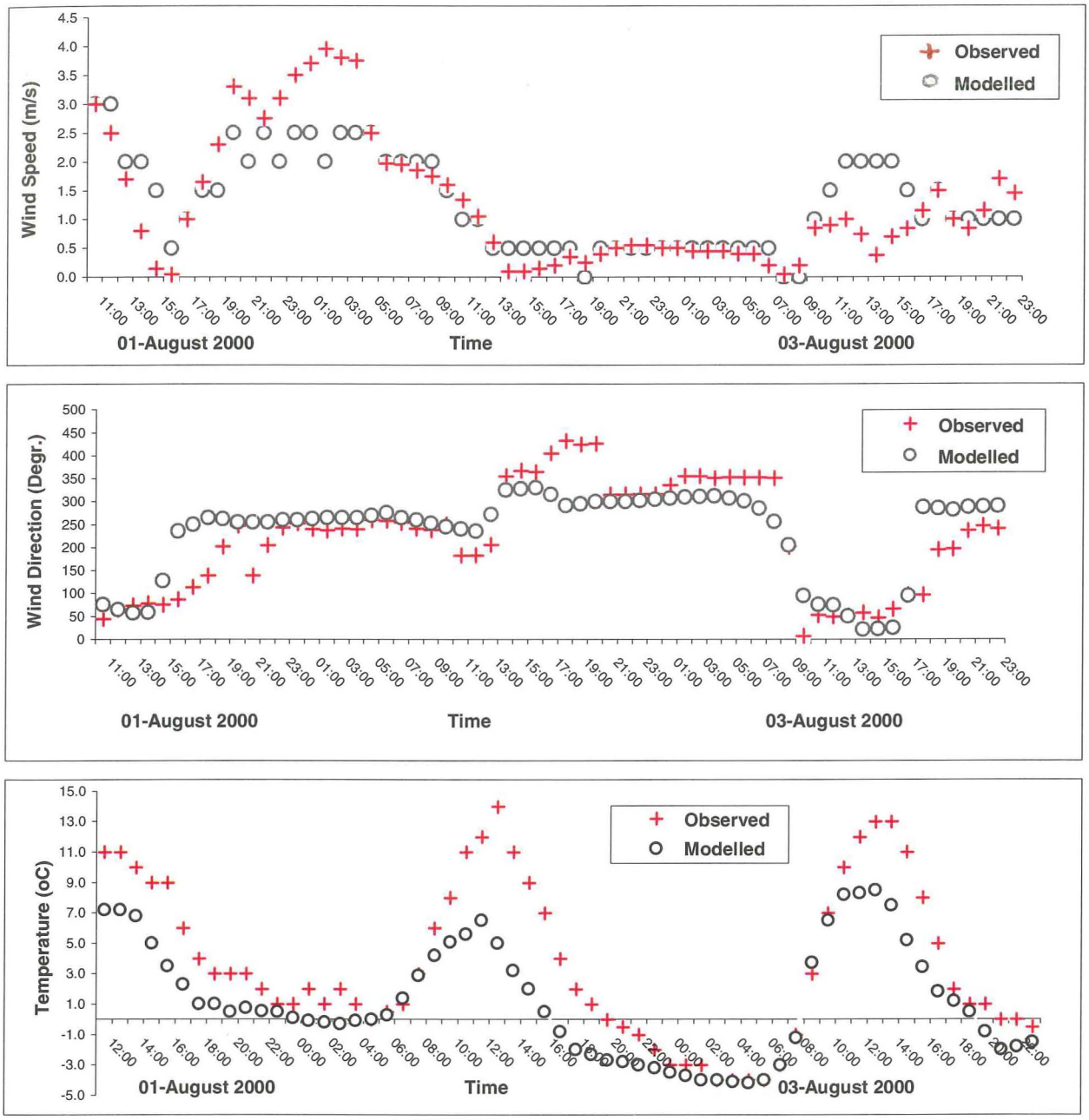

Figure 4.9 Modelled (open circle) and observed (red cross) wind speed, wind direction and near-surface temperature compared for Coles Place: experiment 4, domain 4, using CAPS2000 data from 1200 NZST on 1 August 2000 to 0000 NZST on 4 August 2000.

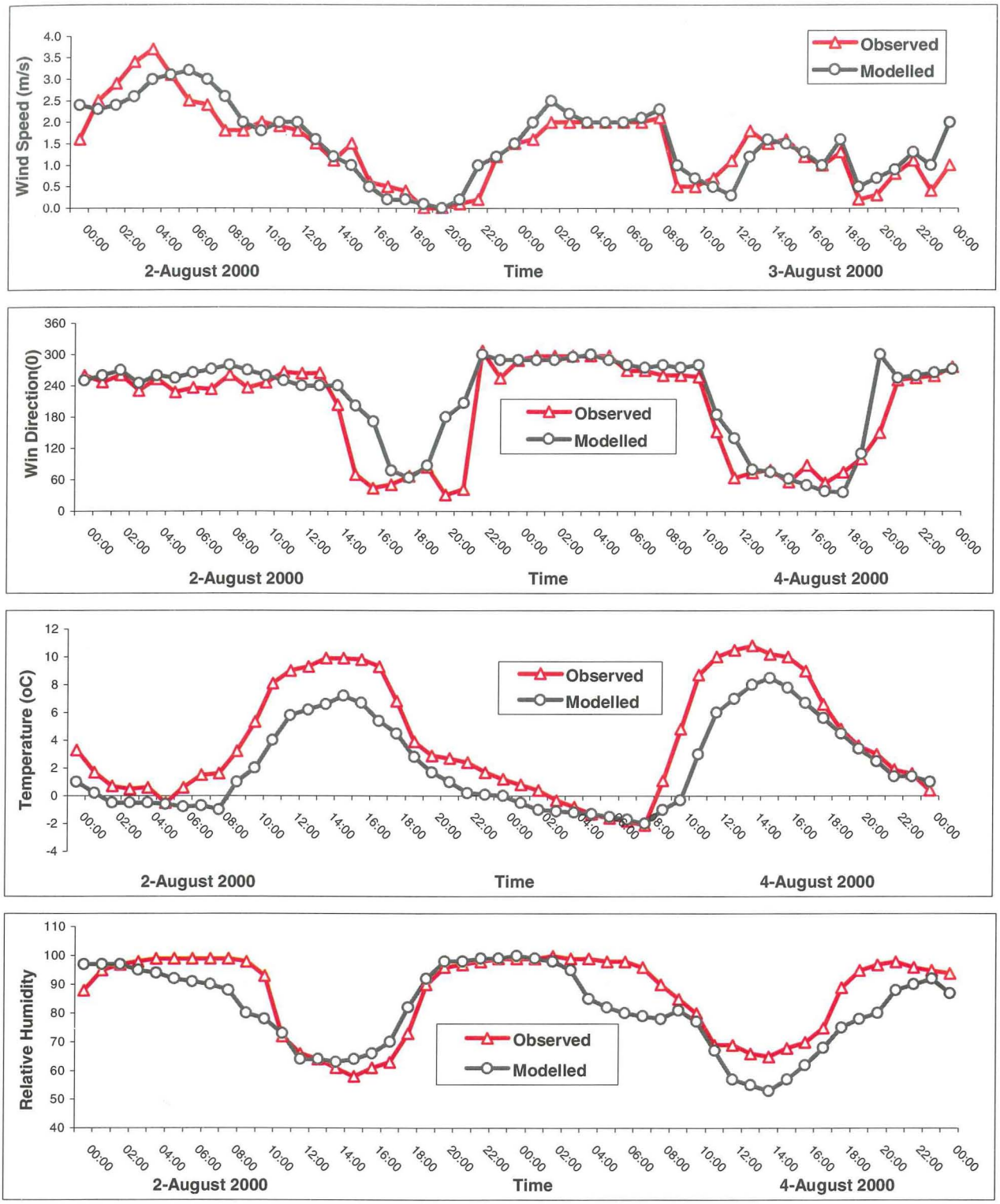

Figure 4.10 Time series of wind (wind speed-m/s & wind direction-degrees), temperature (^{0}C) and relative humidity (%), compared with observations at Colombo St.: experiment 4, grid 4, σ=0.999 (7.0–8.5 metres), using CAPS2000 data from 0000 NZST on 2 August 2000 to 0000 NZST on 4 August 2000.

Modelled and observed values of the near-surface wind speed, wind direction, temperature and relative humidity for the Colombo Street observation site (CAPS2000, the Department of Geography) for the time period 0000 NZST on 2 August 2000 to 0000 NZST on 4 August 2000

are compared in Figure 4.10. The modelled meteorological time trends were obtained from grid 4 by application of the special MM5 plotting package *MM5toGrADS*. The good fit of MM5 results is shown by the ability of the modelled wind direction (black circles) to follow the rapid westerly to easterly wind direction change observed at the measurement site (red triangle line).

General results of three MM5 experiments compared with the observations of all available observation sites (hourly and 6-hourly) during CAPS2000 over the Canterbury Plains for the time period from 0000 NZST on 1 August 2000 to 0000 NZST on 4 August 2000 are shown in Table 4.4. The results of MM5 grids 2 and 3 (spatial resolution 9 km and 3 km respectively) were also used to compare with observed data for points outside the Christchurch area (see Table 4.2).

Table 4.4 Index Of Agreement (IOA), Pearson Correlation Coefficient (PCC), Systematic & Unsystematic Root Mean Square Errors (S-RMSE & U-RMSE), and additional statistics for observed-modelled data for the time period 0000 NZST on 1 August 2000 to 0000 NZST on 4 August 2000 for experiments 3-4: near-surface wind (m/s), temperature (^{0}C) and relative humidity (%).

EXPERMENT	NUMBER OF OBSERATIONS	OBSERVED MEAN	MODELLED MEAN	OBSERVED DEVIATION	MODELLED DEVIATION	PCC	S-MSE	U-RMSE	IOA
WIND SPEED (m/s)									
Experiment 3	320	2.3	2.1	2.3	2.4	0.89	0.31	1.08	0.94
Experiment 4a	643	1.5	1.2	0.9	1.1	0.78	0.50	0.55	0.77
Experiment 4b	305	1.6	1.3	1.2	1.5	0.89	0.61	0.66	0.73
Experiment 4c	650	2.2	2.4	1.4	1.7	0.79	0.27	1.04	0.87
Experiment 4d	366	2.1	2.2	1.2	1.6	0.70	0.10	1.17	0.81
AVERAGE	**457**	**1.9**	**1.8**	**1.4**	**1.6**	**0.81**	**0.36**	**0.90**	**0.82**
U-COMPONENT (m/s)									
Experiment 3	320	0.5	1.0	2.5	2.4	0.53	1.36	2.08	0.74
Experiment 4a	643	0.3	0.7	2.4	2.4	0.80	1.15	1.25	0.74
Experiment 4b	305	0.2	0.3	1.4	1.5	0.78	0.78	0.80	0.67
Experiment 4c	650	0.8	1.2	1.9	2.2	0.70	0.52	1.58	0.83
Experiment 4d	366	-0.1	0.6	1.8	2.0	0.69	0.85	1.46	0.80
AVERAGE	**457**	**0.3**	**0.7**	**2.0**	**2.1**	**0.64**	**0.93**	**1.43**	**0.73**
V-COMPONENT (m/s)									
Experiment 3	320	-0.3	0.1	2.1	1.8	0.36	1.52	1.65	0.61
Experiment 4a	643	0.0	0.0	1.5	1.8	0.68	0.86	0.92	0.71
Experiment 4b	305	0.0	0.2	0.8	0.7	0.71	0.33	0.35	0.65
Experiment 4c	650	-0.3	0.1	1.5	1.5	0.54	0.85	1.14	0.72
Experiment 4d	366	-0.1	0.6	1.6	1.6	0.30	1.30	1.56	0.60
AVERAGE	**457**	**-0.2**	**0.2**	**1.5**	**1.5**	**0.50**	**0.97**	**1.12**	**0.66**

Table 4.4 (continuation)

TEMPERATURE (^{0}C)									
Experiment 3	224	3.7	2.4	3.6	3.4	0.78	2.15	2.11	0.85
Experiment 4a	460	3.3	0.7	4.1	3.6	0.85	2.02	2.13	0.69
Experiment 4b	306	3.8	1.4	4.2	3.8	0.77	1.98	2.56	0.68
Experiment 4c	650	3.2	2.4	4.3	3.5	0.93	1.31	1.31	0.94
Experiment 4d	366	4.5	3.2	3.8	3.3	0.92	1.49	1.32	0.92
AVERAGE	**438**	**3.7**	**2.1**	**4.0**	**3.5**	**0.83**	**1.77**	**1.71**	**0.82**
RELATIVE HUMIDITY (%)									
Experiment 3	224	80.7	78.9	13.4	14.4	0.84	2.27	7.91	0.90
Experiment 4a	460	76.6	76.5	15.7	14.4	0.86	5.81	6.02	0.68
Experiment 4b	306	78.5	75.9	15.6	15.8	0.83	5.78	6.24	0.71
Experiment 4c	650	76.6	76.2	15.7	15.2	0.92	1.81	6.02	0.96
Experiment 4d	366	79.6	79.1	15.1	12.9	0.67	6.47	9.56	0.81
AVERAGE	**438**	**78.6**	**77.4**	**14.9**	**14.5**	**0.81**	**4.42**	**7.15**	**0.79**

The number of observations varied from 220 to 650 in each of the five groups represented in Table 4.4. MM5 output results for domains 2, 3 and 4 were dumped hourly during experiment 4, and 6-hourly for experiment 3 (without relative humidity modelled output data in the first two MM5 experiments). IOA is good and close to 0.80 for wind speed and wind components (except the average IOA for meridional wind). For near-surface temperature and relative humidity, IOA and Pearson's correlation coefficient are generally higher than 0.80 and in some cases exceeding 0.90.

It is important to point out that the smoothing effect of input global assimilation analysis data used for initialisation and nudging of MM5 during a run, and the lack of additional local meteorological information has decreased the 24-hour amplitude in the variation of modelled wind and temperature compared with observations. The following paragraphs illustrate possibilities for improving the ability of MM5 to reproduce more closely variations in observations for the Christchurch area.

4.3.2 Series of runs with different levels of nesting

The use of global analysis data and the absence of any possibility to initialise fine grid domains (i.e. grids 3 and 4 that cover the Christchurch region) with additional meteorological observations from the regional meteorological network (i.e. using RAWINsondes) led to the use of global analysis data only for nudging of the local air circulation during MM5 runs.

Experiment 4x1 was specially undertaken to try to reduce the influence of global analysis time trends in MM5 domain 4 on model output.

Experiment 4x1 consisted of 2 stages: in the first stage, the first 3 domains (grids 1, 2 and 3) were run with exactly the same configuration and physical and dynamical parameterisation approach that had been used in experiment 4 (see Section 4.3.1) for the same time period. The output information for grid 3 was damped hourly and (after the end of the first stage of the experiment) was interpolated as input and used as hourly nudging data to run domain 4 over the same 48 hours (from 1200 UTC on 1 August 2000 to 1200 UTC on 3 August 2000) as in experiment 4, but with input data from domain 3 (not from the global analysis dataset). The second step involved using input data that were created by the first step, as well as local observation data assimilated by MM5 during the run of the first three domains with coarse resolution. Therefore, during the first run, 3 grids were evaluated simultaneously with two-way interaction, and during the second stage of experiment 4x1 only the fourth domain was computed with a condition of relaxation on the boundaries and with input data that had been received from grid 3 (at 3 km spatial resolution) as 1-hourly output.

The 4x1 experiment was run with the following MM5 parameterisation of physical processes (grid 4):

1. Moisture scheme is Dudhia's simple ice scheme
2. Cumulus parameterisation is switched off
3. Boundary layer parameterisation is the Blackadar scheme (suitable for fine spatial grids)
4. Radiation scheme was cloud-radiation scheme
5. Five-layer soil model with bucket soil moisture scheme was applied
6. Shallow convection mechanism was switched on and the roughness model was Zilitinkevich's scheme.

The first three grids (step 1 of the experiment) started at 1200 UTC on 31 July 2000 and finished in 72 hours, the fourth grid was started at 1200 UTC on 1 August 2000 and finished in 48 hours. Accumulated central processor time to run the experiment was approximately 260 hours (40 hours less than for experiment 4).

Results: Figure 4.11 shows wind fields for domain 4 of MM5 for σ-level=0.999 (7.0-8.5 metres above topography surface) for two times during the 4x1 experiment: at 1700 NZST on 3 August 2000 with daytime easterly–northeasterly winds over the Christchurch area (daytime breeze – Figure 4.11a) and at 0000 NZST on 4 August 2000 with obvious westerly–northwesterly near-surface winds (nocturnal drainage winds – Figure 4.11b). The time points are the same as for experiment 4, allowing easy comparison with the results.

a) b)

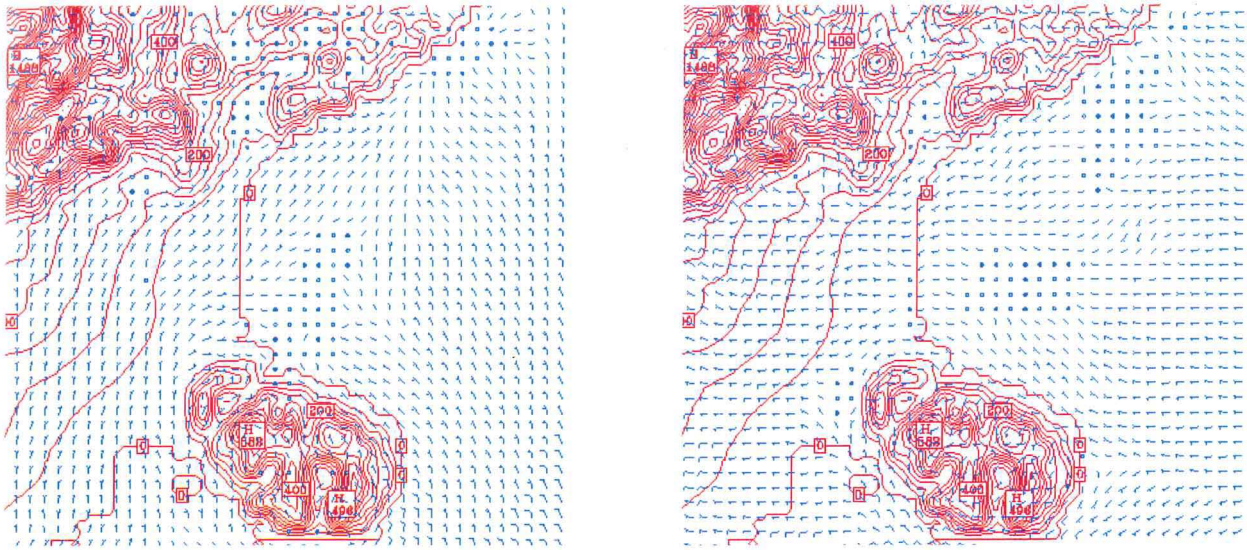

Figure 4.11 Spatial distribution of MM5 modelled near-surface wind for experiment 4x1, grid 4, σ=0.999 (7.0-8.5 metres): a) 1700 NZST on 4 August 2000 (41 hour forecast); b) 0000 NZST on 4 August 2000 (48 hour forecast).

The results of experiment 4x1 once again illustrate the ability of MM5 to accurately reproduce rapid day-night changes of near-surface wind direction as a result of realistically replicating the main features of the real atmosphere circulation resulting from the effects of very complex terrain over the Christchurch area. In Figure 4.12, vertical profiles of dry-bulb, dew-point temperatures and wind output from MM5 are presented for the Christchurch Airport location for domain 4 at 1700 NZST on 3 August 2000 (Figure 4.12a) and at 0000 NZST on 4 August 2000 (Figure 4.12.b). Both profiles represent basically stable conditions, although the midnight nocturnal dry-bulb temperature profile illustrates a much stronger vertical temperature inversion near the ground surface.

a) b)

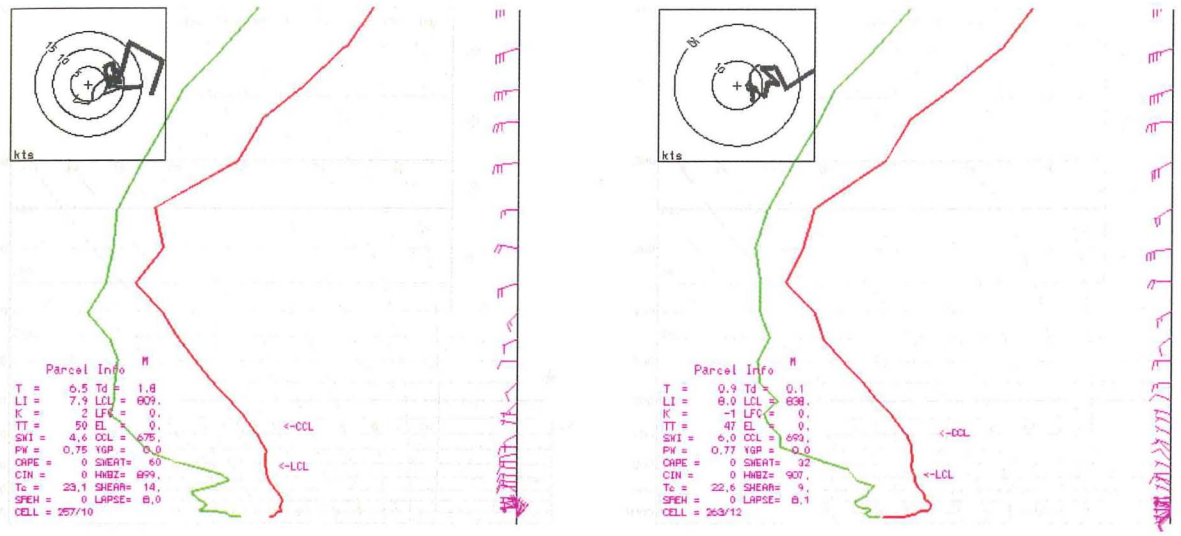

Figure 4.12 Vertical profiles of modelled wind direction, and dry-bulb (red) and dew-point (green) temperatures for experiment 4x1, grid 4: a) 1700 NZST on 3 August 2000 (41 hour forecast); b) 0000 NZST on 4 August 2000 (48 hour forecast).

IOA, Pearson correlation coefficient and additional statistical parameters for modelled and observed data are represented in Table 4.5 to allow comparison of modelled near-surface fields of wind, temperature and relative humidity with observations for sites from CAPS2000 for the Christchurch area, including boundary layer measurements on Jade Stadium (20 and 40 metre heights) and Greers Road (16 and 36 metre heights) towers (see Table 4.2). All the observations shown in Table 4.5 were taken from 25 surface observation sites that had been run during CAPS200 by Ecan, NIWA, the Geography Department of the University of Canterbury and Christchurch City Council.

Table 4.5 Index Of Agreement (IOA), Pearson Correlation Coefficient (PCC), Systematic & Unsystematic Root Mean Square Errors (S-RMSE & U-RMSE), and additional statistics of observed-modelled data for the time period 0000 NZST on 2 August 2000 to 0000 NZST on 4 August 2000, for experiment 4x1: near-surface wind (m/s), temperature (^{0}C), relative humidity (%).

EXPERMENT	NUMBER OF OBSERATIONS	OBSERVED MEAN	MODELLED MEAN	OBSERVED DEVIATION	MODELLED DEVIATION	PCC	S-MSE	U-MSE	IOA
WIND SPEED (m/s)									
Experiment 4x1a	342	1.6	1.7	0.7	0.9	0.80	0.17	0.61	0.87
Experiment 4x1b	245	1.4	1.6	0.8	0.8	0.80	0.22	0.47	0.88
Experiment 4x1c	643	2.2	2.4	1.4	1.6	0.83	0.26	0.90	0.89
Experiment 4x1d	294	2.0	2.1	1.1	1.1	0.85	0.21	0.60	0.92
AVERAGE	**381**	**1.8**	**2.0**	**1.0**	**1.1**	**0.82**	**0.21**	**0.64**	**0.89**
U-COMPONENT (m/s)									
Experiment 4x1a	342	0.6	1.2	1.3	1.8	0.80	0.64	1.11	0.83
Experiment 4x1b	245	0.5	0.8	1.3	1.4	0.94	0.28	0.48	0.96
Experiment 4x1c	643	0.8	1.2	1.9	2.2	0.68	0.51	1.61	0.82
Experiment 4x1d	294	0.8	1.1	1.9	1.9	0.89	0.42	0.85	0.93
AVERAGE	**381**	**0.7**	**1.1**	**1.6**	**1.8**	**0.83**	**0.46**	**1.01**	**0.88**
V-COMPONENT (m/s)									
Experiment 4x1a	342	0.2	0.2	0.9	0.8	0.55	0.47	0.69	0.74
Experiment 4x1b	245	0.0	-0.1	0.8	0.7	0.63	0.29	0.57	0.78
Experiment 4x1c	643	-0.2	0.1	1.5	1.5	0.54	0.82	1.14	0.72
Experiment 4x1d	294	0.1	0.1	1.2	1.0	0.51	0.66	0.87	0.71
AVERAGE	**381**	**0.0**	**0.1**	**1.1**	**1.0**	**0.56**	**0.56**	**0.82**	**0.74**
TEMPERATURE (^{0}C)									
Experiment 4x1a	195	4.0	2.7	4.2	3.4	0.91	1.29	1.40	0.94
Experiment 4x1b	245	4.1	2.5	3.8	3.1	0.91	1.82	1.29	0.90
Experiment 4x1c	643	3.2	2.4	4.3	3.5	0.93	1.31	1.31	0.94
Experiment 4x1d	196	4.3	2.6	3.9	3.1	0.89	2.06	1.43	0.88
AVERAGE	**320**	**3.9**	**2.5**	**4.0**	**3.3**	**0.91**	**1.62**	**1.36**	**0.91**
RELATIVE HUMIDITY (%)									
Experiment 4x1a	195	80.3	79.4	13.5	14.2	0.83	2.13	7.69	0.91
Experiment 4x1b	196	79.5	78.1	14.8	13.6	0.81	4.17	7.83	0.90
Experiment 4x1c	643	80.7	78.9	13.4	14.4	0.84	2.29	7.93	0.90
Experiment 4x1d	196	86.3	82.8	12.5	12.9	0.81	4.08	7.54	0.88
AVERAGE	**400**	**81.7**	**79.8**	**13.6**	**13.8**	**0.82**	**3.17**	**7.75**	**0.90**

Comparing the results of Table 4.5 with corresponding values of IOA in Table 4.3 (the Christchurch region statistics only) it should be noted that IOA has increased for all basic meteorological parameters, and especially for near-surface temperature (from 0.69 to 0.90 on

average for 4 groups). That is very important for the modelled wind speed in the PBL (the IOA for wind characteristics on average has increased from 0.65–0.75 to 0.75-0.85). For near-surface relative humidity, Pearson's correlation coefficient and Index of Agreement are mostly more than 0.80 and in some groups reach a level of correlation of 0.90, showing strong agreement between modelled and observed data.

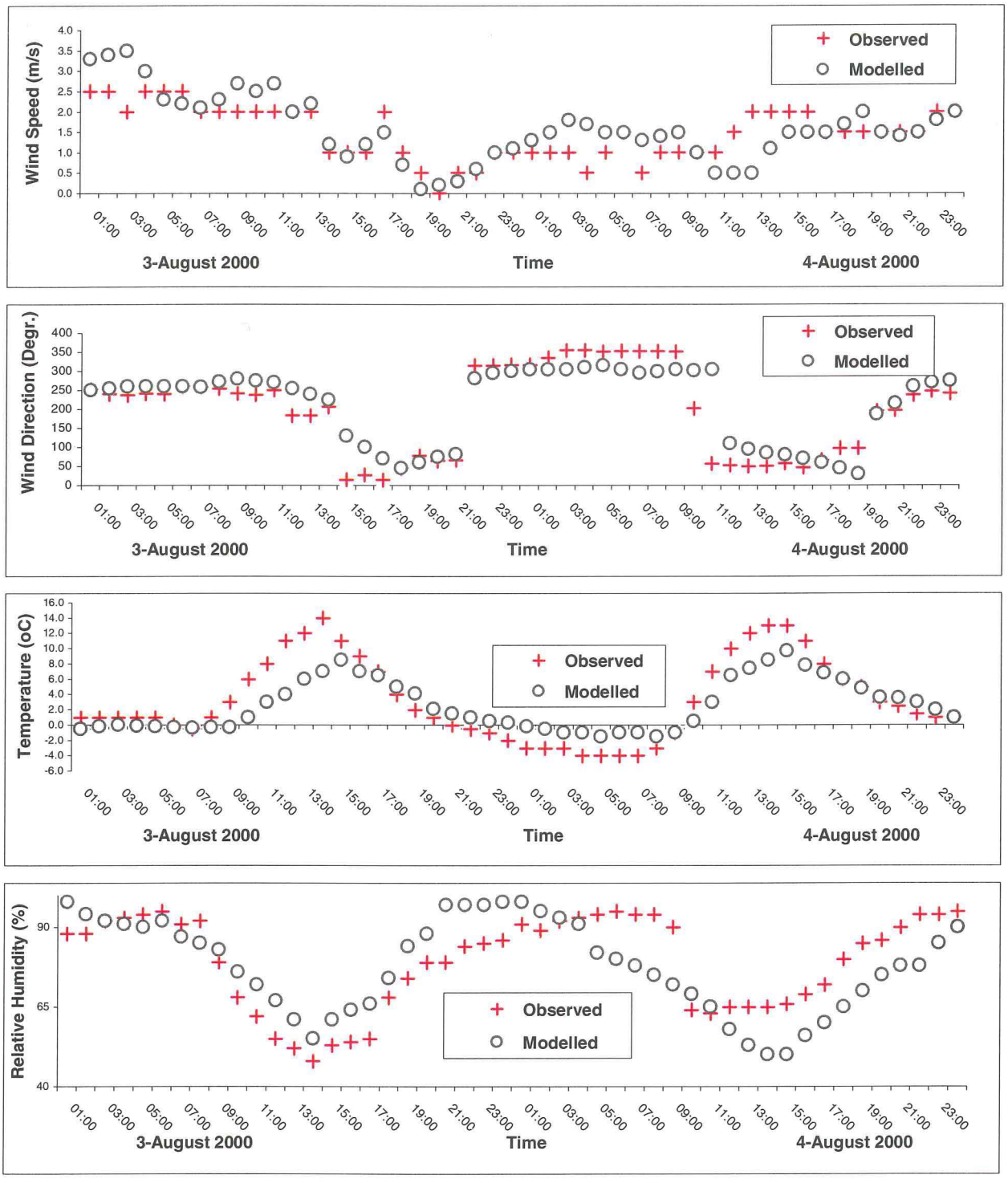

Figure 4.13 Time series of modelled (open circle) and observed (red cross) wind speed, wind direction, near-surface temperature and relative humidity compared for site Coles Place: experiment 4x1, grid 4, time period from 0000 NZST on 3 August 2000 to 0000 NZST on 5 August 2000.

Time trends of the modelled near-surface wind magnitude and direction, temperature and relative humidity modelled values (black open circles) calculated from MM5 grid 4 output are represented in Figure 4.13 allowing comparison with the observation data values (red crosses) from Coles Place (St. Albans) in Christchurch. Inter-comparison of data in Figures 4.9 and 4.13 provides distinctive evidence of the improvement of the modelled temperature and wind direction time trends in experiment 4x1 relative to the experiment 4 results.

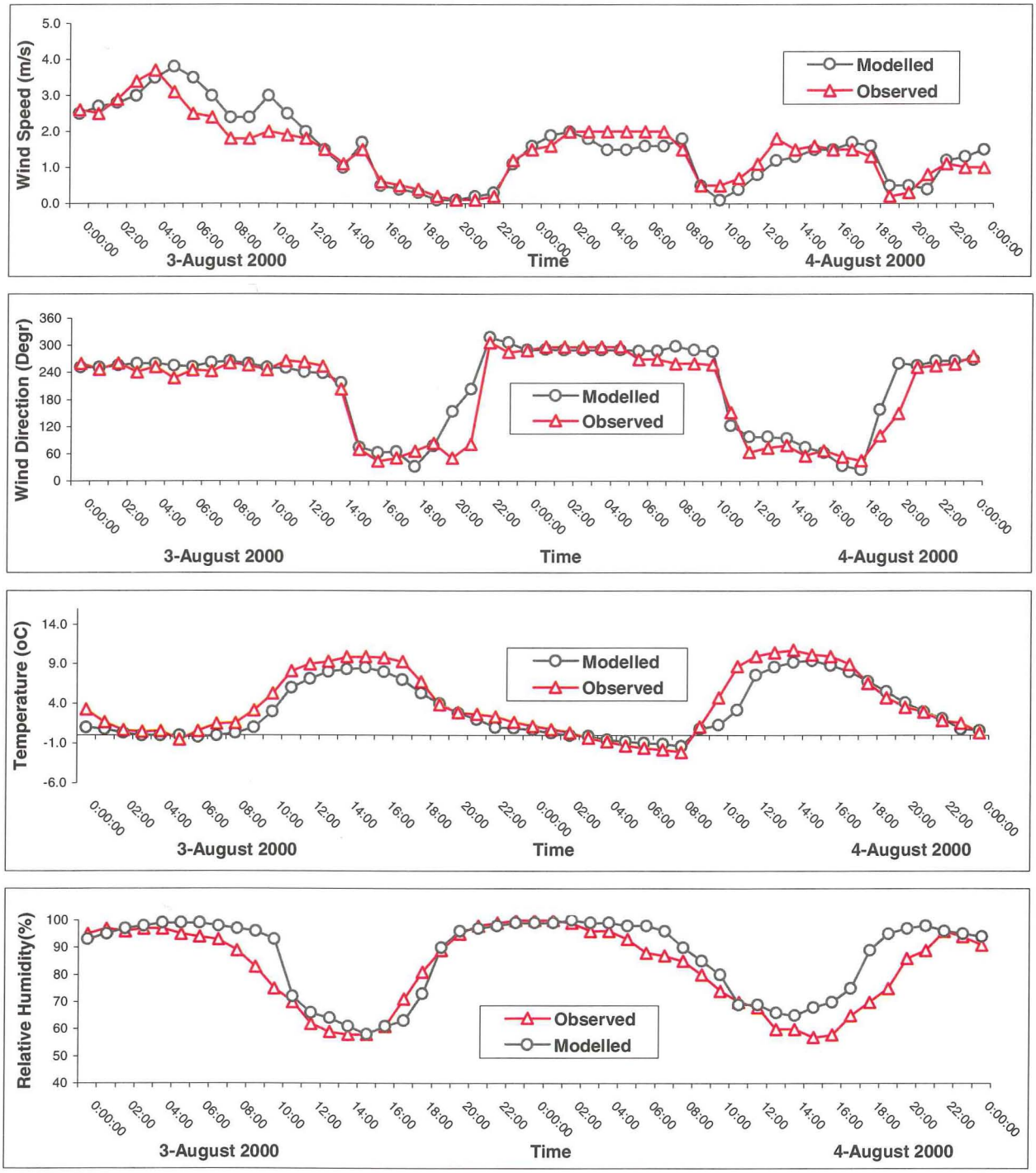

Figure 4.14 Time series of wind (wind speed and wind direction), temperature (^{0}C) and relative humidity (%) compared with observations at Colombo Street: 0000 NZST on 2 August 2000 to 0000 NZST on 4 August 2000, experiment 4x1, grid 4, $\sigma = 0.999$ (7.5-8 metre height).

Modelled and observed time series of the near-surface wind, temperature and relative humidity for the Colombo Street site for the time interval 0000 NZST on 2 August 2000 to 0000 NZST on 4 August 2000 are represented in Figure 4.14. Once again, it is important to note the ability of MM5 modelled wind (black circles/line) to follow the observed daily rapid wind changes (red triangles/line) between westerlies and easterlies, and improvement of the modelled temperature trend compared with the results of experiment 4 (see Figure 4.10). Evidence of this improvement is illustrated not only by comparison of temperature IOA for experiments 4 and 4x1 (Tables 4.3 and 4.5), but also by the time series of near-surface meteorological characteristics.

4.3.3 CAPS2000 and MM5 fine tuning for the Christchurch region

During two subsequent MM5 experiments (experiments 5 and 6) major effort was focused on improvement of MM5 output for domain 4, as this is important for aerosol modelling using CAMx4. Long time period runs (up to 7 days, or 168 hours) of the first three MM5 domains simultaneously or separately were therefore completed, producing MM5 grid 3 output. This was then used as input to domain 4 during model runs at a shorter time interval (from 36 to 48 hours). Hourly and 3-hourly nudging was achieved using domain 3 output with different physical parameterisations of atmospheric boundary layer. This strategy is described in experiments 5-6.

During experiment 5, initially 3 grids (domains 1–3) were run over a 7-day time period using the following numerical and physical schemes:

1. Calculation of all three grids started at the same time ('cold' start): 1200 UTC on 30 July 2000 (0000 NZST on 1 August 2000) and finished all together 1200 UTC on 6 August 2000 (0000 NZST on 7 August 2000)
2. Two-way interaction ('mother–daughter') grids was stipulated for all levels of nesting during the whole run, with the output information dumped hourly for grid 3
3. Grids 1-3 were nudged by global analysis data every six hours
4. The explicit Reisner1 mixed phase moisture scheme was used for all 3 domains
5. Cumulus parameterisation was the Kain-Fritsch scheme 1 for grids 1 and 2 and there was no convection in grid 3
6. Boundary layer MRF (ECMWF global model scheme) parameterisation was used in domains 1–2 and the Blackadar scheme in domain 3
7. Radiation scheme was cloud-radiation scheme for all 3 grids
8. Five-layer soil model was switched on in all 3 domains with a bucket soil moisture scheme
9. Zilitinkevich's roughness parameterisation scheme was chosen.

In the second step, domain 4 only was run with 1-hourly input meteorological information that had been obtained as output from domain 3, with application of a special interpolation program NESTDOWN. All physical parameterisation schemes used to run grid 4 were the same as for domain 3 in the first step of experiment 5. Grid 4 simulations were undertaken several times using a 7-day time period of input data from grid 3. Weekly and monthly global sea surface temperature (SST) analysis data (ds277.0) at 1 x 1 degree resolution were obtained from NCEP for these and the following experiments. The weekly results of the ds277.0 analysis for the South Island of New Zealand were compared with the data obtained during CAPS2000, and a 2-point weighted filter (0.5–0.5) was applied to the basic input SST data for every MM5 domain.

Results: Figure 4.15 shows the wind fields obtained for domain 4 of MM5 for σ-level = 0.999 (7–8.5 metre height) for two times during experiment 5: at 1500 NZST on 1 August 2000 with daytime easterly–northeasterly weak winds over the Christchurch area (daytime breeze circulation – Figure 4.15a), and at 2200 NZST on 1 August 2000 with obvious westerly–south-westerly winds and a more developed near-surface air circulation (nocturnal cold air drainage – Figure 4.15b).

a) **b)**

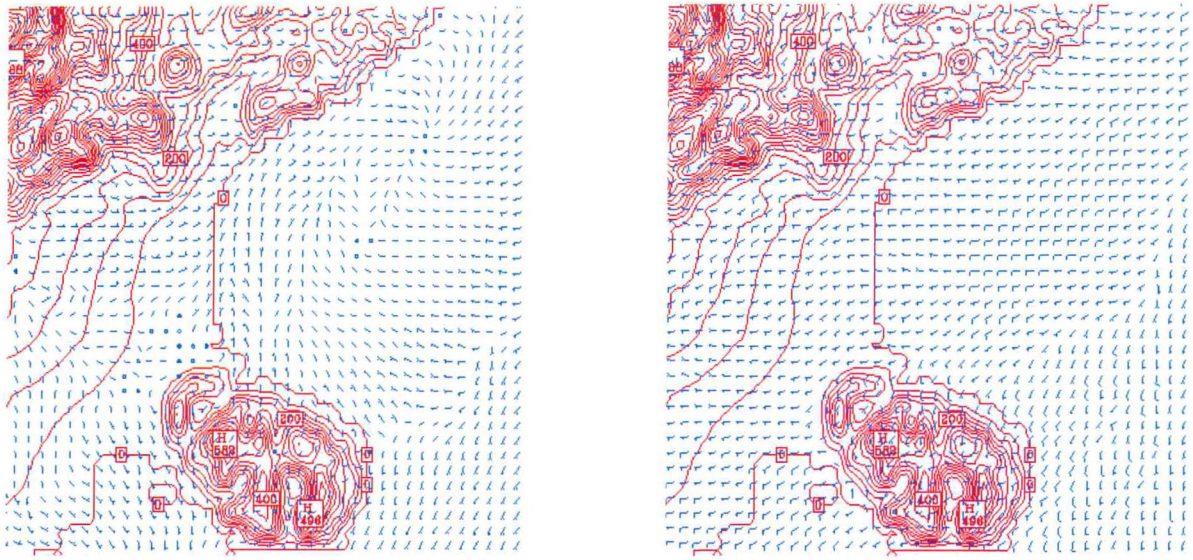

Figure 4.15 Spatial distribution of MM5 modelled near-surface wind for experiment 5, grid 4, σ= 0.999 (7.0–8.5 metres: a) 1500 NZST on 1 August 2000 (39 hour forecast); b) 2200 NZST on 1 August 2000 (46 hour forecast).

Vertical profiles of dry-bulb (red solid line) and dew-point temperatures (green solid line) and vertical change of wind derived for Christchurch Airport from MM5 domain 4 output at 1500 NZST on 1 August 2000 are illustrated in Figure 4.16. The daytime dry-bulb temperature

profile indicates neutral stability near the surface with more stable air aloft (Figure 4.16a) while the late evening dry-bulb temperature profile shows a strong temperature inversion in the lowest 100–150 metres (Figure 4.16b).

a) b)

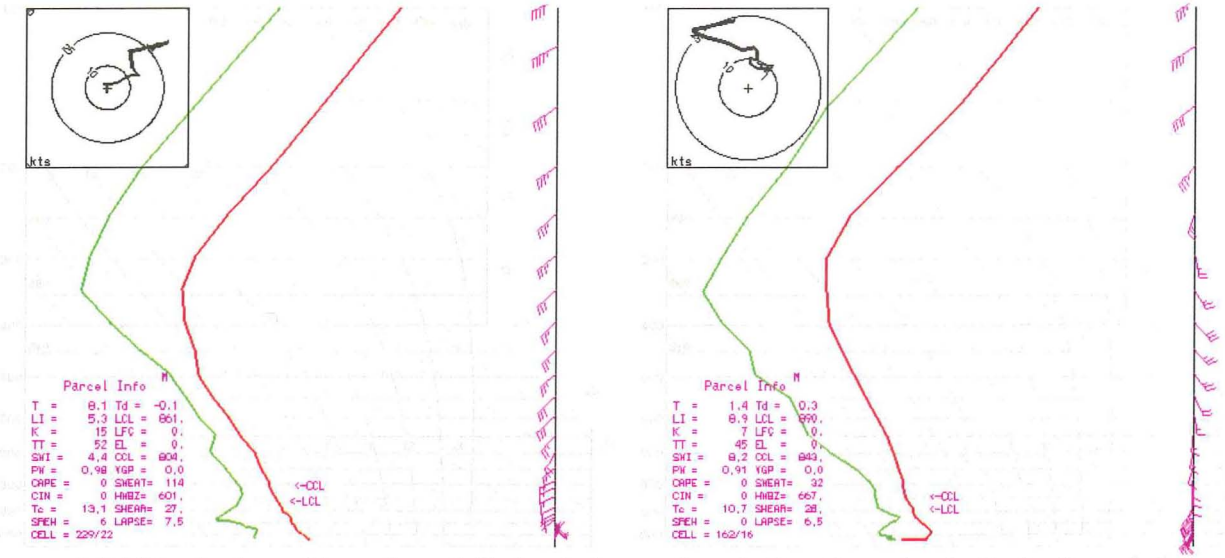

Figure 4.16 Vertical profiles of modelled wind speed and direction, dry-bulb (red) and dew-point (green) temperatures for experiment 5, grid 4: a) 1500 NZST on 1 August 2000 (39 hour forecast); b) 2200 NZST on 1 August 2000 (46 hour forecast).

Index of agreement (IOA), correlation coefficient and additional statistical parameters (number of observations for surface sites that were compared with grid 4 output for the main meteorological parameters, mean and standard deviation of observed and modelled values, systematic and unsystematic root mean square errors) for modelled output and observations are represented in Table 4.6. Comparison of modelled near-surface fields of wind, temperature and relative humidity with the observed ones at CAPS2000 measurement sites for the Christchurch area was undertaken for grid 4 (with 1 km spatial resolution over Christchurch only) for the time period between 1–7 August 2000. All the observations shown in Table 4.6 were obtained from 12 different surface observation sites that were operated during CAPS200.

Table 4.6 Index Of Agreement (IOA), Pearson's Correlation Coefficient (PCC), Systematic & Unsystematic Root Mean Square Error (S-RMSE & U-RMSE), additional statistics of observed and modelled data for 1-7 August 2000 for experiment 5: near-surface wind (m/s), temperature (^{0}C) and relative humidity (%).

EXPERMENT	NUMBER OF OBSERATIONS	OBSERVED MEAN	MODELLED MEAN	OBSERVED DEVIATION	MODELLED DEVIATION	PCC	S-RMSE	U-RMSE	IOA
WIND SPEED (m/s)									
Experiment 5a	245	1.61	1.88	0.70	0.94	0.65	0.28	0.71	0.75
Experiment 5b	141	1.63	1.77	1.63	0.81	0.77	0.17	0.51	0.87
AVERAGE	**193**	**1.62**	**1.83**	**1.16**	**0.88**	**0.71**	**0.23**	**0.61**	**0.81**
U-COMPONENT (m/s)									
Experiment 5a	245	0.61	1.12	1.38	1.57	0.79	0.53	0.96	0.86
Experiment 5b	141	0.86	1.09	0.86	1.48	0.91	0.23	0.61	0.95
AVERAGE	**193**	**0.74**	**1.11**	**1.12**	**1.53**	**0.85**	**0.38**	**0.77**	**0.91**
V-COMPONENT (m/s)									
Experiment 5a	245	0.09	0.27	0.89	0.79	0.53	0.73	0.76	0.65
Experiment 5b	141	0.09	0.18	0.69	0.61	0.59	0.37	0.49	0.76
AVERAGE	**193**	**0.09**	**0.22**	**0.79**	**0.76**	**0.56**	**0.55**	**0.64**	**0.71**
TEMPERATURE (^{0}C)									
Experiment 5a	139	6.04	5.15	4.50	2.94	0.91	2.04	1.23	0.90
Experiment 5b	141	5.73	5.35	5.73	2.89	0.94	1.37	2.90	0.70
AVERAGE	**140**	**5.89**	**5.25**	**5.12**	**2.91**	**0.92**	**1.70**	**2.06**	**0.80**
RELATIVE HUMIDITY (%)									
Experiment 5a	135	87.90	81.68	15.07	13.45	0.86	7.10	6.68	0.89
Experiment 5b	105	81.97	84.44	81.97	12.02	0.87	5.41	5.82	0.91
AVERAGE	**120**	**84.96**	**83.14**	**49.43**	**12.64**	**0.87**	**6.26**	**6.24**	**0.90**

A higher IOA for the zonal component of wind and a lower one for the meridional component are evident compared with the results of experiment 4 (Table 4.5). The decrease of meridional wind accuracy in the MM5 results can be explained by initially very weak meridional wind speeds during the research period for domain 4, which resulted in an increase of relative error of the V-component magnitude. Any way, the Christchurch area during wintertime is dominated by zonal synoptic and mesoscale winds that make modelled zonal air circulation more strongly in agreement with observations compared with the more variable meridional flow (see mean observed and mean modelled values of wind in Tables 4.3, 4.4 and 4.6).

Experiment 6 consisted of three stages: in the first stage only one (coarse) grid (domain 1) was run over a 7-day period using the following numerical and physical schemes:

1. Calculation of mother grid separately: started at 1200 UTC on 30 July 2000 and finished at 1200 UTC on 6 August 2000
2. Grid 1 was nudged using global analysis data every six hours and output information dumped every 3 hours of the model run
3. Dudhia's moisture scheme and Grell cumulus parameterisations were used for the coarse grid
4. Boundary layer MRF parameterisation and cloud-radiation scheme were used
5. Five-layer soil model was switched on
6. 43 vertical levels used, including 12 levels in the PBL and a top level of σ=0.010.

In the second stage, domains 2 and 3 were initialised using domain 1 output (using the NESTDOWN procedure). The model settings were as follows:

1. Time period was the same: from 1200 UTC on 30 July 2000 to 1200 UTC on 6 August 2000;
2. Domains 2 and 3 were nudged by the mother grid output data six-hourly and output information was dumped every hour for grid 3
3. Dudhia's moisture scheme and the Kain-Fritsch cumulus parameterisation were used for mother domain (grid 2) and cumulus parameterisation was switched off for nested grid 3
4. Boundary layer parameterisation was MRF for grid 2 and Blackadar for grid 3
5. Rapid Radiative Transfer Model (RRTM) was used in both grids
6. The five-layer soil model was switched on
7. 43 vertical levels including 12 levels in PBL with near-surface σ=0.999 and top level for σ=0.010.

In the third stage, grid 4 only was run with 3-hourly nudging using output data from domain 3. All physical parameterisation schemes used to run grid 4 were the same as for domain 3 of the second step of experiment 6. Grid 4 was modelled only once for the time period from 1200 UTC on 1 August 2000 to 1200 UTC on 3 August 2000 (on 48 hours with 15 vertical layers in the atmospheric boundary layer, and with a top layer equal to 100 hPa (σ = 0.100). The results of the third stage of the experiment 6 (grid 4) were dumped hourly.

Results: Index of agreement, correlation coefficient, number of observation surface sites that were compared with grid 4 output, mean and standard deviation of observed and modelled values, systematic and unsystematic root mean square error for modelled output and observations are represented in Table 4.7 for grid 3 (second stage of the experiment 6) and for grid 4 (final stage).

Comparison of modelled near-surface fields of wind, temperature and relative humidity with the observed ones at study points of the CAPS2000 for the Christchurch area, included the BL measurements on Jade Stadium and Greers Road towers, as for grids 3 and 4 (with 3 and 1 km spatial resolution) for the same observation points in August 2000. All the observations

shown in Table 4.7 were taken from 12 different surface observation sites that were operated during CAPS200 (see Table 4.2).

Table 4.7 Index Of Agreement (IOA), Pearson's Correlation Coefficient (PCC), Systematic & Unsystematic Root Mean Square Error (S-RMSE & U-RMSE), and additional statistics of observed and modelled data for the time period 1–7 August 2000 for experiment 6: near-surface wind (m/s), temperature (^{0}C) and relative humidity (%).

EXPERMENT	NUMBER OF OBSERATIONS	OBSERVED MEAN	MODELLED MEAN	OBSERVED DEVIATION	MODELLED DEVIATION	PCC	S-RMSE	U-RMSE	IOA
WIND SPEED (m/s)									
Experiment 6a	738	2.21	2.71	0.98	1.15	0.72	0.48	0.90	0.76
Experiment 6b	738	2.31	2.06	0.93	1.45	0.86	0.22	0.72	0.91
AVERAGE	**738**	**2.26**	**2.38**	**0.95**	**1.30**	**0.79**	**0.35**	**0.81**	**0.84**
U-COMPONENT (m/s)									
Experiment 6a	738	0.54	0.95	1.86	2.19	0.83	0.41	1.32	0.88
Experiment 6b	738	0.57	1.07	1.80	1.79	0.82	0.62	1.01	0.88
AVERAGE	**738**	**0.56**	**1.01**	**1.83**	**1.99**	**0.83**	**0.52**	**1.16**	**0.88**
V-COMPONENT (m/s)									
Experiment 6a	738	-0.98	-0.42	1.39	1.67	0.47	0.91	1.55	0.62
Experiment 6b	738	-0.92	0.52	1.31	1.32	0.67	0.54	0.97	0.94
AVERAGE	**738**	**-0.95**	**0.05**	**1.34**	**1.50**	**0.57**	**0.73**	**1.26**	**0.78**
TEMPERATURE (^{0}C)									
Experiment 6a	546	4.39	4.77	3.66	2.95	0.85	1.13	1.42	0.92
Experiment 6b	546	4.89	4.29	3.54	3.29	0.93	1.15	1.20	0.95
AVERAGE	**546**	**4.77**	**4.53**	**3.60**	**3.12**	**0.89**	**1.14**	**1.31**	**0.94**
RELATIVE HUMIDITY (%)									
Experiment 6a	109	84.90	80.34	13.26	14.18	0.85	3.98	6.34	0.91
Experiment 6b	109	84.24	81.24	13.06	13.42	0.92	3.78	5.27	0.95
AVERAGE	**109**	**84.57**	**80.79**	**13.16**	**13.80**	**0.89**	**3.88**	**5.81**	**0.93**

When comparing the statistics for grids 3 and 4 of Table 4.7, a significant improvement is evident in grid 4 results, especially for the wind components. This is very important for future use of the modelled near-surface wind fields in the CAMx4 model for accurate aerosol dispersion calculations. It should also be noted that although the procedure adopted in experiment 6 seems to be very complex and lengthy, the accumulated CPU time for both experiments 5 and 6 is approximately the same (nearly 250 hours). However, the improvement of near-surface wind is significant compared with all other experiments (see Tables 4.1, 4.2, 4.3 and 4.4 for Christchurch – grid 4). Obviously, such a complex computation scheme cannot be applied when using MM5 for real-time modelling.

It is practical to compare modelled and observed time trends of short-wave downward radiation (W m^{-2}) and net radiative balances (W m^{-2}) for different measuring points for CAPS2000, to establish the level of reliability of the radiation balance for MM5 grid 4 output over the Christchurch area. Figure 4.17 shows modelled (grid 4) and observed values of short wave downward radiation (at the University of Canterbury) and the net radiation balance (at Jade Stadium 20 m and Greers Road 15 m) for the time period from 0000 NZST on 1 August 2000 to 0000 NZST on 4 August 2000. These were the only observation sites, at which radiation components were measured.

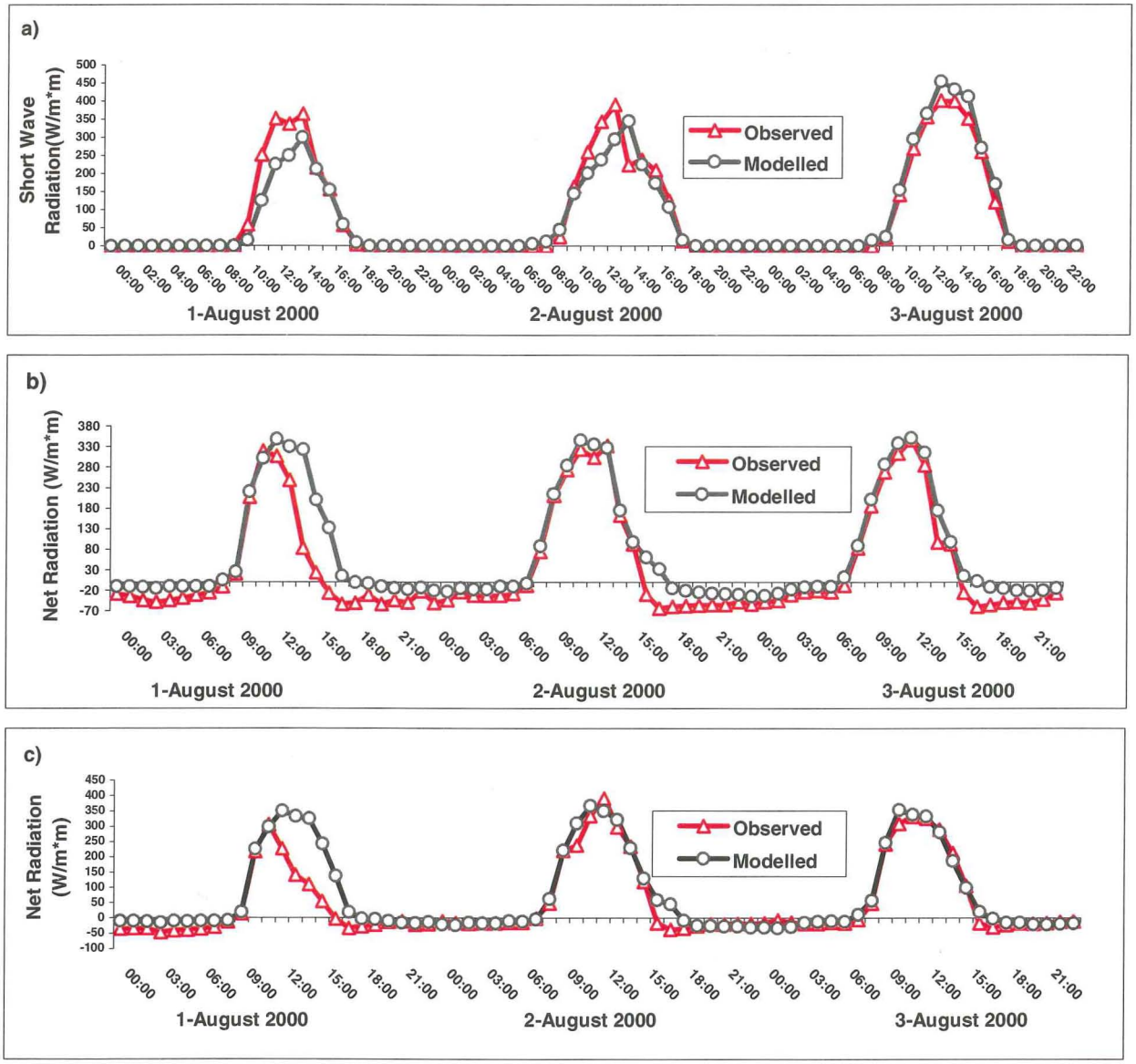

Figure 4.17 Near-surface time trends: a) short wave downward radiation (Wm^{-2} –the University of Canterbury); b) net radiation balance (Wm^{-2} –Jade Stadium), c) net radiation balance (Wm^{-2} –Greers Road): observed (red) and modelled (black); experiment 5, grid 3, 0000 NZST on 1 August 2000 to 0000 NZST on 4 August 2000.

From Figure 4.17, it is obvious that there is good coincidence of the modelled and observed net radiation balances, but an overprediction of the net balance daytime values by MM5 on the first day compared with the observations. Some underprediction can also be noticed for short wave downward radiation measured at the University of Canterbury on the first two days. One of the reasons for the differing radiative values can be a difference in height between modelled results (they were taken for 7.0–8.5 metres height for σ-level = 0.999) and observed data (observation heights were not less than 15–16 metres above the surface). A second argument could be that the cloud-radiative scheme used is not appropriate in this case. In experiment 6, the cloud-radiation scheme was substituted by the Rapid Radiative Transfer Model (RRTM) for grids 2, 3 and 4 and was retained only for the mother domain (grid 1) in the first stage of the 3-stage experiment (see the experiment description above).

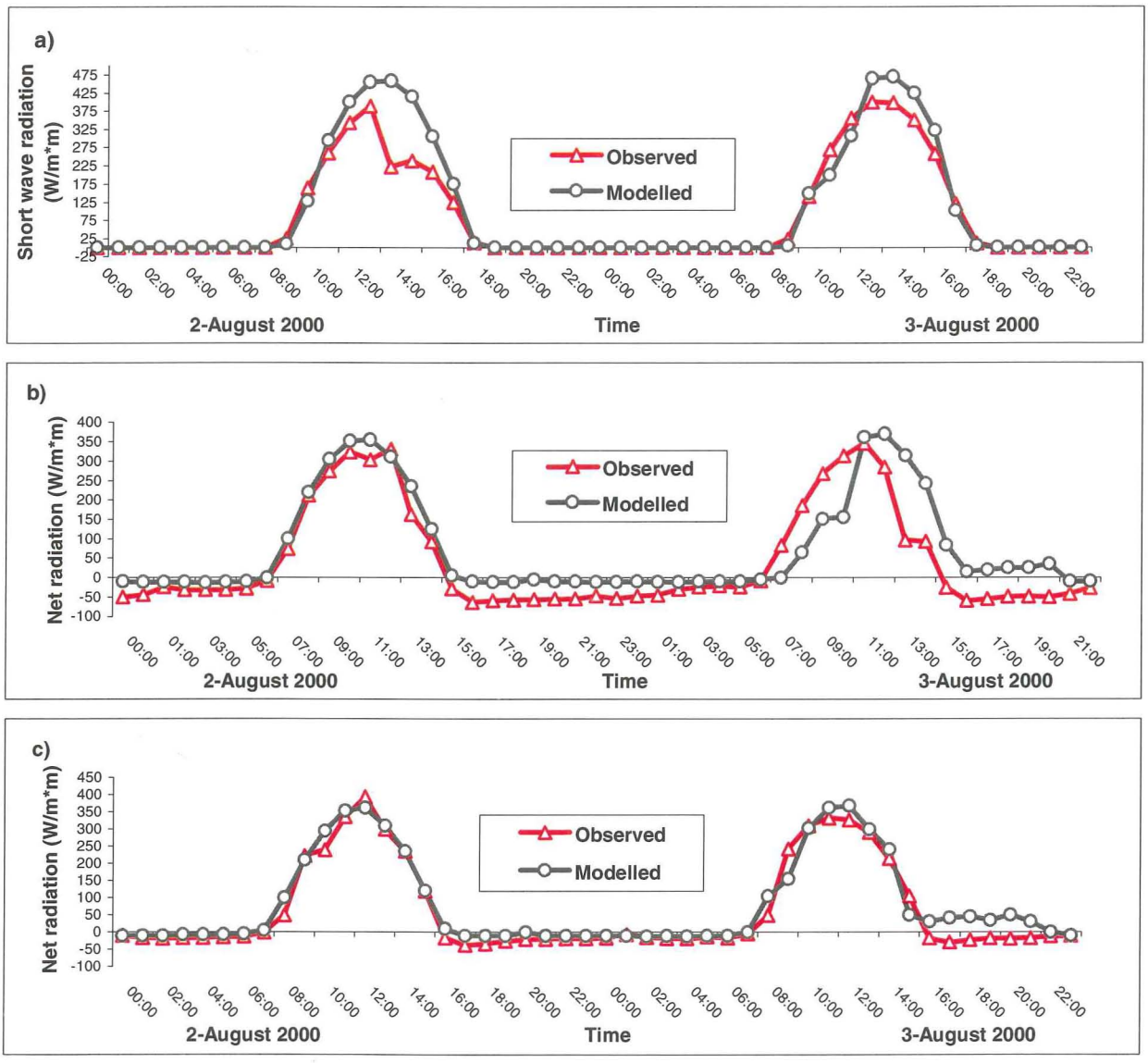

Figure 4.18 Near-surface time trends: a) short wave downward radiation (Wm^{-2} –University of Canterbury); b) net radiation balance (Wm^{-2}-Jade Stadium); c) net radiation balance (Wm^{-2} –Greers Road), observed (red) and modelled (black): experiment 6, grid 4, 0000 NZST on 2 August 2000 to 0000 NZST on 4 August 2000.

In Figure 4.18, a slight overestimation of the modelled net radiation daytime values is seen compared with observations (Figures 4.18 b and c; graphs are given for grid 4 and a time period of 48 hours starting at 0000 NZST on 2 August 2000). This seems to relate to a more significant overestimation of downward short-wave radiation at the University of Canterbury site (Figure 4.18a). The radiative scheme accuracy plays an essential role in valid reproduction of values for all components of the modelled near-surface net radiation balance, which is very important for determining modelled air temperatures. Pearson's correlation coefficient for radiation balance components for experiment 5 was between 0.85–0.90, increasing up to 0.95 in experiment 6.

4.3.4 Particulars of 2003 winter modelling

Winter 2003 in Christchurch experienced more heavy pollution nights than during winter 2000. The most prominent peaks of air pollution occurred in the second half of July 2003, as evident from measurements of particulate matter made in St. Albans (Coles Place). Figure 4.19 shows the time trend of 24-hour average PM_{10} during winter 2003 for Coles Place with the red line indicating the health guideline.

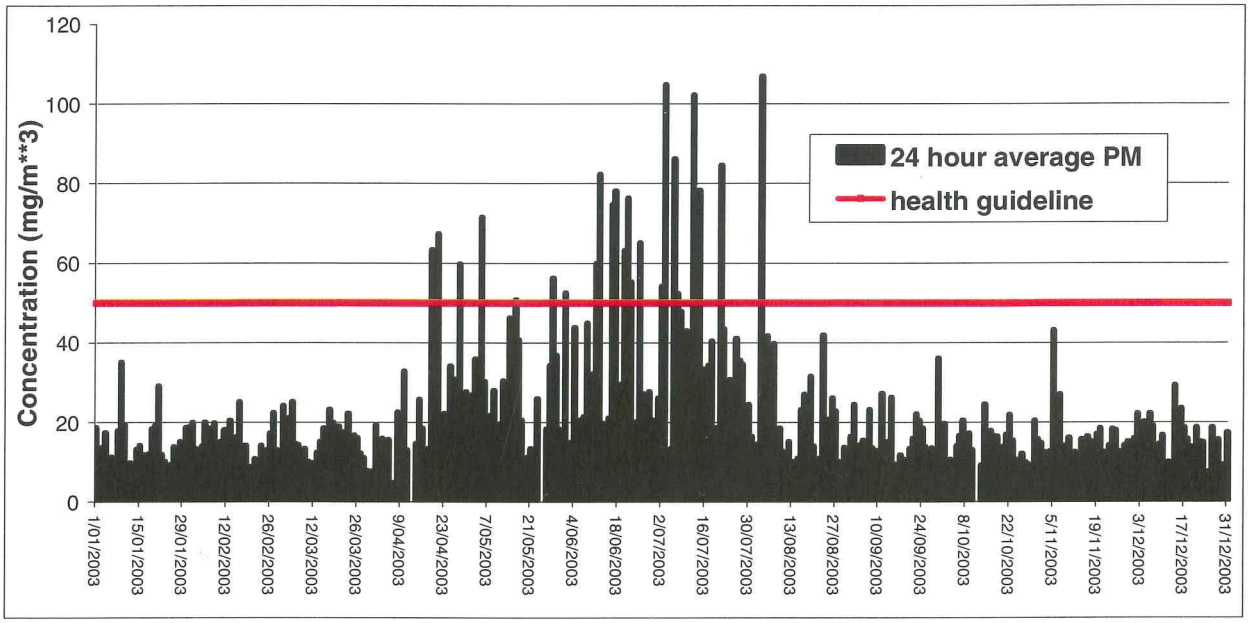

Figure 4.19 24-hour averaged values of PM_{10} ($\mu g\ m^{-3}$), at Coles Place, St. Albans (Christchurch), 2003 (after Aberkane, 2004).

Global analysis data for winter 2003 experiments was easily obtained, as the NCEP ds083.2 division had opened their database for free downloading of data for any year after 2001. All necessary meteorological information (with 6 hour time resolution) was downloaded and archived. The main problem was not in acquiring input data for the MM5–CAMx4 numerical system, but in obtaining observation data to compare with the model output.

In Christchurch during the cold half of 2003 there were only three observation sites functioning (installed and maintained by Environment Canterbury) that measured not only basic near-surface meteorology, but also 10-minute particulate matter level ($\mu g\ m^{-3}$) and CO (or NO) (in number of particles per million/billion – ppm/ppb): Coles Place (St. Albans), Hoon Hay and Aranui. The latter two were temporary measurement sites that had been placed in the Christchurch area for only one year.

Two time periods of stagnant synoptic situation and high level of air pollution were chosen for modelling by MM5: 21 July 2003 to 23 July 2003 and 3 August 2003 to 6 August 2003. A satellite image for 21 July 2003 is presented in Figure 4.20 to illustrate the synoptic situation, which was dominated by a stable anticyclone.

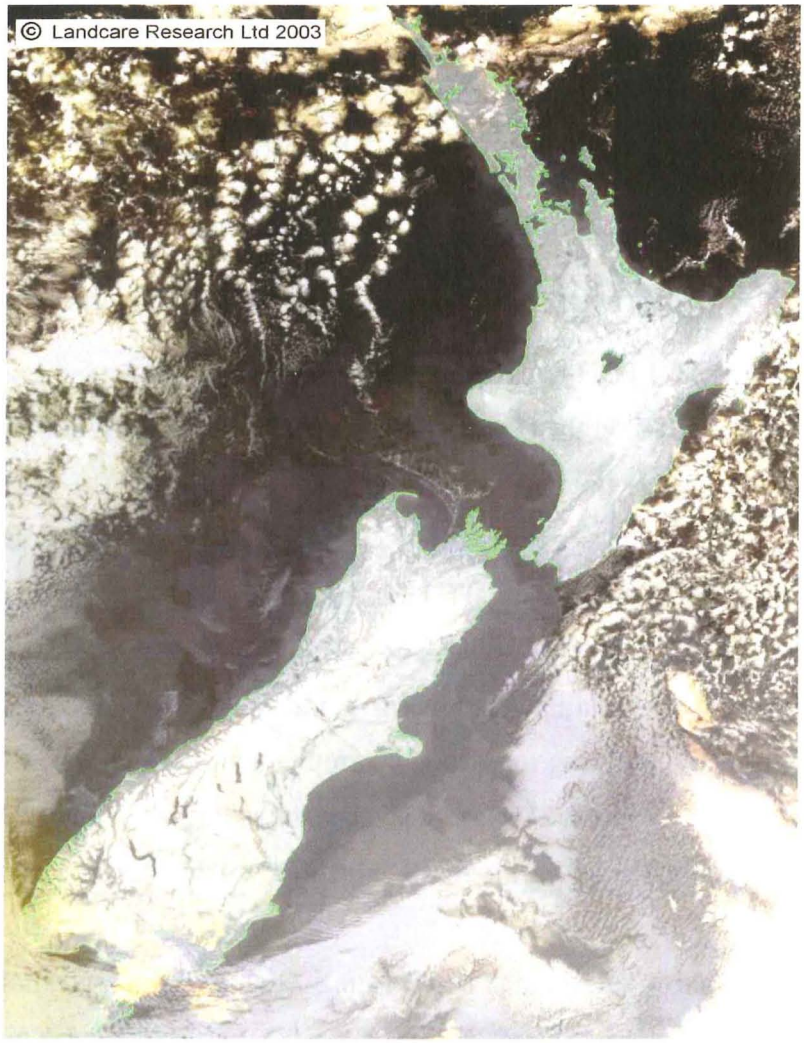

Figure 4.20 NOAA satellite image of the synoptic situation over New Zealand: 1930 NZST on 21 July 2003 (Landcare Research).

It is important to point out that during the period 21–23 July 2003, balloon vertical profiling of wind, temperature and particulate matter was undertaken in the lowest 400–500 metres at English Park, St. Albans, Christchurch (Sturman *et al.*, 2003; McKendry *et al.*, 2004).

This coincided approximately with the average upper boundary of the ABL over Christchurch during wintertime (see Section 4.2.3 and Figure 4.3). The diurnal time trend of PM_{10} concentration exceeded the 24-hour average health guideline for a significant period during the night of 21–22 July 2003, in spite of a moderately strong northeasterly wind (Figure 4.21).

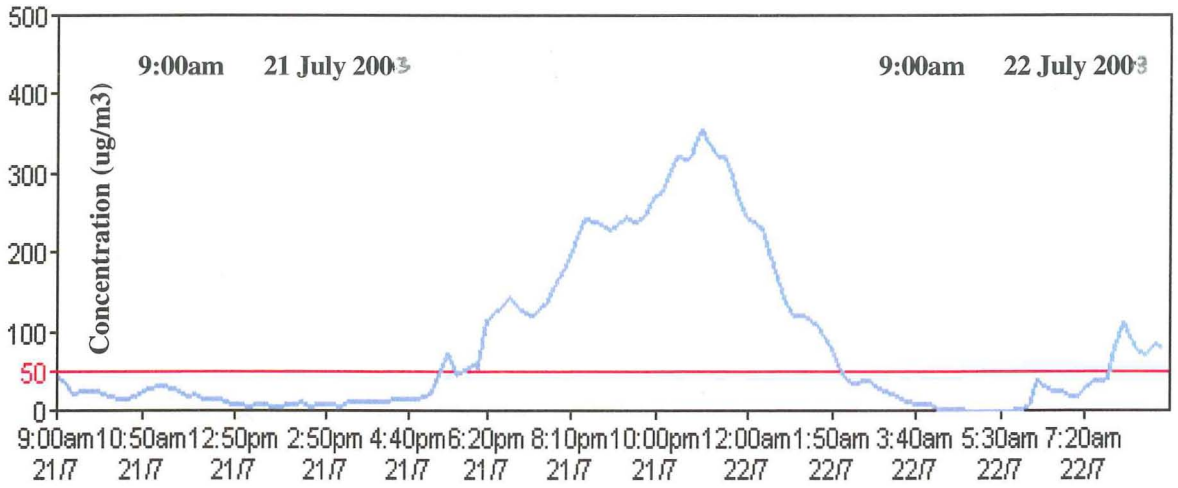

Figure 4.21 Diurnal cycle of PM_{10} ($\mu g\ m^{-3}$) at Coles Place, St. Albans, for the time period: 0900 NZST on 21 July 2003 to 0900 NZST on 22 July 2003 with the red line representing the health guideline (50 $\mu g\ m^{-3}$) (after Ecan, 2003).

MM5 experiment 3-03 was run for the time period 1200 UTC on 20 July 2003 to 1200 UTC on 23 July 2003 (0000 NZST on 21 July 2003 to 0000 NZST on 24 July 2003). In the first stage of experiment 3-03, MM5 was run over a 72-hour period using grids 1-3 and the following physical schemes:

1. All three domains started together at 1200 UTC on 20 July 2003 (0000 NZST on 21 July 2003) and finished together at 1200 UTC on 23 July 2003 (0000 NZST on 24 July 2003)
2. Two-way interaction 'mother–daughter' grids was stipulated for all levels of nesting during the run with the output information dumped hourly for grid 3
3. Grids 1-3 were nudged by global analysis data every 12 hours
4. Explicit Reisner1 mixed phase moisture scheme was used for grid 1 and the simple ice scheme for domains 2-3
5. Cumulus parameterisation was the Kain-Fritsch scheme for grids 1–2 and convection was switched off in grid 3
6. Boundary layer the MRF parameterisation was used for domain 1 and the Blackadar scheme for grid 2–3
7. The radiation scheme was the cloud-radiation scheme for 1–2 grids, with none–for grid 3
8. The five-layer soil model was switched on in all 3 domains, with a bucket soil moisture scheme

9. Sea-surface temperature was set at 277 K for the coarse domain and to 276 K for nested grids 2–3 (from ds277.0 of NCEP).

In the second stage, domain 4 was run for 72 hours with 3-hourly input meteorological data that had been received as output from grid 3 (the mother domain). The physical parameterisation used to run grid 4 was the same as for domain 3, except for use of the RRTM radiation scheme instead of the cloud-radiation one.

Results: Near-surface wind fields for MM5 grid 4 are presented in Figure 4.22 for two times of experiment 3-03: at 0000 NZST on 23 July 2003 showing obvious westerly–south-westerly nocturnal drainage winds (Figure 4.22a) and at 1000 NZST on 23 July 2003 with daytime easterly–north-easterly airflow over the Christchurch area (Figure 4.22b).

a) **b)**

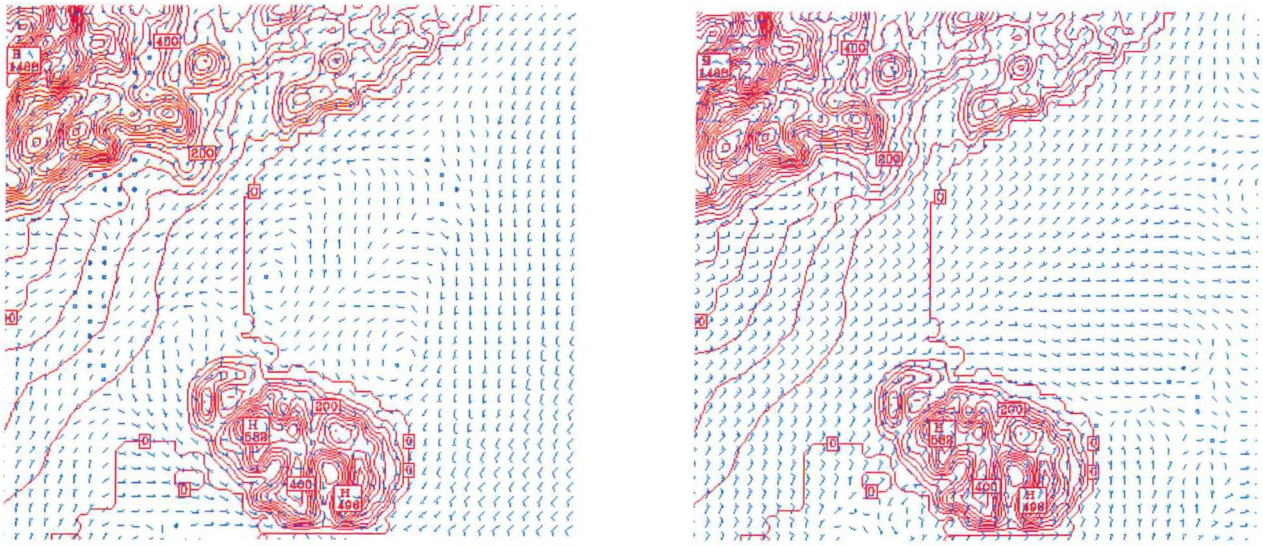

Figure 4.22 Spatial distribution of MM5 modelled near-surface wind for experiment 3-03, grid 4, $\sigma = 0.999$ (7.0–8.5 metres): a) 0000 NZST on 23 July 2003 (48 hour forecast); b) 1000 NZST on 23 July 2003 (58 hour forecast).

Vertical profiles of dry-bulb (red solid line) and dew-point temperatures (green solid line) and wind change with height obtained for Christchurch airport from MM5 grid 4 output at 0000 and 1000 NZST on 23 August 2003 are shown in Figure 4.23. The night dry-bulb temperature profile reflects a weakly stable boundary layer (Figure 4.23a) while a more strongly stable (isothermal) near-surface layer is evident in the morning vertical temperature profile (Figure 4.23b). At both times high humidity in the lowest few hundred metres is indicated by the dew-point temperature profile (Figure 4.23a and b).

a) b)

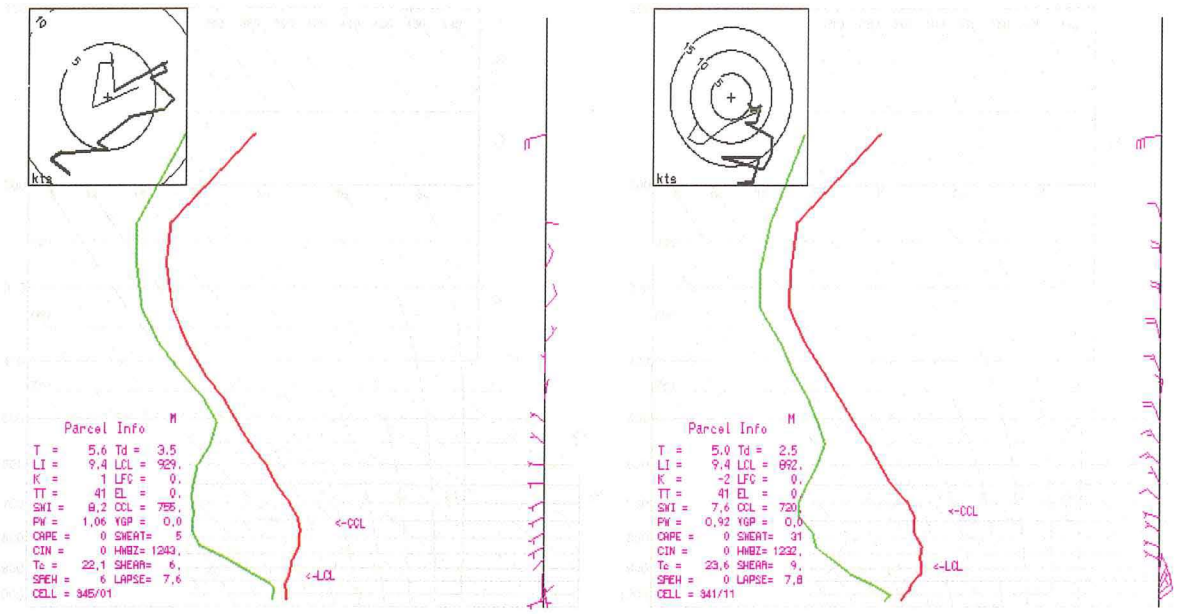

Figure 4.23 Vertical profiles of modelled dry-bulb (red) and dew-point (green) temperatures and wind for experiment 3-03, grid 4: a) 0000 NZST on 23 July 2003 (48 hour forecast), b) 1000 NZST on 23 July 2003 (58 hour forecast).

Index of agreement (IOA), correlation coefficient (PCC) and accompanying statistics, including the total number of values of MM5 output and observations are presented in Table 4.8. Comparison of modelled near-surface fields of wind, temperature and relative humidity for Coles Place, Hoon Hay and Aranui measurement sites was undertaken for the finest grid with a 1 km spatial resolution (domain 4) for the time period from 0000 NZST on 21 July 2003 to 0000 NZST on 23 July 2003 (relative humidity was measured only at Coles Place).

Table 4.8 Index Of Agreement (IOA), Pearson's Correlation Coefficient (PCC), Systematic & Unsystematic Root Mean Square Error (S-RMSE & U-RMSE), and additional statistics of observed and modelled data for the time period 0000 NZST on 21 July 2003 to 0000 NZST on 24 July 2003, experiment 3-03: near-surface wind (m/s), temperature (^{0}C) and relative humidity (%).

EXPERMENT	NUMBER OF OBSERATIONS	OBSERVED MEAN	MODELLED MEAN	OBSERVED DEVIATION	MODELLED DEVIATION	PCC	S-RMSE	U-RMSE	IOA
WIND SPEED (m/s)									
Experiment 3-03a	72	1.05	0.82	0.78	0.65	0.77	0.36	0.41	0.86
Experiment 3-03b	72	1.09	1.12	0.48	0.49	0.83	0.08	0.27	0.91
Experiment 3-03c	72	1.30	1.16	0.70	0.51	0.76	0.33	0.33	0.86
AVERAGE	**72**	**1.15**	**1.03**	**0.65**	**0.55**	**0.79**	**0.26**	**0.34**	**0.88**
U-COMPONENT (m/s)									
Experiment 3-03a	72	0.42	0.43	0.80	0.80	0.68	0.16	0.48	0.89
Experiment 3-03b	72	-0.10	-0.17	0.94	0.94	0.94	0.14	0.39	0.96
Experiment 3-03c	72	0.43	0.23	1.27	1.27	0.94	0.30	0.39	0.96
AVERAGE	**72**	**0.25**	**0.16**	**1.00**	**1.00**	**0.85**	**0.20**	**0.42**	**0.93**
V-COMPONENT (m/s)									
Experiment 3-03a	72	0.35	0.09	0.89	0.51	0.57	0.65	0.42	0.68
Experiment 3-03b	72	0.17	0.02	0.72	0.46	0.31	0.59	0.44	0.69
Experiment 3-03c	72	0.13	-0.04	0.64	0.59	0.33	0.47	0.55	0.71
AVERAGE	**72**	**0.21**	**0.02**	**0.75**	**0.52**	**0.40**	**0.57**	**0.47**	**0.69**
TEMPERATURE (^{0}C)									
Experiment 3-03a	72	4.59	2.77	4.69	3.32	0.87	2.55	1.63	0.86
Experiment 3-03b	72	4.98	2.28	3.54	2.22	0.83	3.18	1.22	0.78
Experiment 3-03c	72	3.57	1.91	4.87	2.44	0.90	3.12	1.06	0.80
AVERAGE	**72**	**4.38**	**2.32**	**4.37**	**2.66**	**0.87**	**2.95**	**1.30**	**0.81**
RELATIVE HUMIDITY (%)									
Experiment 3-03a	72	83.4	84.8	9.9	6.3	**0.83**	4.83	3.50	**0.86**
Experiment 3-03b									
Experiment 3-03c									
AVERAGE	**72**	**83.4**	**84.8**	**9.9**	**6.3**	**0.83**	**4.83**	**3.50**	**0.86**

It should be noted that there is very good agreement between observed and modelled data for wind speed and the zonal component of wind (IOA ranges between 0.85–0.95), but lower IOA for the meridional component: mean IOA is close 0.70 (Table 4.8). Agreement for temperature and relative humidity (RH) exceeded 0.80. The lower level of meridional wind IOA is a result of weak mesoscale and local scale meridional wind absolute magnitudes for the Christchurch area that leads to increase of absolute and relative errors of V-component values in MM5. Christchurch during wintertime is more frequently under the influence of zonal synoptic and mesoscale airflow, which creates more robust agreement of zonal flow with the observations

compared with the more variable meridional flow (see 'Observed mean' for U and V wind components in Tables 4.3, 4.4, 4.6 and 4.8).

In Figure 4.24, vertical profiles of modelled temperature are represented (experiment 3-03, domain 4) and compared with the results of the vertical temperature profiling (at English Park, St. Albans, Christchurch) undertaken during heavy smog nights on 21, 22 and 23 July 2003 (Sturman *et al.*, 2003; McKendry *et al.*, 2004).

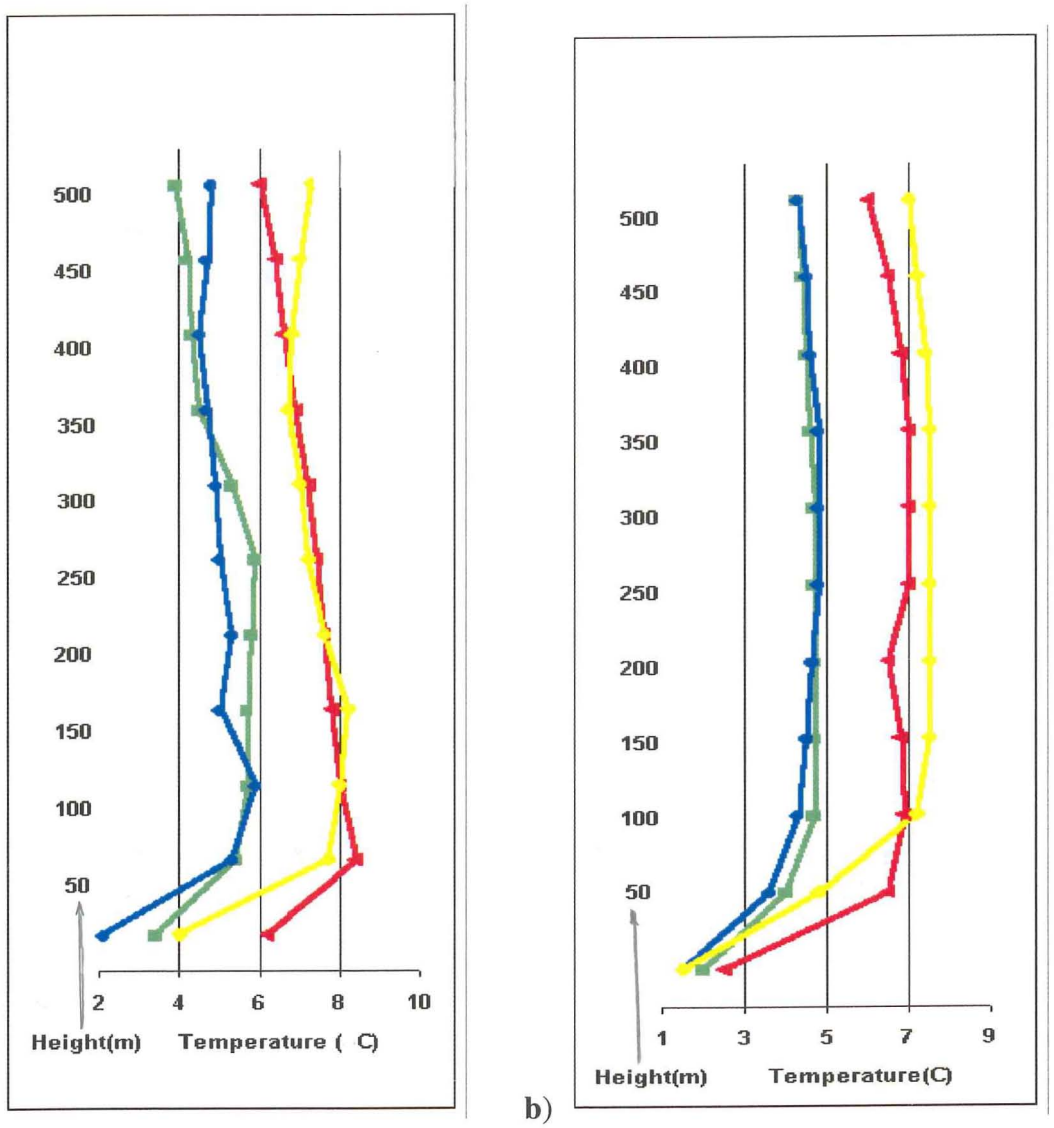

Figure 4.24 Vertical profiles of modelled and measured temperatures (English Park, St. Albans) for experiment 3-03, grid 4: a) 1800 NZST (green-modelled, red-observed) & 2000 NZST (blue-modelled, yellow-observed) on 21 July 2003; b) 2200 NZST (green-modelled, red-observed) & 2400 NZST (blue-modelled, yellow-observed) on 21 July 2003.

Comparing the profiles for the four times (1800, 2000, 2200 and 2400 NZST), it is obvious that the MM5 fine grid run managed to reproduce the vertical tendency shown in the observed temperature profiles in the Christchurch ABL, with correlation coefficients between 0.85 (Figure 4.24a) and 0.95 (Figure 4.24b). However, it is evident that the tendency for underestimation of the modelled temperature values compared with the observations can be associated not only with absence of local input data and the model's BL parameterisation errors, but also with the difficulty of obtaining precise balloon temperature measurements from the vertical profiling plots from the average of up and down balloon movements.

4.3.5 Meteorological Service MM5 parameterisation

As the Meteorological Service (MetService, Wellington) uses the same model for regional weather forecasts over New Zealand, it was decided to run MM5 with the four domains, but with input nudging data received from Wellington (for 20–24 July 2003) and with MM5 physical parameterisations that were used in MetService for operational forecasting. The results were compared with the output of experiment 3-03.

This experiment was named as experiment 4-03 (MetService) and was run over 72 hours for grids 1–3 (1200 NZST on 20 July 2003 to 1200 NZST on 23 July 2003) and on 48 hours for domain 4 (1200 NZST on 21 July 2003 to 1200 NZST on 23 July 2003). For experiment 4-03 the NCEP assimilated data were available 6-hourly for basic meteorology and daily for sea-surface temperature (SST), but SOIL and SNOW files had to be created from NCEP global analysis data, as there were no SOIL temperature data for the Land Surface Model in the MetService database.

Differences in 3-dimensional structure of experiment 3-03 data and MetService input data includes:

1. Data from MetService cover all 4 our domains, SST depends of time
2. MetService data are for 30 vertical levels (1000, 998, 995, 990, 985, 980, 970, 965, 960, 955, 940, 910, 875, 850, 835, 785, 750, 725, 700, 625, 600, 500, 400, 300, 250, 200, 150, 125, 100 hPa) with the top level at 100 hPa
3. Absence of soil files implies that MetService uses standard tables for evaluation of the Land Surface Model.

In the first stage of experiment 4-03, domains 1–3 were run over 72 hours using the following physical scheme:

1. All three domains started together at 1200 UTC on 20 July 2003 (0000 NZST on 21 July 2003 NZST) and finished together at 1200 UTC on 23 July 2003 (0000 NZST on 24 July 2003)
2. Two-way interaction of 'mother–daughter' grids was stipulated for all levels of nesting during the run, with the output information dumped hourly for grid 3

3. Grids 1–3 were nudged 6-hourly by MetService data
4. The Reisner mixed phase moisture scheme was used for all three grids
5. Grell's scheme was used for cumulus parameterisation in domains 1 and 2, and convection was switched off in domain 3
6. Boundary layer MRF parameterisation was used for domains 1–2 and the Blackadar scheme for grid 3
7. The radiation scheme was RRTM for all 3 domains
8. The five-layer soil model was switched on in all 3 domains, with bucket soil moisture scheme
9. SST was used from separately distributed input files.

In the second stage, domain 4 was run over 48 hours with 3-hourly input meteorological data that had been received as output from domain 3 (the mother domain).

After analysis of grid 3 output, a near-surface wind direction day–night change was observed for the Christchurch region, but the amount of wind turn over time was lower than that predicted in experiment 3-03 (domain 3). The physical parameterisation used to run grid 4 was left the same as for domain 3, but the 30 levels of domain 3 data were interpolated to the 43 vertical levels of experiment 3-03 using the slow but very precise positive finite difference method of the NESTDOWN program. This was done with the aim of increasing the resolution of the MM5 atmosphere to achieve more accurate replication of the air circulation over the complex terrain of the Christchurch area.

Results: Near-surface wind fields are represented in Figure 4.25 for MM5 (grid 4) for two times of experiment 4-03: at 0000 NZST on 23 July 2003, showing westerly nocturnal drainage winds (Figure 4.25a); and at 1000 NZST on 23 July 2003, with daytime northerly winds over the Christchurch area (Figure 4.25b). This can be compared with westerly–southwesterly nocturnal winds (Figure 4.22a) and easterly–northeasterly daytime winds (Figure 4.22b) of experiment 3-03.

a) b)

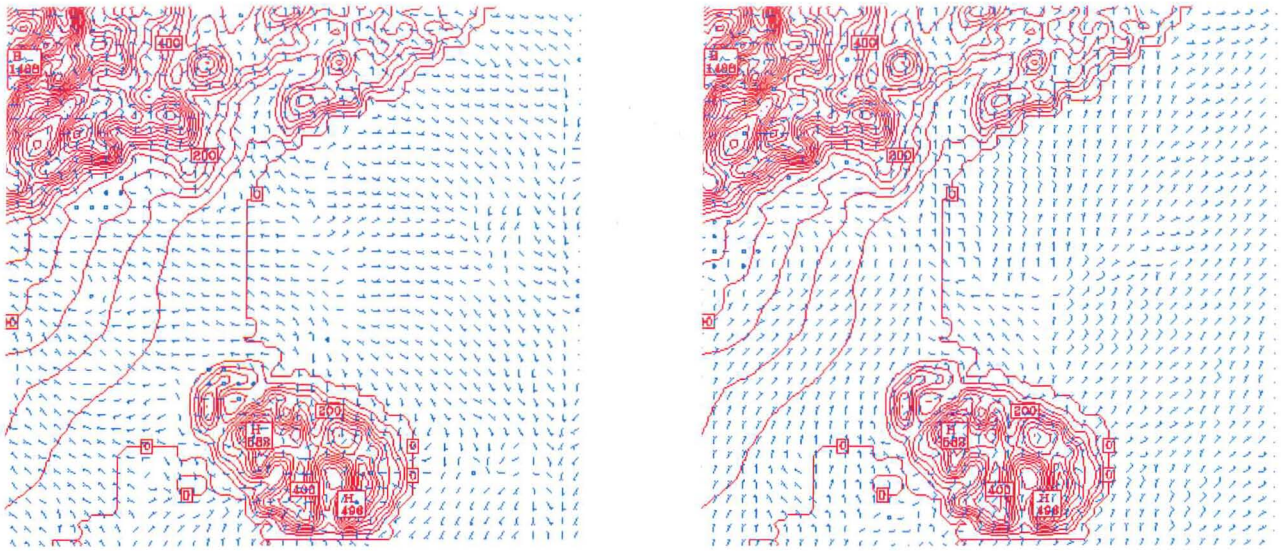

Figure 4.25 Spatial distribution of MM5 modelled near-surface wind for the experiment 4-03, grid 4, σ=0.999 (7.0–8.5 metres): a) 0000 NZST on 23 July 2003 (48 hour forecast); b) 1000 NZST on 23 July 2003 (56 hour forecast).

Vertical profiles of dry-bulb (red solid line) and dew-point temperatures (green solid line) and wind change with height in the ABL are shown in Figure 4.26, as extracted from MM5 grid 4 output for Christchurch Airport at 0000 and 1000 NZST for 23 August 2000. The nighttime dry-bulb temperature profile indicates strong negative buoyancy (Figure 4.26a) in the near-surface layer (compared with weaker stability shown in Figure 4.23a) associated with warm ocean winds (north-easterly airflow) above the ABL, and an elevated inversion above the sea breeze return circulation. The morning vertical temperature profile is characterized by a residual inversion, especially in the lowest 100–150 metres, with a weakened elevated inversion that has descended towards the surface in the warmer northeasterly airflow from the ocean (Figure 4.26b). The dew-point temperature profile indicates a very moist layer below the elevated temperature inversion where the airflow is dominated by an onshore component.

a) b)

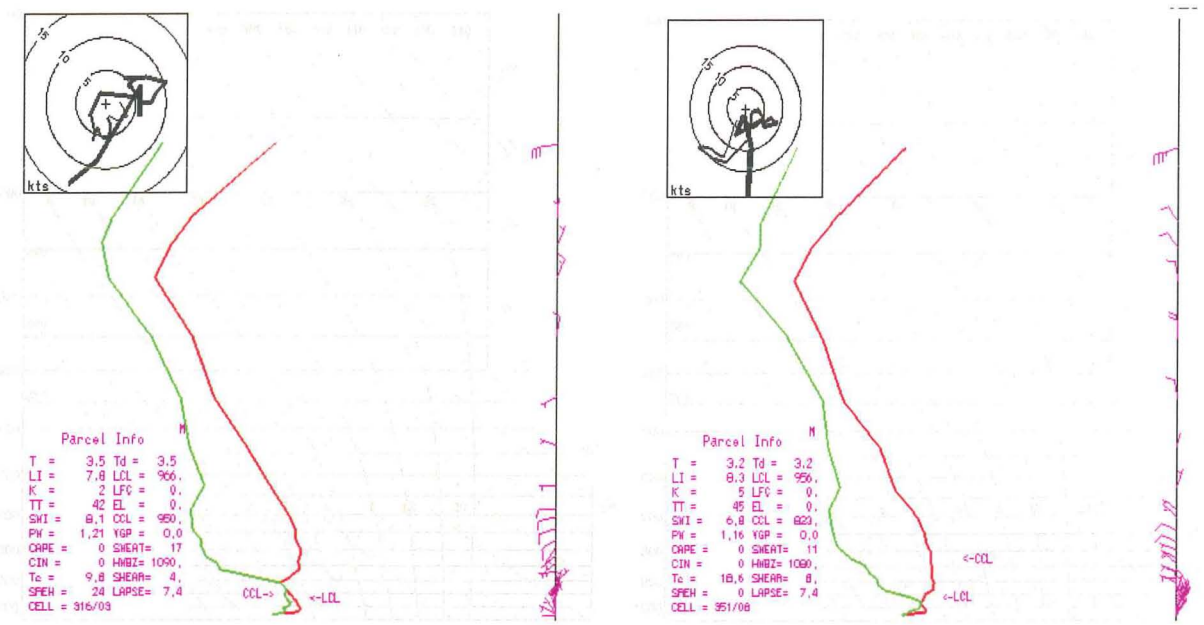

Figure 4.26 Vertical profiles of modelled dry-bulb (red) and dew-point (green) temperatures and wind for experiment 4-03, grid 4: a) 0000 NZST on 23 July 2003 (48 hour forecast); b) 1000 NZST on 23 July 2003 (56 hour forecast).

Vertical profiles of temperature in experiment 4-03 more realistically reflect vertical variation of horizontal air movement than in experiment 3-03 (Figure 4.23a, b), while the near-surface wind distribution and night–day wind rotation is closer to observations in experiment 3-03 (compare Figures 4.22 & 4.25).

Figure 4.27 represents time series of modelled near-surface wind direction (black circles) for experiment 3-03 (Figure 4.27a) and for experiment 4-03 (Figure 4.27b) compared with observations from the Coles Place site (red triangles) during 21–23 July 2003 (48 hour runs, gride 4). Both modelled time trends are very close to the observations (see Figure 4.25).

a)

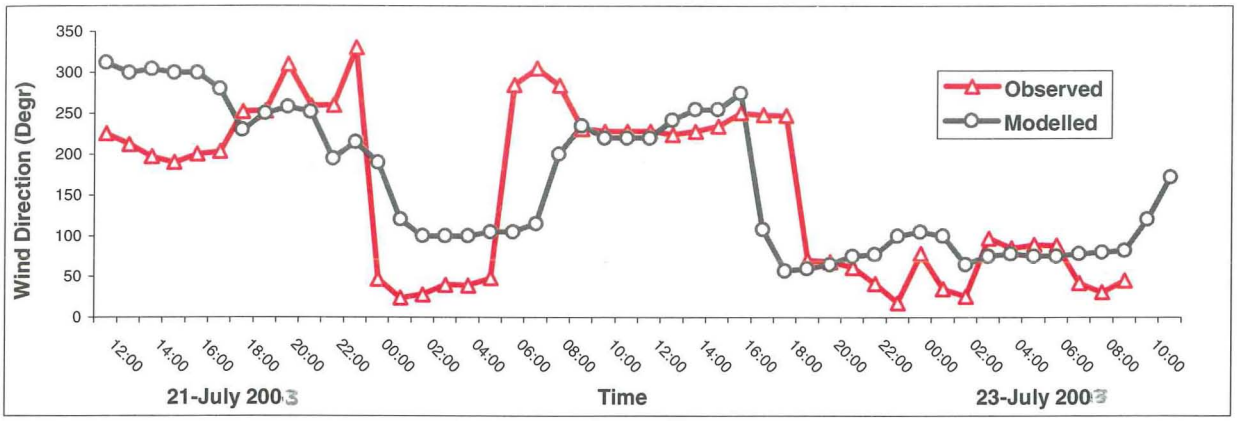

b)

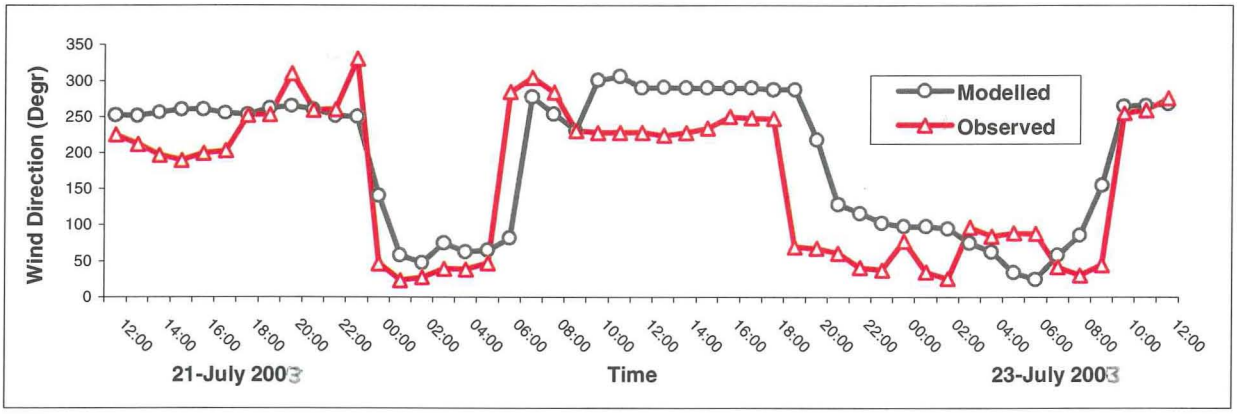

Figure 4.27 Time series of modelled wind direction for a) experiment 3-03 and for b) experiment 4-03 grid 4, σ = 0.999 (7.0-8.5 metres) compared with observations (Coles Place, St. Albans) for the time period 1200 UTC on 21 July (00 NZST on 22 July) to 1200 UTC on 23 July (00 NZST on 24 July) 2000.

Index of agreement, correlation coefficient and accompanying statistics for MM5 experiment 4-03 output and observations are presented in Table 4.9. Comparison of the modelled near-surface fields of wind, temperature and relative humidity for Coles Place, Hoon Hay and Aranui measurement sites was undertaken for the finest grid with 1 km spatial resolution (domain 4) for the time period from 0000 NZST 21 July 2003 to 0000 NZST to 23 July 2003 (relative humidity was measured only at Coles Place).

Table 4.9 Index Of Agreement (IOA), Pearson's Correlation Coefficient (PCC), Systematic & Unsystematic Root Mean Square Error (S-RMSE & U-RMSE), and additional statistics of observed and modelled data for the time period 0000 NZST 22 to 0000 NZST 24 July 2003 for experiment 4-03: near-surface wind (m/s), wind components (m/s), temperature (^{0}C) and relative humidity (%).

EXPERMENT	NUMBER OF OBSERATIONS	OBSERVED MEAN	MODELLED MEAN	OBSERVED DEVIATION	MODELLED DEVIATION	PCC	S-RMSE	U-RMSE	IOA
WIND SPEED (m/s)									
Experiment 4-03a	103	1.31	1.49	0.84	0.89	**0.77**	0.24	0.56	**0.87**
Experiment 4-03b	103	1.25	1.56	0.71	0.77	**0.72**	0.35	0.53	**0.81**
Experiment 4-03c	103	1.67	1.66	0.68	0.76	**0.72**	0.13	0.53	**0.84**
AVERAGE	**103**	1.41	1.57	0.74	0.81	**0.74**	0.24	0.54	**0.84**
U-COMPONENT (m/s)									
Experiment 4-03a	103	0.43	0.40	1.05	0.70	**0.85**	0.26	0.70	**0.89**
Experiment 4-03b	103	0.12	0.24	1.14	1.39	**0.87**	0.14	0.67	**0.92**
Experiment 4-03c	103	0.78	0.40	1.44	0.70	**0.90**	0.27	0.55	**0.95**
AVERAGE	103	0.44	0.35	1.21	0.93	**0.88**	0.23	0.64	**0.92**
V-COMPONENT (m/s)									
Experiment 4-03a	103	0.35	0.49	1.01	0.88	**0.75**	0.51	0.70	**0.77**
Experiment 4-03b	103	0.15	0.43	0.86	0.93	**0.75**	0.32	0.61	**0.84**
Experiment 4-03c	103	0.14	0.39	0.76	0.84	**0.53**	0.40	0.71	**0.71**
AVERAGE	103	0.21	0.44	0.88	0.88	**0.68**	0.41	0.67	**0.77**
TEMPERATURE (^{0}C)									
Experiment 4-03a	103	4.37	4.22	4.43	2.66	**0.82**	2.26	1.53	**0.84**
Experiment 4-03b	103	5.45	4.31	3.51	2.77	**0.89**	1.55	1.26	**0.90**
Experiment 4-03c	103	3.74	4.03	4.45	2.96	**0.92**	1.76	1.19	**0.92**
AVERAGE	103	4.52	4.18	4.13	2.79	**0.87**	1.85	1.33	**0.88**
RELATIVE HUMIDITY (%)									
Experiment 4-03a	103	83.0	81.9	9.6	10.7	**0.77**	1.72	6.74	**0.87**
Experiment 4-03b									
Experiment 4-03c									
AVERAGE	103	83.0	81.9	9.6	10.7	**0.77**	1.72	6.74	**0.87**

It should be noted that there is a good agreement between observed and modelled data for wind speed, and zonal and meridional components of wind. Agreement for temperature and relative humidity (RH) exceeded 0.85. The level of meridional wind IOA is higher than in experiment 3-03, but wind speed is better modelled (closer to real mean wind values) in case of the deep atmosphere of experiment 3-03, with IOA about 0.90 against 0.85 in case of the MetService data (see 'WIND SPEED' in Tables 4.8 and 4.9). This is very important as wind speed (and wind direction) plays a fundamental role in redistribution and dry scavenging of aerosol concentrations over time.

Figure 4.28 presents vertical profiles of modelled temperature (experiment 4-03, domain 4) for times 1800, 2000, 2200 and 2400 NZST on 21 July 2003 compared with the profiles of the temperature obtained from tethered balloon soundings (English Park, St. Albans, Christchurch) collected during the observational study of the ABL vertical structure on nights of heavy smog: 21, 22 and 23 July 2003 (Sturman *et. al.*, 2003).

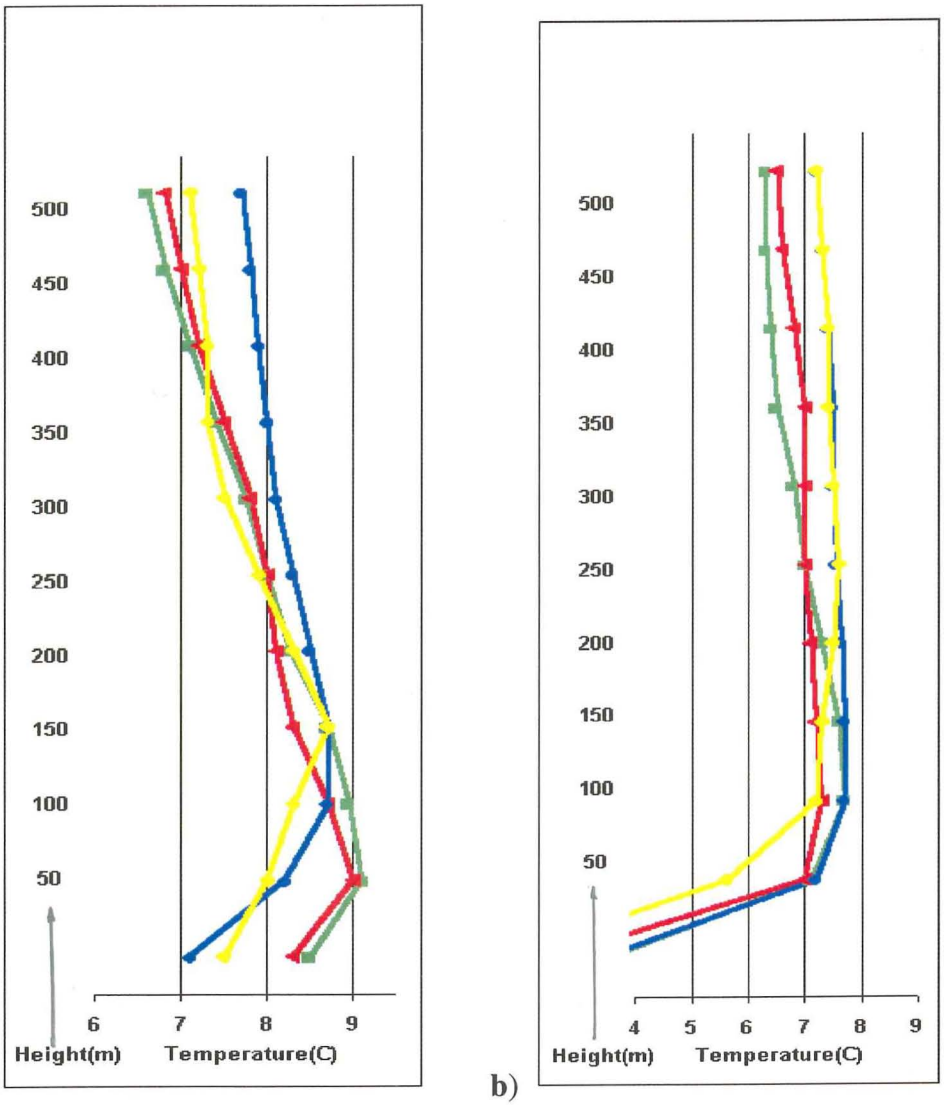

Figure 4.28 Vertical profiles of modelled and measured temperatures (English Park, St. Albans) for experiment 4-03, domain 4: a) 1800 NZST (green-modelled, red-observed) & 2000 NZST (blue-modelled, yellow-observed) on 21 July 2003; b) 2200 NZST (green-modelled, red-observed) & 2400 NZST (blue-modelled, yellow-observed) on 21 July 2003.

Comparison with real data and the results of experiment 3-03 at four times (1800, 2000, 2200 and 2400 NZST) clearly shows that the fine grid run of experiment 4-03 has managed to reproduce the vertical distribution of observed temperature profiles more accurately (see Figure 4.24), with correlation coefficients between 0.90 (Figure 4.28a) and 0.95 (Figure 4.28b). The tendency for underestimation of modelled temperature values compared with observations was less than one degree on average. This probably reflects with more realistic SST input and

nudging data. However, it should be stressed that in the case of experiment 4-03, obtaining observed temperature profiles from the tethered balloon data was simplified and only upward balloon movement information was used to minimize the measurement error (the total time of up-down balloon movement usually takes about 1.5–2.0 hours).

4.3.6 Case study days and error analysis

In this section, the influence of the use of global analysis data on underprediction (type I error) and overprediction (type II error) of near-surface wind field will be assessed. The accuracy of the wind field is of fundamental importance for the effectiveness of predictions of air pollution dispersion using the numerical modelling system MM5–CAMx4.

As already discussed, air circulation in the boundary layer over Christchurch is the result of interaction of the prevailing synoptic scale flow assimilated by the model from input and nudging files of the global analysis and the mesoscale circulation created during MM5 runs by local factors of the Christchurch area.

The probability of a heavy smog night occurrence under stagnant meteorological conditions (i.e. low synoptic winds) can be considered as the null hypothesis (H_0). Weak initial and nudging pressure gradient fields in the ABL (that produce weak wind fields) derived from global data assimilation can lead to underestimation of near-surface wind speed in an experiment and have no serious influence on the time variation of near-surface wind direction. The underestimation of the local to mesoscale wind speeds under settled synoptic scale conditions leads to overprediction of aerosol pollution values during nighttime. Therefore, when high PM concentrations do not occur under such circumstances during nighttime in Christchurch we have a type II error, as H_0 is accepted when it is wrong (underestimation of local airflow velocity and overestimation of PM concentration). The type II error is the combined effect of the global analysis data and the MM5 model settings and leads to false warnings (hoax alert) but does no serious harm practically.

The effect of the global analysis data on overestimation of the intensity of synoptic scale processes for New Zealand and the resulting suppression of local air circulation over the Christchurch region during MM5 runs creates a type I error, because the null hypothesis H_0 (high concentrations of PM at night) is rejected in the forecast with a high level of reliability (generated by dominant strong air flow) when a heavy smog night is actually observed. The rejection of a heavy smog night forecast when it is true could lead to serious health problems in Christchurch and its vicinity, which is not the case for overprediction of aerosol pollution (the type II error).

Experiments 2_1 and 2_2 were run for the time period 22–24 July 2000. This period was affected by strong southwesterly winds (from global analysis data) and by heavy pollution at night between 23 and 24 July 2000 (see Figure 3.6), implying stagnant near-surface airflow with local circulation dominating over synoptic scale effects.

A short description of the 3-dimensional structure of experiments 2_1 and 2_2 (winter 2000) includes 43 vertical layers for 4 domains with 14 vertical layers in the atmospheric boundary layer and the top σ-level equal to 0.010 hPa.

In the first stage of experiment 2_1, domains 1 to 3 were run together over a 72 hours period starting at 0000 NZST on 22 July and finishing at 0000 NZST on 25 July 2000 using 6-hourly global analysis nudging. In experiment 2_2, the mother domain was run first for 80 hours (1200 NZST on 21 July 2000 to 0000 NZST on 25 July 2000) with 6-hourly nudging, and grids 2 and 3 were evaluated using input from domain 1 output 6-hourly over the time period 0000 NZST on 22 July 2000 to 0000 NZST on 25 July 2000.

The following physical parameterisations were used in both experiments:

1. Reisner mixed phase moisture scheme was used for all three grids
2. The Grell scheme was used for cumulus parameterisation in domains 1 and 2, and convection was switched off in domain 3
3. The boundary layer MRF parameterisation scheme was used for domains 1–2 and the Blackadar scheme for grid 3
4. The radiation scheme was the RRTM method for all 3 domains
5. The soil model was switched on with a bucket soil moisture scheme in all 3 domains
6. SST was the NCEP global sea-surface temperature analysis.

In the second stage, grid 4 was run over 24 hours (1200 NZST on 23 July 2000 to 1200 NZST on 24 July 2000) with initialisation and hourly nudging using meteorological data output from domain 3. The physical parameterisation used in grid 4 was left the same as for domain 3, but the number of levels in domain 4 was decreased from 43 to 40 levels (the top σ-levels 0.010, 0.020 and 0.030 were removed) using the precise positive finite difference interpolation method of the NESTDOWN procedure.

Results: Near-surface wind fields for MM5 (grid 4) for two times of experiment 2_2 are presented in Figure 4.29: at 0000 NZST on 24 July 2000 under strong south-westerly anti-cyclonic winds (Figure 4.29a) and at 1000 NZST on 24 July 2000 under the same strong south-westerly near-surface airflow over the Christchurch area (Figure 4.29b) inherited by MM5 (grid 4) from the global objective analysis and assimilated during the model run.

a) b)

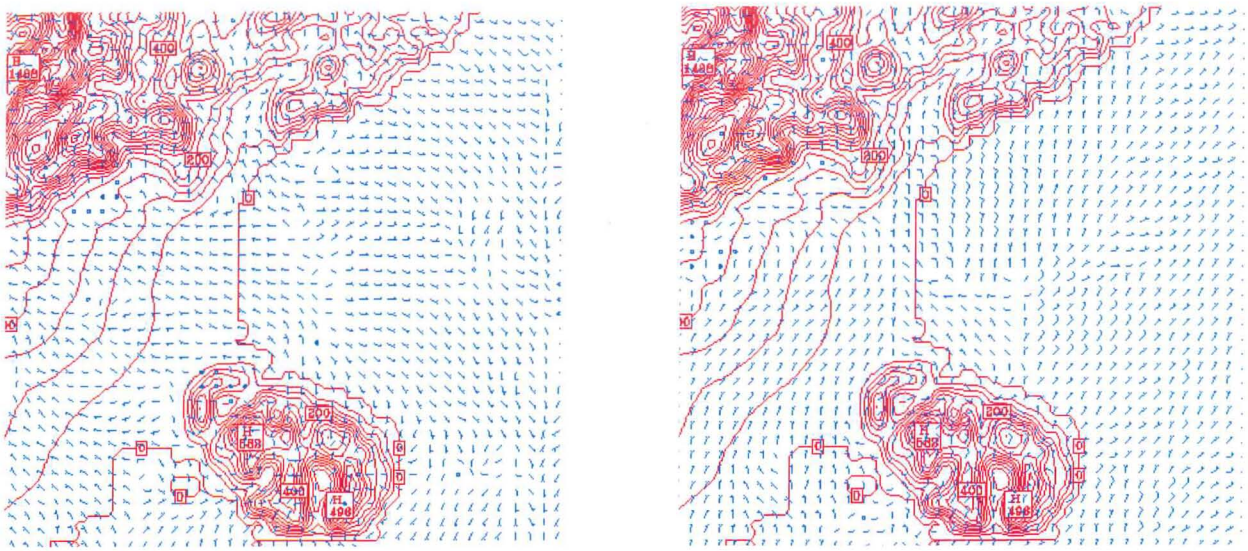

Figure 4.29 Spatial distribution of MM5 modelled near-surface wind for experiment 2_2, domain 4, σ=0.999 (7.0–8.5 metres): a) 0000 NZST on 24 July 2000 (12 hour forecast); b) 1000 NZST on 24 July 2000 (22 hour forecast).

Vertical profiles of dry-bulb temperature for both these times (grid 4) show the elimination of the nighttime temperature inversion in the boundary layer as a result of very active quasi-barotropic air advection.

In Figure 4.30, time series of modelled near-surface wind direction (black circles) for Coles Place (Figure 4.30a) and Cracroft (Figure 4.30b) observation sites are compared with observations (red triangles) for the time period from 1200 NZST on 23 July 2000 to 1200 NZST on 24 July 2000 (24 hours runs, grid 4). Both modelled time series of near-surface wind have failed to predict the night-time wind change that is obvious from the observations, which appears to result from the strong influence during this run of south-westerly winds taken from the global data assimilation database.

a)

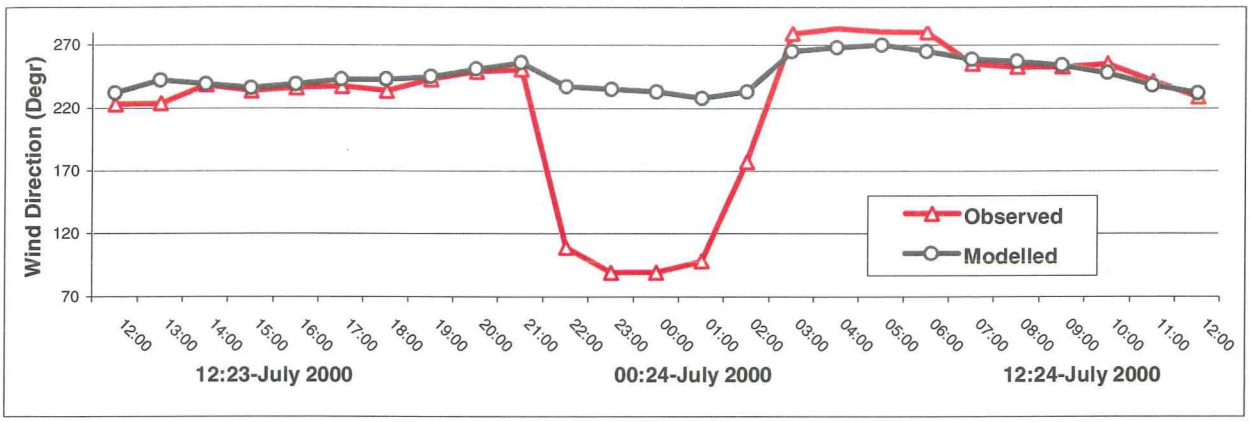

b)

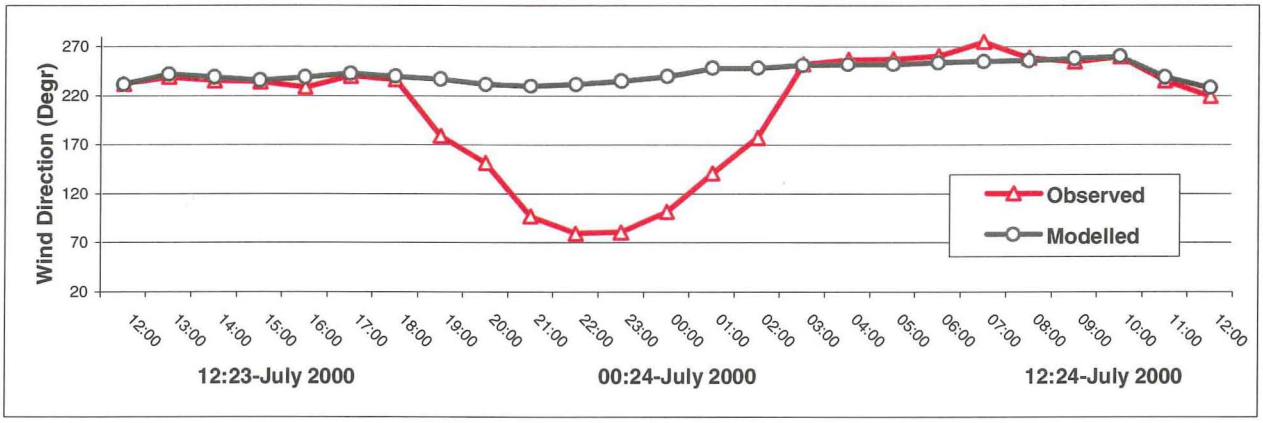

Figure 4.30 Time series of the modelled near-surface wind direction for a) Coles Place and b) Cracroft (grid 4) compared with observations, for experiment 2_1, over the time period from 1200 NZST on 23 July 2000 to 1200 NZST on 24 July 2000.

Time series of the modelled near-surface wind magnitude (Figure 4.31a) and direction (Figure 4.31b) derived from the output of experiment 2_1 grid 4 were also evaluated against the observed wind characteristics (red crosses) taken from the Coles Place observation site (St. Albans). Comparison of modelled and observed data provides evidence of reasonable agreement regarding wind magnitudes and the failure of MM5 to reproduce the observed near-surface wind direction change.

a)

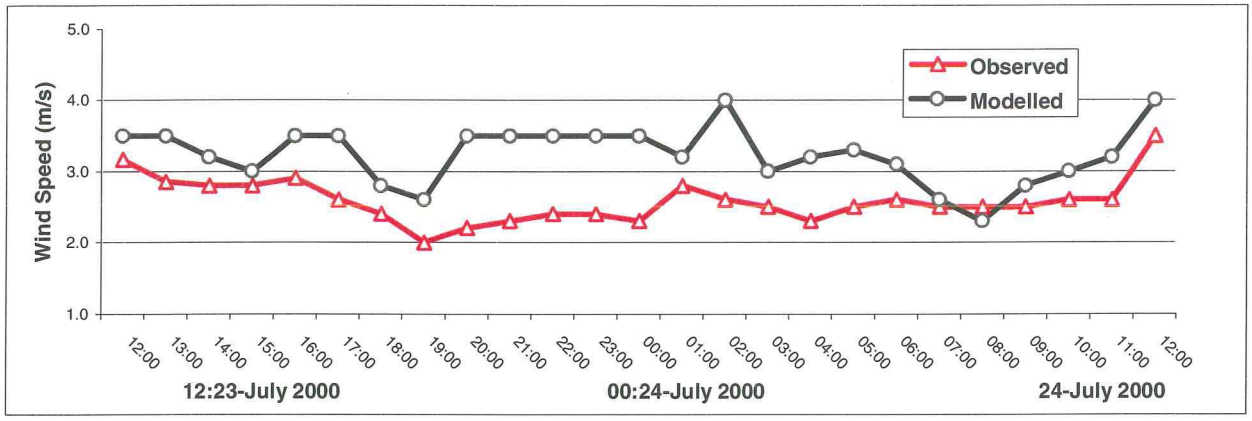

b)

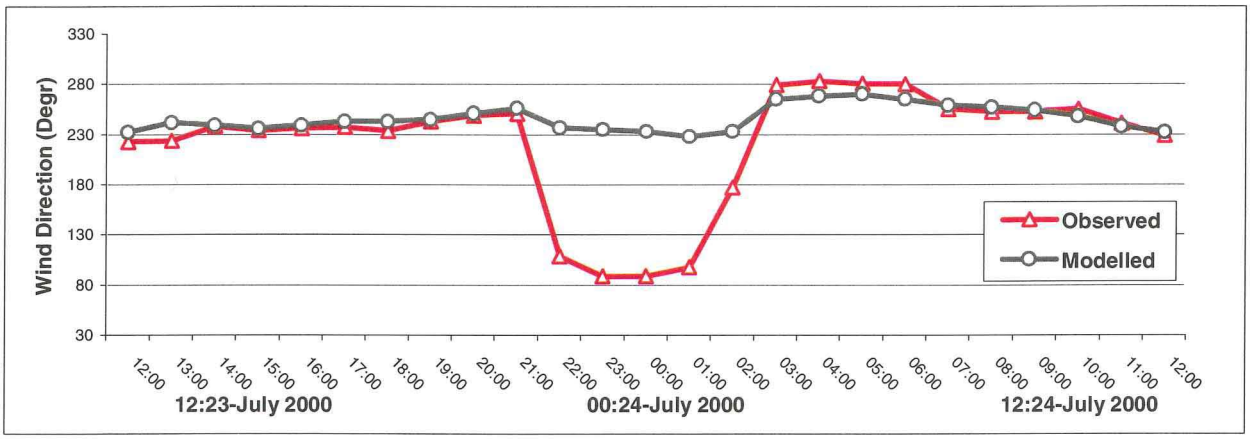

Figure 4.31 Time series of modelled (black circle) and observed (red cross) near-surface wind speed and wind direction: experiment 2_1, grid 4, for Coles Place, over the time period from 1200 NZST on 23 July 2000 to 1200 NZST on 24 July 2000.

Index of agreement, correlation coefficient and additional statistics for MM5 experiments 2_1 (grids 3, 4) and 2_2 (grid 4) near-surface meteorology are represented in Table 4.10. Comparison of modelled near-surface fields of wind, temperature and relative humidity were taken for 24 observation sites (the Christchurch area only) for the time interval from 1200 NZST on 23 July 2000 to 1200 NZST on 24 July 2000. The number of temperature and relative humidity measurements, as always, was less than the number of wind measurements). Description of the experiments is given in Table 4.2.

Table 4.10 Index Of Agreement (IOA), Pearson's Correlation Coefficient (PCC), Systematic & Unsystematic Root Mean Square Error (S-RMSE & U-RMSE), and additional statistics (observed and modelled data) for the time period 1200 NZST on 23 July 2000 to 1200 NZST on 24 July 2000 for experiments 2_1 and 2_2: near-surface wind (m/s), wind components (m/s), temperature (^{0}C) and relative humidity (%).

EXPERMENT	NUMBER OF OBSERATIONS	OBSERVED MEAN	MODELLED MEAN	OBSERVED DEVIATION	MODELLED DEVIATION	PCC	S-RMSE	U-RMSE	IOA
WIND SPEED (m/s)									
Experiment 2_1a	515	2.63	3.83	1.32	1.56	0.60	1.25	1.23	0.68
Experiment 2_1b	200	2.93	3.53	0.66	0.72	0.68	0.62	0.52	0.71
Experiment 2_2	224	3.05	3.72	0.73	0.80	0.71	0.70	0.56	0.72
AVERAGE	**313**	**2.87**	**3.70**	**0.91**	**1.03**	**0.66**	**0.86**	**0.77**	**0.70**
U-COMPONENT (m/s)									
Experiment 2_1a	515	0.83	2.32	2.04	2.73	0.68	1.54	2.01	0.75
Experiment 2_1b	200	1.86	3.08	1.67	0.59	0.44	1.88	0.54	0.49
Experiment 2_2	224	1.89	3.15	1.74	0.66	0.53	1.93	0.55	0.48
AVERAGE	**313**	**1.53**	**2.85**	**1.82**	**1.33**	**0.55**	**1.78**	**1.03**	**0.57**
V-COMPONENT (m/s)									
Experiment 2_1a	515	0.83	0.82	1.77	1.99	0.54	0.88	1.77	0.67
Experiment 2_1b	200	1.22	1.56	1.16	0.84	0.67	0.69	0.62	0.77
Experiment 2_2	224	1.30	1.79	1.24	1.00	0.64	0.78	0.72	0.78
AVERAGE	**313**	**1.11**	**1.39**	**1.39**	**1.27**	**0.62**	**0.78**	**1.04**	**0.74**
TEMPERATURE (^{0}C)									
Experiment 2_1a	243	8.78	8.89	3.56	2.84	0.92	0.96	1.12	0.95
Experiment 2_1b	100	6.67	6.60	3.74	2.63	0.94	1.26	0.89	0.94
Experiment 2_2	112	6.98	6.88	3.65	2.61	0.95	1.18	0.85	0.94
AVERAGE	**152**	**7.47**	**7.46**	**3.65**	**2.70**	**0.93**	**1.13**	**0.95**	**0.94**
RELATIVE HUMIDITY (%)									
Experiment 2_1a	183	71.62	69.53	11.12	9.96	0.79	3.87	6.12	0.87
Experiment 2_1b	100	71.66	67.81	10.53	6.91	0.88	5.85	3.23	0.86
Experiment 2_2	112	71.43	67.21	10.10	7.34	0.89	5.53	3.33	0.87
AVERAGE	**132**	**71.57**	**68.18**	**10.58**	**8.07**	**0.85**	**5.08**	**4.23**	**0.87**

There is good agreement between observed and modelled data for temperature and relative humidity, with IOA more than 0.85 for RH and more than 0.93 for temperature in both experiments. However, for wind magnitude and zonal and meridional components, the IOA fluctuates in the range 0.57 (U-component) to 0.74 (V-component), and close to 0.70 for wind speed. The most interesting result is that correlation between zonal modelled and observed winds

is lower than the correlation between modelled and observed meridional winds. The only rational explanation for this phenomenon (as in all previous studies, the modelled V-component always had a lower IOA compared with the U-component) is that the decrease of modelled zonal wind IOA is generated by the superimposition of two different scale processes that in this situation oppose each other. The nudging by synoptic scale stable southwesterly winds and the modelled mesoscale circulation trying to maintain the cycle of local air circulation. This example of the excessive dominance of the global analysis input data on MM5 output illustrates a type I error resulting from the use of global assimilation data.

It is interesting to examine the results of MM5 experiment 2_6 run over 24 hours for the time interval from 1200 NZST on 23 July to 1200 NZST on 24 July 2000, which was completed in two steps (using grids 1 to 3 and grid 4 separately) using the same parameterisation scheme as in experiments 2_1 and 2_2, but without nudging by global analysis data (global analysis as a source of initial input data only). This experiment could help to show more clearly the ability of MM5 to reproduce the complex air circulation over the Christchurch area that operates over different time-scales, using initial global analysis input data.

Near-surface wind fields for MM5 (grid 4) for two times during experiment 2_6 are illustrated in Figure 4.32. First, at 1400 NZST on 23 July 2000, weak south-westerly winds and southerly winds occur along the Christchurch coast (Figure 4.32a), while at 1400 NZST on 24 July 2000 strong south-westerly near-surface airflow occurs closer to the grid 4 boundaries (reflecting the influence of global analysis boundary condition data), with weak and variable (mostly following the local orography) south-westerly to westerly and north-westerly winds over Christchurch and the Canterbury plains (Figure 4.32b). These demonstrate a very different type of modelled air circulation (locally produced airflow) compared with the strong south-westerly day and night winds at all points of MM5 domain 4 shown in Figure 4.29.

a) b)

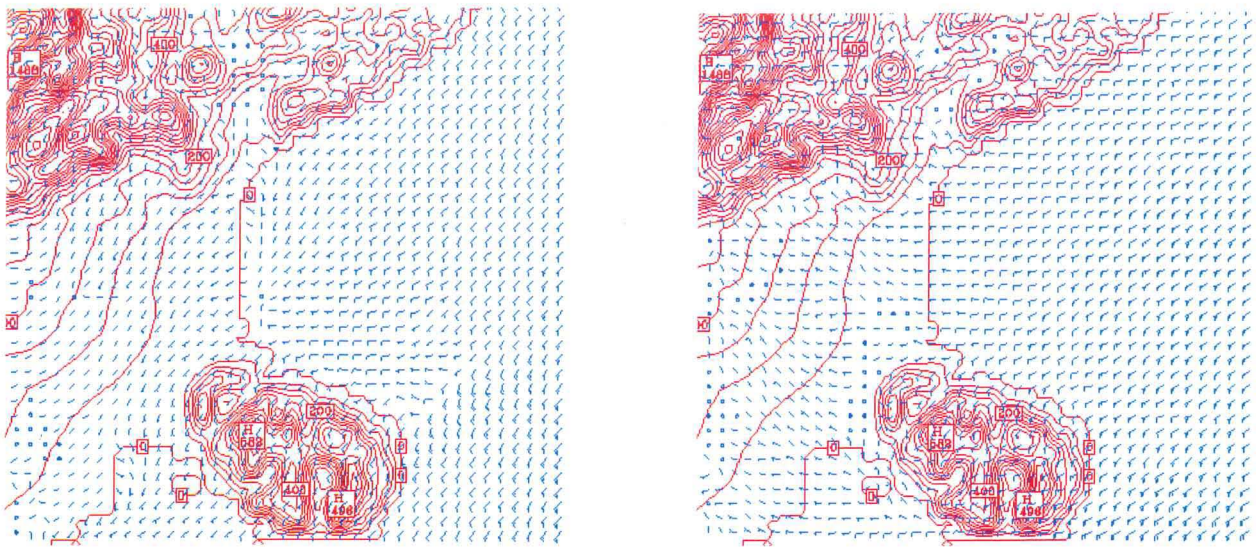

Figure 4.32 Spatial distribution of MM5 modelled near-surface wind for experiment 2_6, domain 4, σ=0.999 (7.0–8.5 metres): a) 1400 NZST on 23 July 2000 (2 hour forecast); b) 0200 NZST on 24 July 2000 (14 hour forecast). The dominance of synoptic scale southwesterly winds can be traced only close to the grid 4 boundaries.

Experiment 2_6 provides evidence of the development of two different scales of process (synoptic scale circulation and local orographical induced airflow) and illustrates once again the real danger of producing type I errors using global analysis input data (i.e. rejection of a high smog hazard forecast when a heavy pollution night actually occurs).

4.3.7 Possibilities and limitations of MM5

In the previous paragraph, it was shown that use of global analysis as input and nudging data could lead to suppression of local mesoscale air circulation in the MM5 model output, as a result of the elimination of local air circulation features during the process of four dimensional data assimilation using global data. The spatial resolution of the global assimilation model and the output resolution of the assimilated analysis are the main restrictions to more accurate reproduction of Christchurch's mesoscale air circulation. As was discussed before, the global analysis data (ds083.2) has a spatial resolution 1^0 x 1^0 over the entire globe. One degree at latitude 45^0 represents approximately 110 km between two grid points – that is 3 times more than the diameter of the Christchurch area. Use of nested grids with additional input information about orography and soils ameliorates this situation, but initial elimination of essential local meteorological information from the input and (especially) from nudging data restricts the level

of precision of MM5 results for coarse and fine grids. The situation can be improved by assimilation of meteorological data from the New Zealand local meteorological network to prevent too big a discrepancy between global analysis and the real synoptic situation.

The second restriction on the maximum quality of an MM5 forecast is the time interval between observations. In our case it is equal to 6 hours, but it is difficult to change the observation time interval, as the 6-hour observation period is the standard one used all over the world (established by the World Meteorological Organization – WMO). It can be changed only during special meteorological studies, like CAPS2000.

The possibility of improvement of MM5 output (using global analysis data) can be achieved by using a finer database of orography than that provided by USGS (30 second data) or other global topographic databases. More precise landuse information could also be obtained, as well as SST information. In addition, the procedure by which MM5 is pre-run using dynamical and physical tuning (including four dimensional data assimilation – FDDA) is one of the main possibilities to improve MM5 winter modelling for the Christchurch area. Experiments 2_3 and 2_4 were run with 3-dimensional analysis data assimilation (experiment 2_4) and without FDDA (experiment 2_3), with the aim of showing how the modelled results can be improved using FDDA analysis. They consisted of two stages: in the first stage of experiment 2_3, domains 1 to 3 were run over a 72-hour time period using the following numerical and physical schemes:

1. Calculation started at 1200 UTC on 18 July 2000 and finished at 1200 UTC on 21 July 2000
2. All grids were nudged by global data analysis six hourly and output information was dumped 3 hourly for domain 3
3. Dudhia's moisture scheme and the Grell cumulus parameterisations were used in domains 1–2
4. Boundary layer parameterisation was the MRF scheme for grids 1 and 2 and the Blackadar for grid 3
5. The RRTM scheme was applied in all 3 grids
6. The five-layer soil model was switched on with the soil moisture scheme
7. 43 vertical levels including 12 levels in the PBL and the top level for σ=0.020.

In the second stage, only grid 4 was run with 3-hourly nudging using the output of domain 3 and an hourly dump of modelled information. All physical parameterisation schemes used to run grid 4 were the same as for domain 3, and grid 4 was simulated for time period 1200 UTC on 19 July 2000 to 1200 UTC on 21 July 2000 over 48 hours with 12 vertical layers in the atmospheric boundary layer and with a top layer equal to 10 hPa (σ=0.020). The difference between the two experiments was that in experiment 2_4, FDDA analysis had been switched on for all 4 domains, and in experiment 2_3 this procedure had been switched off.

Results: The time period 19–22 July 2000 was characterised by intensification of westerly

to south-westerly warm foehn winds with advection of warm air and a consequential increase of near-surface temperature, which lasted for some time. This event is difficult to imitate using MM5 especially for near-surface wind speed and temperature time trends. Time series of the modelled near-surface wind magnitude (black circles) for experiment 2_4 (Figure 4.33a) and experiment 2_3 (Figure 4.33b) were evaluated against observed wind speed (red crosses) obtained at the Coles Place observation site in St. Albans (Christchurch). Comparison of modelled and observed data provides clear evidence of better agreement between modelled and observed wind magnitudes when using FDDA (Figure 4.33a). The mean level of modelled wind speed in experiment 2_4 is very close to the observations.

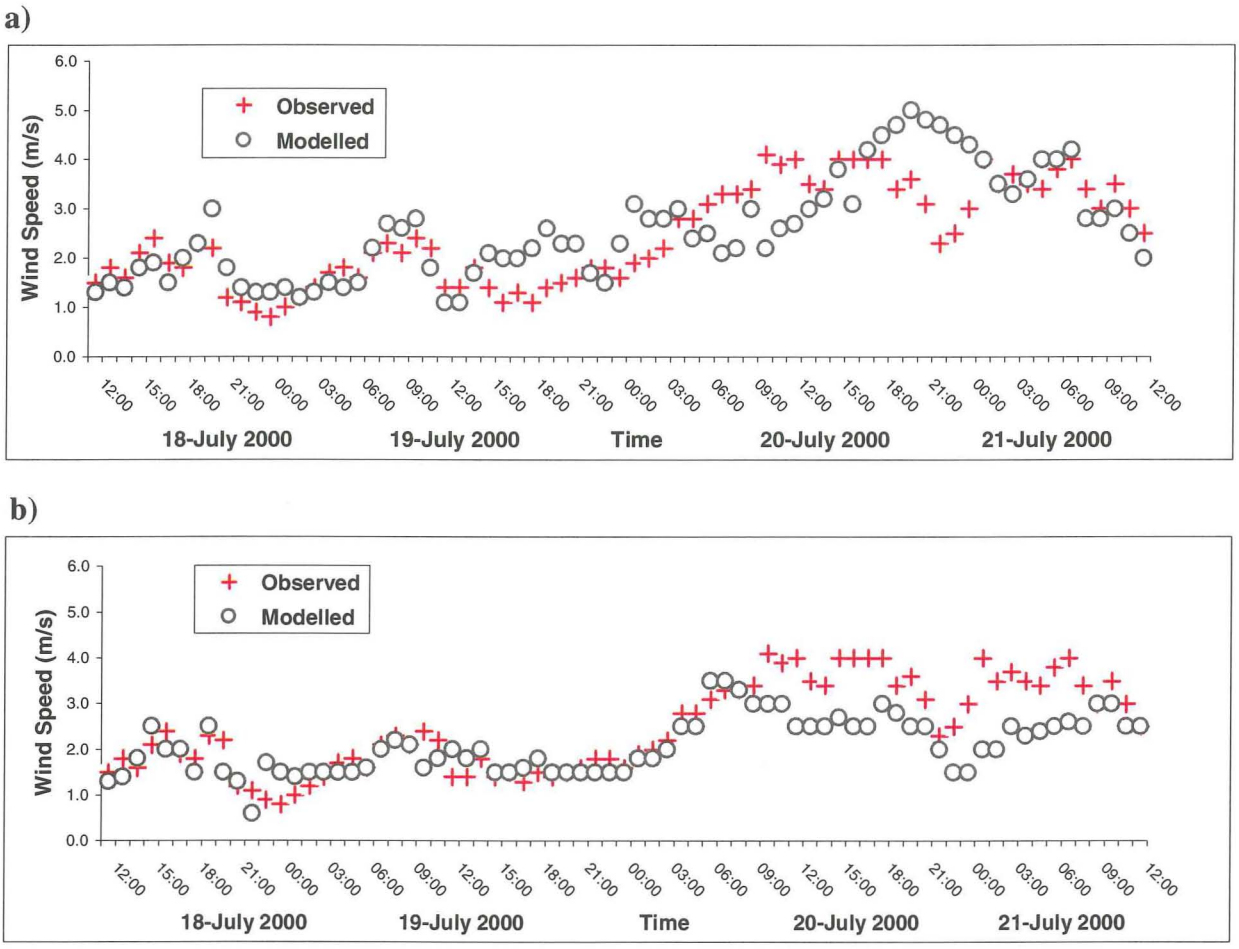

Figure 4.33 Time series of modelled (black circles) and observed (red crosses) near-surface wind speed for a) experiment 2_4, domain 4, and b) experiment 2_3 at Coles Place over the time period from 1200 NZST on 18 July to 1200 NZST on 21 July 2000.

Time series of the modelled near-surface temperature (black circles) are shown in Figure 4.34 for experiment 2_4 (Figure 4.34a) and experiment 2_3 (Figure 4.34b), compared with Coles Place observations once again (red crosses). The investigation of the observed data shows a distinct time tendency of near-surface temperature increase associated with warm air advection in the Christchurch area by accelerating winds (see Figure 4.33). Comparison of modelled and

observed data for the two experiments provides evidence of an improvement in prediction of the temperature trend in the experiment with 3-dimensional analysis data assimilation (Figure 4.34a). Once again, the number of modelled points in experiment 2_3 doesn't coincide with the number in experiment 2_4. However, this fact doesn't influence the general near-surface temperature time trends in the experiment without FDDA (Figure 4.34b), which shows serious underestimation of modelled temperature values compared with observations. Temperature trends for experiment 2_4 are very close to observations (Figure 4.34b) and it is clear that the FDDA MM5 run managed to replicate the near-surface warm air advection event (Figure 4.33b), which produced the general temperature increase.

a)

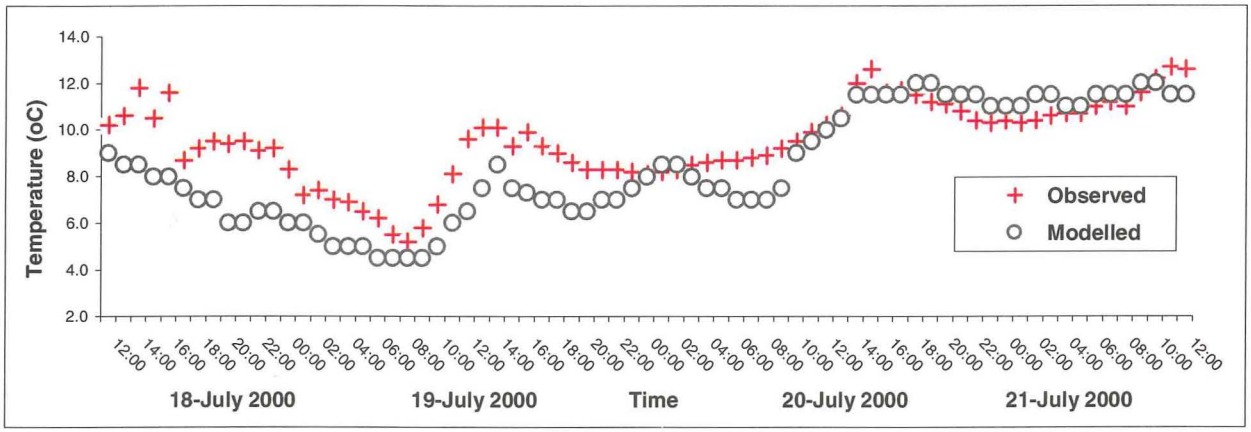

b)

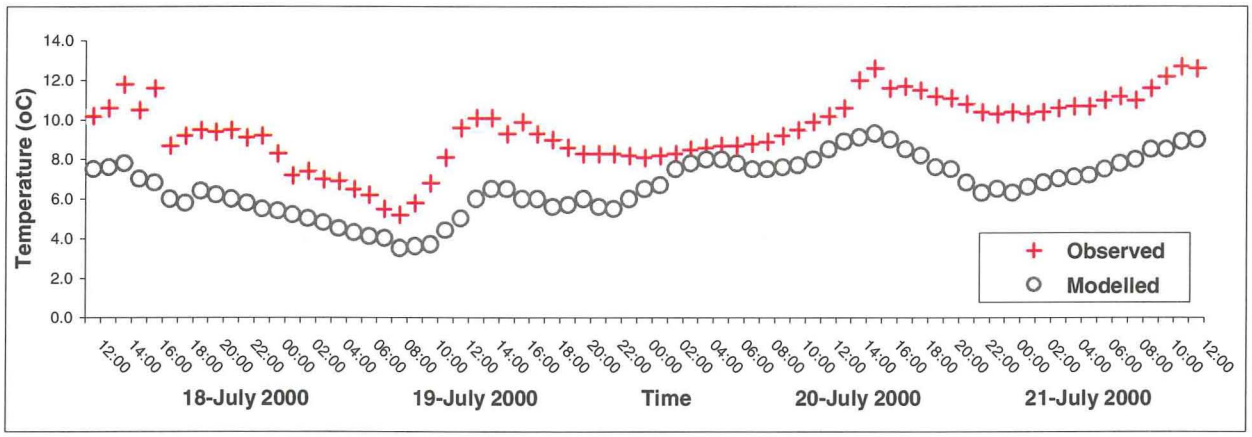

Figure 4.34 Time series of modelled (black circles) and observed (red crosses) near-surface temperature for a) experiment 2_4, domain 4 and b) experiment 2_3, 20 observation sites, time period from 1200 NZST on 19 July 2000 to 1200 NZST on 21 July 2000.

Index of agreement, correlation coefficient and additional statistics for experiments 2_3 (grid 4) and 2_4 (grid 4) near-surface meteorology are represented in Table 4.9. Comparison of modelled near-surface fields of wind, temperature and relative humidity were taken for 20 observation sites (Christchurch only – Table 4.2) for the time interval from 1200 NZST on 19

July 2000 to 1200 NZST on 21 July 2000 (the number of relative humidity measurements was less than the number of other measurements).

Table 4.11 Index Of Agreement (IOA), Pearson's Correlation Coefficient (PCC), Systematic & Unsystematic Root Mean Square Error (S-RMSE & U-RMSE), and additional statistics, from 1200 NZST on 19 July 2000 to 1200 NZST on 21 July 2000, experiments 2_3 and 2_4: near-surface wind (m/s), wind components (m/s), temperature (^{0}C), relative humidity (%).

EXPERMENT	NUMBER OF OBSERATIONS	OBSERVED MEAN	MODELLED MEAN	OBSERVED DEVIATION	MODELLED DEVIATION	PCC	S-RMSE	U-RMSE	IOA
WIND SPEED (m/s)									
Experiment 2_3	511	2.25	2.06	1.11	0.72	0.80	0.57	0.43	0.84
Experiment 2_4	511	2.84	2.75	1.42	1.33	0.84	0.32	0.73	0.91
AVERAGE	**511**	**2.54**	**2.40**	**1.26**	**1.03**	**0.82**	**0.44**	**0.58**	**0.88**
U-COMPONENT (m/s)									
Experiment 2_3	511	-1.17	-0.95	1.93	1.72	0.87	2.08	1.88	0.87
Experiment 2_4	511	-2.11	-1.77	1.13	1.94	0.88	0.51	0.77	0.87
AVERAGE	**511**	**-1.59**	**1.47**	**1.53**	**1.84**	**0.88**	**1.29**	**1.26**	**0.87**
V-COMPONENT (m/s)									
Experiment 2_3	511	-0.18	0.18	1.10	0.94	0.79	1.15	0.89	0.74
Experiment 2_4	511	-0.46	-0.53	1.13	1.47	0.83	0.22	1.11	0.74
AVERAGE	**511**	**-0.32**	**-0.29**	**1.11**	**1.25**	**0.82**	**0.68**	**1.00**	**0.74**
TEMPERATURE (^{0}C)									
Experiment 2_3	292	8.92	6.77	1.31	1.51	0.75	2.16	1.01	0.60
Experiment 2_4	292	9.97	8.56	1.92	2.66	0.90	1.49	1.17	0.84
AVERAGE	**292**	**9.46**	**7.16**	**1.56**	**1.58**	**0.83**	**1.83**	**1.09**	**0.72**
RELATIVE HUMIDITY (%)									
Experiment 2_3	292	87.71	90.92	7.65	6.69	0.90	3.59	2.88	0.90
Experiment 2_4	292	87.78	88.79	7.64	7.09	0.93	1.46	2.62	0.96
AVERAGE	**292**	**87.75**	**89.85**	**7.65**	**6.39**	**0.91**	**2.53**	**2.71**	**0.93**

There is very good agreement between observed and modelled data for wind speed and temperature in experiment 2_4, with IOA of more than 0.90 for wind and more than 0.80 for temperature, compared with 0.84 (for wind) and 0.60 (for temperature) in experiment 2_3 without FDDA. The IOA for other meteorological parameters (U- and V-components of wind and RH) are similar in both experiments. Therefore, we can summarize that using FDDA during MM5 runs gives additional possibility for improvement of model output of basic meteorology using global analysis input data.

4.4 *Methods of CAMx4 modelling of Particulate Matter over the Christchurch region*

4.4.1 *Tuning CAMx4 using meteorological model output data*

Chemistry model CAMx4 uses MM5 output fields of heights above sea level, wind, temperature, water vapour, coefficient of viscosity and information about clouds and cloud water content as meteorological information on levels determined in the CAMx4 input informational file, and these levels coincide with boundary layer levels of MM5. CAMx uses MM5 basic meteorology for initialisation and for boundary conditions, as well as for nudging data at certain time intervals. It is therefore possible to evaluate the most successful MM5 experiments (compared with CAPS2000 observation data) and provide the most realistic input for fine tuning the dispersion model, ensuring that the processes of aerosol dispersion, advection and scavenging are reproduced by the chemistry model as accurately as possible given the background boundary layer meteorology. On the other hand, the output of CAMx4 runs provides an additional possibility to design future MM5 experiments based on the results of the chemistry model output – the so-called postponed correlation bond in the numerical system.

All the experiments using the coupled MM5–CAMx4 numerical system had the spatial resolution of the MM5 fourth grid, from which meteorological fields were obtained for use in the dispersion model. This coincided with the spatial resolution (and number of nodes) of CAMx4, while the number and heights of the vertical levels of the chemistry model always matched the MM5 vertical levels in the boundary layer. This precaution was stipulated initially to minimise loss of meteorological information during the processes of conversion of MM5 output information into the CAMx4 input format. Additional programs can also be written for the MM5–CAMx4 system, as CAMx4 works with a large number of so-called 'before and after modelling' special software that are used to create additional input files (such as gridded emissions files, landuse files, gridded concentration files and so on) for the chemical model, and allowing utilization of the output of CAMx4 runs by statistical programs and space–time visualisation software, described later in Chapter 4.

Initial analysis of the near-surface air circulation on smog nights (nights with near-surface high pollutant concentrations and low visibility) has relied on observations from the Christchurch sites established during CAPS2000 (Kossmann and Sturman, 2004) and this was useful for more detailed understanding of the 24-hour cycle of aerosol concentrations. This was used to tune CAMx4 with MM5 basic input meteorology to reproduce observed dispersion characteristics as well as possible. In Figure 4.35 wind roses are shown for smog nights (data were collected and averaged for winter months of the CAPS2000 field

experiment) for evening (Figure 4.35a) and early morning (Figure 4.35b) to show the basic redistribution of PM_{10} concentrations over the Christchurch urban zone (shaded).

a) **b)**

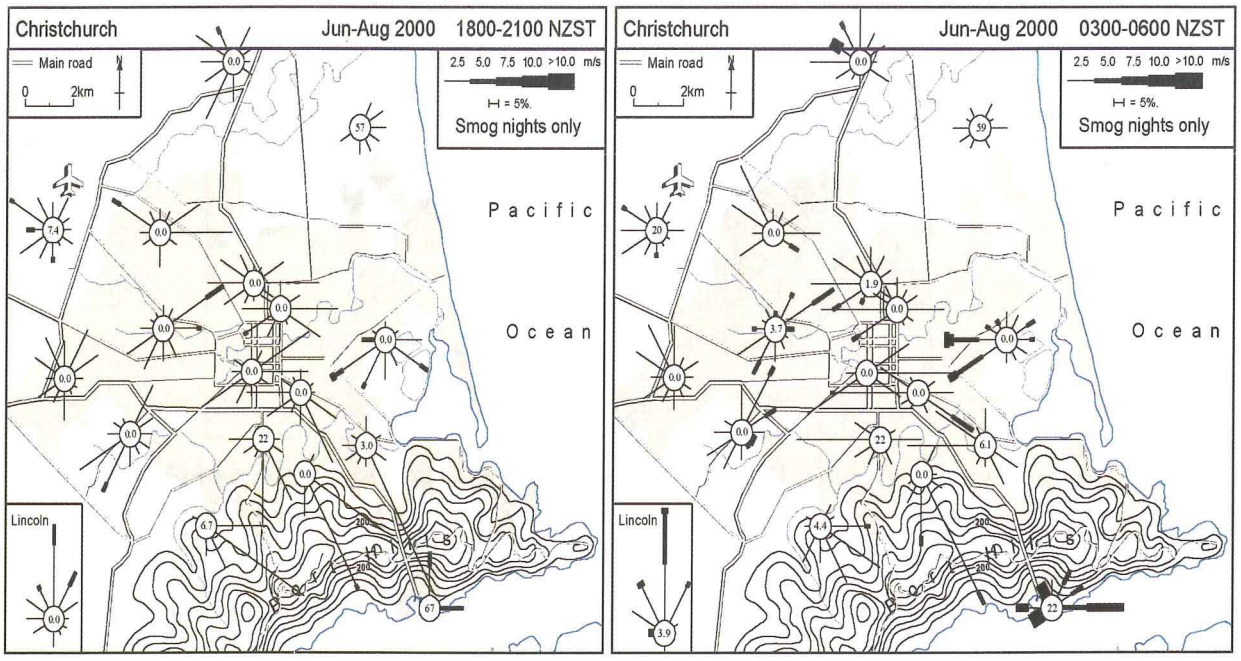

Figure 4.35 Observed near-surface wind speed and direction distribution for 16 observation sites in the Christchurch area during CAPS2000, averaged for June–August, smog nights only: a) 6pm–9pm, b) 3am–6am (after Kossmann and Sturman, 2004).

From Figure 4.35, it is evident that the drainage winds from the Canterbury Plains and Port Hills create a convergence zone (or some kind of localised frontal zone) of cold dense air in the evening under stagnant synoptic situations, with advection of PM_{10} emissions toward the central part of Christchurch (Figure 4.35a) during evening. Subsequently, movement of high aerosol concentrations occurs towards coastal areas and the ocean (Figure 4.35b) as a result of the coupled nocturnal land breeze and air movement from the converged drainage flow from the Canterbury Plains. This is shown schematically in Figure 4.36. The night-time (from 6pm up to 6am) cycle of the air pollution frontal zone involves the increase in levels of PM_{10}, first toward the centre of Christchurch (approximately till midnight), and then the drifting of the pollution towards the coastal districts (Spronken-Smith *et al.*, 2004).

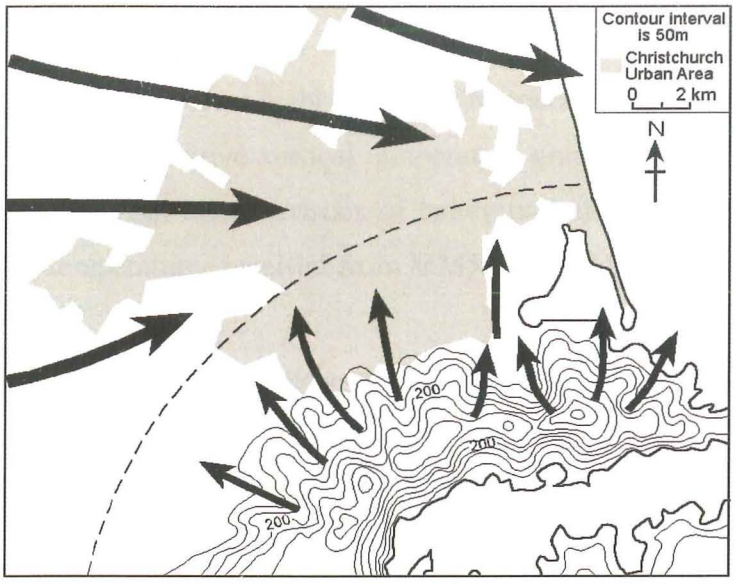

Figure 4.36 Schematic mesoscale air circulation in the ABL over the Christchurch urban area during smog nights (after Sturman *et al.*, 2001)

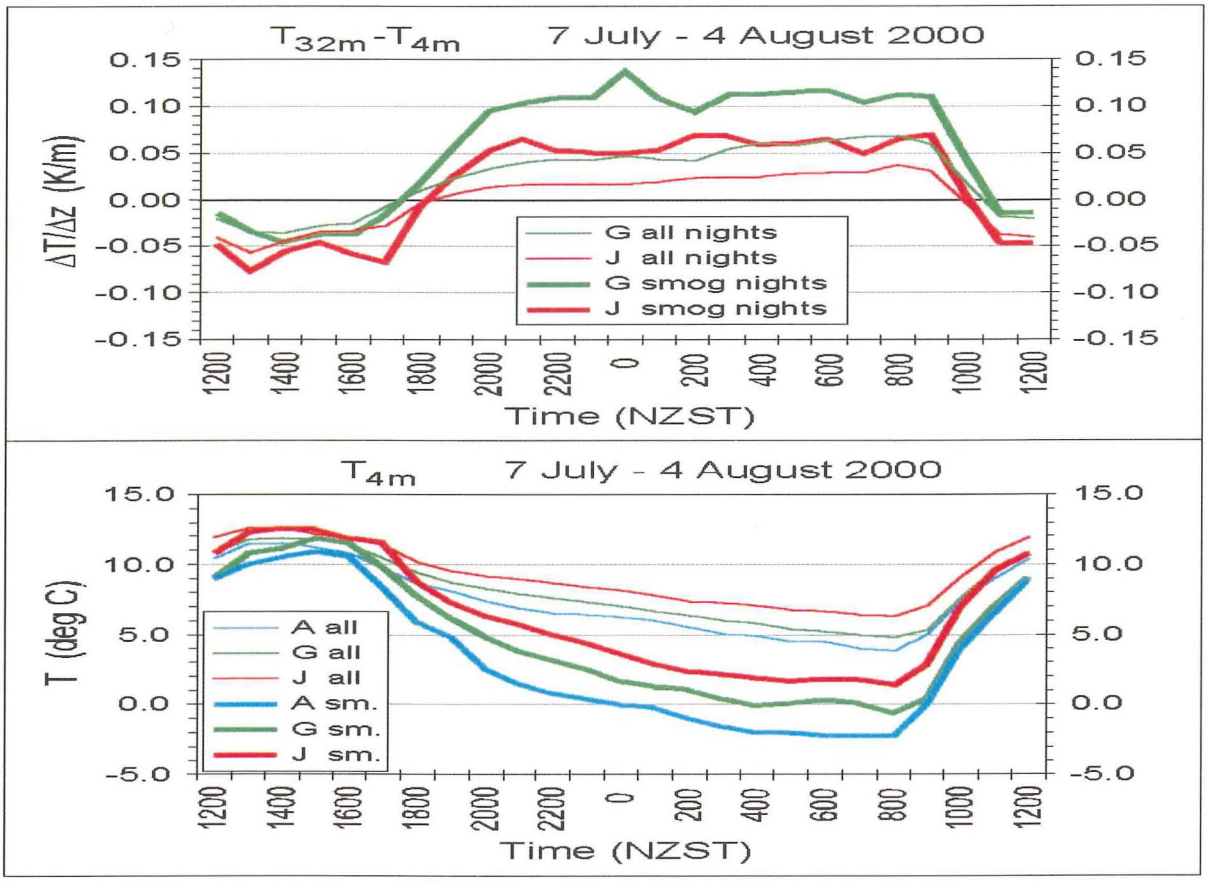

Figure 4.37 Time variability of the average vertical temperature gradient (top) and near-surface temperature (bottom) during all nights and smog nights between 7 July and 4 August 2000 (after Sturman *et al.*, 2001).

In Figure 4.37, time variability of the near-surface temperature and vertical temperature gradient (indicative of vertical atmosphere stability) is shown for smog nights (sm.) averaged for

Jade Stadium tower (J), Christchurch Airport (A), Greers Road tower (G), and for all nights. The differences between sites are the result of the effect of the urban area. From Figure 4.37, it is evident that the distinctively lower night minimum temperatures for smog nights (especially for Christchurch Airport) and positive vertical temperature gradients (negative buoyancy), indicate typical mean meteorological characteristics of heavy pollution nights which can be compared with CAMx4 input temperatures received from MM5 fine grid (domain 4) runs.

4.4.2 Tuning CAMx4 using particulate material monitoring data

Fine-tuning of the CAMx4 chemical model included firstly, reconfiguration, adjustment and time smoothing of the average hourly gridded PM_{10} and $PM_{2.5}$ concentrations used for initialising and nudging. Observed particulate matter data collected during CAPS2000 at three observation sites (Coles Place, Polytechnic and Packe Street) were available for the time period from early July up to the middle of August 2000.

The observations collected at three Ecan sites during winter 2000 provided a very good opportunity for comparison with output from the chemical model run with input meteorology from MM5. Figure 4.38 illustrates the near-surface time trends of PM_{10} and CO measured with a 10-minute frequency for 23–24 July 2000.

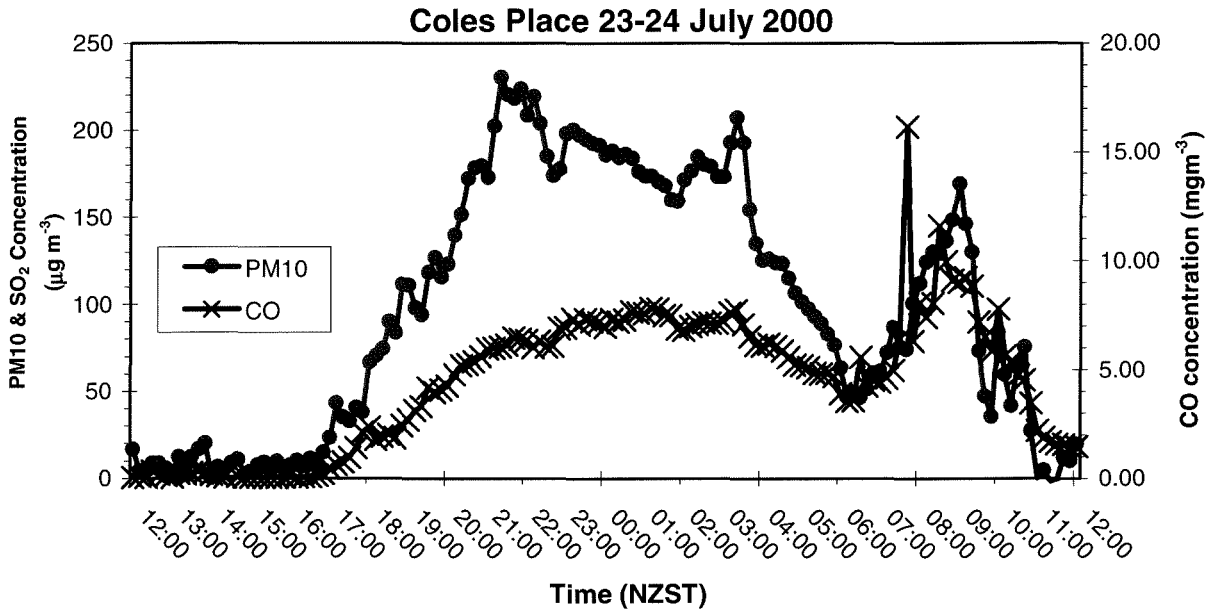

Figure 4.38 24-hour time series of 10 minute averaged PM_{10} ($\mu g\ m^{-3}$) and CO ($mg\ m^{-3}$) recorded at Coles Place (St. Albans, Christchurch) for 23–24 of July 2000 (after Kossmann *et al.*, 2002).

The time series of PM_{10} (red line) in Figure 4.38 shows two peaks of particulate pollution in Christchurch: the big evening/night peak (between 5–6pm and 23pm–2am next day) that is

predominantly a result of home heating using open-fires and log-burners (domestic pollution), and the second lower peak during early morning (between 6–7am and 9 am) that is considered to be the combined result of home heating (domestic) and high traffic activity under stable boundary layer conditions dominated by a strong temperature inversion. In the CAMx4 experiments we used surface air pollution observations from three sites to make adjustments to the operation of the chemical model, including investigating the effect of different numbers of vertical levels, and changes of the initial emissions values.

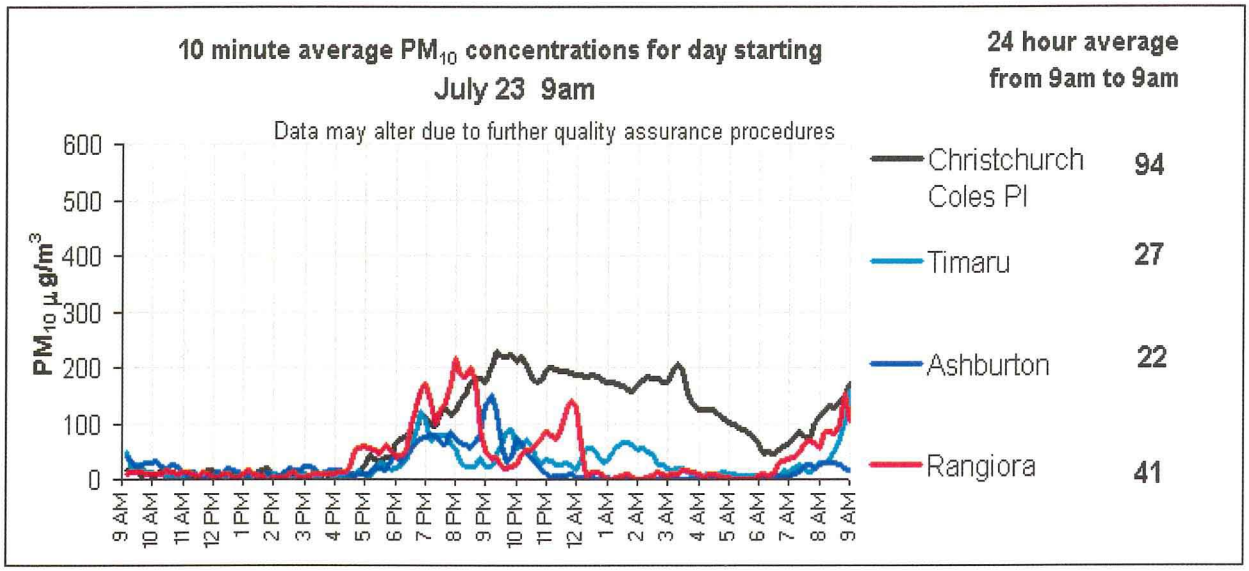

Figure 4.39 24-hour time series of 10 minutes average PM_{10} (µg m^{-3}) in Christchurch, Timaru, Ashburton and Rangiora for 23–24 July 2000 (obtained from Ecan).

Figure 4.39 shows the time series of PM_{10} for the morning of 23 July to the morning of 24 July 2000 for Christchurch, Timaru, Ashburton and Rangiora sites. Nighttime PM_{10} maxima were above the health guideline (50 µg m^{-3}) at all 4 places, while high levels were maintained in Christchurch until around 6 am the following morning. Some secondary peaks occurred early in the morning at Timaru and Rangiora. The example shown in Figure 4.39 illustrates the greater significance of the PM_{10} pollution problem in Christchurch compared with surrounding small towns.

It is important to stress that observed PM concentration data for the Christchurch area have been used not only for comparison with CAMx4 output, but also in the generation of the chemical model gridded input emission file as explained in Section 4.4.4.

4.4.3 Landuse distribution and dry deposition over Christchurch

Landuse distribution input files play an essential role in regard to the dry deposition mechanism of CAMx4. They contain time-invariant (for CAMx4 runs) two-dimensional gridded

fields of landuse distribution for the whole grid (in our case, the finest grid is domain 4 from MM5, with 1 km spatial resolution). In CAMx4, the information from these files (or from one file if nested grids are not used) is used for calculation of dry deposition and scavenging speeds, reflecting the roughness of the each landuse category.

The model options offer the ability to generate the landuse file only for the coarse grid, as during a CAMx4 run the coarse landuse distribution information can be interpolated onto finer grids. However, as was mentioned before, it is best to avoid possible generation of errors due to additional interpolation. In Table 4.12, landuse categories are listed with the default surface roughness values (in metres) assigned to each category and background ultraviolet albedo used within CAMx4 for near-surface ozone calculations. The categories marked **bold** are those chosen for the current experiments for the Southern Island of New Zealand.

Table 4.12 CAMx categories and those used in our calculations (marked as **bold**) and the default surface roughness values (m) with ultraviolet albedo.

Category Number	Land Cover Category	Surface Roughness (metres)	UV Albedo
1.	**Urban**	**1.5**	**0.8**
2.	**Agricultural**	**0.25**	**0.05**
3.	**Rangeland**	**0.05**	**0.05**
4.	**Deciduous forest**	**1.00**	**0.05**
5.	**Coniferous forest including Wetlands**	**1.00**	**0.05**
6.	**Mixed forest**	**1.00**	**0.05**
7.	**Water**	**0.0001**	**0.04**
8.	**Barren land**	**0.002**	**0.08**
9.	**Non-forest wetlands**	**0.15**	**0.05**
10.	Mixed agricultural and range	0.15	0.05
11.	Rocky (with low shrubs)	0.15	0.05

The main problem with the landuse files was that ENVIRON International Corporation (Novato, California) suggests that all users use USGS CTG (Composite Theme Grid) data if they work in the USA, or develop their own landuse files compatible with the CTG format fields of CAMx4 input if they work elsewhere. The people from ENVIRON suggested the use of only 3 categories: urban, water and non-urban, arguing that CAMx was not very sensitive to landuse. However, with the assistance of John Thyne (GIS Manager, Department of Geography), it was possible to create 8 landuse categories for all 4 domains of MM5 at 1 km spatial resolution, and

then to interpolate this information onto the coarser domains – 3, 2 and 1. The input information was created for UTM (Universal Transversal Mercator) projection, and a special program written (*UTMtoCTG*) to transform the 2-dimensional input data with landuse characteristics received from GIS New Zealand landuse sites into CTG input format for use in CAMx4 for all four MM5 domains. The interpolation is of the second level of precision as it was done from fine (daughter) grids onto coarse (mother) grids.

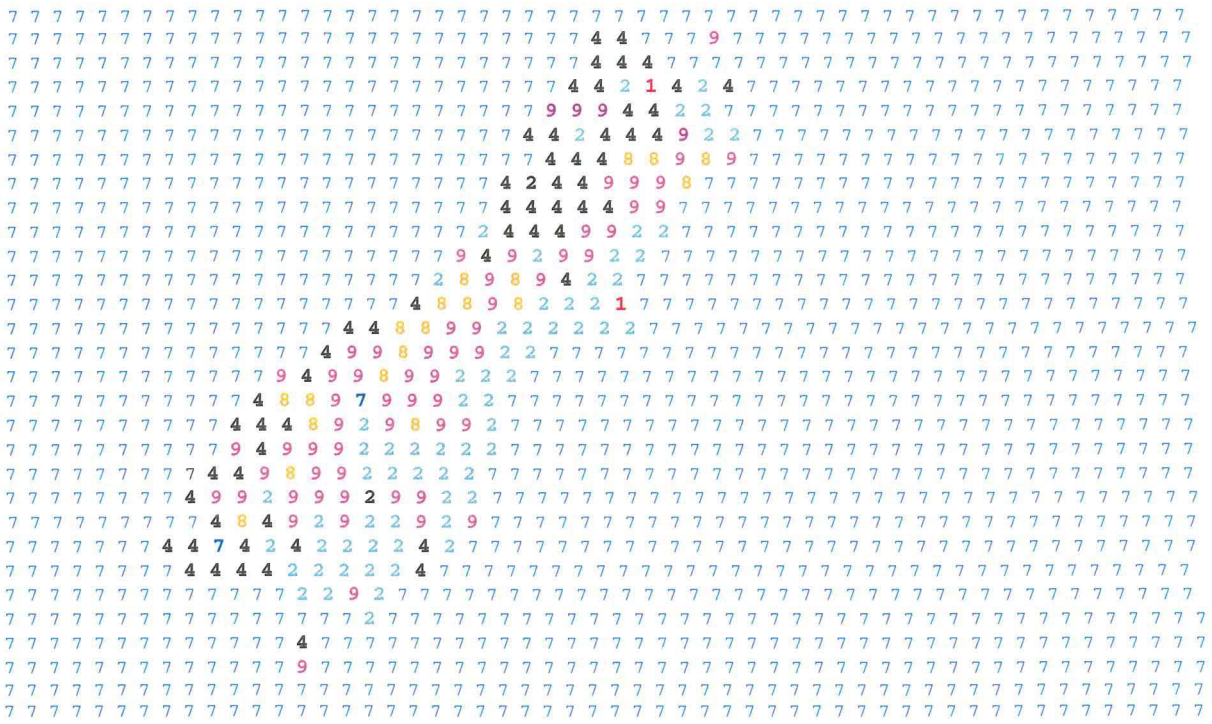

Figure 4.40 Landuse distribution for 8 categories (see Table 4.12) for domain 1 (the MM5 coarse mother domain) that covers all the South Island of New Zealand.

Figure 4.40 is an example of the landuse file created for domain 1 of MM5, based on the eight categories marked **bold** in the Table 4.12. Landuse categories 10 (mixed agricultural and range) and 11 (rocky, with low shrubs) were replaced by category 9, as they had the same physical parameters, and there were technical difficulties with assimilation of 2 digit categories using available software. Category number 4 (Deciduous forest) was not found for the South Island of New Zealand. Future plans to use MM5–CAMx4 with a special super-fine resolution up to 333 metres will demand more precise input information, including calculation of new landuse files, and the possible addition of new landuse categories to allow more precise investigation of the dry deposition mechanism over the South Island.

4.4.4 Gridding and adjusting emission input fields for CAMx4

Gridded input concentration fields of PM and gases play an essential role in evaluation of the ability of CAMx4 to investigate temporal variation of spatial patterns of aerosols and gases in

the lowest 50–100 metres of the atmospheric boundary layer in the Christchurch area under temperature inversion conditions. Spatial fields of gridded concentrations of PM_{10}, $PM_{2.5}$, CO_x, NO_x, SO_x and VOC (Volatile Organic Components), based on emissions inventory data from Environment Canterbury, were used as initial data in creating CAMx4 input gridded emission files. The gridded files of particulate matter and gas concentrations have a 1 km spatial resolution (coinciding with the resolution of the finest MM5 grid), covering all of Christchurch with 34 x 39 horizontal nodes with units of (kg m^{-3} hr^{-1}). A special program was written to transform input concentration files with 34 x 39 number of regular grid points into an MM5 (with the same 1 km spatial resolution) 121 x 121 number of regular grid points (grid 4 of MM5), with an additional check procedure to ensure that central points coincide.

The initial concentration fields were averaged for the whole wintertime (late May to early September) for the Christchurch area, and split into four groups according to the origin of the pollutant emission (see Figure 3.5). This produced a 'domestic' group – of home use of open fires and log burners with different qualities of fuel (see Figure 3.7); an 'industry' group – of wood/coal combustion for industrial purposes; a 'vehicle' group – from transport during rush-hours, and a 'total' group – that includes all three former groups. As the 'domestic' and 'industry' groups are the main contributors to the aerosol (PM) air pollution (up to 95–98 % of pollutants are derived from these groups and up to 90–92 % from the 'domestic' group alone – see Figure 3.5), all experiments with the coupled MM5–CAMx4 system used the group 'total', which is dominated by processes of solid fuel combustion.

The level of aerosol and gas concentrations in the input gridded emission files varies not only in space (over Christchurch) but also in time throughout the day. As a result, for all 4 groups, the day was split into four time intervals with differing levels of pollution emission depending on the time period's 'pollution production' activity:

1. Night time: 10pm–6am next day (mostly reduced activity);
2. Morning time: 6am–10am (morning secondary 'vehicle–industrial' peak);
3. Midday time: 10am–4 pm (industrial subpeaks);
4. Evening time: 4pm–10 pm (the maximum peak of pollution–'domestic' factor).

The mean and grid-point values of aerosol and gas emissions in the gridded fields differ significantly between one time period and another, so that a 5 time-point filter (TPF) was applied to all initial concentration fields to smooth the difference of concentration values between different time periods for all 4 groups. So, if moving from one time interval to another a TPF factor for the current time group will be:

1. $TPF = 0.00$ $(t = t_b - 2)$;
2. $TPF = 0.75$ $(t = t_b - 1)$;

3. TPF = 0.50 ($t = t_b$);
4. TPF = 0.25 ($t = t_b + 1$);
5. TPF = 0.00 ($t = t_b + 2$).

Where t_b is the border time between two time groups (6am, 10am, 4pm or 10pm) and t is the current time in the current time group. Application of the TPF allowed more even initial fields of pollutant emissions to be obtained throughout the day for all three different origin emission groups and for the 'total' group emissions.

The next step in assimilation of initial gridded emissions fields for CAMx4 involved splitting of the aerosol (PM_{10} and/or $PM_{2.5}$) and gas (CO, NO_x, SO_x and VOC) components based on the species in the input gridded emission file for CAMx4 chemistry mechanism 4 (CB-IV – see the model description in Section 2.6.2), and transforming units from (kg m^{-3} hr^{-1}) in (μg m^{-3} hr^{-1}).

For particulate matter, four main species were chosen that make up nearly 100% of the PM (Ryan, 2002), with the Split Mass Factor (SMF) for each species defined for high pollution nights dominated by wood smoke (the group 'domestic') as:

1. Pollutant Elemental Carbon (PEC) with SMF = 0.53;
2. Pollutant Organic Aerosol (POA) with SMF = 0.46;
3. Pollutant SO_4 with SMF = 0.0089;
4. Pollutant NO_3 with SMF = 0.0011.

The sum of the four species split mass factors tends to 1.00 and therefore the influence of any other species on the summed value of PM at any point or time is considered negligible. A special program was written to transform the initial gridded fields of PM emissions into fields of CAMx4 input species: PEC, POA, PSO_4 and PNO_3. It should be stressed that the split mass factor weighting adopted here represents the dominancy of the 'domestic' group in air pollution over Christchurch, and SMF weights should be revised in the case of 'vehicle' only pollution research.

For gases, the procedure of input data preparation was easier for CO, NO_x and SO_x, as it demanded only knowledge of the molecular weight of a species to apply an equation to convert the input (kg m^{-3} hr^{-1}) units to ppm (parts per million) units, because all gas species were represented in ppm in CAMx4. However, for organic gases the process is different, as emissions of organic gases are typically reported in emission inventories only as aggregate organics, either as VOC or as Reactive Organic Gases (ROG). The specification profiles used to split aggregate organic gas estimates into individual compounds are based on those outlined for total organic gases in Ryan (2002), which includes methane and ethane. The lumping molecular approach in the CB-IV mechanism, where individual compounds with similar reactivity characteristics or

carbon bond structures are grouped into a single mechanism species, involves three steps in the specification of VOC: assignment of a speciation profile, conversion of VOC to TOG (Total Organic Gases), and multiplication of the assigned profile's split factors by the TOG estimate to create emissions estimates for the species used in the model. The final step in specification of VOC emissions consists of generation of input species in either molar (ppm) or mass form using the specification profiles from the CB-IV profiles file. Any way, VOC is split into 8 species for the CAMx4 input emission file, and all 8 species are listed with the molar split factor for every species in parentheses: ETH (0.006213904), FORM (0.005709348), NTR (0.010482527), OLE (0.002893959), PAR (0.014575323), TOL (0.000149776) XYL (0.000133326) and ALD2 (0.002175308).

After the above pre-processing of initial aerosol and gas spatial fields, the emission input file contained fifteen CAMx4 gridded input species representing the complex compounds in the atmosphere over Christchurch. A special program was written to compile all the input species together and to create the single input emissions binary file containing aerosol and gas concentrations for the CAMx4 experiments. These were run from several hours up to four days, and with a nudging time interval from 1.5 minutes up to several hours depending on the nature of the problem being investigated.

4.4.5 Optimal coupling of MM5 – CAMx4

Details of the method used for optimal coupling of MM5 and CAMx4 will be described in Chapter 5, based retrospectively on the reliability of predictions of particulate matter dispersion over the Christchurch region. However, two important aspects of optimisation of the MM5–CAMx4 numerical system are outlined:

1. Input data play the dominate role in assessing the quality of the output from the MM5–CAMx4 coupled numerical system, especially over short periods of the PM_{10} forecast (12–24 hours);
2. Direct use of input/output data by CAMx4-MM5 without additional interpolation and/or re-interpolation procedures provides the opportunity to provide more realistic numerical simulations of PM_{10} spatial distribution, from the point of view of the real air pollution space-time dispersion during heavy smog nights over Christchurch.

4.4.6 Research and quasi-operation possibilities of the MM5–CAMx4 system

The research regime of the MM5–CAMx4 system includes two steps, in the first of which the MM5 experiment is run using the final fine grid 4 (all details of this step have been described earlier in Chapter 4), while in the second the chemical model is used, with all necessary input

data files being configured for a case study experiment. The initialisation file for CAMx4, including all the input parameters and references to the files that are necessary for CAMx4 to successfully run, will now be described.

First of all, the CAMx4 information file contains all parameters that determine the time period of the run, the number of days and hours in the run, the number of grids (including nested grids), the characteristics of every grid in the mother/daughter domain, and also the time step, the maximum allowed advective time step and the output dump time interval in minutes.

CAMx4 has several modes of operation that consist of:

1. A simple run using the basic chemistry mechanism compiler (CMC), input meteorology, the albedo/haze/ozone input file and photolysis rates input file for one grid with averaged (hourly or several hourly) output species of ozone and total values of dry and wet scavenged deposition only (calculated from MM5 input wind and water vapour files). This can be made a little more complicated if the SAPRC-99 gas chemical mechanism is used instead of chemical mechanism 3 (see Chapter 2). The accumulated Central Processor Run (CPR) time for such a run is no more than 1 to 1.5 hours per each day of the experiment, running on a PC Pentium 5 or Pentium 6, depending on the number of horizontal nodes and vertical levels (vertical node number can range from 2 to 12 depending on the number of vertical levels in the MM5 ABL);
2. Addition of landuse files allows switching on of the dry deposition advection, dispersion and scavenging mechanisms in CAMx4, that are vitally important for any research into the chemical modelling of gases and aerosols (particulate matter). Total CPR time increases up to 4–6 hours;
3. Application of the gridded emission data file to the input information file for partitioning aerosols and gases (a description of the gridded emission data file was provided earlier in Chapter 4) allows investigation of variations over time of the spatial distribution and levels of hourly accumulated concentrations of PM (PM_{10} and $PM_{2.5}$), which is the main aim of the application of the coupled MM5–CAMx4 system. The number of averaged output aerosol and gas species in this study is equal to 27, including both primary and secondary species. Total CPR time varies from 10–12 hours for a 2 level CAMx4 model run, and up to two days in case of a 6 level CAMx4 run using the finest MM5 grid only (grid 4 with 1 x 1 km spatial resolution). Addition of more coarse (or more fine) grids in the chemical model can increase the total computer run time significantly, eliminating any chance to create a quasi-operational forecast numerical system;
4. Inclusion of PiG (Plume-in-Grid) technology in a run increases the central processor run time by no more than 10-15 % compared with the run time without it (this is shown by the

experimental data received with CAMx4 distribution).

This short description of CAMx4 resource requirements provides an initial understanding of the timetable for quasi-operational application of the MM5–CAMx4 numerical system. In the situation of the quasi-operational MM5-CAMx4 regime the time wasted on □meteorological data calculation (MM5) and on utilization of CAMx4 input data for an actual run is the most important criteria for the modelling system application (on the background of the computer possibilities). This problem of real-time forecasting of atmospheric pollutants is discussed by Jacobs *et al.* (1995). The research strategy investigates not only the accuracy of the modelled output compared with observed data (that will be done in Chapter 5) and the tuning of the model to produce more accurate predictions, but also allows assessment of the universality of the system. The approximate time spent obtaining the PM dispersion results can also be evaluated, along with the possibility of decreasing the total time cycle of the MM5–CAMx4 system to improve options for quasi-operational application. Possible steps include:

1. Use of grid 3 of MM5 instead of grid 4 (the finest) for generating a 24–36 hour MM5 forecast, or reduction of the number of spatial nodes in all 4 MM5 domains with a general (cold) start for all grids;
2. Use of a 2 level version of CAMx4 instead of a multi-layer version for aerosol dispersion forecasts over 24-36 hours starting from midday. The two-level CAMx4 version, as will be shown in the Chapter 5, compares favourably with the 6-level version in case of PM_{10} prediction. This step allows a reduction of several hours of computer time that is very important for the quasi-operational application of the numerical system work;
3. Reduction of the number of spatial nodes in both the MM5 and CAMx4 models and calculation only of the most vulnerable (most polluted) districts (with highest night/morning aerosol pollution);
4. And the last, but most effective, remedy is the use of a more powerful computer including transfer of the MM5–CAMx4 system to a parallel processing computer system (such as the Linux Duval PC).

4.5 Summary

The first part of Chapter 4 describes the requirements for successful numerical modelling, as well as the process of global analysis data assimilation, and the comparison of CAPS2000 field experiment observations with modelled output for both MM5 and CAMx4.

Methods of MM5 modelling over Christchurch are discussed in the second part of this chapter including single runs, series of runs with different levels of nesting for MM5 fine tuning over the Christchurch region, and also the particulars of 2003 winter modelling. Case study days

and possibilities and limitations of MM5 were also considered.

In the last part of the chapter, the dependence of CAMx4 PM_{10} modelling quality on such important factors as MM5 output BL meteorology, landuse distribution mapping, the reliability of gridded emission input fields and their adjustment for CAMx4 work regime was shown. In addition, the research and quasi-prognostic regimes of MM5–CAMx4 were considered.

Chapter 5

Modelling PM_{10} dispersion using the MM5-CAMx system

5.1 Introduction

The first part of this chapter describes the main results of chemical modelling of particulate matter (PM_{10}) dispersion for winter 2000 (the CAPS2000 field experiment) during weak synoptic scale circulation, when local topography is a dominant factor in the airflow patterns of the Christchurch region. The results of several numerical model runs are described, using CAMx4 over different time periods and starting at different times. These results are compared with observations obtained from Ecan meteorological and air pollution monitoring sites. Night-time patterns of PM distribution over the city are also considered.

The second part of Chapter 5 describes the results of 2003 winter PM_{10} modelling over different time periods (but not more than 48 hours) in regard to the possibility of creating a quasi-operational modelling system based on the MM5–CAMx4 system. Comparison with observed data from three Ecan sites provides the opportunity to find the optimal 'warm-up' time for the chemical model to produce the best agreement between CAMx4 output PM concentrations compared with observed data for nights with high levels of pollutant concentrations. All conclusions are supported by statistical analysis.

5.2 Results of PM_{10} modelling using the MM5-CAMx system – winter 2000

During winter 2000 (CAPS2000), particulate matter values (in $\mu g\ m^{-3}$) were measured (at 10 minute intervals in the near-surface layer) at three observation sites operated by Environment Canterbury: Coles Place (St. Albans), the Polytechnic (City Centre) and Packe Street (St. Albans). A series of modelling experiments were run using CAMx4 with different experimental run times, input near-surface meteorological data from the finest MM5 grid (1 km spatial resolution), and with gridded emissions input data for PM and various gases (15 input species). The main purpose was to investigate the ability of CAMx4 to reproduce PM_{10} time trends observed at all three sites. To characterize the stability of the chemical model output (with regard to the length of a run period and to the start time) several modelling periods were chosen for the evaluation. These are: 72 hour forecast starting at midday (1200 NZST), 48 hour runs starting at midday (1200 NZST) and midnight (2400 NZST), and a 30 hour run starting in the evening (1800 NZST). The runs in the model experiments were generally started during daylight hours in

spite of active near-surface turbulence, which is considered to limit the ability to undertake such research (Arya, 1999; Zawar-Reza and Sturman, 2001). This was done to 'warm up' the chemical model, as the main focus was on night-time and morning peaks of particulate matter (see Figure 4.38 and 4.39), which were the main target of the research.

In Figure 5.1 time series of observed (red line) and modelled 2-level (green line) and 6-level (blue line) CAMx4 averaged concentrations of PM_{10} ($\mu g\ m^{-3}$) are shown for Coles Place, the Polytechnic and Packe Street. They are derived from a 72 hour run, starting at 1200 NZST on 18 July and finishing at 1200 NZST on 21 July 2000, using meteorological data from MM5 grid 4 output and gridded PM emissions for initialisation, and hourly nudging during the experiment.

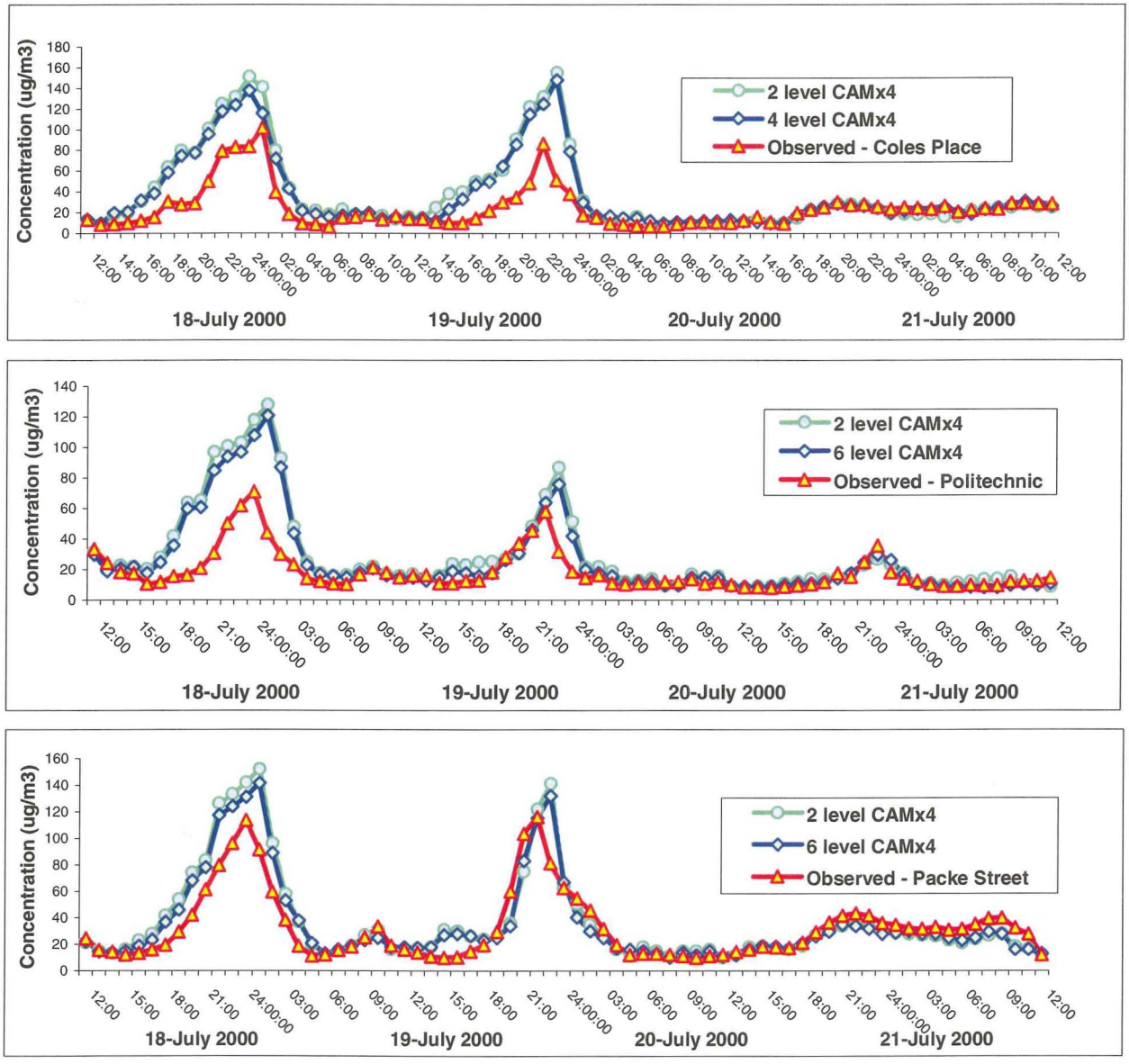

Figure 5.1 Time series of modelled (green line – 2-level CAMx4, blue line – 6-level CAMx4) and observed (red line) near-surface PM_{10} concentration ($\mu g\ m^{-3}$) for Coles Place, the Polytechnic and Packe Street observation sites: 1200 NZST on 18 July 2000 to 1200 NZST on 21 July 2000 (observed data from Ecan).

In all of the experiments with CAMx4, we used 2 versions of the chemical model: 2-level (lower level 7.0–8.5 metres, upper level 38–45 metres) to allow future quasi-operational work, and 6-level (upper level about 360–400 metres) for research and comparison purposes. It should be noted that the chemical model with MM5 input near-surface meteorology has managed to reproduce night peaks of aerosol air pollution for two nights (18–19 and 19–20 July 2000) at all three sites, with overestimation of the maxima for the first run night at Coles Place and Polytechnic compared with real data. It has also succeeded to imitate the secondary increase of PM concentrations during the morning rush time (especially at Packe Street and the Polytechnic). Pearson's correlation coefficient between modelled and observed PM_{10} concentration ranges between 0.82 for Polytechnic and 0.88–0.90 for Coles Place and Packe Street, while 72-hour averaged values of particulate matter for all three modelled points have exceeded observation values on 30–35 % of occasions. For instance, at Coles Place the 2-level CAMx4 average PM concentration is equal to 37.6 $\mu g\ m^{-3}$ compared to the observed value of 25.7 $\mu g\ m^{-3}$. It is important to stress that during the nights of 18–19 and 19–20 July, the meteorological situation over Christchurch was stagnant with quite weak near-surface winds and strong temperature inversions (see Figure 4.32a, b and Figure 4.33a, b). However, the situation changed to strong westerly to southwesterly winds starting from the 20 July 2000 (under the influence of an occluded front), as reflected by the MM5 grid 4 run (Figure 4.32a), with the advection of warm air leading to an increase in near-surface temperatures (Figure 4.33a). Such a rapid change in the meteorological situation over Christchurch led to the disappearance of night and morning maxima of PM_{10} from the observations (Figure 5.1 for Coles Place, the Polytechnic and Packe Street).

The difference in values of particulate matter concentration between 2-level and 6-level versions of CAMx4 is considered to be negligible from the point of view of underestimation of PM concentrations (compared to the 50 $\mu g\ m^{-3}$ health guideline) for the Christchurch region. It is therefore hopeful that the 2-level version of CAMx4 could be used as the basis for quasi-prognostic application of the MM5–CAMx4 system. The agreement of 2-level and multi-level CAMx4 results with observations is not so good for gases, but this will be examined in more detail in future research.

Figure 5.2 shows the time series of observed (red line) and modelled 2-level (green line) CAMx4 and 6-level (blue line) CAMx4 hourly mean concentrations of PM_{10} (in $\mu g\ m^{-3}$) for Coles Place, the Polytechnic and Packe Street for a 48 hour run starting at 0000 NZST on 31 July and finishing at 0000 NZST on 1 August 2000. Meteorological data from MM5 finest domain near-surface output (the lowest 6 levels for the 6-level chemical model and the lowest 2 levels for the 2-level one) and gridded aerosol emissions values were used as initial and hourly nudging

information during the 48 hour run. The experiment was started at midnight when small-scale air turbulence is at its weakest.

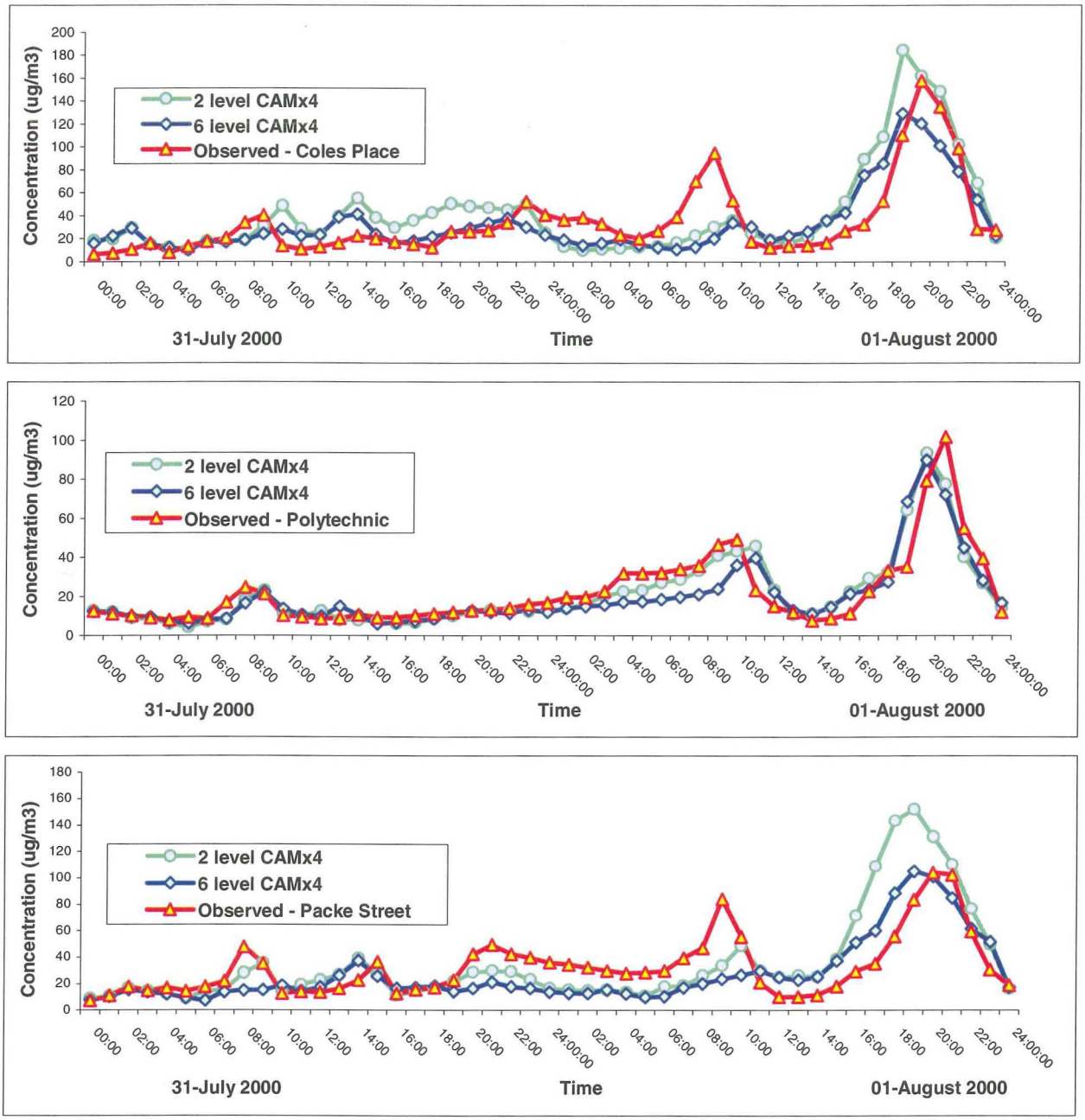

Figure 5.2 Time series of modelled (green line – 2-level CAMx4, blue line – 6-level CAMx4) and observed (red line) near-surface PM_{10} concentration ($\mu g\ m^{-3}$) for Coles Place, the Polytechnic and Packe Street observation sites: 0000 NZST on 31 July to 0000 NZST on 1 August 2000 (observed data from Ecan).

The chemical model using MM5 input boundary layer basic meteorology has managed to reproduce morning and night peaks of PM_{10} for 1 August 2000 at all three observation sites, but underestimated the morning peak's maximum values (especially at Coles Place and Packe Street

compared with observed concentrations). CAMx4 managed to imitate the secondary morning peak of PM concentrations for 31 July (it is especially evident for Coles Place and the Polytechnic – Figure 5.2). Pearson's correlation coefficient for modelled and observed PM_{10} concentrations ranges between 0.72 and 0.77 for Coles Place and Packe Street, and is nearly equal to 0.90 for the Polytechnic, being a little bit better in the case of the 2-level chemistry model. Modelled 48-hour averaged values of particulate matter for Coles Place exceed observations 10–15 % of the time. For example, the Coles Place 2-level CAMx4 average is equal to 41.2 $\mu g\ m^{-3}$ against 36.7 $\mu g\ m^{-3}$ from the observed values. However, the modelled and observed values nearly coincide for the other two sites (21.30 $\mu g\ m^{-3}$ modelled against 22.1 $\mu g\ m^{-3}$ observed at the Polytechnic). A table with the general statistics for winter 2000 is shown later in Section 5.1 (Table 5.1).

For the time period modelled, the meteorological situation over the Christchurch region was stagnant with quite weak near-surface winds and temperature inversions during the second part of the run, on 1 August 2000 (see Figure 4.32a, b; Figure 4.33a, b). However, it was characterised by relatively strong pressure gradients and quite high wind speeds on 31 July when two fronts passed over the region (Figure 5.3a), and then calmed down on 1 August (Figure 5.3b). These meteorological conditions reduced the evening maximum of PM_{10} over Christchurch, and this situation was represented well by the results of the CAMx4 output, both for 2-level and 6-level versions. Slightly better results were achieved with the CAMx4 2-level version (with the upper level approximately 38–45 m above the surface).

a)

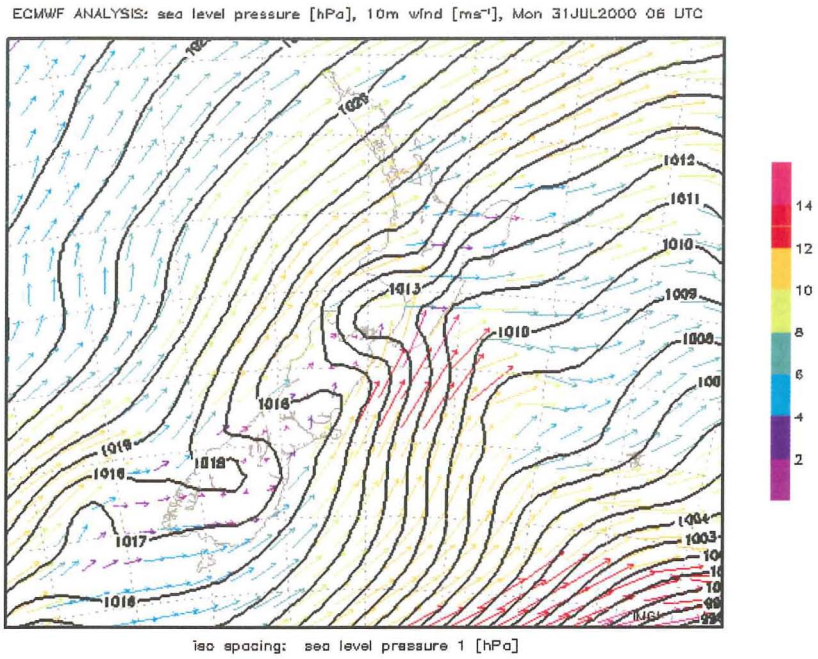

b)

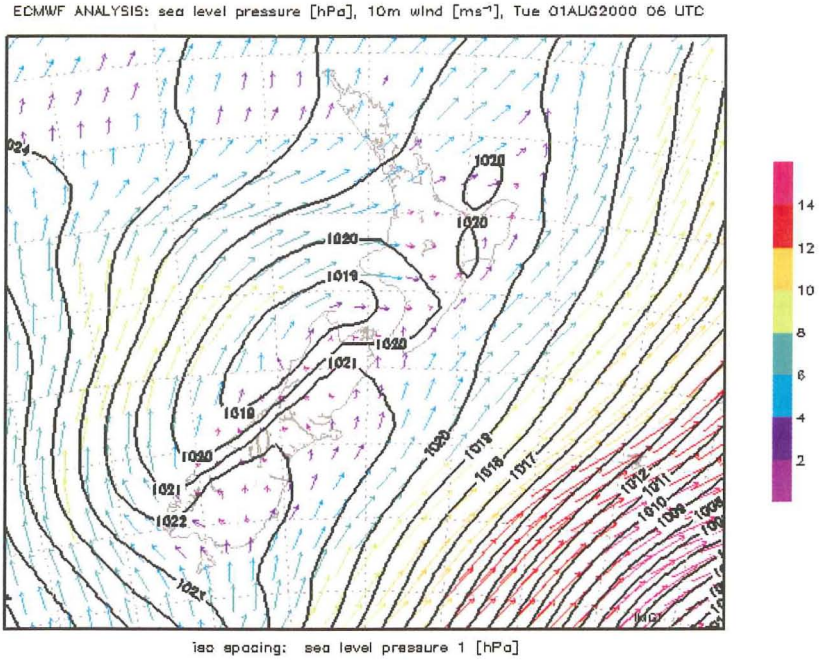

Figure 5.3 Synoptic situation over New Zealand: a) 1800 NZST on 31 July 2000, b) 1800 NZST on 1 August 2000 (after Meteorological Service, Wellington).

The results of the 48-hour CAMx4 run are available from midday under conditions of maximum near-surface air turbulence and minimum particulate matter concentration. Figure 5.4 shows the time trends of observed (red line) and modelled 2-level (green line) CAMx4 and 6-

level (blue line) CAMx4 hourly mean concentrations of PM_{10} ($\mu g\ m^{-3}$) for Coles Place, the Polytechnic and Packe Street, for the 48 hour run starting at midday 4 August and finishing at midday 6 August 2000. Initial and hourly nudging data were obtained from the meteorological output from domain 4 (MM5) and the specially generated gridded aerosol and gas emissions file described earlier (see Section 4.4.4).

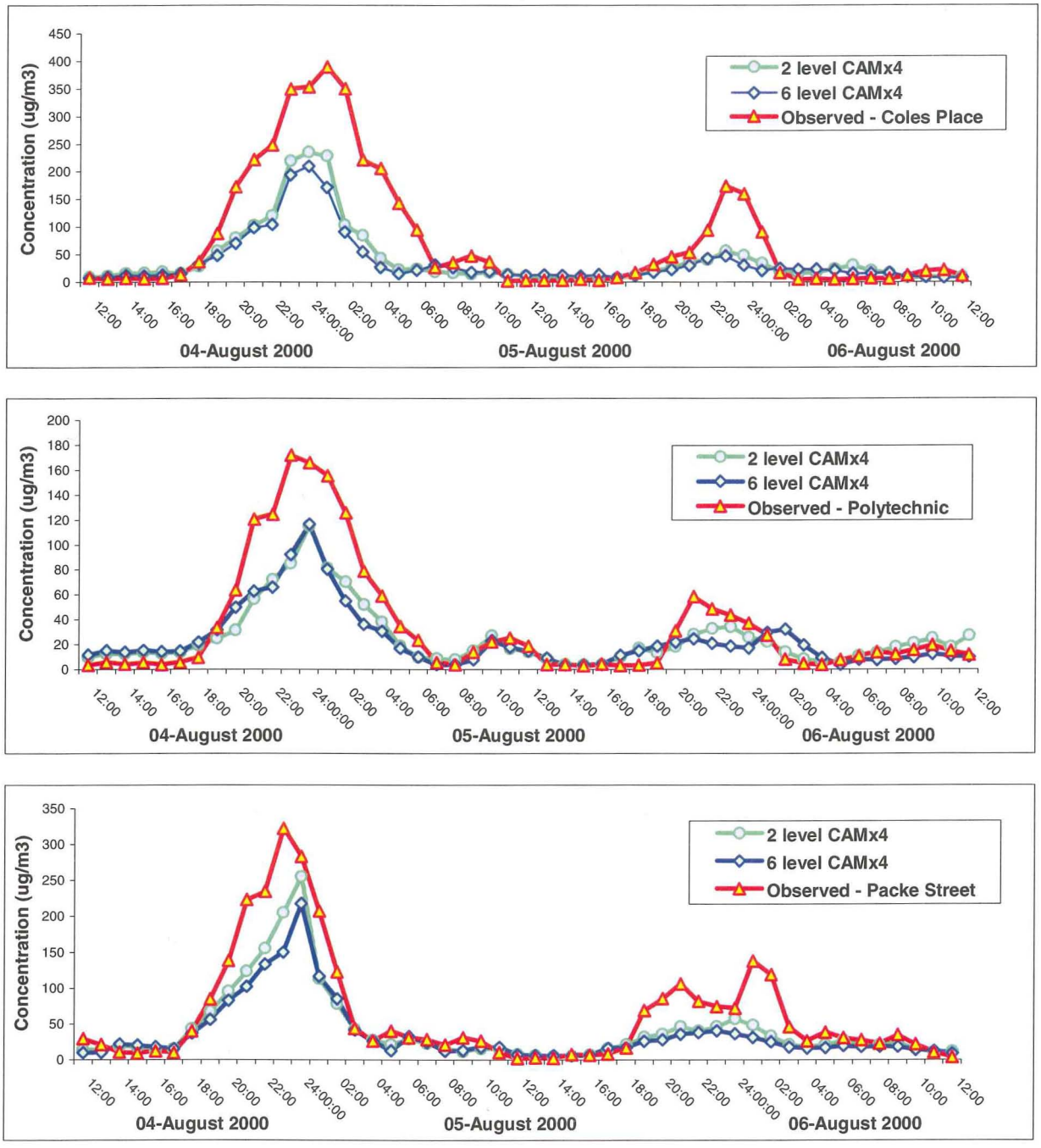

Figure 5.4 Time series of modelled (green line – 2-level CAMx4, blue line – 6-level CAMx4) and observed (red line) near-surface PM_{10} concentration ($\mu g\ m^{-3}$) at Coles Place, the Polytechnic and Packe Street observation sites: 1200 NZST on 4 August to 1200 NZST on 6 August 2000 (observed data from Ecan).

It should be noted that the chemical model using MM5 grid 4 input meteorology has

reproduced the night and morning peaks of PM_{10} quite well for 4–6 August 2000 at all three observation sites, although the principal evening peak's maximum values were underestimated (especially at Coles Place). However, the CAMx4 forecast has exceeded the health guideline of PM_{10}=50 μg m^{-3} by a factor of 4–5 times, and there is only a one hour time lag between observed and modelled maximum values at night for all three observation sites. The chemistry model has reproduced the secondary morning peaks of PM_{10} for both modelled mornings of early August (particularly for the Polytechnic and Packe Street – Figure 5.4). Pearson's correlation coefficient for modelled/observed PM_{10} concentrations ranges between 0.90 and 0.95 for all three data collection sites, for both 2-level and 6-level CAMx4 runs. Averaged 48-hours particulate matter concentrations for Coles Place, the Polytechnic and Packe Street are less than observed values for 30–50 % of the time (for instance, at Coles Place the 2-level CAMx4 average is equal to 51.8 μg m^{-3} compared with the observed value of 77.8 μg m^{-3}), because of underestimation of the very high concentration maximum on 4–5 August 2000. See Table 5.1 for the general statistics for winter 2000.

The meteorological situation over the Christchurch region was stagnant with quite weak near-surface winds and temperature inversions (see Figures 4.13, 4.14 and 5.5a) during the first part of the run (5 August 2000) when very high levels of particulate pollution were recorded. However, it changed under the influence of strengthening gradient winds (and increased wind speeds) as a result of an approaching strong cyclone from the southwest (Figure 5.5b).

a)

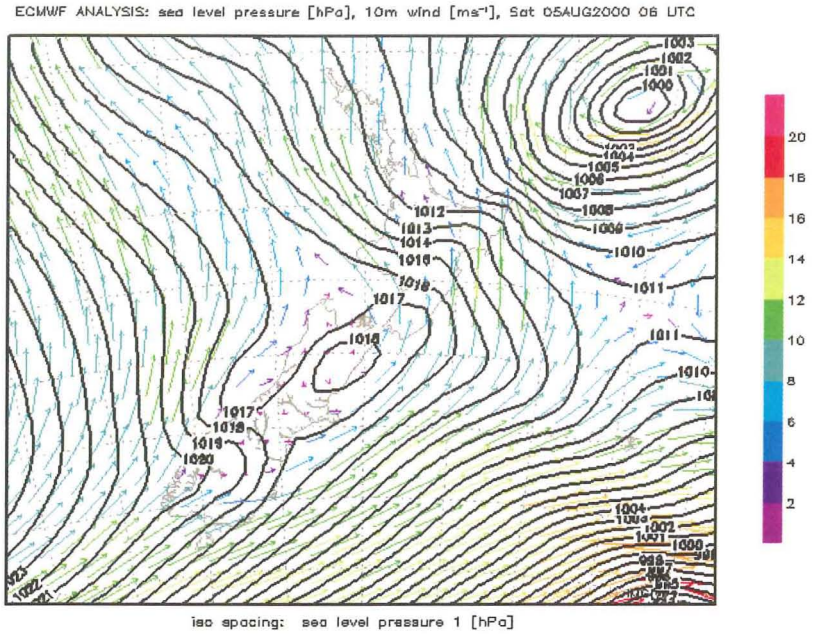

b)

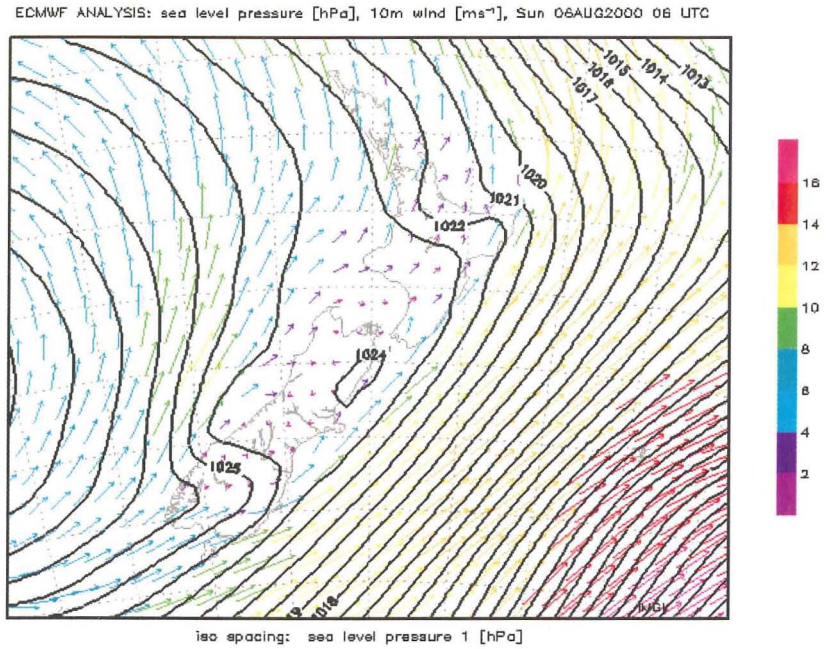

Figure 5.5 Synoptic situation over New Zealand: a) 1600 NZST on 5 August 2000, b) 1600 NZST on 6 August 2000 (after Meteorological Service, Wellington).

The change of synoptic situation over Christchurch (increased wind) reduced the 6 August particulate material evening maximum (Figures 5.4 and 5.5) and this was reproduced by the CAMx4 experiment for the 2-level and 6-level runs, with slightly better results in the case of the 2-level version.

a)

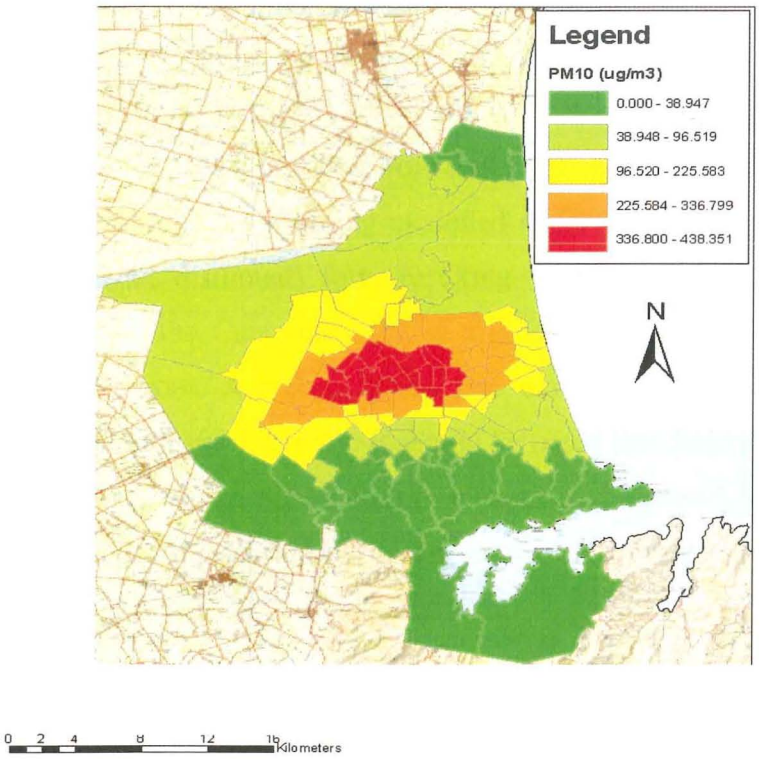

b)

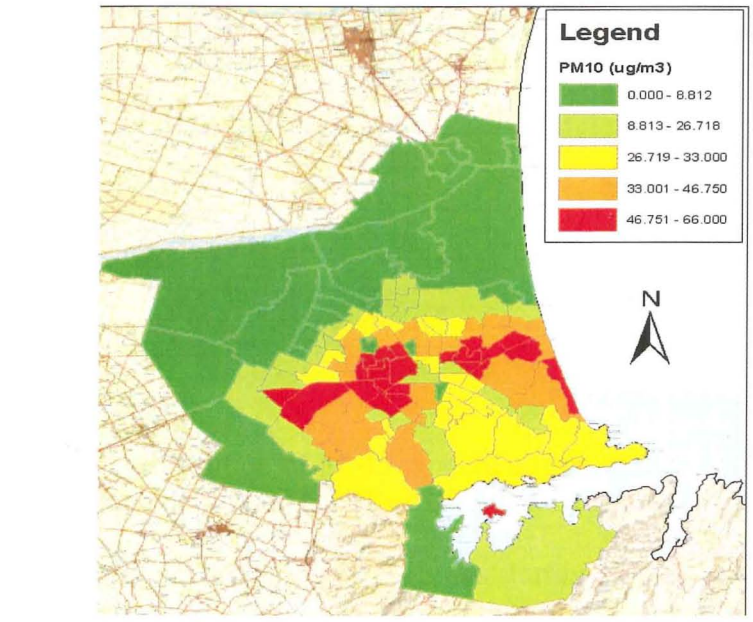

Figure 5.6 Spatial near-surface distribution of PM_{10} concentration ($\mu g\ m^{-3}\ hr^{-1}$): a) 0000 NZTS on 5 August 2000; b) 0900 NZST on 5 August 2000. Note the different scales used to represent concentrations on the two maps.

From the modelled spatial aerosol distribution, it is evident that maximum concentrations of PM_{10} at midnight (Figure 5.6a) have an elongated shape and is located over the city centre (a region with a lot of working fire-places in old homes, plus emission of aerosol from private transport and industry). A secondary maximum is located in the districts situated near to the city centre and towards the ocean, resulting from the effect of the inward sea breeze and the nocturnal drainage winds (Figure 5.7a). Morning modelled spatial PM_{10} distribution is also characterized by an elongated (but disrupted) form resulting from the influence of active southwesterly drainage winds from the Canterbury Plains and Port Hills (Figure 5.7b) on redistribution of night-time concentrations. A high pollution area along Blenheim Road appears to result from morning traffic and industrial activity. It should be noted that the concentration of particulates in the air is significantly less in Figure 5.6b (see caption of Figure 5.6a, b), because of night/early morning advection of PM_{10} toward the ocean, and partially because of dry and wet scavenging.

a) **b)**

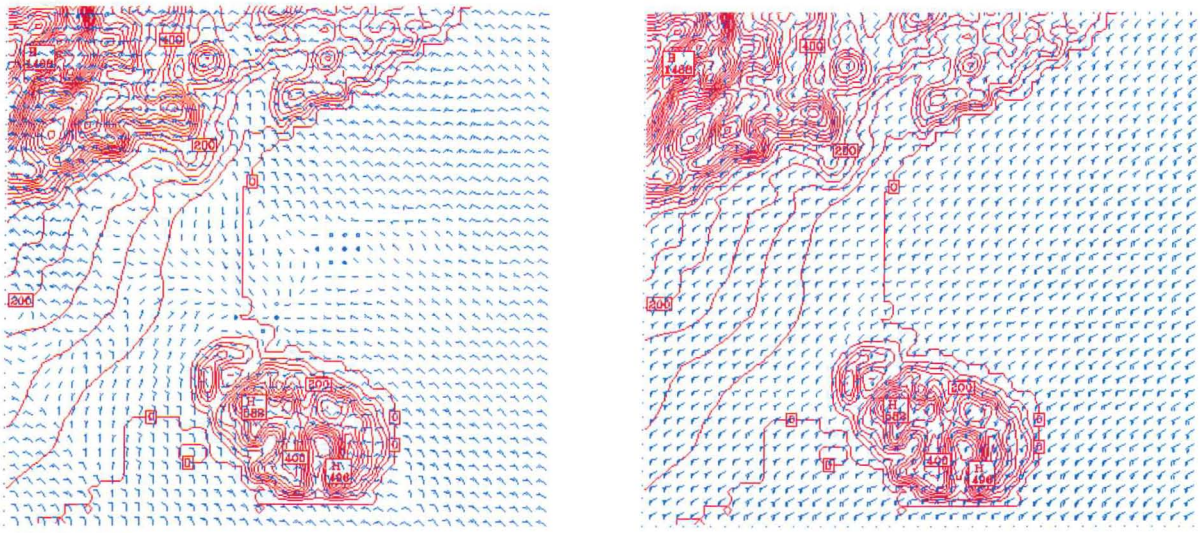

Figure 5.7 Spatial distribution of MM5 modelled near-surface wind, domain 4, σ=0.999 (7.0–8.5 metres): a) 0000 NZST on 05 August 2000, b) 0900 NZST on 05 August 2000.

Finally, CAMx4 was run for over 30 hours starting in the evening (6pm) during a period of reduced near-surface air turbulence and particulate matter accumulation under a weak developing temperature inversion. Figure 5.7 presents a time series of observed (red line) and modelled 2-level (green line) and 6-level (blue line) CAMx4 hourly mean concentrations of PM_{10} (in $\mu g\ m^{-3}$) for Coles Place, the Polytechnic and Packe Street. This is for a 30 hour run starting at 1800 on 31 August and finishing at 0000 on 2 August 2000. The meteorological data from domain 4 (MM5) and gridded aerosol/gas emissions files were used as initial and nudging

fields for CAMx4.

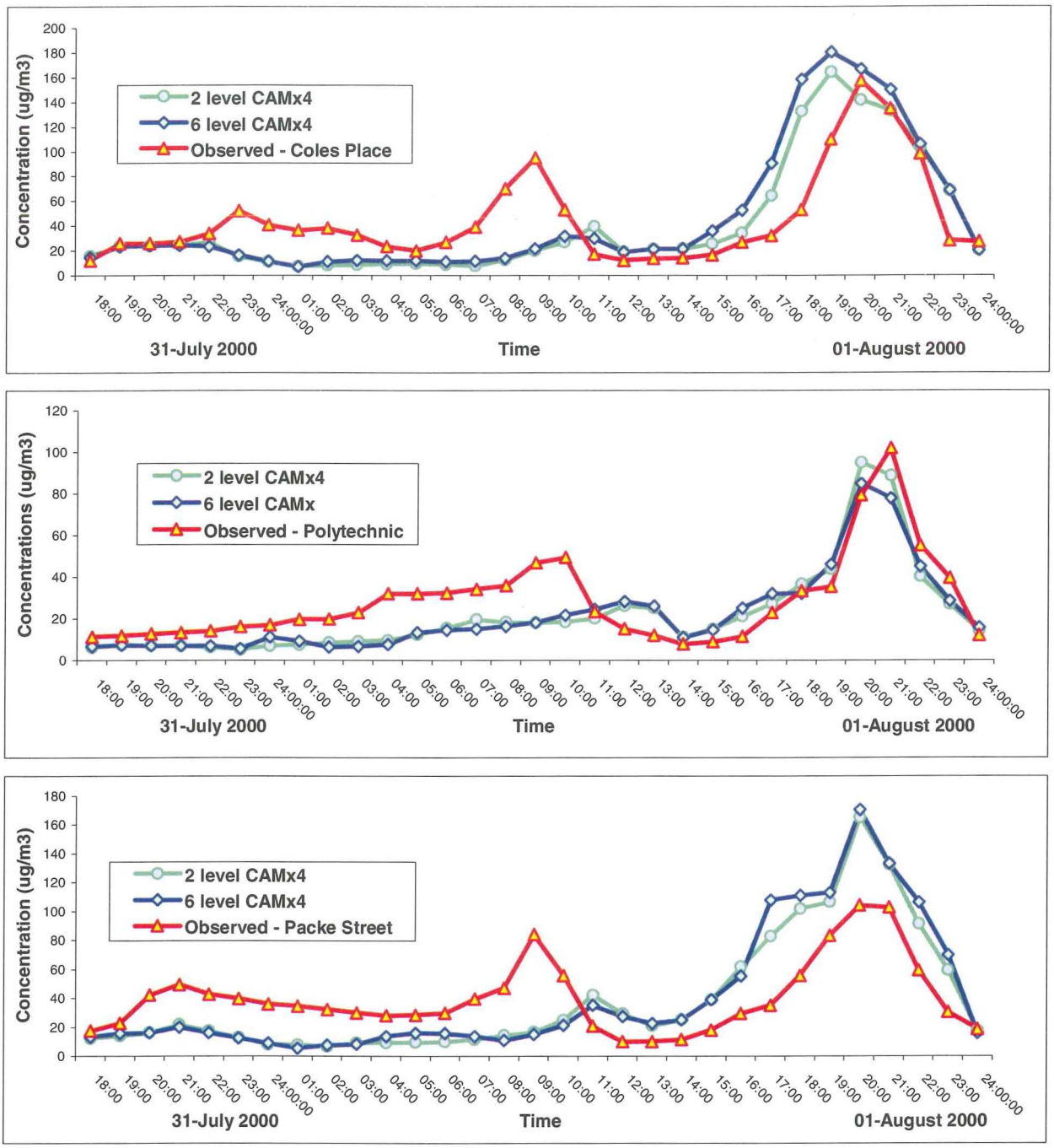

Figure 5.8 Time series of modelled (green line – 2-level CAMx4, blue line – 6-level CAMx4) and observed (red line) near-surface PM_{10} concentration ($\mu g\ m^{-3}$) for Coles Place, the Polytechnic and Packe Street observation sites: 0600 NZST on 31 July to 0000 NZST on 2 August 2000 (observed data from Ecan).

The CAMx4 30-hour run using MM5 input meteorology managed to reproduce very closely the night-time peak of PM_{10} for 1 August (especially at Coles Place and the Polytechnic – Figure 5.8) and weakly imitate the morning secondary maximum of PM with a two-hour delay for all 3 sites. This appears to reflect the importance of the so-called 'warm-up' time period (not less than 10–12 hours) for the chemical model before CAMx4 can provide predicted values

comparable with real PM concentrations. Because of the above-mentioned reasons, the correlation coefficient for modelled/observed PM_{10} concentrations dropped to range between 0.70–0.84 for Coles Place and Packe Street, and a little more than 0.80 for the Polytechnic site. Averaged 30-hour particulate matter concentrations for Coles Place, the Polytechnic and Packe Street in are quite close to observed data (at Coles Place the 2-level CAMx4 average is equal to 41.8 $\mu g\ m^{-3}$ compared to the observed value of 44.8 $\mu g\ m^{-3}$), because the model underestimation was not for the evening concentration maximum, but for the secondary morning peak. See Table 5.1 with the general statistics for winter 2000 below. The synoptic situation and air circulation over the Christchurch region has already been described earlier in this chapter (see Figures 5.2 and 5.3).

Pearson's correlation coefficient, index of agreement and additional statistics for the MM5–CAMx4 calculations of near-surface PM_{10} night and day concentrations (hourly output) are compared for three observation sites and represented in Table 5.1. Comparison is provided for the experiments using CAMx4 for the following run times: 72, 66, 60, 54, 48, 42, 36, 30 and 24 hours.

Table 5.1 Index Of Agreement (IOA), Pearson's Correlation Coefficient (PCC), Root Mean Square Error (RSME), Systematic and Unsystematic Root Mean Square Error (S-RMSE & U-RMSE), observed mean and modelled mean particulate matter concentrations (in $\mu g\ m^{-3}hr^{-1}$) for the 2-level CAMx4 version (winter 2000).

Run Time (Hours)	Observed Mean	Modelled Mean	PCC	RMSE	S-RMSE	U-RMSE	IOA
72 hours	25.6	34.8	0.84	27.23	13.91	20.74	0.92
66 hours	26.7	36.3	0.86	23.73	12.56	17.70	0.94
60 hours	27.0	32.5	0.86	20.03	6.77	14.00	0.95
54 hours	25.2	28.4	0.87	15.58	3.50	14.95	0.97
48 hours	30.3	32.6	0.85	21.60	2.63	21.53	0.95
42 hours	32.5	32.0	0.78	17.31	5.08	16.62	0.95
36 hours	34.4	35.0	0.79	19.31	3.22	19.13	0.94
30 hours	38.0	33.6	0.73	25.87	4.88	25.55	0.92
24 hours	40.6	36.3	0.71	23.98	5.78	23.43	0.91

From Table 5.1, a very good agreement between modelled 2-level CAMx4 and observed PM_{10} concentrations (see IOA and PCC) is evident for all experiments, but it should be noted that in the case of one-dimensional arrays, the correlation coefficient is considered to be a more reliable statistic than the index of agreement (more appropriate to one dimensional arrays).

However, it is evident from the table that maximum values of correlation coefficient (and IOA), minimum differences between observed and modelled mean and minimum systematic root mean square error (S-RMSE) are characterized by the experiments with run periods from 36 hours to 48 hours (1.5–2 day forecasts). It should be stressed that 48, 42 and 36-hours runs were all started at midday or in the evening, giving CAMx4 a 'warm-up' time period to more accurately reproduce the particulate material peaks. The results in Table 5.1 for time periods no longer than 48 hours will be compared with the output of the chemistry model for winter 2003.

5.3 Results of 2003 winter PM_{10} modelling

Winter 2003 was colder than winter 2000 (see Figure 4.21, for instance), with more PM_{10} peaks exceeding the health guideline (50 $\mu g\ m^{-3}$). Particulate matter was measured (at 10 minute intervals in the near-surface layer) at three observation sites: at the main Environment Canterbury site at Coles Place (St. Albans), and additional sites in Aranui and Hoon Hay. Several MM5-CAMx4 experiments were completed with different experimental run times (but not more than 48 hours), with input near-surface meteorology received from MM5 grid 4 output, and input of aerosol/gaseous (15 input species) gridded emissions from the data file generated specially for the purpose (as described earlier in Section 4.4.4). The aim is to evaluate the possibility of applying the MM5–CAMx4 numerical system for future quasi-operational forecasting of aerosol air pollution, using the winter 2003 synoptic conditions (runs were done over 48, 42, 36, 30 and 24 hours).

However, it is necessary to explain first why the 2-level version of the chemistry model reproduces time series of PM hourly mean concentrations no worse, and a little better, than the 6-level CAMx4 version. As already mentioned, the height of the upper (second) level of the 2-level chemical model ranged between 38–45 metres (see Section 5.2). From Figure 5.9, representing vertical temperature and PM concentrations measured on 21–22 of July 2003 (night time), it can be seen that the dominant part of the aerosol (more than 90%) is contained in the lowest 35–40 metres, in the lowest section of the temperature inversion. It is therefore not surprising that the 2-level CAMx4 provides useful PM_{10} predictions.

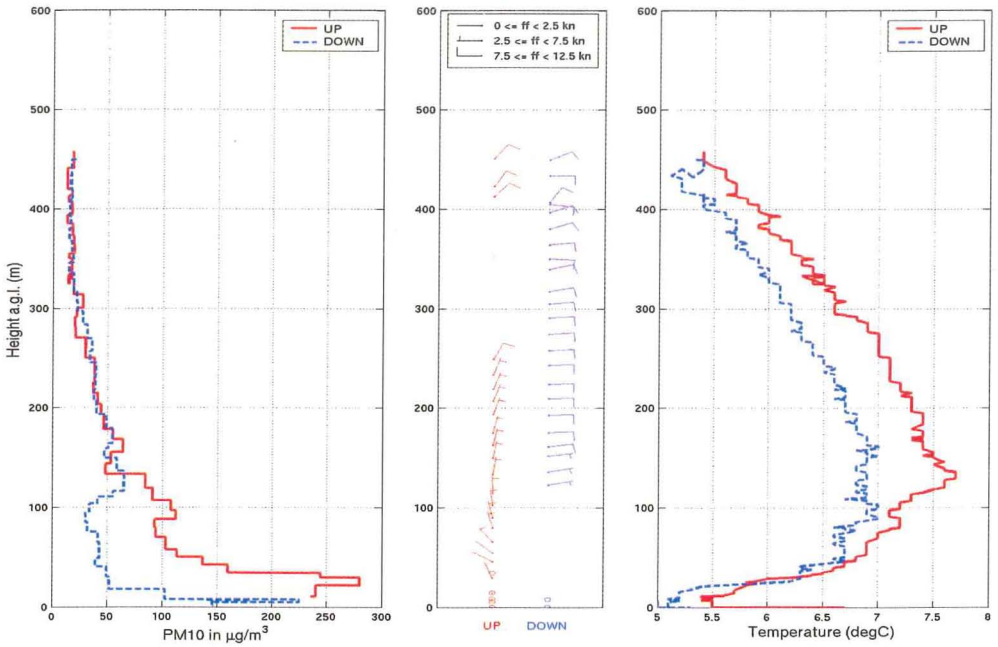

Figure 5.9 Vertical profiles of PM_{10} concentrations ($\mu g\ m^{-3}$), wind and temperature (°C): English Park, St. Albans, Christchurch, 2300 NZST on 22 July 2003 to 100 NZST on 23 July 2003 (after Sturman et al., 2003, pers.comm.).

Figure 5.10 represents time trends of observed (red line) and modelled 2-level (green line) and 6-level (blue line) CAMx4 hourly averaged concentrations of PM_{10} ($\mu g\ m^{-3}$) for Coles Place, Aranui and Hoon Hay over a 48 hour run, starting at 1200 NZST on 21 July and finishing at 1200 NZST on 23 July 2003, with input MM5 meteorological data and the gridded PM emissions file used for CAMx4 initialisation and hourly nudging.

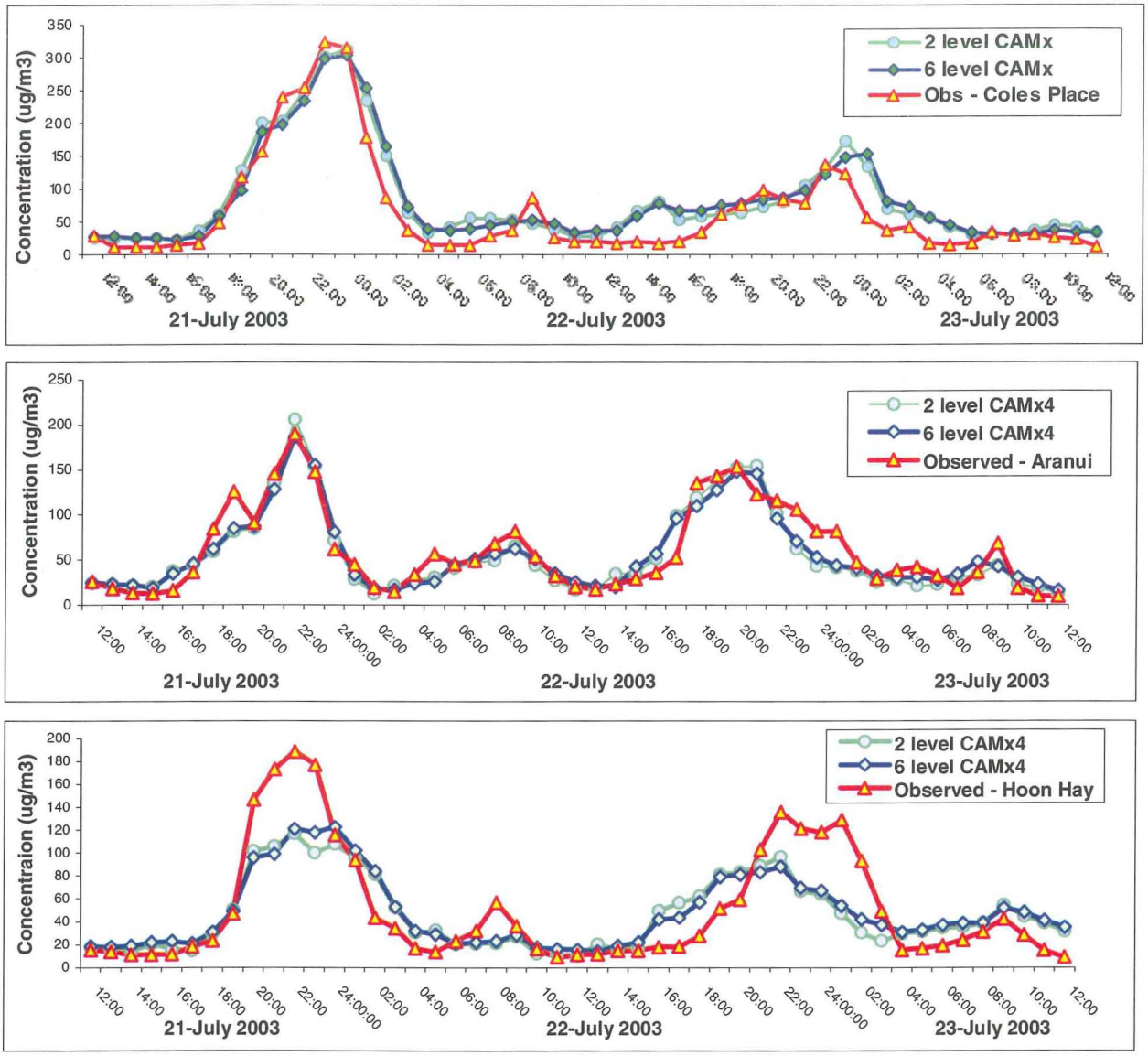

Figure 5.10 Time series of modelled (green line – 2-level CAMx4, blue line – 6-level CAMx4) and observed (red line) near-surface PM_{10} concentration ($\mu g\ m^{-3}$) for Coles Place, Aranui and Hoon Hay observation sites: 1200 NZST on 21 July to 1200 NZST on 23 August 2003 (observed data from Ecan).

The chemical model with MM5 input meteorology adequately reproduces night and morning peaks of PM_{10} for 22 and 23 July 2003 for all three monitoring sites (especially in the case of Coles Place and Aranui – Figure 5.10). However, the model underestimates night-time maxima, with a 2 hour time lag for Hoon Hay, which may be due to the complex local nocturnal airflow for this location, which is the closest to the Port Hills (see Figure 4.33). The 48-hour CAMx4 run has replicated the secondary morning peak of PM_{10} for all 3 observed sites (especially for Coles Place and Aranui – Figure 5.10). Pearson's correlation coefficient for modelled/observed PM_{10} concentrations ranges between 0.90 and 0.95 for Aranui and Coles Place, but is as low as 0.80 for Hoon Hay (for 2-level and 6-level CAMx4 versions). Particulate

matter 48-hour averaged concentrations for all three modelled points fluctuate by not more than 15% of the observed values, except for the Hoon Hay case (for example, Aranui: 2-level CAMx4 average is 55.4 μg m^{-3} compared with the observed value of 59.8 μg m^{-3}). In Table 5.2, the general statistics of the MM5–CAMx4 air pollution experiments for July 2003 are shown. It should be said that the synoptic situation over the South Island of New Zealand was stagnant (anticyclonic) during all 3 days chosen for the modelling experiments, with weak mesoscale air advection and dominant local wind systems.

Time series of observed (red line) and modelled (2-level CAMx4 – green and light blue line, 6-level CAMx4 – dark blue line) hourly averaged concentrations of PM_{10} (in μg m^{-3}) at Coles Place, Aranui and Hoon Hay are shown in Figure 5.11 for a 36 hour run, starting at 1200 NZST on 21 July and at 0000 NZST on 22 July for the 2-level CAMx version, and at 0000 NZST on 22 July 2003 for the 6-level CAMx4 version. Input data consisted of MM5 grid 4 meteorological data and gridded aerosol and gas emissions file for CAMx4 initialisation and hourly nudging.

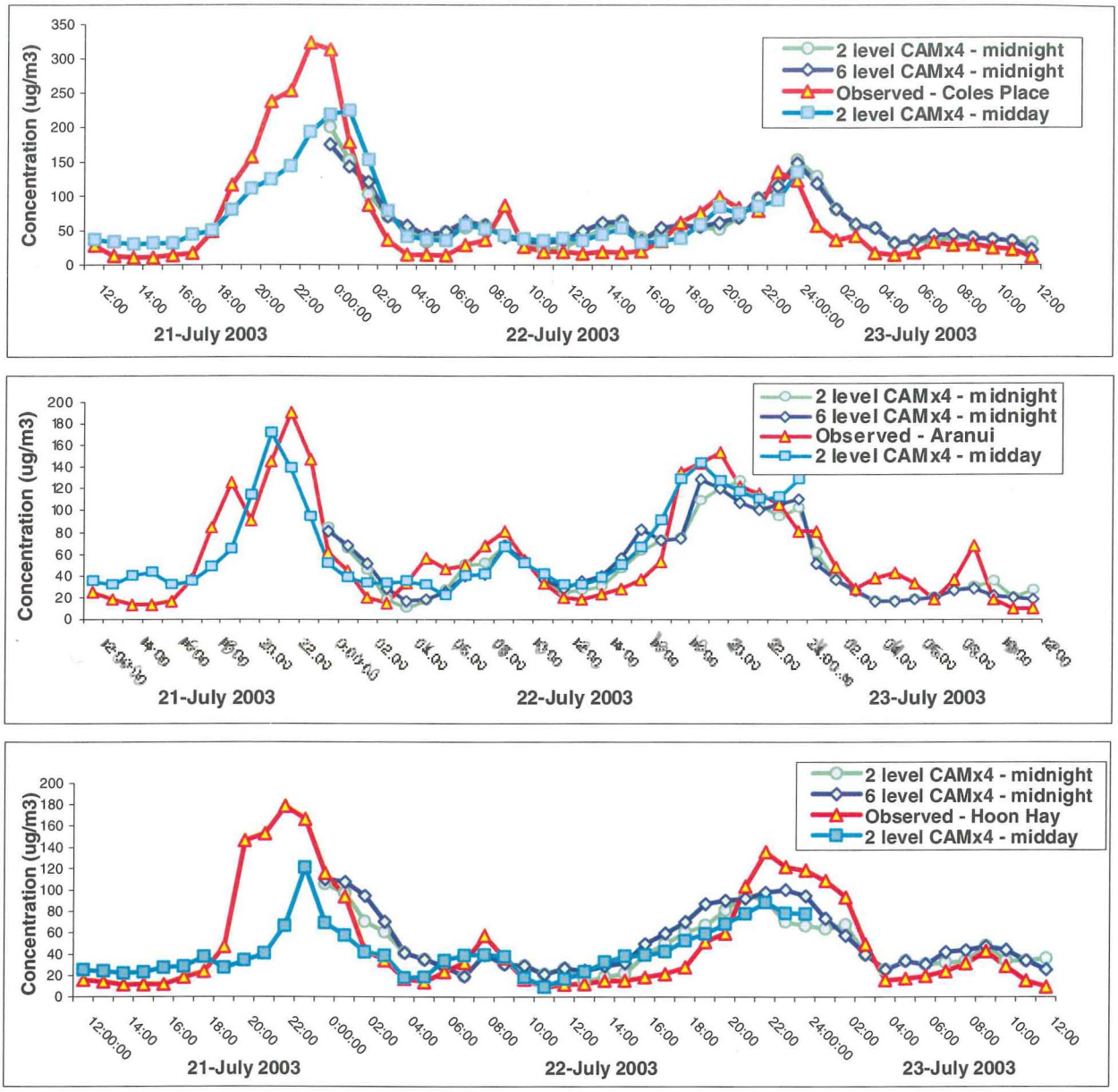

Figure 5.11 Time series of modelled (green line, light blue line – 2-level CAMx4, dark blue line – 6-level CAMx4) and observed (red line) near-surface PM_{10} concentration ($\mu g\ m^{-3}$) for Coles Place, Aranui and Hoon Hay: 36 hour run, starting 12 NZST on 21 July & 00 NZST on 22 for the 2-level CAMx4, and 00 NZST on 22 July 2003 for the 6-level CAMx4 (observed data from Ecan).

MM5–CAMx4 numerical system has accurately replicated the night and morning peaks of PM_{10} for 22-23 July 2003 for all three observed sites, especially in the case of Aranui, which is closest to the ocean and under the influence of the day–night cycle of the sea breeze. Underestimation of 21–22 July observed peak values with a 1 hour time lag of PM maximum concentrations for Coles Place and Hoon Hay can be explained by the absence (in the CAMx4 run) of a 10–12 hour 'warm-up' period, the significance of which was discussed in Section 5.1 (see Figures 5.2 and 5.8). The most important result of this 36-hour run is the evidence of the universality of CAMx4 with regard to it's 'start time'. Pearson's correlation coefficient between modelled and observed PM concentrations ranges between 0.80 and 0.88 for all three observed sites and does not depend strictly on 'start time'. It depends only on the length (in hours) of the 'warm-up' period before night-time.

Particulate matter 36-hour averaged concentrations for Coles Place, Aranui and Hoon Hay deviate by not more than 10% from the observed values. For example, at Hoon Hay 2-level CAMx4 averages are 47.3 $\mu g\ m^{-3}$ and 42.9 $\mu g\ m^{-3}$ compared to the observed values 44.8 $\mu g\ m^{-3}$. In Table 5.2 (lower) are shown all the general statistics of the MM5–CAMx4 air pollution experiments for July 2003. The modelled spatial distribution of PM_{10} is illustrated in Figure 5.12 at midnight (Figure 5.12a) and in the morning (9am) next day (Figure 5.12b).

a)

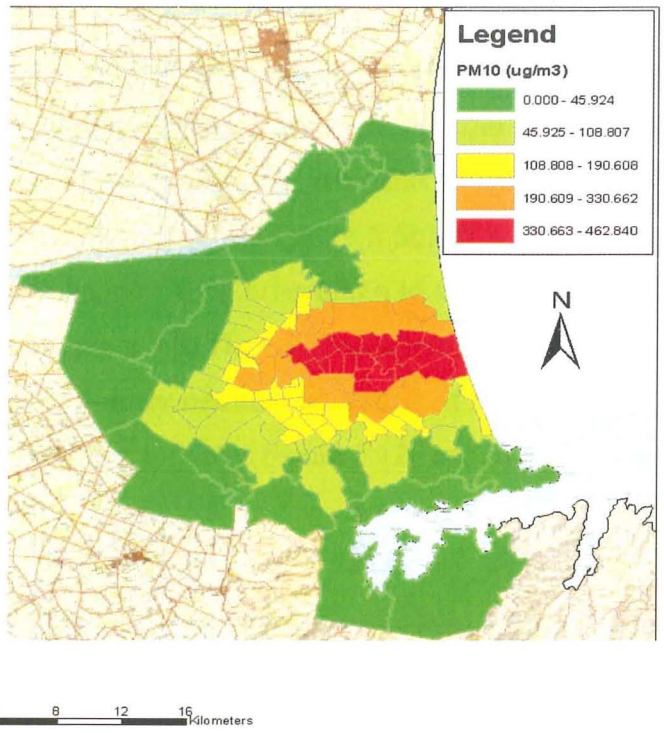

b)

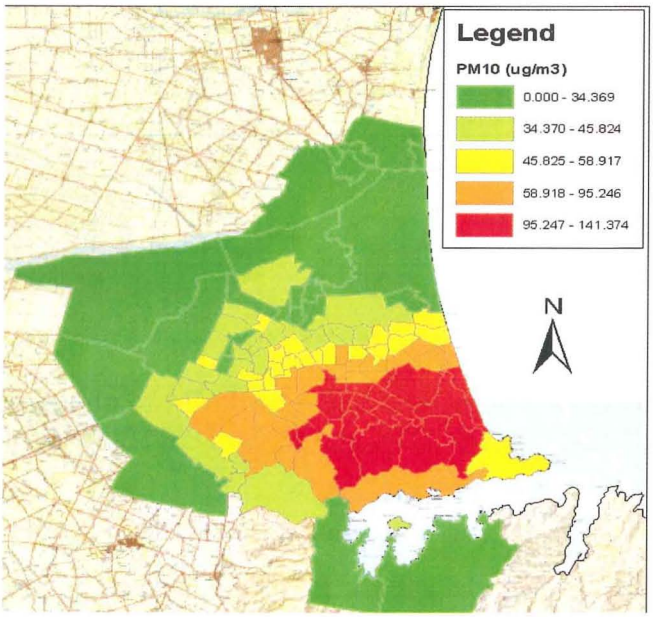

Figure 5.12 Spatial near-surface distribution of PM_{10} concentration ($\mu g\ m^{-3}\ hr^{-1}$): a) 0000 NZST on 22 July 2003, b) 0900 NZST on 22 July 2003. Note the different scales used to represent concentrations on the two maps.

From Figure 5.12a and b, it is obvious that modelled PM_{10} spatial distribution at midnight (Figure 5.12a) has an elongated shape and significant shift toward the ocean from the city centre (compared with Figure 5.6a) under the influence of nocturnal drainage winds from the

Canterbury Plains (Figure 5.13a), with a secondary maximum in the neighbouring districts. Morning modelled spatial PM_{10} distribution (Figure 5.12b) is also characterized by an evident spatial shift, not only in the direction of the ocean but also towards the southeast. This indicates the dominance of the Canterbury Plains night-morning cold air drainage over the Port Hills drainage winds (Figure 5.13b), especially comparing this situation with the spatial distribution of PM for the morning of 5 August 2000 (see Figure 5.6b). It is necessary to note that the spatial aerosol night–morning distribution over Christchurch in the case of winter 2003 is closer to the classical situation shown in Figure 3.3. The concentrations of PM_{10} in air are significantly less in Figure 5.12b, because of night–early morning advection of PM_{10} toward the ocean and partially by scavenging processes (see the caption of Figure 5.12a and b).

a) **b)**

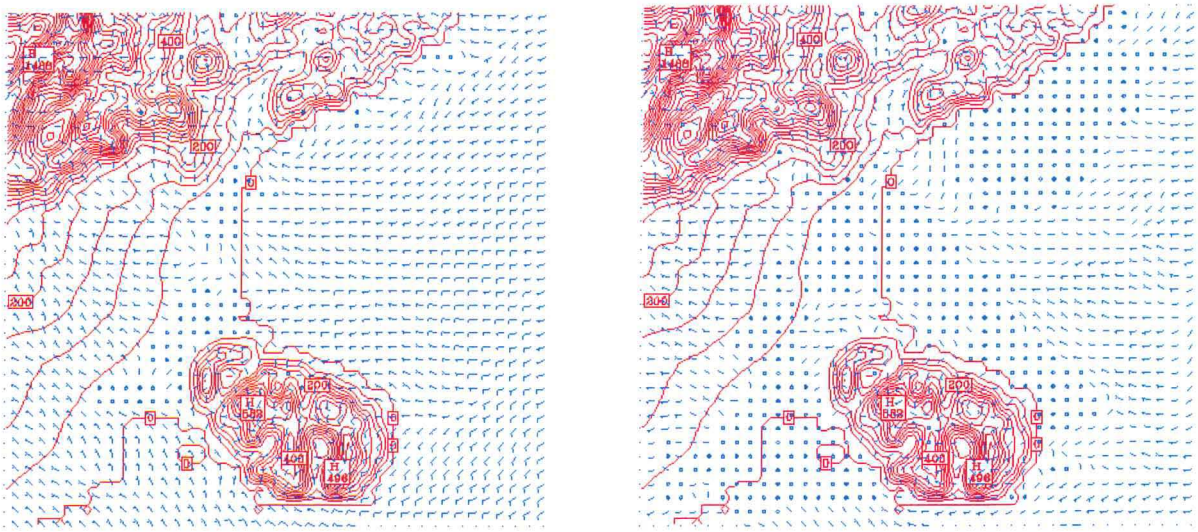

Figure 5.13 Spatial distribution of MM5 modelled near-surface wind, domain 4, σ=0.999 (7.0–8.5 metres): a) 0000 NZST on 22 July 2003, b) 0900 NZST on 22 July 2003.

Finally, it is interesting to present the results of a very short, 12 hour CAMx4 run, which started in the evening during particulate matter accumulation under a developing temperature inversion, and ending in the morning under strong temperature inversion conditions. In Figure 5.14, time series of observed (red line) and modelled 2-level (green line) CAMx4 version and 6-level (blue line) CAMx4 version hourly mean concentrations of PM_{10} (in $\mu g\ m^{-3}$) are presented for Coles Place, Aranui and Hoon Hay sites. The 12 hour run was started at 1800 NZST on 21 and finished at 0600 NZST on 22 July 2003, and meteorological data from MM5 grid 4 and the gridded emissions file were used for initialisation and nudging.

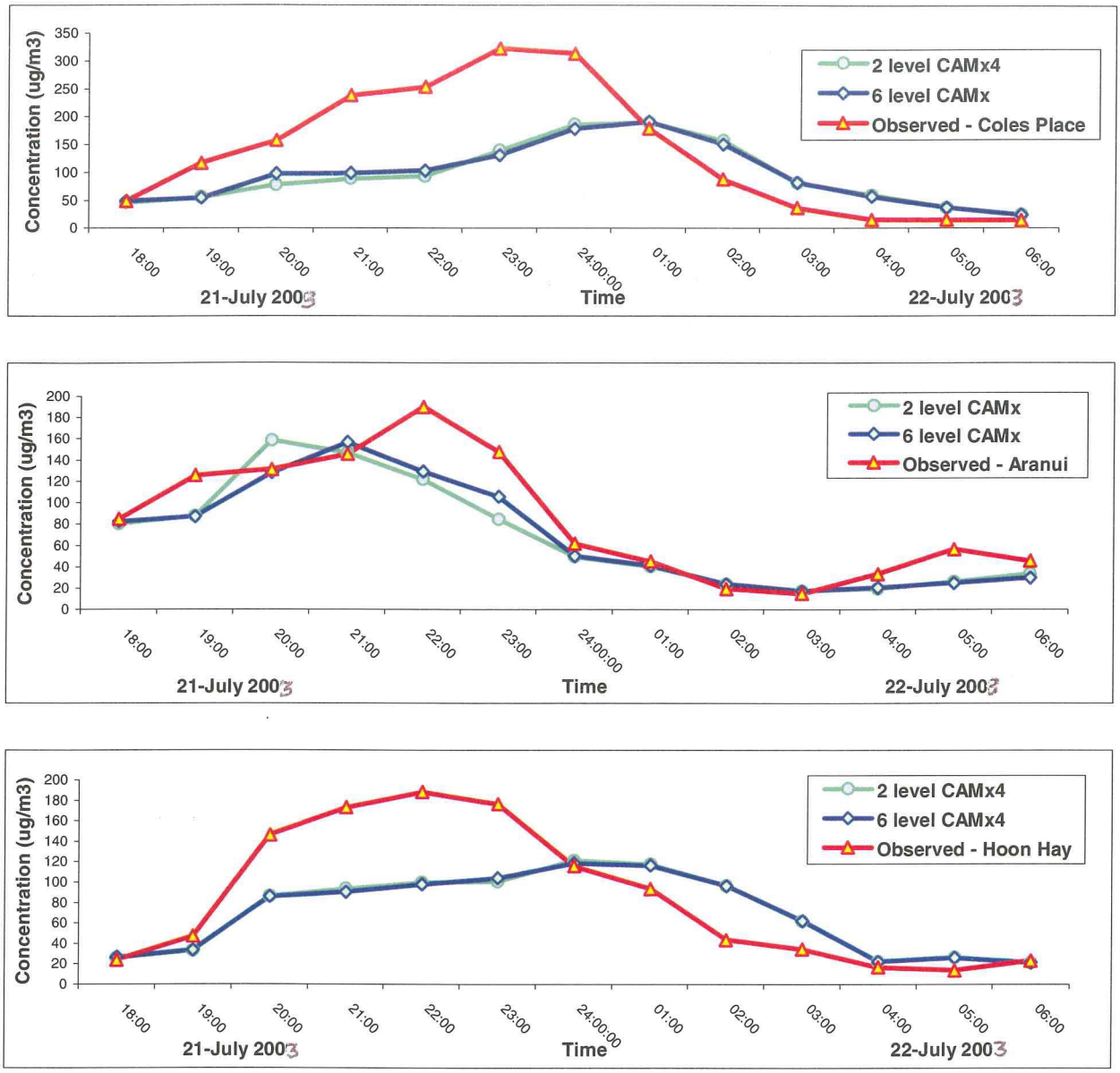

Figure 5.14 Time series of modelled (green line – 2-level CAMx4, blue line – 6-level CAMx4) and observed (red line) near-surface PM_{10} concentration ($\mu g\ m^{-3}$) for Coles Place, Aranui and Hoon Hay observation sites: 1800 NZST on 21 July to 0600 NZST on 22 July 2003 (observed data from Ecan).

Over such a short run time, CAMx4 has not adequately reproduced the night peak of PM_{10} between 21-22 July 2003 compared with observations, except at Aranui (Figure 5.14). It has also produced a time lag between the observed and predicted peaks of PM_{10}, particularly at Hoon Hay and Coles Place. The correlation coefficient for modelled/observed PM_{10} concentrations ranges between 0.65 and 0.70 for Coles Place and Hoon Hay, and is about 0.85 for Aranui (for the 2-level CAMx4 version). Particulate matter 12-hour averaged concentrations for all three sites deviate from the observed mean values by more than 35-45% (Coles Place: 2-level CAMx4 average is 94.2 $\mu g\ m^{-3}$ compared with the observed value of 137.6 $\mu g\ m^{-3}$). This example stresses the very important role of the 'warm-up' time period (it's better to have not less than 10–12

modelled hours before estimation of the first night-time PM concentrations), or there will always be a high probability of making a type I error – with the model failing to predict the observed heavy pollution night.

Pearson's correlation coefficient, Index of Agreement and additional statistics for MM5 – CAMx4 calculations of near-surface PM_{10} night-day concentrations (with hourly output) are compared for 3 observation sites and represented in Table 5.2. Comparison is made between the CAMx4 runs using the different time intervals: 48, 42, 36-I (CAMx4 starts at midday), 36-II (CAMx4 starts at midnight), 30 and 24 hours. The 12-hour case study is not included in Table 5.2, as it was undertaken to identify the smallest lead time for forecast consistency of the MM5–CAMx4 numerical system.

Table 5.2 Index Of Agreement (IOA), Pearson's Correlation Coefficient (PCC), Root Mean Square Error (RSME), Systematic and Unsystematic Root Mean Square Error (S-RMSE & U-RMSE), observed mean and modelled mean particulate matter concentrations ($\mu g\ m^{-3}hr^{-1}$) for the 2-level CAMx4 version (winter 2003).

Run Time (Hours)	Observed Mean	Modelled Mean	PCC	RMSE	S-RMSE	U-RMSE	IOA
48 hours	51.3	61.2	0.89	28.34	12.37	25.51	0.97
42 hours	64.9	59.1	0.85	34.72	27.02	21.86	0.96
36 hours-I	51.3	54.9	0.85	25.46	18.23	19.05	0.96
36 hours-II	50.8	53.3	0.84	26.56	18.74	19.46	0.96
30 hours	58.8	63.5	0.88	30.91	17.42	25.11	0.96
24 hours	50.2	52.4	0.81	24.36	17.74	16.80	0.95

Table 5.2 shows a good agreement between modelled and observed PM_{10} concentrations for all 2-level CAMx4 version experiments (see IOA and PCC). Table 5.2 makes it evident that for good numerical system output, the length of any run should be not less than 30–36 hours (for MM5 and for CAMx), as maximum values of the correlation coefficient, and minimum differences between observed and modelled mean and minimum systematic root mean square error (S-RMSE) are associated with the experiments with run periods of 36 and 48 hours. CAMx4 48 and 36-hour runs were started at midday, which gave CAMx4 a 'warm-up' time to replicate more accurately the magnitude of observed particulate matter peaks.

5.4 Summary

The details of PM_{10} modelling over different time periods using the MM5-CAMx system for winter 2000 were considered. Most appropriate start times of CAMx4 and 'warm-up' periods were identified. Results of the 2003 winter PM_{10} numerical modelling were also analysed.

Chapter 6

Conclusions and future research

6.1 Re-examination of research objectives

This study has presented the results of particulate matter numerical modelling over the Christchurch region using the coupled numerical system MM5–CAMx4 (meteorological–chemical model) for wintertime, and comparing the output with observed data for 2000 and 2003 winters. Aerosol air pollution in Christchurch results from use of domestic fires during cold winter nights, and for many years has been considered to be the most serious environment problem in the region during winter. The level of aerosol pollution is increased by the combined effects of the complex orography of the Christchurch local area, and regular stable synoptic conditions in winter, leading to supremacy of the local meteorological conditions with strong near-surface temperature inversions in the lowest 100–150 metres of the boundary layer. The aim of this study is to create a numerical modelling system by coupling limited area meteorological and chemical models, and to assess the ability of the system to reproduce PM_{10} dispersion over time. The research also aims to try and identify the optimal MM5–CAMx4 operational regimes that most closely reproduce the night and morning peaks in PM observed at the main air pollution monitoring sites in Christchurch. The aims were more specifically expressed as four principal objectives:

1. To utilize MM5 and to identify the optimal parameterisation for accurate simulation of Christchurch winter air circulation
2. To utilize CAMx version 4 and to create all essential input information for PM_{10} dispersion modelling
3. To develop and apply a numerical system consisting of the meteorological and chemical models
4. To identify the optimal parameters for the model system that produce the most reliable results, particularly with regard to improving accuracy of predictions of PM dispersion over space and time for both future research and developing quasi-operational forecast system.

These objectives were met through very careful use of the numerical system to research the possibilities of prediction of PM_{10} levels during winter, using special case study days and comparison of the model system output with observed data for winters 2000 and 2003. The purpose of this chapter is to briefly summarise the results and discuss their implications. The chapter concludes by discussing the limitations identified during the study and suggestions for

future research.

6.2 Summary of main findings

This section summarizes the findings from the result chapters (3 to 5) with regard to the four principal research objectives. Chapter 3 dealt with the first objective, as the synoptic scale and mesoscale circulation over the Christchurch region during wintertime was investigated using MM5. Origins of the observed-analysed meteorological data that could be used in the MM5 tuning process were discussed. The main part of Chapter 4 was devoted to realization of the first objective, while the last part of the chapter described the details of the application of CAMx4. This included description of preparation of necessary input files, including not only chemical information, but also the near-surface meteorology (objectives 2 and 3). Chapter 5 focused on researching the different regimes of the MM5–CAMx4 numerical system, and in particular developing a more detailed understanding of the numerical system behaviour, and identifying the most appropriate configurations of MM5–CAMx4 to achieve adequate results using less computer time (objectives 3 and 4).

The main consideration of the analysis of the meteorological and air pollution situation in Christchurch (Chapter 3) is the well-known influence of the complex air circulation over the region. The regime of the near-surface circulation depends on processes that operate at different meteorological scales, ranging from the macro-synoptic scale to the meso-miscroscale, including the migration of the drainage wind convergence zone in the city during night-morning hours. The influence of complex topography and the ocean on the local near-surface air circulation regularly creates very acute air pollution situations at a time when night-time domestic heating is at a maximum. This leads to accumulation of aerosol pollution in the lower boundary layer as a result of very strong negative near-surface buoyancy. The complexity of the problem determined the importance of precise tuning of MM5 to the meteorological conditions of the Christchurch area (objective 1).

Chapter 4 provided described the origins of meteorological data for MM5 initialisation and nudging (global analysis), and how the observational data were collected during the CAPS2000 experiment. The latter were compared with MM5 grid 4 (with 1 km spatial resolution) output so that more realistic MM5 near-surface meteorological output could be produced. Chapter 4 also described the principle results of MM5 modelling of the local air circulation over Christchurch and showed that the use of a 'deep' numerical atmosphere (top level at the height of 33–36 km) and increased PBL resolution in MM5 (up to 12-13 levels) allowed the production of more realistic results for the winters of 2000 and 2003 (objective 1). Details of the application of

global analysis data and FDDA analysis were also examined. The last part of Chapter 4 examined possibilities of creating input data for CAMx4, including landuse and gridded emission files, including aerosol and gaseous concentration files for the Christchurch region (objective 2). Input and nudging chemical data, as well as the input near surface meteorological data derived from MM5 output, are very important for accurate PM_{10} dispersion modelling using CAMx4 and for efficiency of the numerical modelling system (objective 3).

Chapter 5 described the principle results of the numerical system MM5–CAMx4 evaluation (objective 3), including the results of PM concentration modelling and the level of correlation between modelled and observed particulate matter time series. Modelling of PM_{10} spatial night-morning distribution is also outlined, as well as the effect of advection on PM_{10} distribution with the aerosol being carried towards the ocean after midnight by cold air drainage (objective 4). Given available input data, an optimal 6–12 hours 'warm-up' time interval was identified for the chemical model to accurately reproduce values of the night (11pm–2am) and morning (8am–10am) air pollution peaks using the MM5-CAMx system. The short 'warm-up' time period provides some optimism with regard to creating a quasi-operational version of MM5-CAMx4 numerical system in the future (objective 4).

6.3 Implications of results

It would be a gross generalisation to conclude that numerical modelling of winter PM_{10} time-space dispersion is a very complicated but possible task to realize. The results of the thesis illustrate the complexity of night-time patterns of particulate matter over Christchurch and its vicinity. However, the development and application of the numerical modelling system should allow improved understanding of the process of PM_{10} dispersion, accumulation and scavenging and improvement in the process of winter air pollution management.

6.4 Suggestions for further research

The MM5–CAMx4 numerical system is a very complex one and has great possibilities in application to environment research. Several of the suggestions listed below were not included in the thesis because of lack of time/space. However, some of them were examined briefly during completion of the research, which helped in the development of an understanding of the workings of the numerical models (or numerical model system), and therefore allowed more sophisticated operation of the numerical system:

1. Use of the RIP (Read, Interpolate, Plot) MM5 plotting program functions to study backward trajectories of air parcels for MM5 experimental results. A backward trajectory option of the

RIP program provides a good opportunity to trace the pathways of air advection through the Christchurch region in the boundary layer at fine resolution and to compare the results with observed near surface air advection

2. Modelling of inflow/outflow air transport over the South Island of New Zealand using special forward/backward trajectory models (FLEXTRA and FLEXPART) and MM5 output wind fields as a basis for different kinds of trajectory experiments
3. Application of the CAMx chemistry model for 2 and 3-dimensional studies of time distribution/accumulation of an instantaneous (or continuous) point (or multi-point) pollutant source for different wind and temperature conditions over the urban area
4. Use of MM5–CAMx4 system for space-time dispersion of gases (CO, NO, CO_2, NO_2, SO_2) in the Christchurch region and in surrounding small towns
5. Use of MM5–CAMx4 numerical system for investigation of multi-scale interaction between local and synoptic scale processes
6. Installation of the numerical modelling system on a multi-parallel computer system (for example, PC Linux) with the aim of applying it to a range of research problems (for different kinds of local air pollution investigations and numerical simulations) and in quasi-operational studies
7. Assimilation of the New Zealand meteorological network observations for more accurate research/forecast numerical modelling.

It is possible to conclude that the numerical modelling system developed here provides an opportunity to investigate the effects of recent and former influences of human activity on the environment at a range of time and space scales, and to predict future states of environmental structure and quality.

List of symbols

A	measure of lapse rate ($=50^0$ K)
c_l	species concentration
c_p	specific heat
c_s	sound speed
D/Dt	total derivative
F^{rad}	radiation function
h	layer interface height
g	acceleration due to gravity
K	turbulence diffusion coefficient
k	thermal conductivity
p	air pressure
p_n	air pressure of level n
p_s	surface air pressure
p_t	constant top air pressure
p_0	near-surface air pressure
p_{00}	sea-level air pressure (1013 hPa)
Q_H	heating function
s	humidity
t	time
T	dry-bulb temperature
T_0	reference air temperature for p_0
T_{s0}	reference air temperature for p_{00}
$\mathbf{u}$	wind vector
$\mathbf{V}_H$	horizontal wind vector
x, y	horizontal coordinates
η	net vertical 'entrainment rate'
σ	vertical terrain-following coordinate
ρ	air density
υ	coefficient of kinematics viscosity
μ	dynamic viscosity
θ	potential temperature
χ_D	water vapor diffusion coefficient

Ω	rotational speed of earth
$2\Omega x$	Coriolis force
∇	Laplacian

Glossary of abbreviations

ABL	Atmospheric Boundary Layer
AHM	Alpine Hydrochemical Model
AMPS	Arctic/Antarctic Mesoscale Prediction System
ATAQM	Advanced Texas Air Quality Model
CAA	Clean Air Act
CALMET	CALifornia METeorology
CALPLOT	CALifornia PLOTting
CALPUFF	CALifornia PUFFing
CAMx4	Comprehensive Air quality Model with extension, version 4
CAPS2000	Christchurch Air Pollution Study 2000
CB	Carbon Bond
CBM	Carbon Bond Mechanism
CCC	Christchurch City Council
CM	Chemistry Mechanism
CMAQ	Community Multiscale Air Quality system
CMC	Chemistry Mechanism Compiler
CTG	Composite Theme Grid
DAQMv2	Denver Air Quality Model Version 2
Ecan	Environment Canterbury
ECMWF	European Centre for Medium-range Weather Forecast
EDSS	Environment Decision Supporting System
EPA	Environment Protection Agency
EURAD	European Air Pollution Dispersion model system
FDDA	Four Dimensional Data Assimilation
FSL	Forecast System Laboratory
ftp	file translate protocol
FWS	Fire Weather System
GAM	Global Atmospheric Model
GD	Global Database
GDAS	Global Data assimilation System
GIS	Geographical Information System
GUI	Graphic User Interface

IEH	Implicit-Explicit Hybrid
IOA	Index Of Agreement
ITCZ	Inter-Tropical Convergence Zone
LAM	Limited Area Model
LSM	Land-Surface Model
MADE	Modal Aerosol Dynamic model for Europe
MAQSIP	Multiscale Air Quality Simulation Platform
MM5	Meteorological Model 5
NCAR	National Centre for Atmospheric Research
NCEP	National Centre for Environment Prediction
NIWA	National Institute of Water and Atmospheric research
NOGAPS	Navy Operational Global Analysis and Prediction System
NZST	New Zealand Standard Time
OSAT	Ozone Source Appointment Technology
OTAG	Ozone Transport Assessment Group
PAVE	Program for Analysis and Visualisation of Environmental data
PEC	Pollutant Elemental Carbon
PBL	Planetary Boundary Layer
PCC	Pearson Correlation Coefficient
PiG	Plume-in-Grid
PM	Particulate Matter
POA	Pollutant Organic Aerosol
PSU	Pennsylvania State University
RACM	Regional Atmospheric Chemistry Modelling system
RADM	Regional Acid Deposition Model
RAMS	Regional Atmospheric Modelling System
RH	Relative Humidity
RIP	Read, Interpolate, Plot
RMSE	Root Mean Square Error
RRTM	Rapid Radiative Transfer Model
ROG	Reactive Organic Gases
RUC	Rapid Update Cycle
S-RMSE	Systematic Root Mean Square Error
SMF	Split Mass Factor
SMOKE	Sparse Matrix Operator Kernel Emission System

SODAR	Sound Direction And Ranging
SPB	Selwyn Plantation Board
SST	Sea Surface Temperature
SVOC	Secondary Volatile Organic Components
TAPM	The Air Pollution Model
TAQS2000	Texas Air Quality Study 2000
TNRCC	Texas Natural Resource Conservation Commission
TOG	Total Organic Gases
TPF	Time Point Filter
U-RMSE	Unsystematic Root Mean Square Error
UAM-V	Urban Airshed Model system V
UCAR	University Corporation for Atmospheric Research
UKMO	United Kingdom Meteorological Office
USGS	United States Geological Survey
UTC	Universal Time Coordinated
UTM	Universal Transverse Mercator
UV	Ultra Violate
VNOC	Volatile Non-Organic Components
VOC	Volatile Organic Components
WPM	Weather Prediction Model
WRF	Weather Research and Forecasting model

References

Ackermann, I.J., Hass, H., Memmesheimer, M.E.A., Binkowski, F.S., Shankar, U., 1998, Modal aerosol dynamics model for Europe: development and first applications, *Atmospheric Meteorology*, vol. 36, pp. 2981–99.

Alexandrova, E., Balgaranova, J., Petkov, A., Pavlova, L., 2003, *Water, air and soil pollution*, Kluwer Academic Publishers, vol. 150, Issue 1–4.

Allwine, K.J., Dabberot, W.F., Simmons, L.L., 1998, Peel review of the CALMET/CALPUFF modelling system, EPA contract N 68-D-98-092, *work assignment*, N 1-03 report.

Arakawa, A. and Lamb, V.R., 1977, Computational design of the basic dynamical processes of the UCLA general circulation model, In *Methods in Computational Physics*, vol. 17, J. Chang (ed.), Academic Press, New York, pp. 173-265.

Arakawa, A., Mintz, Y., 1974, *The UCLA general circulation model, Notes from a Workshop on Atmospheric Modelling*, 25 March-4 April 1974, Department of Meteorology, University of California at Los Angeles, 404 pp.

Arakawa, A., Schubert, W.H., 1974, Interaction of a cumulus cloud ensemble with the large scale environment, Part I. *Journal of the Atmospheric Sciences*, vol. 31, pp. 674-701.

Arya, S.P., 1988, *Introduction to Micrometeorology*, Academic Press, New York, 307 pp.

Arya, S.P., 1999, *Air pollution meteorology and dispersion*, Oxford University Press, New York, 310 pp.

Baldasano, J.M., Delgado, R., Calbo, J., 1998, Applying receptor models to analyze urban/suburban VOCs air quality in Martorell (Spain), *Environmental Science and Technology*, vol. 32, pp. 405–12.

Bao, J.-W., McKeen, S.A., Grell, G.A., Trainer, M., Hsie, E.-Y., 2002, A comparison of meteorological observations with the output of a real-time weather – chemistry forecasting model during Texas AQS 2000 field experiment, *Preprints of the 4th Conference on Atmospheric Chemistry*, AMS, 13–17 January 2002, Orlando, Florida.

Baty, J.S., 1999, *Particulate deposition velocities in Christchurch city*, Master Thesis, Department of Geography, University of Canterbury, Christchurch, New Zealand.

Bergin, M.S., Russell, A.G., Milford, J.B., 1998, Effects of chemical mechanism uncertainties on the reactivity quantification of volatile organic compounds using a three-dimensional air quality model, *Environmental Science and Technology*, vol. 32, pp. 694–703.

Beyea, J., Hatch, M., 1999, Geographic exposure modelling: a valuable extension of geographic information systems for use in environmental epidemiology, *Environmental Health Perspectives*, vol. 107, pp. 694–703.

Bischoff-Gauss, I., Kalthoff, N., Fiedler, F., 1998, The impact of secondary flow systems on air pollution in the area of Sao Paolo, *Journal of Applied Meteorology*, vol. 37, pp. 269–87.

Blackadar, A. K., 1979, High resolution models of the planetary boundary layer, *Advances in Environmental Science and Engineering*, edit by J.R. Pfaffin and E.N. Ziegler, Gordon and Breach, Newark, N.J., pp. 50–85.

Bott, A., 1989, A positive definite advection scheme obtained by non-linear renormalization of the advective fluxes, *Monthly Weather Review*, vol. 117, pp. 1006–15.

Boucouvala, D., Bornstein, R., Wilkinson, J., Miller, D., 2003, MM5 simulations of a SCOS97 – NARSTO ozone episode, *Atmospheric Environment*, vol. 37, Supplement 2, pp. 95–117.

Bourke, W., 1974, A Multi-Level Spectral Model. I. Formulation and Hemispheric Integrations, Monthly *Weather Review*, vol. 102, pp. 687-701.

Brandt, J., Bastrupbirk, A., Christensen, J.H., Mikkelzen, T., Thykiernielsen, S., Zlatev, Z., 1998, Testing the importance of accurate meteorological input fields and parameterizations in atmospheric transport modelling using DREAM – validation against ETEX-1, *Atmospheric Environment*, vol. 32, pp. 4167–86.

Brown, M.J., Locatelli, J.D., Stoelinga, M.T. and Hobbs P.V., 1999, Numerical modelling of precipitation cores on cold fronts. *Journal of the Atmospheric Sciences*, vol. 56, pp. 1175-96.

Buckland, A.T., Middleton, D.R., 1999, Nomograms for calculating pollution within street canyon, *Atmospheric Environment*, vol. 33, pp.1017–36.

Byun, D.W. and Ching K.S., 1999, *Science algorithms of the EPA Model-3 Community Multiscale Air Quality (CMAQ) Modeling System*, EPA-600/R-99/030, U.S. EPA.

Byun, D.W. and Ching K.S., 1999, Science algorithms of the EPA Model-3 CMAQ modeling system, Washington, DC, U.S. *Environmental Protection Agency, Office of Research and Development.*

Carter, W.P.L., 2000, Implementation of the SAPRC-99 Chemical Mechanism into the Models-3 Framework, *Other Documents and Presentations,* Final Report to the United States Environmental Protection Agency. January 2000.

Chalouakau, A., Assimacopoulos, D., Lekkas, T., 1999, Ozone concentrations in the Athens Basin, *Environmental Monitoring and Assessment*, vol. 56, pp. 97–112.

Chang, J.S., Brost, R.A., Isaksen, I.S.A., Madronich, S., Middleton, P., Stockwell, W.R. and Walcek, C.J., 1987, A three-dimensional Eulerian Acid Deposition model (EURAD): physical concepts and formulation, *Journal of Geophysical Research*, vol. 92, N 14, pp. 681–700.

Chen, Q., Bai, L., Bromwich, D.H., 1996, A Harmonic-Fourier spectral limited-area model with an external wind lateral boundary condition, *Monthly Weather Review*, vol. 125, pp. 143–67.

Chilton, R.L., 1999, *Meteorological influences on air pollution of a Canterbury town:*

Ashburton, New Zealand, MSc thesis, Department of Geography, University of Canterbury, Christchurch, New Zealand.

Cirillo, M.C., Tamponi, M., Zanini, G., 1997, Italian debate on the role of regulatory models in the framework of the new European Directives on air quality, *International Journal of Environment and Pollution*, vol. 8, pp. 817–24.

Clai G., Kerschbaumer, A., Tosi, E., Tibaldi, S., 1998, Analysis of urban atmospheric pollution data in the Bologna area, *Environmental Monitoring and Assessment*, vol. 52, pp. 149–57.

Coats, C.J., Tryanov, Jr.A., McHenry J.N., Xiu, A., Gibbs-Lario, A. and Peters-Lidard, C.D., 1999, An extension of the EDSS/Model-3 I/O API for coupling concurrent environmental models, with applications to air quality and hydrology, Paper J10.6, *Preprint volume: 14th Conference on Hydrology, American Meteorology Society, Dallas, Texas.*

Cogliani, E., 2001, Air pollution forecast in cities by an air pollution index highly correlated with meteorological variables, *Atmospheric Environment*, vol. 35, pp. 2871–77.

Colella, P. and Woodward, P.R., 1984, The Piecewise Parabolic Method (PPM) for gas-dynamical simulations, *Journal of Computational Physics*, vol. 54, pp. 174–201.

Cox, R.M, Sontowski, J., Fry, R.N.Jr., Dougherty, C.M. and Smith, T.J., 1998, Wind and diffusion for complex terrain, *Journal of Applied Meteorology*, vol. 37, pp. 996–1006.

de Haan, P., Rotach, M.W., 1998, A novel approach to atmospheric dispersion modelling: the puff-particle model, *Quarterly Journal of the Royal Meteorological Society*, 124, pp. 2771 – 92.

de Haan, P., Rotach, M.W., Werfeli, M., 1998, Extension of an operational short-range dispersion model for applications in an urban environment, *International Journal of Vehicle Design*, vol. 20, pp.105–14.

Dailey, P.S., Keller, J.L., Modeling of extreme wind events using MM5: approach and verification, *MM5 Workshops, Division 3*, **www.mmm.ucar.edu/mm5/workshop/workshop-program-2002.html.**

Davis, J.M., Eder, B.K., Nychka, D., Yang, Q., 1998, Modeling the effects of meteorology on ozone in Houston using cluster analysis and generalized additive models, *Atmospheric Environment*, vol. 32, pp. 2505–20.

Dockerty, D.B. and Pope, C.A., 1994, Acute respiratory effects of particulate air pollution, *Annual review of Public Health*, vol. 15, pp.107-32.

Dudhia, J., 1993, A non-hydrostatic version of the Penn State/NCAR mesoscale model: Validation tests and simulation of an Atlantic cyclone and cold front, *Monthly Weather Review*, vol. **121**, pp. 1493-513.

Dudhia, J., 2002, MM5: current status and plans, *MM5 Workshops, Division 1*, **www.mmm.ucar.edu/mm5/workshop/workshop-program-2002.html**.

Dudhia, J. and Bresch, J.F., 2000, A global version of MM5. *Tenth Annual PSU/CAR Mesoscale Model User's Workshop*, Boulder CO, June 2000, pp. 23–26.

Dudhia, J., Grell, G.A., Guo, Y., Manning, K., Wang, W., Chiszar, J., 2000, *PSU/NCAR mesoscale modelling system tutorial class notes and user's guide: MM5 modelling system Version 3*, Mesoscale and Microscale Meteorology Division, NCAR, Boulder, Colorado, USA.

Ebel, A., Elbern, H., Feldmann, H., Jakobs, H.J, Kessler, C., Memmesheimer, M., Obberreuter, A., Piekorz, G., 1997, *Air pollution studies with the EURAD Model System (3): EURAD-European air pollution dispersion model System*, Mitteilungen aus dem Institut fur Geophysik und Meteorologie der Universitat Koln, vol. 120, pp. 172.

ENVIRON International Corporation, 2003, Comprehensive Air quality Model with extensions (CAMx), version 4.00, Novato, California.

Fast, J.D., O'Steen, B.L., Addis, R.P., 1995, Advanced atmospheric modelling for emergency response, *Journal of Applied Meteorology*, vol. 34, pp. 626–49.

Finardi, S., Morselli, M.G., Brusasca, G., Tinarelli, G., 1997, A 2-D meteorological preprocessor for real-time 3-D ATD models, *International Journal of Environment and Pollution*, vol. 8, pp. 391–400.

Foster, E., 1996, *Health effects of suspended particulate.* Canterbury Regional Council, Technical report, Environmental management group.

Gardner, M.W., Dorling, S.R., 1998, Artificial neural networks (the multilayer perception) – a review of applications in the atmospheric science, *Atmospheric Environment*, vol. 32, pp. 2627–36.

Gardner, M.W., Dorling, S.R., 1999, Neural network modelling and prediction of hourly NO_x and NO_2 concentrations in urban air in London, *Atmospheric Environment*, vol. 33, pp. 709–19.

Gery, M.W., Whitten, G.Z., Killus, J.P. and Dodge, M.C., 1989, A photochemical kinetics mechanism for urban and regional scale computer modelling, *Journal of Geophysical Resources*, vol. 94, pp. 925 – 56.

Gill, A.E., 1982, *The Atmosphere – Ocean Dynamics*, Cambridge, England, 385 pp.

Goldfrey, J.J., Clackson, T.S., 1998, Air quality modelling in a stable polar environment – Ross Island, Antarctica, *Atmospheric Environment*, vol. 32, pp. 2899–911.

Gordon, T., Stern, B., 1974, Spectral Modelling at GFDL, *GARP Programme on Numerical Experimentation*, 103 pp.

Goudie, A., Atkinson, B.W., Gregory, K.J., Simmons, I.G., Stoddart, D.R., Sugden, D., 1994, *The Encyclopedic dictionary of Physical Geography*, Blackwell, Oxford, 611 pp.

Gray, G., 1910, Dissolved matter in rainwater, *Canterbury Agricultural College Magazine*, pp. 183–95.

Grell, G.A., Dudhia, J. and Stauffer D., 1994, A description of the Fifth-Generation Penn

State/NCAR Mesoscale Model (MM5). *NCAR Tech Note NCAR/TN-398+STR*, 138 pp.

Grell, G.A., McKeen, S.A., Michalakes, J., Bao, J.-W., Trainer, M., Hsie, E.-Y., 2002, Real-time simultaneous prediction of air pollution and weather during Houston 2000 Field Experiment, *Preprint of the 4th Conference on atmospheric chemistry*, AMS, 13–17 January 2002, Orlando, Florida.

Haggkvist, K., 1997, Evaluation of dispersion models for an urban environment – an example from Stockholm, Sweden, *International Journal of Environment and Pollution*, 8, pp.638–45.

Hauge, G., Hole, L.R., 2002, Simulation of surface temperature inversions in complex terrain and implementation of slope irradiance, *MM5 Workshops, Division 4*, **www.mmm.ucar.edu/mm5/workshop/workshop-papers_ws02.html**.

Hernandez, J.F., Cremades, L., Baldasano, J.M., 1997, Simulation of tracer dispersion from elevated and surface releases in complex terrain, *Atmospheric Environment*, vol. 31, pp. 2337–48.

Holton, J.R., 1992, *Dynamic meteorology*, New York, Academic Press, 456 pp.

Hurley, P., 2002, *The Air Pollution Model (TAPM) Version 2. Part 1: Technical Description*, CSIRO, Australia, 49 pp.

Jacobs H.J., Feldmann, H., Hass, H., Memmesheimer, M., 1995, The use of nested models for air pollution studies: An application of the EURAD model to a SANA episode, *Journal of Applied Meteorology*, vol. 34, pp. 1301–19.

Jaeckervoirol, A., Lipphardt, M., Martin, B., Quandalle, P., Salles, J., Carissimo, B., Dupont, E., Mussongenon, L., Riboud, P.M., Aumont, B., Bergametti, G., Bey, I. And Toupance, G., 1998, A 3D regional scale photo-chemical air quality model application to a 3 day summertime episode over Paris, *Revue de l'Institut Francais du Petrole*, 53, pp. 225 – 37.

Jakobs, H.J., Friense, E., Memmesheimer, M. and Ebel, A., 2002, Real-time forecast of atmospheric pollutants over Europe and Germany, *MM5 Workshops, Division 5*, **www.mmm.ucar.edu/mm5/workshop/workshop-papers_ws02.html**.

Jonhstone, S.J., 2000, *The interaction of inversion development and katabolic winds: implications for air pollution in Christchurch*, Unpublished MSc thesis, Department of Geography, University of Canterbury.

Kain, J.S., Fritsch, J.M., 1993, Convective parameterization for mesoscale models: The Kain-Fritsch scheme, *The Representation of cumulus in numerical models, Meteorological Monographs*, vol. 46, American Meteorological Society, pp. 165–77.

Kallos, G., Kotroni, V., Lagouvardos, K., Papadopoulos, A., 1998, On the long-range transport of air pollutants from Europe to Africa, *Geophysical Research Letters*, vol. 25, pp. 619–22.

Klaussmann, A.M., deFoy, B., Godfrey, J., Scire, J., 2001, MM5 simulation over New Zealand – Application to the America's Cup races, *MM5 Workshops, Division 4*,

www.mmm.ucar.edu/mm5/workshop/workshop-program-2001.html.

Klemp, J.B., Skamarock, W.C., Dudhia, J., 2000, Conservative split-explicit time integration methods for the compressible non-hydrostatic equations, draft manuscript, *WRF Eulerian prototype model equations, height and mass vertical coordinates*, NCAR, Boulder, Colorado.

Kossmann, M. and Sturman, A.P., 2002, Analysis of surface wind fields in Christchurch and Canterbury (NZ) during winter smog nights – results from the CAPS2000, *16th International clean air and environmental Conference of the Clean Air Society of Australia and New Zealand, Christchurch, New Zealand 18 – 22 August 2002*, pp. 452–58.

Kossmann, M. and Sturman, A.P., 2004, The surface wind field during winter smog nights in Christchurch and coastal Canterbury, New Zealand, *International Journal of Climatology*, vol. 24, pp. 93-108.

Kotroni, V., Kallos, G., Lagouvardos, K., Varinou, M., Walko, M., 1999, Numerical simulations of the meteorological and dispersion conditions during an air pollution episode over Athens, Greece, *Journal of Applied Meteorology*, vol. 38, pp. 432–447.

Kotroni, V., Lagouvardos, K., 2002, MM5 fine scale simulations for the support of Athens 2004 Olympic Games: evaluation of the first year of operational activities, *MM5 Workshops, Division 3*, **www.mmm.ucar.edu/mm5/workshop/workshop-program-2003.html**.

Krichak, S.O., Tsidulko, M. and Pinhas, A., 2002, A study of an INDOEX period with aerosol transport to the eastern Mediterranean area, Journal of Geophysical Research, vol. 107, N. D18, pp. 18/1–18/9.

Krishnamurti, T.N., Ingles, K., Cocke, S., Kitade, T., Pasch, R., 1984, Details of low latitude medium range numerical weather prediction using a global spectral model, *Journal of the Meteorological Society of Japan*, vol. 62, pp. 613-49.

Kuo, L., 1974, Further studies of the parameterisation of the influence of cumulus convection on large-scale flow, *Journal of the Atmospheric Sciences*, vol. 31, pp. 1232-40.

Kurihara, Y., 1965, Numerical integration of the primitive equations on a spherical grid, *Monthly Weather Review,* vol. 93, N 7, pp. 399-416.

Lamprecht, R., Berlowitz, D., 1998, Evaluation of diagnostic and prognostic flow fields over prealpine complex terrain by comparison of the Lagrangian prediction of concentrations with tracer measurements, *Atmospheric Environment*, vol. 32, pp. 1283–300.

Lighthill, M.J., 1966, Dynamics of rotating fluids, a survey, *Journal of Fluid Mechanics*, vol. 26, pp. 411–31.

Low-Nam, S., Davis, C., 2002, Development of a Tropical Cyclone bougussing scheme for the MM5 system, *MM5 Workshops, Division 6*, **www.mmm.ucar.edu/mm5/workshop/workshop-program-2002.html**.

Makviladze, G.M., Roberts, J.P., Yakush, S.E., 1995, Modelling of atmospheric pollution by explosions, *Environmental Software*, vol. 10, pp. 117–27.

Manabe, S., Hahn, D.G., 1981, Simulation of atmospheric variability. *Monthly Weather Review*, vol.109, pp. 2260-86.

Mass, C.F., Ovens, D., Westrick, K. and Colle B.A., 1997, Does increasing horizontal resolution produce more skilful forecast, *Bulletin of the American Meteorological Society*, vol. 83, pp. 407–430.

McCauley, M.P., Sturman, A.P., 1999, A study of orographic blocking and barrier wind development upstream of the Southern Alps, New Zealand, *Meteorology and Atmospheric Physics*, vol. 70, pp. 121–31.

McGill, A.J., 1987, *Sea breeze circulation about Auckland, New Zealand Meteorological Service Scientific Report 29*, New Zealand Meteorological Service, Wellington, New Zealand, 36 pp.

McGowan, H.A., Sturman, A.P., 1993, Synoptic and local effects on the climate of the Waimate area, South Canterbury, *Weather and Climate*, vol. 13, pp. 22–23.

McKendry, I.G., 1983, Spatial and temporal aspects of the surface wind regime on the Canterbury Plains, New Zealand, *Journal of Climatology*, vol. 3, pp. 155–166.

McKendry, I.G., 1989, Numerical simulation of sea breezes over the Auckland, New Zealand – Air Quality Applications, *Boundary Layer Meteorology*, vol. 49, pp. 7–22.

McKendry, I.G., Sturman, A.P., 1983, The significance of the Canterbury wind regime. In Bedford, R, D, Sturman, A, P, *Canterbury at the crossroads: issues for the eighties*, New Zealand Geographical Society, Miscellaneous Series, N 8, University of Canterbury, Christchurch, pp. 126–37.

McKendry, I.G., Sturman, E.P., Owens I.F., 1986, A study of interacting multi-scale wind systems, Canterbury Plains, New Zealand, *Meteorology and Atmospheric Physics*, vol. 35, pp. 242–52.

McKendry, I.G., Sturman, E.P., Owens, I.F., 1987, The Canterbury Plains northeasterly, *Weather and Climate*, vol. 7, pp. 61–74.

Michelson, S.A., Bao, J.-W., McKeen, S.A., White, A., Grell, G.A., 2002, An evaluation of real-time forecasts from a weather-chemistry forecasting model using observations from the Texas AQS 2000 field experiment, *MM5 Workshops, Division 4*, **www.mmm.ucar.edu/mm5/workshop/workshop-program-2003.html**.

Miranda A.I., Borrego, C., 1996, A prognostic meteorological model applied to the study of a forest fire, *International Journal of Wildland Fire*, vol. 6, pp. 157–63.

MM5/RAMS fine grid meteorological modelling for September 8 – 11, 1993 Ozone Episode, Final Report, Texas Natural Resource Conservation Commission, 12118 Park Circle, Austin, Texas, 31 August 2001.

Moody, T., 1983, Air pollution in Canterbury: into the '80s or back to the '30s? In *Canterbury at the crossroad: Issues for the eighties* (Bedford R.D. & Sturman A.P., eds.), pp. 138–66.

Morse, P.M., 1964, Thermal Physics, Benjamin, New York, 355 pp.

Nunnari, G., Nucifora, A.F.M., Randieri, C., 1998, The application of neural techniques to the modelling of time-series of atmospheric pollution data, *Ecological Modelling*, vol. 111, pp. 187–205.

Odman, M.T., Wilkinson, J.G., MacNair, L.A., Russell, A.G., Ingram, C.L. and Houyoux, M.R., 1996, *Horizontal advection solver uncertainty in the Urban Airshed Model*, Prepared for California Air Resources Board and California EPA, April.

Oke, T.R., 1978, *Boundary layer climates*, Methuen: London.

Otte, T.L., Using MM5v3 with ETA analysis for air-quality modelling at the EPA, *MM5 Workshops, Division 7*, **www.mmm.ucar.edu/mm5/workshop/workshop-program-2001.html**.

Otte, T.L., Locser, A., 2001, Implementation of an urban canopy parameterization for fine-scale simulations, *MM5 Workshops, Division 5*, **www.mmm.ucar.edu/mm5/workshop/workshop-program-2001.html**.

Owens, I.F., Tapper, N.J., 1977, The influence of meteorological factors on air pollution occurrences in Christchurch, In *Proceedings of the air and environment conference*, Rotorua, New Zealand, pp. 403–20.

Pedlosky, J., 1979, *Geophysical Fluid Dynamics*, vol. I-II, Springer-Verlag, Berlin and New York.

Peters-Lidard, C.D., McHenry, J.N. and Coats, C.J., 2002, Design and evaluation of the coupled MM5/TOPLATS modeling system for Texas air quality accidence episode, *MM5 Workshops, Division 4*, **www.mmm.ucar.edu/mm5/workshop/workshop-papers_ws02.html**.

Pielke, R.A., 1984, *Mesoscale meteorological modelling*, Academic Press, New York, 267 pp.

Pielke, R.A., Cotton, W.R., Walko, R.L., Tremback, C.J., Lyons, W.A., Grasso, L.D., Nicholls, M.E., Morgan, M.D., Wesley, D.A., Lee, T.J., Coperald, J.H., 1992, A comprehensive meteorological modelling system – RAMS, *Meteorology and Atmospheric Science*, vol. 49, pp. 69–91.

Pietrowicz, J., 2002, Testing of mesoscale meteorological models as a tool to forecast pollen concentration, *MM5 Workshops, Division 6*, **www.mmm.ucar.edu/mm5/workshop/workshop-papers_ws02.html**.

Reisner, J., Rasmussen, M.R. and Bruintjes, R.T., 1998, Explicit forecasting of supercooled liquid water in winter storms using the MM5 mesoscale model. *Quarterly Journal of the Royal Meteorological Society*, vol. 124, pp. 1071-107.

Rostkier-Edelstein, D., Berkovic, S. and Givati, R., 2002, Statistical evaluation of high resolution MM5 surface winds and temperatures over complex terrain, *Division 2*, **www.mmm.ucar.edu/mm5/workshop/workshop-papers_ws02.html**.

Russel, A., 1997, Regional photochemical air quality modelling – model formulations, history,

and state of the science, *Annual Review of Energy and the Environment*, 22, pp. 537–88.

Ryan, A.P., 1975, Low level airflow patterns in Christchurch on nights of high air pollution potential, *Proceedings of the 8th Clean Air and Environment conference*, Rotorua, New Zealand, pp. 403–20.

Ryan, A.P., 1987, *The climate and weather of Canterbury (including Aorangi)*, New Zealand Meteorological Service, Miscellaneous Publication, 115 (17), 66 pp.

Ryan, R., 2002, Specification profiles and assignment files located on EMCH, *Memorandum*, EPA, U.S.A.

Seika, M., Harrison, R.M., Metz, N., 1998, Ambient background model (ABM): development of an urban Gaussian dispersion model and application to London, Atmospheric Environment, vol. 32, pp. 1881–91.

Smagorinsky, J., 1963, 'General Circulation Experiments with the Primitive Equations', *Monthly Weather Review*, vol. 91, N 3, pp. 99-164.

Smagorinsky, J., 1983, The Beginnings of Numerical Weather Prediction and General Circulation Modelling: Early Recollections, *Advances in Geophysics*, vol. 25, pp. 3-37.

Smallcomb, C., 2002, Using an operational MM5 in the Fire Weather Forecast process for West Texas and Southeastern New Mexico, *Division 5*, **www.mmm.ucar.edu/mm5/workshop/workshop-papers_ws02.html**.

Someshwar, D., Dudhia, J., Baker, D. and Moncreiff, M., 2002, A heavy rainfall episode over the west coast of India using analysis nudging in MM5, *Division 2*, **www.mmm.ucar.edu/mm5/workshop/workshop-papers_ws02.html**.

Sorteberg, A., Berge, E., Eastwood, S., 2001, Results from high-resolution operational meteorological forecasts in complex terrain during wintertime inversions, *Division 6*, **www.mmm.ucar.edu/mm5/workshop/workshop-papers_ws01.html**.

Souto, J.A., Perez-Munuzuri, V., de Castro, M., Souto, M.J., Casares, J.J. and Lucas, T., 1998, Forecasting and diagnostic analysis of plume transport around a power plant, *Journal of Applied Meteorology*, vol. 37, pp. 1068–1083.

Spronken-Smith, R.A., Sturman, A.P., Wilton, E., 2001, The air pollution problem in Christchurch, New Zealand, Progress and Prospects, *Clean Air and Environmental Quality*, vol. 36, pp. 23–8.

Spronken-Smith, R.A., Sturman, A.P., Kossman, M., Zawar-Reza, P., 2002, An overview of the Christchurch Air Pollution Study (CAPS) 2000, *16th International clean air and environmental Conference of the Clean Air Society of Australia and New Zealand, Christchurch, New Zealand 18 – 22 August 2002*, pp. 758–63.

Spronken-Smith, R.A., Kossmann, M., Zawar-Reza, P., 2004,Where does all the energy go? *Energy partitioning in suburban Christchurch under stable wintertime conditions. Theoretical and applied climatology.* [accepted; selected by the International Association for Urban Climate (IAUC) for inclusion in a special issue].

St. John, J.C., Chameides, W.L., 1997, Climatology of ozone exceedences in the Atlanta Metropolitan area: 1-hour vs. 8-hour standard and the role of plume recirculation air

pollution episodes, *Environmental Science and Technology*, vol. 31, pp. 2797–804.

Stauffer, D.R., Seaman, N.L., 1994, Multiscale four-dimensional data assimilation, *Journal of Applied Meteorology*, vol. 33, pp. 416–434.

Steenburg, W.J., Onton, D.J., Siffert, A.J., Cheng, L., Haymore, B., 2001, MM5 based modelling and model output statistics for the 2002 Olympic winter games, Division 6, **www.mmm.ucar.edu/mm5/workshop/workshop-papers_ws01.html**.

Stein, A.E., Lamb, D., Draxler, R.R., 2000, Incorporation of detailed chemistry into a three-dimensional Lagrangian – Eulerian hybrid model: application to regional tropospheric ozone, *Atmospheric Environment*, vol. 34, pp. 4361–72.

Sturman, A.P., 1985, Examination of the role of local wind systems in the concentration and dispersion of smoke pollution in Christchurch, New Zealand, *New Zealand Geographer*, vol. 41, pp. 67–76.

Sturman, A.P., 1986, Atmospheric circulation and precipitation patterns in the Canterbury plains and High County, New Zealand, *Weather and Climate*, vol. 6, pp. 7–14.

Sturman, A.P., 1998, Dynamic and thermal effects on surface airflow associated with Southerly Changes over the South Island, New Zealand, *Meteorology and Atmospheric Physics*, vol. 47, pp. 229–36.

Sturman, A.P., 2000, Applied Meteorology, *Progress in Physical Geography*, vol. 24, pp. 129–139.

Sturman, A.P., 2000, Applied Climatology, *Progress in Physical Geography* (progress report), vol. 24, N 1, pp.129–39.

Sturman, A.P., 2000, Impact of meteorology on air pollution in Canterbury, *Invited paper to the air pollution and health Conference, Christchurch, 3 – 6 August, 2000.*

Sturman, A.P., Fitzsimons, S.J., Holland, L.M., 1985, Local winds in the Southern Alps, New Zealand, *Journal of Climatology*, vol. 5, pp.145–60.

Sturman, A.P., Kossmann, M., Spronken-Smith, R.A. and Zawar-Reza, P., 2001, The Christchurch Air Pollution Study (CAPS) 2000 – An overview and preliminary results, *Proceedings of the Third Urban Air Quality Symposium: Measurement, Modelling and Management*, Loutraki, pp. 68–72.

Sturman, A.P., Kossmann, M., Spronken-Smith, R.A., Zawar-Reza, P., 2001, Meteorological controls of dispersion of air pollution in Christchurch. *2001 Geography, a spatial odyssey – hosted by the Otago branch of the New Zealand Geographical Society, Dunedin, New Zealand, 29 January – 2 February, 2001.*

Sturman, A.P., Kossmann, M., Zawar-Reza, P., Spronken-Smith, R.A. and Boorer, S., 2002, Air pollution meteorology of Timaru, South Canterbury, New Zealand. *16th International Clean Air and Environment Conference of the Clean Air Society of Australia and New Zealand*, Christchurch, New Zealand 18–22 August, 2002, pp. 764–770.

Sturman, A.P., Kossmann, M., Zawar-Reza, P., Vergeiner, J., 2003, Vertical structure of the

atmospheric boundary layer during high air pollution events in Christchurch, New Zealand, *National Clean Air Conference: Linking Air Pollution Science, Policy and Management, Newcastle, Australia, November 23-27, 2003.*

Sturman, A.P., McKendry, I.G., 1984, Detailed analysis of the structure of local wind systems in Canterbury, New Zealand, *Proceedings of the Nowcasting II Symposium*, Norrkoping, Sweden, European Space Agency, Sp-208, pp. 81–5.

Sturman, A.P., Tapper, N.J., 2002, *The weather and climate of Australia and New Zealand*, Oxford University Press, Melbourne, 476 pp.

Sturman, A.P., Trewinnard, A., Gorman, P., 1984, A study of atmospheric circulation over the South Island, New Zealand (1961–1980), *Weather and Climate*, vol. 4, pp. 53–62.

Sturman, A.P., Tyson, P.D., 1981, See breezes along the Canterbury coast in vicinity of Christchurch, New Zealand, *Journal of Climatology*, vol. 1, pp. 203–19.

Sturman, A.P., Tyson, P.D., 1981, Sea breezes along the Canterbury coast in the vicinity of Christchurch, New Zealand, *Journal of Climatology*, vol. 1, pp. 203–19.

Sturman, A.P., Zawar-Reza, P., 2000, Application of analytical tools to the assessment of air pollution transport over the Christchurch area, *Fresh perspectives, Annual Conference of the Meteorological Society of New Zealand, Christchurch, New Zealand, 20 – 24 November, 2000.*

Sturman, A.P., Zawar-Reza, P., 2001, *Application of back-trajectory techniques to the delimitation of a Clean Air Zone for the Christchurch airshed*, Technical Report, U01/3, Environment Canterbury, Christchurch, 23 pp.

Sturman, A.P., Zawar-Reza, P., 2002, Application of back-trajectory techniques to delimitation of urban clean air zones, *Atmospheric Environment*, vol. 36, pp. 3339–3350.

Sun, P., Allen, D.T., McDonald-Buller, E.C., Chang, S., Kimura, Y., Mullins, C.B., Yarwood, G., Neece, J.D., 2000, Development of chlorine mechanism for use in the carbon bond IV chemistry model, *Journal of Geophysical Researches*, vol. 108 (D4), pp. 41-45.

Tao, W.K. and Simpson, J., 1993, Goddard Cumulus Ensemble Model. Part I: Model description. *Terrestrial, Atmospheric and Oceanic Sciences,* vol. 4, pp. 19-54.

Titov, M., 2003, List of observation sites during CAPS200.

van Der Assem, S., Fisher, G.W., Sturman, A.P., 1996, Christchurch air quality study: progress report 3, *National Institute of Water and Atmospheric Research*, Report AK96029, 29 pp.

Wang, W., MM5 pre- and post-processing programs' update, *MM5 Workshops, Division 1*, **www.mmm.ucar.edu/mm5/workshop/workshop-papers_ws02.html**.

Wilkinson, L., 1959, *The air pollution problem in the Christchurch area*, Unpublished PhD Thesis, Environmental Science, Department of Geography, University of Canterbury, 175 pp.

Wilmott, C.J., Ackleston, S.G., Davis, R.E., Feddema, J.J., Klink, K.M., Legates, D.R., O'Donnell, J., Rowe, C.M., 1985, Statistics for the evaluation and comparison of models, *Journal of Geophysical Research*, vol. 90 (C5), pp. 8995–9005.

Wilton, E., Aberkane, T., Harvey, M., 2002, *Annual air quality monitoring report 2000*, Environment Canterbury, Christchurch, New Zealand, Report no. U02/32, **www.Ecan.govt.nz/Air/reports/U02-32.pdf**. [31v October 2003].

Wilton, E., Sturman, A.P., 2002, Assessing source of visibility degradation in Christchurch, *16th International clean air and environmental Conference of the Clean Air Society of Australia and New Zealand, Christchurch, New Zealand 18–22 August 2002*, pp. 884–89.

Yarwood, G., Morris, R.E., Yocke, M.A., Hogo, H. and Chico, H., 1996, Development of a methodology for Source Appointment of Ozone concentration estimates from a photochemical grid model, *Presented at the 89th AWMA annual meeting, Nashville TN, June 23–28.*

Zaengl, G., 2002, An improved method for computing horizontal diffusion in a sigma-coordinate model and its application to simulations over mountainous topography. *Monthly Weather Review*, vol. 130, pp. 1423–1432.

Zawar-Reza, P., Sturman, A.P., 2001, Assessing the impact of industry on air quality and the environment using atmospheric mathematical models, *Proceedings of the 3rd International seminar of Iranian industry & mines R & D centres*, Tehran, 2001, pp. 517–21.